
# MEASUREMENT OF PHASE EQUILIBRIA FOR OXYGENATED HYDROCARBON SYSTEMS

**By**

**Samuel Ayodele Iwarere**

B.Sc.Industrial Chemistry (Hons)

University of Ilorin, Kwara State, Nigeria

Submitted in fulfilment of the academic requirements for the degree of Master of Science in Engineering to the Faculty of Engineering, School of Chemical Engineering, University of KwaZulu-Natal, Durban.

**December 2009**

# PREFACE

The work presented in this thesis was carried out under the Thermodynamic Research Group of the School of Chemical Engineering at the University of KwaZulu-Natal, Durban, from February 2009 to November 2009 under the supervision of Professor D. Ramjugernath and Doctor P. Naidoo.

This thesis is submitted as the full requirement for the degree M.Sc. in Chemical Engineering.

I, Samuel Ayodele Iwarere, therefore declare that:

(i) The research reported in this thesis, except where otherwise indicated, is my original work.

(ii) This thesis has not been submitted for any degree or examination at any other university.

(iii) This thesis does not contain other persons' data, pictures, graphs or other information, unless specifically acknowledged as being sourced from other persons.

(iv) This thesis does not contain other persons' writing, unless specifically acknowledged as being sourced from other researchers. Where other written sources have been quoted, then:
a) their words have been re-written but the general information attributed to them has been referenced;
b) where their exact words have been used, their writing has been placed inside quotation marks, and referenced.

(v) This thesis does not contain text, graphics or tables copied and pasted from the Internet, unless specifically acknowledged, and the source being detailed in the thesis and in the References sections.

_____

S. A. Iwarere

As the candidate's supervisor, I, Prof. D. Ramjugernath, approved this thesis for submission.

_____

Professor D. Ramjugernath

As the candidate's co-supervisor, I, Dr. P Naidoo, approved this thesis for submission.

_____

Dr. P. Naidoo

# ACKNOWLEDGEMENTS

I wish to acknowledge some of the people who contributed directly or indirectly to the successfully completion of this work and for some of those who may have made significant input on this project but whose name may be omitted in this acknowledgement. Please kindly accept my apologies in good faith as to err is human, to forgive divine. I love and appreciate you all.

- My supervisors, Professor D. Ramjugernath and Doctor P. Naidoo for their support and guidance in the course of my research. Without their knowledge, ideas and experience this project would not have been possible.

- My colleagues in the Chemical Engineering Department and, in particular, Ayanda, Avumile, Francois, Jim, Linda, Kaniki, Khalid, Khulekani, Marc, Margreth, Travis, and Shalini for their valuable company and assistance.

- SASOL Ltd., the National Research Foundation (NRF) of South Africa and the University of KwaZulu-Natal Scholarships Office for financial support.

- My brothers in Christ, (mostly from His People Christian Church) who has made my stay in South Africa so far a memorable one.

- My beloved parents, Mr & Mrs F.O. Iwarere, my brother Babs and my sister Buky. I also wish to acknowledge my Undergraduate project supervisor and spiritual mentor Prof. E.O. Odebunmi who believed so much in my life and what God can achieve through me, thus motivating me to come back to the Academic world. The last but not the least, I acknowledge my fiancée Olufunsho D. Oni for all her understanding, support, encouragement and motivation. I love you and I will always do.

- Finally, to the greatest one who rules over the whole Heaven and Earth, The Pillar that holds my life. The one I live for. The source of my existence- Jesus Christ, my Lord and Personal Saviour. I love you Lord.

# ABSTRACT

A number of industrially relevant separation processes involve carboxylic acids. Carboxylic acids are also amongst the various oxygenated products found in aqueous waste streams or as by-products of industrial operations in Sasol's Fischer Tropsch processes. Other by-products include alcohols and ketones. Accurate vapour-liquid-equilibrium (VLE) data are required for the efficient and optimal modeling and simulation of these processes. In addition, removing and separating these components will help to prevent their pollution and the associated impact on the environment. For this project, the new systems (2-Propanol (1) + Butyric Acid (2), 2-Butanol (1) + Butyric Acid (2) and 2-Methyl-1-butanol (1) + Butyric Acid (2) binary mixtures were measured at three isotherms of 333.15, 353.15 and 373.15 K respectively. These measurements were carried out using the Stainless steel VLE apparatus of Reddy (2006) and the glass VLE apparatus of Raal (1992) which was later modified by Joseph (2001) and Scott (2003). The two apparatus could operate in both isobaric and isothermal modes, with the temperature and pressure being regulated via a pulse-width modulation control strategy (Joseph et al. 2001) while the stainless steel apparatus was controlled using a graphical user interface run on the computer with the pressure controlled to within 0.01 kPa of the set-point pressure.

The accuracy of the measured temperature was estimated to be within ±0.02K for the two VLE apparatus, while the accuracy of the temperature control varied between 0.01 and 0.05 K. The pressure accuracy was estimated as ±0.03 and ±0.02 kPa for the stainless steel and glass still respectively and controlled to within 0.01 kPa for isobaric operation, while the accuracy of the equilibrium composition measurement using a Shimadzu GC2010 gas chromatography was estimated to be ±0.002 of a mole fraction.

The thermodynamic behaviour of the carboxylic acid and alcohol mixtures is known to be strongly affected by specific interactions like association (hydrogen bonding) and electrostatic interactions of permanent or induced dipoles. The modeling of associating systems has been a challenge due to fact that the commonly used models do not explicitly account for these specific interactions. In this project, the modeling of data for the newly measured systems was performed using two different reduction techniques; the combined (gamma-phi) method and the direct (phi-phi) method. For the combined method, NRTL (1968) liquid-phase activity coefficient model was used to successfully correlate the VLE data, while the vapour phase imperfections were accounted for using virial equation of state with Tsonopoulos correlation (1974) and the Hayden and O'Connell (1975) correlation with the chemical theory approach. The Soave-Redlich-Kwong (1972) equation of state in conjunction with the Wong and Sandler mixing rule and NRTL Gibbs excess energy model

(SRK/WS/NRTL), and the Stryjek-Vera (1986) form of Peng–Robinson (1976) equation of state in conjunction with the Wong and Sandler mixing rule and NRTL Gibbs excess energy model (PRSV/WS/NRTL) were utilized in the direct method, with both liquid and vapour phase non-idealities represented by fugacity coefficients.

The associating effects of the carboxylic acid and alcohol systems are represented by Chemical theory considering that the acid have one association site (monomer-dimer formation) and the alcohol have two association sites. Hence, the one site in the acid cross-associate with both sites in the alcohol. Thus, it is considered that the chain length will be shorter in the mixture than in the pure alcohol taking the explanation of (Fu and Sandler) that when acids and alcohol associate, the chain terminates. The calculation was based on two assumptions made by (Prausnitz et al., 1980).

The direct method and the combined method gave a good fit with the chemical theory accounting for the chemical interaction by correlating the vapour phase more accurately. All the data sets passed the highly rigorous direct test (Van Ness, 1995) for thermodynamically consistency. However, the point test (Van Ness et al. 1973) gave a better indication of the thermodynamic consistency of the carboxylic acid-alcohol binary systems.

# TABLE OF CONTENTS

# LIST OF FIGURES

## Chapter 1



## Chapter 2



## Chapter 3



## Chapter 4

## Chapter 5



## Chapter 6

## Chapter 7

## Appendix C



## Appendix D

## Appendix D

# LIST OF TABLES

## Chapter1



## Chapter3



## Chapter 6



## Chapter 7

## Appendix A



## Appendix C

# NOMENCLATURE

## English Letters

| | |
|---|---|
| A | Constant in the Antoine or Wagner vapour pressure equations |
| a | Intermolecular attraction force parameter in the Soave Redlich-Kwong(1972) and Peng and Robinson Stryjek and Vera EOS |
| a´ | Parameter in the Tsonopoulos (1974) correlation |
| AAD | Absolute average deviation |
| $a_i$ | Activity defined in equation (3.42) |
| B | Constant in the Antoine or Wagner vapour pressure equations |
| $B^0$ | Parameter in the Pitzer-Curl [1957] correlation |
| $B^1$ | Parameter in the Pitzer-Curl [1957] correlation |
| $B_{ii}$ | Second virial coefficient of pure component i [$cm^3$/mol] |
| $B_{ij}$ | Second virial coefficient for species i - species j interaction [$cm^3$/mol] |
| b | Molecular size parameter in Soave Redlich-Kwong (1972) and Peng-Robinson (1976) EOS |
| b´ | Parameter in the Tsonopoulos (1974) correlation |
| C | Constant in the Antoine or Wagner vapour pressure equations |
| c | Numerical constant defined in equation (B.36 and B.37) |
| CPA | Cubic Plus Association |
| D | Constant in the Wagner vapour pressure equation |
| $D^o$ | Summation term in the Wong-Sandler (1992) mixing rule (equation (B.29)) |
| $E_i$ | Energy of a particular configuration i in a simulation [J/mol] |
| EOS | Equation of state |
| f | Fugacity [kPa] |
| $\hat{f}$ | Fugacity in solution [kPa] |
| G | Molar or specific Gibbs energy [J/mol] |
| $G_{12}$ | Parameter in the NRTL (1968) model |
| $G_{21}$ | Parameter in the NRTL (1968) model |
| $\overline{G}$ | Partial molar Gibbs energy [J/mol] |
| $g_{ij}$-$g_{ii}$ | Parameter representing energy interactions between species in the NRTL (1968) model |

| | |
|---|---|
| GCA | Group contribution with associating |
| $g^E$ | Excess Gibbs energy |
| H | Enthalpy [J/mol] |
| HPVLE | High Pressure Vapour Liquid Equilibrium |
| $\Delta H_{vap}$ | Enthalpy of vapourization [J/mol] |
| K | Equilibrium constant |
| k | Mixing rule parameter |
| $k_B$ | The Boltzmann constant [1.381 x $10^{-23}$ J/mol.K] |
| $k_{ij}$ | Binary interaction parameter |
| LPVLE | Low Pressure Vapour Liquid Equilibrium |
| M | Represents a general thermodynamic property |
| $M_W$ | Molecular weight [g/mol] |
| $N_A$ | Avogadro's number (6.022137 x $10^{23}$ $mol^{-1}$) |
| n | Number of moles |
| $n_{exp}$ | Number of experimentally measured points (section 7.2) |
| P | System pressure [kPa] |
| P´ | Parachor |
| $P_c$ | Critical Pressure |
| $P_r$ | Reduced Pressure defined in equation (3.68) |
| Q | Quadratic sum of second virial coefficients |
| R | Universal gas constant [J/mol.K] |
| $R_d$ | Mean radius of gyration [Å] |
| S | Molar or specific entropy [$cm^3$/mol] |
| T | System temperature [ K] |
| $T_c$ | Critical Temperature [ K] |
| $T_r$ | Reduced Temperature |
| $V_m$ | Molar or specific volume [$cm^3$/mol] |
| x | Liquid phase mole fraction (or composition) |
| y | Vapour phase mole fraction (or composition) |
| Z | Compressibility factor |
| $Z^{assoc}$ | Compressibility factor for the Association Part of CPA EOS |
| $Z^{Phys}$ | Compressibility factor for the Physical Part of CPA EOS |
| $z_i$ | True mole fraction of species i |

## Greek Letters

| | |
|---|---|
| $\alpha$ | Scaling factor in Soave-Redlich-Kwong and Peng-Robinson (1976) equation of state |
| $\alpha_{12}$ | Parameter in NRTL (1968) model representing solution non-randomness |
| $\delta$ | Denotes a residual (e.g. $\delta$P) |
| $\delta_{ij}$ | Term relating the second virial coefficients |
| $\varepsilon_A$ | Tolerance in the flow diagrams for the bubblepoint iterations |
| $\varepsilon_B$ | Tolerance in the flow diagrams for the bubblepoint iterations |
| $\varepsilon_X$ | Tolerance in the flow diagrams for the bubblepoint iterations |
| $\varepsilon_\Pi$ | Constant temperature term in the direct test (Van Ness, 1995); defined by equation (3.68) |
| $\varepsilon_{\Pi P}$ | Constant in the Peng-Robinson (1976) equation of state |
| $\varepsilon_T$ | Constant pressure term in the direct test (Van Ness, 1995); defined by equation (3.69) |
| $\Phi$ | Ratio of fugacity coefficients, with the Poynting correction factor |
| $\phi$ | Fugacity coefficient |
| $\hat{\phi}$ | Fugacity coefficient in solution |
| $\phi^*$ | True species fugacity coefficient |
| $\Gamma_i$ | Temperature dependent constant of integration |
| $\gamma$ | Activity coefficient |
| $\eta$ | Solvation (unlike species) and association (pure species) parameters |
| $\kappa$ | Characteristic constant in Stryjek and Vera (1986) alpha correlation in Peng- Robinson |
| $\mu$ | Dipole moment [debye] |
| $\mu_i$ | Chemical potential of component i |
| $\mu_i^m$ | Molecular dipole |
| $\rho$ | Density [kg/m$^3$ or mol/cm$^3$] |
| $\sigma$ | Constant in the Peng-Robinson (1976) equation of state |
| $\tau_{12}$ | Parameter in the NRTL (1968) model |
| $\tau_{21}$ | Parameter in the NRTL (1968) model |
| $\omega$ | Acentric factor |

## Subscript

| | |
|---|---|
| 1 | Denotes component 1 |
| 2 | Denotes component 2 |
| Ant | Denotes the Antoine equation |
| avg | Denotes an average value |
| b | Denotes the boiling point |
| c | Denotes a critical property |
| calc | Denotes a calculated value |
| exp | Denotes an experimental value |
| i | Denotes component i |
| lit | Denotes a literature value |
| m | Denotes a mixture property |
| r | Denotes a reduced property |
| Wagner | Denotes Wagner equation |

## Superscript

| | |
|---|---|
| D | Denotes the "dimerized" contribution to the second virial coefficient in the Hayden and O'Connell method (1975) |
| E | Denotes an excess property |
| Exp | Denotes an experimental value in the direct test of thermodynamic consistency (Van Ness, 1995) |
| F | Denotes the "free" contribution to the second virial coefficient in the Hayden and O'Connell method (1975) |
| id | Denotes an ideal solution |
| ig | Denotes an ideal gas |
| l | Denotes the liquid phase |
| sat | Denotes a saturated value |
| v | Denotes the vapour phase |
| ∞ | Denotes the infinite pressure value |

CHAPTER
1

# INTRODUCTION

Distillation is still the most widely used separation process in the chemical and petrochemical industry. The basis of distillation is phase equilibrium, specifically, vapour-liquid equilibrium (VLE) and in some cases vapour-liquid-liquid equilibrium (VLLE). It can effect a separation among chemical components only if the compositions of the vapour and liquid phases that are in phase equilibrium with each other are different.

The designing of separation processes requires a knowledge of the behaviour of vapour-liquid equilibrium, which is also frequently used in distillation and reactor design. However, there is much difficulty experienced in the experimental measurement of a VLE dataset. Hence, estimation methods have proven to be valuable tools for the chemical engineer in the preliminary stage of design, but there is still a need for VLE measurements, especially for non-ideal systems. However, for the final design of a distillation column, accurate information based on experiments is essential, due to the considerable capital investment of the chemical production facilities. Further development of estimation methods, however requires more VLE data to be published. For successful modeling, accurate physical properties must be provided at conditions of practical interest (Schad, 1998 and Carlson, 1996). Lack or inadequate knowledge of the physical properties can severely reduce the accuracy of process simulations (Turton et al. 1998). This is because the physical properties in a process can vary greatly from component to component. Hence, different types of apparatus may be required in VLE measurements as determined by the physical properties of the components in the systems being measured.

## 1.1 BACKGROUND TO THE RESEARCH PROBLEM

This project, which requires the measurement of phase equilibrium data for some oxygenated hydrocarbon systems, namely carboxylic acid and alcohol systems that are of importance in processes that SASOL are developing. The Thermodynamic Research Unit at the School of Chemical Engineering has undertaken some previous phase equilibrium measurements involving carboxylic acids binary systems. Sewnarain (2002) measured butyric acid and valeric acid at isobaric conditions, Hlengwere measured isobutyric (1) + hexanoic acid (2) at 20 kPa, 408.15 and 423.15 K, valeric (1) + hexanoic acid (2) at 15 kPa, 423.15 and 433.15 K. Clifford (2003) measured propanoic (1) + valeric acid (2), as well as isobutyric (1) + valeric acid (2) binary systems at isobaric and isothermal conditions. Pillay (2009) measured 1-propanol (1) + butyric acid (2) at 333.15 and 353.15 K. All the carboxylic acids systems measured to date employed a dynamic glass VLE apparatus originally designed by Raal *(*Raal and Mühlbauer, 1998) and modified by Joseph (2001), except for Clifford (2003) who set up a similar VLE glass apparatus to that of Joseph (2001). However, for this project, a novel VLE measurement apparatus designed by Reddy (2006) was employed. The glass VLE apparatus, which was setup by Clifford (2003) as mentioned earlier, was also used for the low-pressure measurements.

Hence, this work is a continuation of the investigation into a stream consisting of the following components (Table 1.1).

| | **Non- Acid Chemicals** |
|---|---|
| 1 | Ethanal - Acetaldehyde |
| 2 | Propanal |
| 3 | 2-Propanone - Acetone |
| 4 | 2-butanone - MEK |
| 5 | Methanol |
| 6 | Ethanol |
| 7 | 1-propanol (n-propanol) |
| 8 | 2-propanol (iso-propanol) |
| 9 | 1-Butanol (n-butanol) |
| 10 | 2-Butanol |
| 11 | 2-Me-1-Propanol ( iso butanol) |
| | **Organic Acids** |
| 12 | $CH_3COOH$ (ethanoic/acetic) |
| 13 | $C_2H_5COOH$ (propanoic/propionic) |
| 14 | $C_3H_7COOH$ (Butanoic/Butyric) |

**Table 1.1: Components in the industrial stream of interest considered for VLE measurements in this study**

A survey of literature was made to determine the VLE data that have been measured for binary and ternary combinations of some of the components tabulated in Table 1.1. The review showed fifteen unmeasured binary systems. Seven out of the fifteen unmeasured systems consisted of ethanal and five of propanal binary systems. It was found that ethanal boils at room temperature making it difficult for measurements on the recirculating dynamic apparatus, which was used for the project, and impossible for the glass still as the measurement would have had to be at pressures as high as 4 to 5 bar, due to temperature difference with the acids. A similar experience came in an attempt to separate the propanal from the carboxylic acid. This lead to the choice of systems eventually measured in the project for which no previous data was available.

## 1.2 OBJECTIVE OF THE STUDY

In this project, a novel VLE measurement apparatus designed by Reddy (2006) was used along with the glass VLE still of Raal (Raal and Mühlbauer, 1998) for measuring the relevant systems in the modeling and design of oxygenate and isooctane technologies.

The project involves:

(a) Setting up and testing suitable apparatus.

(b) Measuring the binary vapour-liquid equilibria (VLE) data for the components.
A survey of the literature was made to determine the VLE data that have been measured for binary and ternary combinations of the components provided in Table 1.1. Thereafter by carefully screening the unmeasured binary combinations by taking into consideration the suitability of the apparatus available, operating conditions, etc. the following systems were deemed appropriate and necessary for measurements. All the systems were measured at three isotherms to be able to have thermodynamics parameters with temperature dependence. The vapour pressures of all the components studied was the first to be measured.

The systems and conditions at which experiments were undertaken were:

- 2-Propanol (1) + Butyric Acid (2) at 333.15, 353.15 and 373.15 K
- 2-Butanol (1) + Butyric Acid (2) at 333.15, 353.15 and 373.15 K
- 2-Methyl-1-Propanol (1) + Butyric Acid (2) at 333.15, 353.15 and 373.15 K

(c) Correlating the measured data with appropriate thermodynamic models.

## 1.3 CHEMISTRY OF CARBOXYLIC ACID AND ALCOHOL

Alcohols are examples of compounds with one or more hydrogen atoms in alkanes replaced by an -OH group while in carboxylic acids, a –COOH group replaces one of the hydrogen atom. Alcohols are generally grouped depending on the position of the -OH group on the chain of carbon atoms. Thus, alcohols are classified as primary, secondary and tertiary. The alcohols used in this project, 2-methyl-1-propanol is classified as a primary alcohol while the 2-propanol and 2-butanol are referred to as the secondary alcohols. One of the generally distinguishing factors for this classification is the ability of primary alcohol to be oxidized to aldehydes and finally the corresponding carboxylic acids, while the secondary alcohols undergo one stage of oxidation to the corresponding ketones. The tertiary alcohol does not undergo any form of oxidation.

### 1.3.1 Hydrogen bonding in Alcohols

Strong attractive forces, such as hydrogen bonding, affect the physical properties of associating compounds (Fu and Sandler, 1995). This attraction occurs between molecules of a hydrogen atom attached to very electronegative elements like fluorine, oxygen or nitrogen. Hydrogen bonds in alcohols occur between the slightly positive hydrogen atoms and lone pairs electrons on oxygen in other molecules.

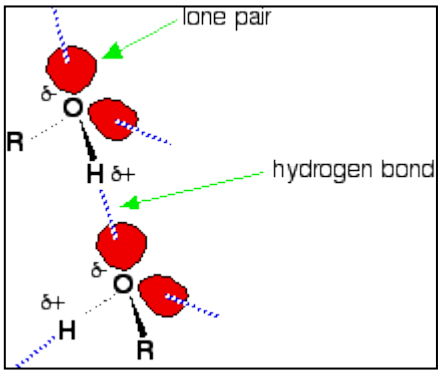


**Figure 1-1: Hydrogen bond formation in alcohols. (http://www.chemguide.co.uk/organicprops/alcohols/background.html accessed on 23 October 2009)**

These properties in alcohols explain the reason for their higher boiling point than the corresponding alkanes with van der Waals dispersion forces as the only intermolecular force. In addition to the above-mentioned properties, alcohols contain dipole-dipole interactions. Although, dipole-dipole interactions and hydrogen bonding is the same for all the alcohols, the dispersion forces will

increase as the alcohols get bigger. The latter becomes stronger as the molecules increase in length with the lone pair electrons also increasing. Hence, the boiling points of alcohol increase as the number of carbon atoms in the chains increases because more energy is needed to overcome the dispersion forces. (http://www.chemguide.co.uk/organicprops/alcohols/background.html accessed on 23 October 2009)

### 1.3.2 Solubility of Alcohols

Alcohols are completely soluble in water up to a carbon chain length of three. Thereafter, solubility decreases with an increase in the carbon chain length.

### 1.3.3 Solubility of Carboxylic acids

Carboxylic acids and alcohols are polar protic solvents. This is because of the hydrogen bond between hydrogen and oxygen. Generally, carboxylic acids are more soluble in water than their corresponding alcohol (Clifford, 2003).Thus, the first four-carbon atom components exhibit complete solubility in water. However, since a branched alkyl group results in greater solubility than a straight-chain alkyl group. The branching minimizes the contact surface of the non-polar portion of the acid. Hence, isobutyric acid is more soluble than butyric acid acids. This same principle applies for the alcohols.

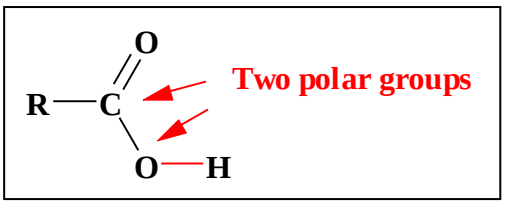


**Figure 1-2: The Polar structure of Carboxylic acids (Clifford, 2003)**

The figure above shows the polar structure of carboxylic acids. The hydrogen bond donors (the hydroxyl) and hydrogen bond acceptors (the carbonyl) both participate in hydrogen bonding and together form the functional group carboxyl.

### 1.3.4 Association in Carboxylic acids

One of the most significant properties of carboxylic acids is their acidity. Carboxylic acids are known to be both Lewis acids (i.e. donate $e^-$ pairs) and Brønsted-Lowry acids (i.e. donate $H^+$ ions).

Carboxylic acids like the alcohols form hydrogen bonds with themselves or with other molecules. This ability of carboxylic acids to form hydrogen bonds (stabilised dimers) with each other explains the reason for their higher boiling points than comparable alcohols. The two molecules can interact via a "head to tail" hydrogen bonding scheme in the vapour phase. Thus, carboxylic acids exist as dimers (pairs of molecules) or trimers and therefore require the addition of more heat for boiling than the corresponding alcohols (Sewnarain, 2002).

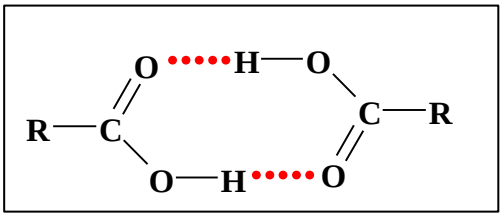

**Figure 1-3: Carboxylic acid dimer formed through double-hydrogen bonding. (Clifford, 2003)**

However, if the dimer or trimer persists in the vapour phase, the molecular weight is in effect doubled while in a case where the dimer or trimer is broken upon boiling, extra energy will be required to break the hydrogen bonds. Although, when the acids form hydrogen bonds with other polar species such as water and alcohols, only a single hydrogen bond is formed. (Sewnarain, 2002)

## 1.4 REACTIONS OF CARBOXYLIC ACID AND ALCOHOL

Although, carboxylic acids undergo different types of chemical reactions, its most useful reaction in industry is the Fischer-Esterification reaction. This reaction occurs when a carboxylic acid is heated with an alcohol in the presence of a catalyst (usually Hydrogen Chloride) and equilibrium is established with the ester and water, which is formed during the course of the reaction. This process can be used to produce esters in high yield when the equilibrium is shifted to the right since the reaction is reversible. Figure 1-4 gives the reaction mechanism for a carboxylic acid and alcohol binary mixture.

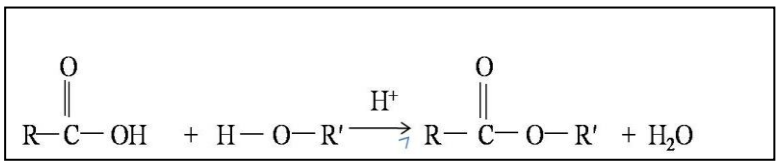

**Figure 1-4: Reaction of carboxylic acid and alcohol**

This reaction is at equilibrium. This means that significant amount of carboxylic acid and alcohol co-exist with ester and water. Hence, by controlling concentration of one of the reactants, the reaction can be pushed either way. Removal of water from the system will result in formation of more ester because the acid and alcohol react to replace water. The resulting formation of ester is called the Fischer esterification.

CHAPTER
2

# A REVIEW OF EQUIPMENT FOR VAPOUR-LIQUID EQUILIBRIUM MEASUREMENT

Generally, classification of vapour-liquid equilibrium (VLE) equipment can be based on the type of operation (static or dynamic), mode of operation (isobaric or isothermal or isopleth), operating conditions (high, moderate or low-pressure), variable measurement (P-T-x-y) and method of phase determination (analytical or synthetic) (Reddy, 2006). The distinction amongst high, medium and low-pressure VLE is of course appropriate in a relative sense (Dohrn and Brunner, 1995) as it depends on an arbitrary assignment of the lower limit.

In the phase determination using high-pressure vapour-liquid equilibrium (HPVLE) static equipment, sampling could be done using an analytical method, synthetic method or a combination of the two methods. Generally, the method of sampling equilibrium phases when using either a static or dynamic equipment in order to analyse the phases and determine their concentrations is referred to as an analytical method. Synthetic method involves preparation of mixtures of known concentration and then observing the behaviour that results from "synthesizing" fluid mixtures in a cell with sight glasses. This method therefore does not need sampling (Nagahama, 1996).

The methods for the direct measurement of VLE are classified according to Hala et al. (1967) into the following groups:

1. Distillation Methods
2. Dynamic Methods (Circulation)
3. Static Methods
4. Flow Methods
5. Dew and Bubble Point Methods

There are many comprehensive reviews of experimental methods and equipment for low pressure VLE and to a lesser extent, except in recent reviews, high-pressure VLE measurement in various literature sources as in the monographs by Hala et al. (1967), Malanowski (1982a,1982b), Deiters and Schneider (1986), Abbott (1986) and Raal and Mühlbauer (1998). In this chapter, no further discussion will be presented on HPVLE methods, as well as low-pressure vapour liquid equilibrium (LPVLE ) methods in general. Greater emphasis will be placed upon the development of dynamic recirculating type VLE stills for moderate pressures and temperature beginning with the VLE apparatus of Harris (2004) which was reviewed by Reddy (2006). The recirculation cell design was adopted in this study.

## 2.1 Dynamic (circulation) equilibrium stills

According to Marsh (1989), the development of the dynamic still type apparatus can be considered to have reached the mature stage of progress. For the dynamic equilibrium stills, the mixture is brought to boil under controlled pressure while the vapour and liquid mixture is separated in the equilibrium chamber and the vapour phase is condensed and returned to the boiling chamber. The liquid phase formed in the equilibrium chamber is also circulated. The composition of the boiling liquid and the vapour change with time until a steady state is achieved (Abbott, 1986). In addition, under dynamic methods, degassing is undertaken in-situ thereby making the process much faster in term of time taken to reach equilibrium when compared with the static method that will be discussed in the next section. In a working still, the steady state represents the true equilibrium values or, in other words, one equilibrium step. The principle of a dynamic equilibrium still is presented in Figure 2.1.

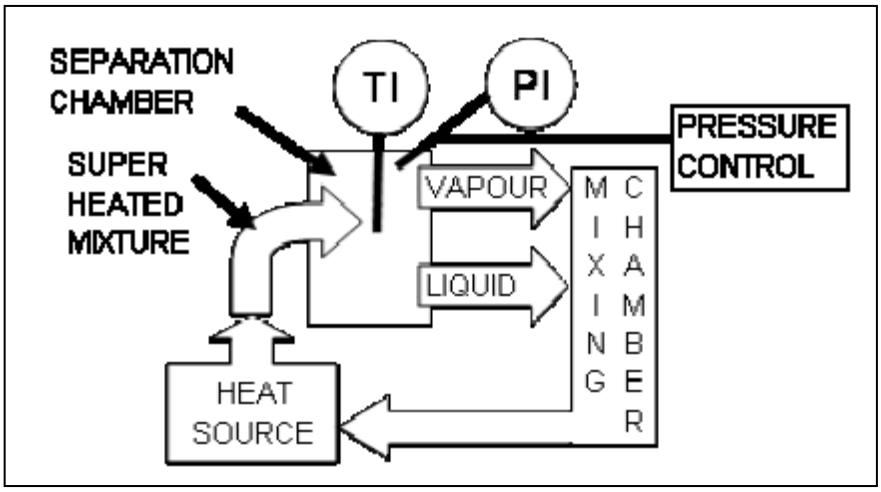


**Figure 2-1: The principle of a dynamic equilibrium still (Uusi-Kyyny, 2004).**

The automation of the dynamic still has helped immensely in the control of pressure and

temperature which are measured variables in vapour-liquid measurement. With the dynamic still, conditions are favourable for measuring one total composition at several pressures, analysing the vapour and liquid samples. The total composition in the still is generally altered by adding and/or removing the components manually; this is the easiest method. One limitation associated with the use of the automated apparatus is the possible need to adjust the heat input to the Cottrell pump.

## 2.2 Static VLE apparatus

The degassing of components is one of the important procedures in the static method. The general principles of the static method are presented in Figure 2.2.

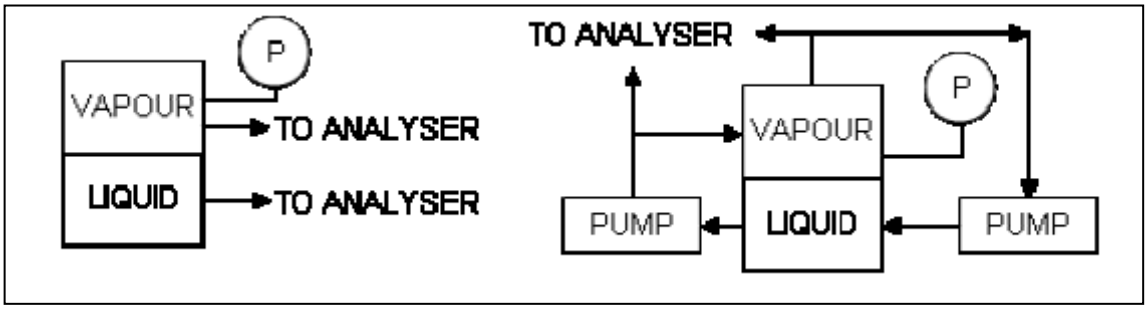


**Figure 2-2: The principles of a static VLE measurement apparatuses (Uusi-Kyyny, 2004).**

However, some limitations still faced with the use of this apparatus includes; the need to ensure that the samples analysed represent the equilibrium state due to the partial condensation of the vapour phase and the partial vaporisation of the liquid phase, during sampling and sample transfer. In addition, the time needed for producing one isotherm is longer when compared with the recirculation dynamic apparatus.

## 2.3 Static total pressure method/ Synthetic method

The static total pressure method is a fast and efficient method for determining VLE for binary mixtures with the additional advantage that the apparatus using the static total pressure method has been successfully computer-controlled (Rarey and Gmehling, 1993). Some of the disadvantages include the inability of the method to be used for measuring reactive mixtures, the problems associated with degassing of the components, the inability to perform a thermodynamic consistency check of the results and difficulty in interpretation of ternary vapour liquid-liquid-equilibrium VLLE data sets (Karre and Gaube, 1988).

## 2.4 Flow through apparatus

In the flow-through method, the system is open and two or more components are charged in a constant flow into the cell until a steady state is attained. The vapour and liquid phases are then analysed. This method is suitable for temperature-sensitive and reactive components (Reichl et al. 1998). The amount of mixture can be high which makes the analysis of the samples easier, but for expensive components, this is not a favourable feature (Nagahama, 1996). Some of the problems experienced by researchers during experimental set-ups are the difficulties with the control of the vapour-liquid interface level in the cell, as well as the component flow rates. However, one advantage of using this method is the short residence time for temperature sensitive components (Nagahama, 1996). The principle of the flow-through method is presented in Figure 2-3.

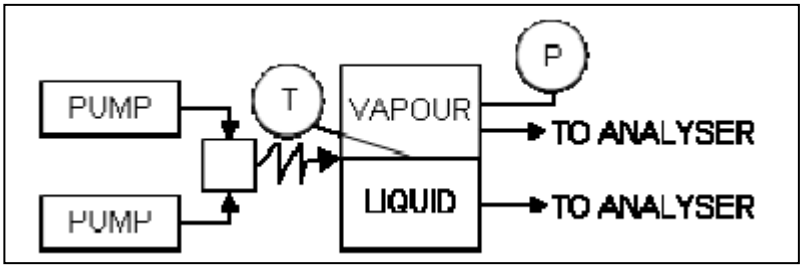


**Figure 2-3: The principle of a flow-through apparatus. (Uusi-Kyyny, 2004)**

## 2.5 Dew and bubble point measurement apparatus

According to Raal and Mühlbauer (1998) and Hala et al. (1967), the development of the latest and efficient methods for the measurement of VLE has led to the dew and bubble point methods losing favour.

However, some advantages of this method include the elimination of the need for sampling and analysis, the measurement of the densities of mixture, as well as determination of the critical point of components. Some of the disadvantages include difficulty in the observation of the dew point, the components used have to be carefully degassed (Malanowski, 1982), and the time needed for the determination of one isotherm is appreciably longer than when using the static total pressure method. For more detailed information, readers are referred to the write-up of Uusi-Kyyny (2004).

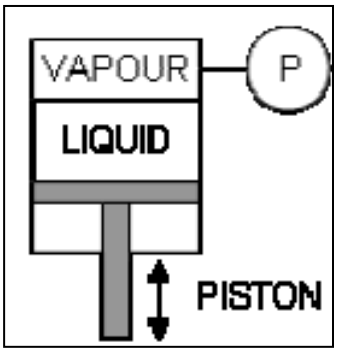


**Figure 2-4. The principle of dew and bubble point measurement method (Uusi-Kyyny , 2004).**

## 2.6 The VLE Still of Joseph et al. (2001)

The VLE still of Raal (Raal and Mühlbauer, 1998) was modified by Joseph (2001). This modified version was used and describe in detail by Joseph et al. (2001) and Sewnarain et al. (2002) to mention a few. An excellent review on the history of the circulating VLE stills in addition to this glass still is available in Raal and Mühlbauer (1998).

## 2.7 The VLE Still of Harris (2004)

The trends that have been observed with the extrapolation of LPVLE methods to elevated pressure ranges quite clearly indicate the difficulties that arise when a design of equipment for elevated pressure and temperature is proposed(Reddy, 2006). Some of the challenges often encountered include the incorporation of sight glasses due to the need for visual observation in high-pressure stills (Griswold et al., 1943). In addition, the need for a pressurizing medium such as a fixed gas results in concerns over the solubility of the gas at higher pressures due to concerns over the solubility of the gas in the system.

Therefore, the need for the measurement of high-temperature VLE in the low to moderate-pressure regions motivated the design of new VLE measurement equipment by Harris (2004) at the Thermodynamic Research Unit of the University of KwaZulu-Natal with the following objectives:

(a)The operating range with respect to temperature would be 300 - 700 K.
(b) The operating range with respect to pressure would be 1 kPa - 30 MPa.
(c) The apparatus would allow for a dual mode of operation *i.e.* both isothermal and isobaric.
(d) The time taken to reach equilibrium would be relatively short.

(e) The apparatus proposed will make provisions for the sampling of both the vapour and liquid phases.

The operation principles of the design of Raal (Raal and Mühlbauer, 1998) was the standard reference for his proposed design. The still was constructed from 316 stainless steel and designed to operate between the temperatures of 300 to 700 K and pressures between 1 kPa to 30 MPa. The details of this equipment and its design flaws has been discussed in greater detail in Chapter 4 of Reddy's thesis (Reddy 2006) as it serves as the basis for the construction of a new moderate-pressure VLE apparatus by Reddy ( 2006) which is used for this project work.

Since the equipment designed could not perform optimally as proposed, Harris (2004) recommended the following for an improved future design:

(a) The overall wall thickness and the bulk of stainless steel used for the construction of the various sections of the apparatus should be reduced in accordance with a reduced pressure capacity for the apparatus. For the design of the reboiler and the equilibrium chamber, a design was suggested to incorporate two pieces that screw into each other, to eradicate the need for flanges in the reboiler and the equilibrium chamber.
(b) It was also suggested that the Cottrell tube should be designed such that a sideways entry of the vapour-liquid mixture occurs, as in the Rogalski and Malanowski (1980) still. It was felt that this would serve to eliminate the conduction of superheat from the Cottrell tube to the equilibrium mixture.
(c) The last suggestion was that a view glass (possibly sapphire) can be incorporated into the design of the equilibrium chamber. There were no reasons provided as to what the advantages of such an arrangement would be.
Although, the only possible reason for the suggestion in (c ) might be a desire to view the phase separation taking place in the equilibrium chamber. However, the general practice is to insulate the equilibrium chamber in most of the glass VLE still used in our laboratory to prevent heat loss, which also make visualization of the equilibrium chamber impracticable. Thus, the suggestion above could be seen to be of little or insignificant value.

The general layout of the VLE apparatus of Harris, as reproduced from the thesis of Harris (2004) is shown in Figure 2.5.

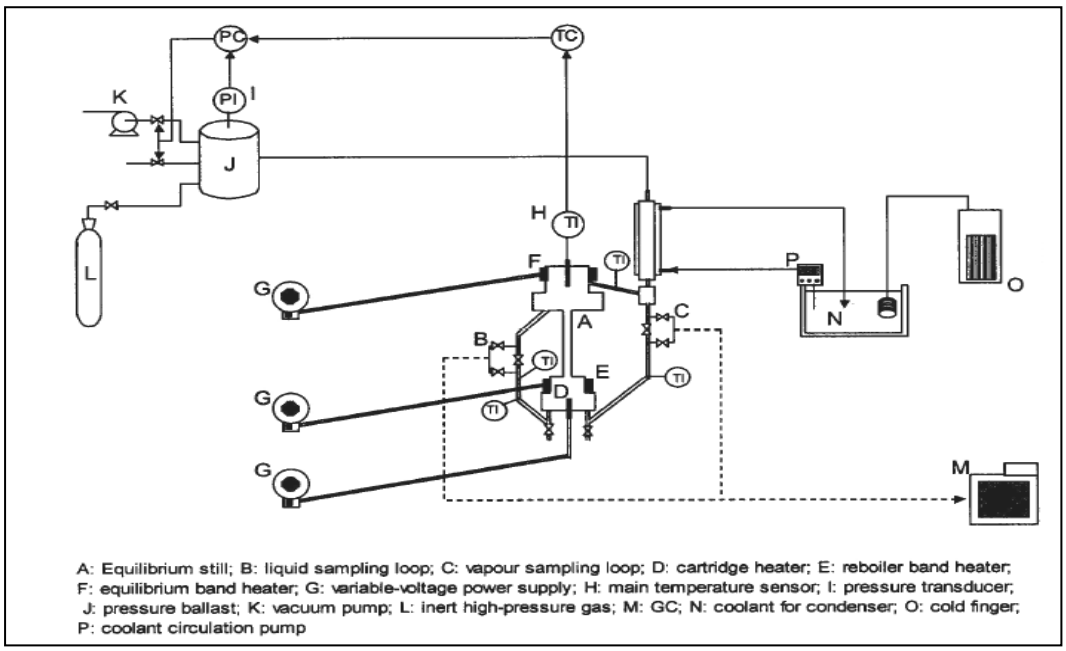


**Figure 2-5: Schematic layout of the VLE still of Harris (2004).**

## 2.8 The VLE Still of Reddy (2006)

A main feature of this design is the equilibrium chamber. The liquid is charged into a reboiler of capacity of approximately 170 ml and heat is thereafter added to the system through a varaic to bring it to boiling. An external heater is included to compensate for the heat losses to the environment.

The boiling generates a vapour-liquid mixture that is forced upward through the vacuum insulated Cottrell tube and then into the equilibrium chamber which is packed with 3 mm rolled 316 stainless-steel wire mesh cylinders in order to provide a large interfacial area that ensures significant contact between the vapour and liquid phases. This arrangement has an advantage of achieving equilibrium rapidly, even for species with a high relative volatility. The liquid flows into a liquid trap while the vapour condensate flows into the vapour trap where samples are drawn for composition analysis, with each line returning to the reboiler via a return line union where the vapour condensate sample trap equalizer tube meet with the liquid trap pressure equalizer tube .

A detailed description of this equipment constitutes Chapter 4 of the thesis of Reddy (Reddy, 2006) and hence the reader can refer for more detail to this chapter.

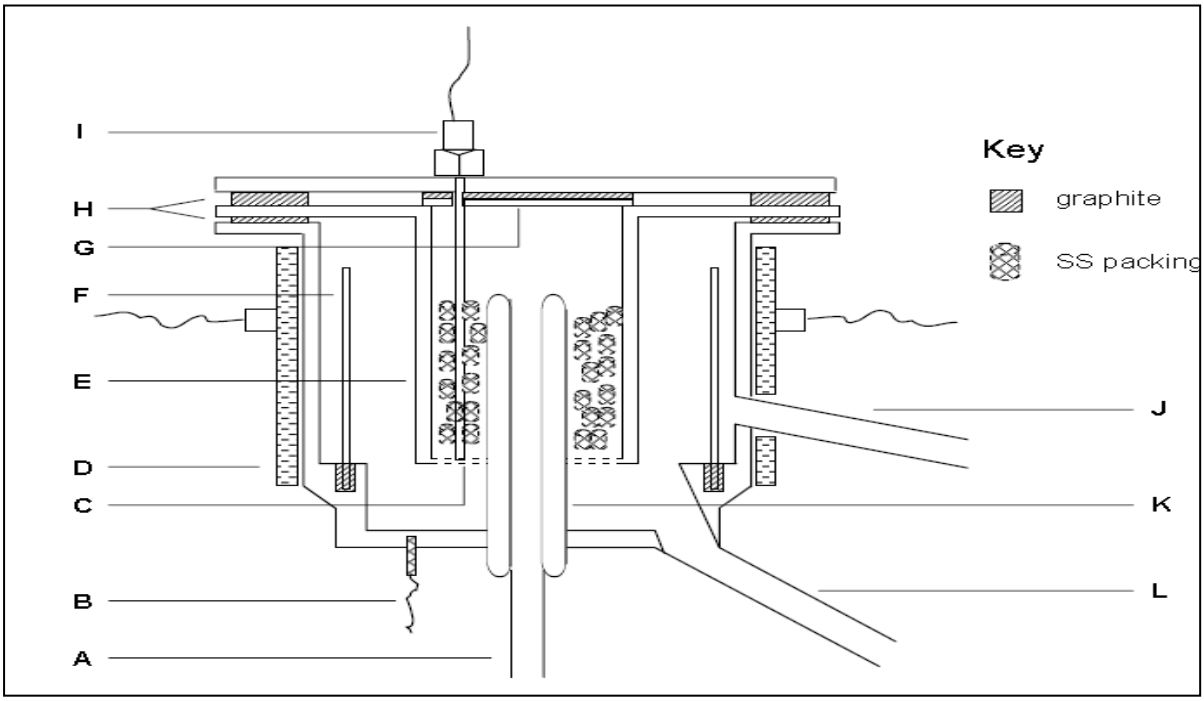


**Figure 2-6: Schematic diagram of the equilibrium chamber (Reddy 2006).**

**A, Cottrell tube; B, main body Pt-100; C, drain holes; D, split band external heater; E, packed section housing, F, thin-walled 316 SS concentric tube; G, graphite-backed 316 SS disc; H, graphite gaskets; I, packed section Pt-100 sensor, J, vapour take-off tube; K, Cottrell tube vacuum jacket; L, liquid take-off tube**

For the design of the VLE still of Reddy to be effective, a synopsis of the assessment of the principal limitations and oversights by Harris coupled with the recommendation from him led to the proposals that were formulated as listed below:

(a)The solitary valid recommendation by Harris (2004) was that of constructing a similar apparatus with much thinner walls coupled with the diminution of the operating pressure limit. As discussed above, the large heat capacity of the large bulk of stainless steel adversely affects the attainment of an internal thermal equilibrium. This produces a very poor thermal response of the VLE apparatus as a function of heat input (in determining the "plateau region") and makes the general operation of the apparatus a very time-consuming procedure (start-up procedures, equilibrium times, etc.). After an examination of trends in the field of VLE measurement for subcritical components coupled with the VLE requirements of industrial concerns, the feasible maximum operating pressure and temperature limits for the apparatus was considered as being 1 MPa and 600 K, respectively.

Also, since the idea of Harris to use the "screw-type" design for the reboiler and equilibrium chamber designs was not feasible, the use of flanges and gaskets, especially with the optimal sealing properties and resilience of graphite-based gaskets was considered as the optimal choice. The latter arrangement would facilitate the servicing (disassembly) of the equipment, as for an apparatus in its tentative developmental stages, frequent disassembly and reassembly of the

apparatus should be anticipated in the modifying of the apparatus to obtain an optimal performance (Reddy, 2006).

(b)The exclusion of any *mechanically agitation* in the design of the VLE apparatus of Harris severely compromised the quality of the data acquired due to the probable occurrence of non-equilibrium vapourization or flashing due to improper mixing of the phases in the reboiler. This of course had manifested in the temperature fluctuations (which were also contributed to by the quite large heat capacity of the large mass of 316 SS) and the erroneous vapour phase compositions.

(c) The incorporation of interior *viewable sections* in key strategic positions in a VLE apparatus facilitates the operation and monitoring of the establishment of equilibrium in the apparatus. The complete lack of any visual observation in the apparatus of Harris created a great deal of uncertainty concerning the optimal amount of material to be charged to the still to sustain the recirculation train. It also draw concern on the efficiency and continuity of the vapour-liquid mixture transported up the Cottrell tube as a function of temperature, the occurrence of any backflow in the return lines (and into the sample traps) and the general fluid flow characteristics of the system as an approach to the equilibrium condition (rate of circulation or drop count). With the necessity for the incorporation of transparent sections to aid with the above, especially for the Cottrell tube and re-designed sample traps, it was anticipated the operating pressure limit of the apparatus would be reduced (Reddy, 2006).

(d) In the design of the *sample traps*, provision was made to ensure that observation of the nature of the flow of the phases (drop count, backflow into the traps, *etc.*) is possibly coupled with magnetic stirring and appropriate sampling provisions (a septum nut and a septum). In the design of Harris (2004), the use of the sampling loops did not allow for the above and were unsatisfactory.

(e) The use of *temperature sensors* in the key sections of the apparatus, in addition to the equilibrium temperature obtained from the packed section should be employed to ensure that the thermal profile of the operational areas could be effectively monitored. The use of a temperature sensor in the reboiler would have allowed for the effective monitoring of the temperature of the reboiler contents as a function of the energy input into the internal and external heaters from the variable-voltage transformers. In this way, the onset of boiling of the mixture and hence the optimal amount of energy input to sustain boiling can be determined by monitoring the temperature of the reboiler. In this way, for an apparatus with a poor thermal response to energy input, monitoring of the reboiler temperature ensures that too much heat is not added too early to prevent the superheating of the mixture. In addition, for the equilibrium chamber, where an external heater is required for the pre-heating of the main body, the use of a temperature sensor in the latter would

be most advantageous to ensure that no excessive heating of the equilibrium chamber occurs. A strategy that has been used frequently has been to maintain the equilibrium chamber a few Kelvin above the equilibrium temperature. Pt-100 temperature sensors of the appropriate dimensions would be incorporated in the above-mentioned sections in the novel VLE apparatus to provide the advantages mentioned above. Temperature sensors would also be used in the return line, as providing feedback to the temperature controller unit, as discussed in (f) (Reddy, 2006).

(f) The design of the *return lines* in the apparatus of Harris was another serious design flaw. The vapour condensate and liquid lines should be combined into a single line a fair distance away from re-entry into the reboiler to allow for some premixing of the phases to occur.

The return line was temperature-controlled in the original design of Harris with a CN-40 digital temperature controller unit and this was incorporated into the new design, however, the design of the temperature control system would have to be to be altered. Ideally, there should be no heating of the return line near the vicinity of the sample traps, as this promotes backflow, which is also caused by excessive heating of the return lines (Reddy, 2006).

(g) The cooling of *liquid and vapour condensate streams* would be a necessary feature due to the sealing materials used in the sample traps *i.e.* Teflon® and Viton®. The sections of the liquid and vapour condensate return lines before the sample traps would be jacketed to allow for the flow of the coolant fluid (Reddy, 2006).

(h) The *pressure stabilization system* would have to be improved together with the implementation of the necessary *safety measures*. As mentioned previously, the insufficient volume of the approximately 3 litre 316 SS ballast vessel used by Harris (2004) is quite ineffective for smoothing or dampening inherent pressure fluctuations for a dynamic VLE still (Reddy, 2006).

A much larger vessel (to be used at higher pressures) with a ballast volume of at least 50 litres would be effective. Safety measures are necessary in the event of the over pressurization of the apparatus, which would be connected to a high-pressure gas cylinder for above-atmospheric operations (Reddy, 2006).

CHAPTER
3

# THERMODYNAMIC PRINCIPLES

It is a known fact that species forming hydrogen bonds often exhibit unusual thermodynamic behaviour (Kontogeorgis et al., 1996). The strong attractive interactions between molecules result in the formation of molecular clusters. These interactions may strongly affect the thermodynamic properties of the fluids. This could be observed in water where the hydrogen bonds explain why it is liquid at room temperature and atmospheric pressure instead of a gas. Therefore, it is important to take the chemical equilibria between associating molecules into account in order to develop a reliable thermodynamic model. In mixtures, hydrogen-bonding interactions may occur between molecules of the same species (self-association) or between molecules of different species (solvation or cross-association). Carboxylic acids are known to form dimers in the vapour phase at low pressures and moderate temperatures. Therefore, using an equation of state to model multicomponent systems containing carboxylic acids becomes complicated. This was observed in this project since most of the measurements were undertaken at low pressures and moderate temperatures.

## 3.1 Equilibrium and Chemical Potential

Equilibrium is defined as a state of balance. Thus it could be described that when the temperature for two systems are the same or their pressures are the same or their chemical potentials are the same, then they are in said to be in thermal, mechanical, as well as diffusive equilibrium respectively . Hence, a system is said to be at equilibrium, if in a completely isolated system, $\Delta S = 0$ or $\Delta A = 0$ at constant temperature and volume, or $\Delta G = 0$ at constant temperature and pressure. By considering the differential form of thermodynamic potentials, $\Delta S$, $\Delta A$ and $\Delta G$, which are the entropy change, Helmholtz free energy and the Gibbs free energy change respectively, can be derived.

However, a system is in equilibrium not only when there is an absence of change but also the absence of any tendency toward change on a macroscopic scale (Smith et al., 1996).

According to Smith et al. (1996), multiple phases at the same T and P are in equilibrium when the chemical potential ($\mu$) of each constituent species is the same in all phases.

For component *i*, in different phases....

$$\mu_i^{\alpha} = \mu_i^{\beta} = ..... = \mu_i^{\pi} \tag{3.10}$$

α, β and π are phases

The derivation can be found in (Smith et al., 1975; Raal and Mühlbauer, 1998; Salzman, 2004). It is important to mention the equation that relates fugacity (which will be discussed in the next section) to chemical potential (at constant temperature):

$$\mu_i = \Gamma_i(T) + RT \ln f_i \tag{3.11}$$

where $\Gamma_i(T)$ is an integration constant that is dependent on temperature only. For a species in solution, Equation (3.11) is given as:

$$\mu_i = \Gamma_i(T) + RT \ln \hat{f}_i \tag{3.12}$$

where the fugacity of a species in solution, $\hat{f}_i$, replaces the pure species fugacity in the expression for chemical potential.

## 3.2 Fugacity and Fugacity Coefficient

Gilbert N. Lewis (1908) introduced the concept of fugacity. It is a calculated property that can be related to chemical potential. This is so because the chemical potential cannot be related to measurable quantities such as T and P and thus, cannot be easily calculated from P-V-T data.

Theoretically, the condition for equilibrium between a liquid phase, l, and a vapour phase, v, at the same temperature and pressure is:

$$\hat{f}_i^{\,v} = \hat{f}_i^{\,l} \tag{3.13}$$

In the equation above, "^" denotes the mixture property.

By defining the fugacities of mixtures as a function of measurable quantities such as temperature, pressure and phase composition:

$$\hat{f}_i^{\,v} = y_i \hat{\phi}_i P \tag{3.14}$$

where P is the total pressure, $y_i$ the mole fraction and $\hat{\phi}_i$ the fugacity coefficient, which can be calculated from one of the following two equations:

$$\ln \hat{\phi}_i = -\int_{\infty}^{V} \left( \left[ \frac{\partial (nZ)}{\partial n_i} \right]_{T,V,n,n_j} - 1 \right) \frac{dV}{V} - \ln Z \tag{3.15}$$

or

$$RT \ln \hat{\phi}_i = \int_{v}^{\infty} \left( \bar{v}_i - RT / P \right) dP \tag{3.16}$$

where both ln *Z* and the derivative lying within the integral are evaluated using a suitable equation of state. This will be discussed further in Appendix B on the equation of states used in this work.

### 3.3 Activity and Activity Coefficient

Activity coefficient is described as the measure of how a specific real system deviates from some reference system that is taken to be ideal. According to Prausnitz et al. (1980), the activity coefficient is completely defined only if the standard-state fugacity is clearly specified. In an ideal mixture, the interactions between each pair of chemical species are the same and, as a result, an expression such as Raoult's law can be used for the properties of the mixtures.

The chemical potential, $\mu$, of a substance *i* in an ideal mixture is given by

$$\mu_i = \mu_i^{\theta} + RT \ln x_i \tag{3.17}$$

where $\mu^{\theta}_i$ is the chemical potential in the standard state and $x_i$ is the mole fraction of the substance in the mixture. For a non-ideal behaviour the equation can be written as:

$$\mu_i = \mu_i^{\theta} + RT \ln a_i \tag{3.18}$$

where $a_i$ is the activity of the substance in the mixture with,

$$a_i = x_i \gamma_i \tag{3.19}$$

and $\gamma_i$ is the activity coefficient. The activity coefficient is assumed unity as the mole fraction $x_i$ approaches 1, thus the substance is said to obey Raoult's law. If the activity coefficient is greater

than unity, substance *i* show positive deviation from Raoult's law and negative deviation when activity coefficient is less than unity.

This approach whereby the fugacity coefficient and the activity coefficient are respectively used to characterize non-idealities in the vapour and liquid phases is known as the combined method of VLE.

$$\hat{f}_i^V = y_i \Phi_i P = \hat{f}_i^L = x_i \gamma_i P_i^{sat} \tag{3.20}$$

$$y_i \Phi_i P = x_i \gamma_i P_i^{sat} \tag{3.21}$$

where

$$\Phi_i = \frac{\hat{\phi}_i}{\phi_i^{sat}} \exp\left[\frac{-V_i^l (P - P_i^{sat})}{RT}\right] \tag{3.22}$$

Equation (3.21) is a useful equation that generally relates the liquid and vapour phases and is the basis for a great deal of the low-pressure VLE theory. The reader is referred to the text of Walas (1985) for a comprehensive review of the many available thermodynamic models and their applications.

## 3.4 Evaluation of Fugacity and Fugacity Coefficients

Fugacity coefficient is the ratio of fugacity to pressure and it's usually set equal to one at low pressure. Hence, fugacity is assumed equal to pressure for an ideal gas. However, for systems containing associating components (as in the case for this project), authors such as Prausnitz et al. (1980) have reported a large deviations from ideal phase behaviour even at very low pressure. This has been attributed to the formation of dimers or trimers in the vapour, as well as in the liquid phase as explained earlier. Dimer formation in carboxylic acids and alcohols has been explained in Section 1.3.

The vapour phase fugacity may be expressed in terms of the fugacity coefficient:

$$\hat{f}_i^v = y_i \hat{\phi}_i P \tag{3.14}$$

while the activity coefficient is related to the liquid phase fugacity:

$$\hat{f}_i^l = x_i \gamma_i f_i \tag{3.23}$$

In literature, researchers (Tamir and Wisniak, 1975; Yoshio Iwai and Yasuhiko Arai, 2001; Wen-Tzong Liu and Chung-Sung Tan, 2002; Sewnarain et al., 2002; Clifford et al., 2003 among others) discuss the problem of vapour phase association in VLE for carboxylic acid binary mixtures. For this work, three models was employed: (1) The simplest models used were the Soave-Redlich-Kwong (1972) and Stryjek-Vera (1986) form of Peng-Robinson (1976) equation of state which account for non-ideality but assume no association in both the liquid and vapour phase . (2) A virial equation of state model (Tsonopoulos, 1974) which takes into account the non-idealities in the vapour phase in calculating the vapour phase fugacity coefficients. (3) A model (Hayden and O'Connell (1975) with Chemical theory) which accounts for association in vapour phase as well as non-ideal solution behaviour in the liquid phase as described by Prausnitz et al. (1980).

### 3.4.1 Calculating Fugacity using Virial Equation of State

The Virial Equation of State (VEOS) was introduced as a model for real gases (which generally do not obey ideal gas behaviour due to intermolecular interaction. Thus, VEOS account for the intermolecular interactions in real gases that do not obey ideal gas EOS at relatively high pressure.

In summary, the primary objectives for the implementation of VEOS therefore are:

- To account for deviation from ideality in the vapour phase, and
- To compare the EOS for its accuracy.

Hence, many generalized virial equations of state have been employed in the past to account for vapour phase imperfections. Some of which includes (Black, 1958; O'Connell and Prausnitz, 1967; Kreglewski, 1969; Nothnagel et al., 1973; Tsonopoulos, 1974; Hayden and O'Connell, 1975).

Prausnitz (1969) explains that since the accuracy of the fugacity and compressibility are about the same for the pressure-explicit and density-explicit equations truncated at the second virial coefficient, and systems are usually specified by temperature, pressure, and composition, the most convenient form of the virial equation to be used is,

$$Z = 1 + \frac{BP}{RT} \tag{3.24}$$

where Z is known as the compressibility factor and is equal to one for an ideal gas. The second virial coefficient, B, is a function of temperature and composition (for mixtures). Thus, in a mixture of *N* components

$$B = \sum_{i=1}^{N}\sum_{j=1}^{N} y_i y_j B_{ij}(T) \tag{3.25}$$

where $y$ is the mole fraction and $B_{ij}(T)$ is the second virial coefficient characterizing pair interactions between an $i$ and a $j$ molecule, and is a function of temperature only. The vapour phase fugacity is given by,

$$\hat{f}_i^{v} = y_i \hat{\phi}_i P \tag{3.14}$$

where the fugacity coefficient is given by

$$\ln \hat{\phi}_i = \left[ 2\sum_{j=1}^{N} y_j B_{ij} - B \right] \frac{P}{RT} \tag{3.26}$$

If the virial equation (truncated after 3 terms) is used to describe the mixture behaviour, then the fugacity coefficients can be calculated by:

$$\ln \hat{\phi}_i = \frac{2}{v}\sum_{j=1}^{N} y_j Bi_j + \frac{3}{v^2}\sum_{j=1}^{N}\sum_{k=1}^{N} y_j y_k C_{ijk} - \ln Z \tag{3.27}$$

where the C represent the third virial coefficient. Hence, virial coefficients for the mixture obtained are:

$$B = \sum_{i=1}^{N}\sum_{j=1}^{N} y_i y_j B_{ij} \tag{3.28}$$

$$C = \sum_{i=1}^{N}\sum_{j=1}^{N}\sum_{k=1}^{N} y_i y_j y_k C_{ijk} \tag{3.29}$$

The virial coefficients for pure substances ($B_{ii}$, $C_{iii}$, etc.) and cross coefficients ($B_{ij}$, $C_{ijk}$, etc.) can be obtained from experimental data. However, Hayden and O'Connell (1975) mentioned that for substances such as carboxylic acids, which associate very strongly, the virial equation is not valid. The "chemical theory" for nonideality can give good correlation, as well as predictions in such cases when an equilibrium constant for association is available (Nothnagel et al., 1973).

Unfortunately, equilibrium constants are not generally available for carboxylic acids in literature.

Also, finding experimental data for species of interest is often difficult; therefore, some satisfactory

correlations for the determination of the second virial coefficients have been developed. Only the Tsonopoulos correlation (1974) and the Hayden O'Connell equations with the Chemical theory will be discussed below.

### 3.4.1.1 The Tsonopoulos Correlation

The Tsonopoulos (1974) correlation, which was one of the correlation models used in this project, is regarded as an extended Pitzer and Curl (1957) correlation and is effective in calculating virial coefficients for both polar and non-polar compounds. Although, the method of Tsonopoulos for estimating virial coefficients is usually recommended for hydrocarbon mixtures at low pressures, it can also be applied in the correlation of associated fluids just like O'Connell and Prausnitz (1967), Hayden and O'Connell (1975), Lee and Chen (1998) and Iglesias-Silva and Hall (2001). For non-polar gases, the equation takes the form:

$$\frac{BP_c}{RT_c} = f^{(0)}(T_r) + \omega f^{(1)}(T_r) \tag{3.30}$$

For the polar systems, the form is:

$$\frac{BP_c}{RT_c} = f^{(0)}(T_r) + \omega f^{(1)}(T_r) + f^{(2)}(T_r) \tag{3.31}$$

where

$$f^{(0)}(T_r) = 0.1445 - \frac{0.330}{T_r} - \frac{0.1385}{T_r^2} - \frac{0.0121}{T_r^3} - \frac{0.000607}{T_r^8} \tag{3.32}$$

and

$$f^{(1)}(T_r) = 0.0637 + \frac{0.331}{T_r^2} - \frac{0.423}{T_r^3} - \frac{0.008}{T_r^8} \tag{3.33}$$

$$f^{(2)}(T_r) = \frac{a'}{T_r^6} \tag{3.34}$$

where $P_c$ and $T_c$ are the critical pressure and temperature, R = 8.314471 $Jmol^{-1}K^{-1}$ is the universal gas constant, B is the second virial coefficient, $T_r$ is the reduced temperature. $f^{(1)}$ is referred to as the nonpolar term while $f^{(2)}$ is a term that accounts for the polar effects and takes an additional

parameter to account for hydrogen bonding effect when a compounds such as C2+ straight-chain 1-alkanols is involved in the expression;

$$f^{(2)}(T_r) = \frac{a'}{T_r^6} - \frac{b'}{T_r^8} \tag{3.35}$$

The parameters *a´* and *b´* are functions of the dipole moment and differ for different compounds. They are obtained by fitting Equations (3.34) and (3.35) to experimental second virial coefficient (*B)* data.

Tsonopoulos uses a similar mixing rule to those given by Pitzer and Curl correlation (1957) for $T_{cij}$ and $\omega_{ij}$ but differ for $P_{cij}$ which are referred to as cross coefficient parameters. Hence, for calculating these parameters, the equations are given:

$$\omega_{ij} = \frac{\omega_i + \omega_j}{2} \tag{3.36}$$

$$T_{cij} = \sqrt{(T_{ci}T_{cj})}(1-k_{ij}) \tag{3.37}$$

$$P_{cij} = \frac{4T_{cij}(P_{ci}V_{ci}/T_{ci} + P_{cj}V_{cj}/T_{cj})}{(V_{ci}^{1/3} + V_{cj}^{1/3})^3} \tag{3.38}$$

For binary mixtures of polar/non-polar, $a_{ij}$ and $b_{ij}$ are set equal to zero (i.e. it is assumed that $B_{ij}$ has no polar term). For binary mixtures of polar/polar, $B_{ij}$ is determined by assuming that the polar term of $B_{ij}$ can be found using $a_{ij} = 0.5(a_i + a_j)$ and $b_{ij} = 0.5(b_i + b_j)$.

Meng and Duan (2007) proposed a new method, a modification of the Tsonopoulos correlation for the second virial coefficients of associated fluids since the $f^{(2)}$ term in equation (3.35) was initially introduced based on an assumption that separate the polar contributions to B from the associated contributions of associating fluids. Thus, they modified the $f^{(2)}$ term to correct the polar as well as the associated contributions.

Meng and Duan (2007), reported the second virial coefficient for 10 alcohols (out of which the three used in this project were included) using the proposed method. The result was compared to the work of Iglesias-Silva and Hall (2001) on alcohols. Both Meng and Duan (2007) and Iglesias-Silva and Hall (2001) correlation were found to give a closer average absolute deviation value for

the 2-propanol and 2-butanol and a much better average absolute deviation value for methanol. However, since methanol was not included in the systems for this project, and the deviations reported in literature using the extended form of Meng and Duan (2007), as well as Iglesias-Silva and Hall (2001) were roughly equal for the polar compounds, it was not necessary to use the model in this work. Hence, only the chemical theory approach was employed to improve the correlations for 2-propanol and 2-butanol. The proposed extended correlation model for second virial coefficient for associating fluids is in Meng and Duan (2007). Therefore, it will not be discussed beyond the comparison made above.

### 3.4.1.2 The Hayden and O'Connell Correlation

A generalized correlation method was proposed by Hayden and O' Connell (1975) for determining the second virial coefficients for simple and complex systems containing polar, non-polar and associating molecules. This method was developed using a corresponding-states formulation of the contributions of various intermolecular forces between pairs of molecules. Thus, it does not offer the simplicity of the Pitzer-type correlations.

However, it is an accurate predictive method that requires only the input properties such as the components critical temperature and pressure, the molecular parameters (i.e. radius of gyration $R_d$ , and dipole moment $m\mu$) that may be estimated from the molecular structure. It sometimes includes an empirical parameter (η) for association between like species or solvation between unlike species. As the method consists of many equations, only the most relevant part of the equation will be discussed in this work. The reader is referred to the publication of Hayden and O' Connell (1975) for further details.

The total second Virial coefficient is considered to be a sum of several contributions:

$$B_{total} = B_{free} + B_{metastable} + B_{bound} + B_{chem} \qquad (3.39)$$

where $B_{free}$ represents the molecular volumes, $B_{metastable} + B_{bound}$ results from the potential energy from more or less strongly-bound pairs of molecules and $B_{chem}$ results from associating substances. The calculation procedure is complex and will not be detailed here. It is however available in Appendix A of Prausnitz et al. (1980).

The critical parameters of most compounds can be obtained from literature for example in Reid et al. (1988), Frendenslund et al. (1977) and the Dortmund Data Bank (DDB, 2009). When there are no experimental values, the Lydersen group contribution method outlined in Reid et al. (1988) as well as a GC method for critical properties (Nannoolal et al. 2007) can be used. Dipole moments are available in McClellan (1974) and can be determined by the method of Smyth (1955). The mean

radius of gyration $R_d$ may be obtained from the parachor P' by the following equation (Hayden and O'Connell, 1975):

$$R_d = -0.2764 + 0.2697\sqrt{P' - 48.95} \tag{3.40}$$

while Harlacher and Braun (1970) gives an expression to describe the relationship between the parachor and the mean radius of gyration:

$$P' = 50 + 7.6R_d + 13.75R_d^2 \tag{3.41}$$

According to Fredenslund et al. (1977) the solvation and association parameters are the most difficult to estimate because they must be determined empirically. Therefore, for interaction between components in a mixture, Hayden and O'Connell (1975) suggest that the association and solvation parameters $\eta$, should be set equal to zero unless the species are in the same group or a special solvation contribution could be justified and empirically determined for each pair of groups. However, association and solvation parameters were found from the tables given by Prausnitz et al. (1980). Prausnitz et al. (1980) suggested that if the exact system in question cannot be found in the tables, then the values for a chemically similar system should be taken. Hence, the values given for the propionic acid and acetic acid system were used for the butyric acids since they belong to the same group of organic acids.

### 3.4.2 Calculating Fugacity Coefficients using an Equation of State

Equation of state is a relation between state variables (Perrot, 1998). It can be use to evaluate fugacity. For vapour-liquid equilibrium, the fugacity of the liquid is equal to the fugacity of the vapour for each phase. Typically, equation of state is used to calculate the fugacity of the vapour phase. The fugacity of the liquid can be calculated either with an equation of state or with activity coefficient model.

The origins of the $\Phi_i$ - $\Phi_i$ **(direct)** approach were largely as a result of a need to overcome the limitations associated with the $\gamma_i$ - $\Phi_i$ **(combined)** method in the treatment of supercritical components (where a standard-state fugacity would be required for the supercritical liquid) and to effectively maximize the advantages of a unified approach in facilitating phase equilibrium computations. In contrast to the $\gamma_i$ - $\Phi_i$ approach, the $\Phi_i$ - $\Phi_i$ approach, allows for the use of the same auxiliary function in the form of $\Phi_i$ for the representation of the real thermodynamic behaviour of both the liquid and vapour phases in a mixture through the use of an equation of state with reliable mixing rules.

The equations for calculating fugacity in an EOS are described by equation 3.13 and 3.14.The fugacity coefficients in equation 3.14 and 3.21 are determined from a suitable EOS together with appropriate mixing rules that allow for the extension of the pure component form of the EOS to mixtures applicable to both phases using the thermodynamic relationships in equation 3.15.

The phase equilibrium ratio is given in the form below as:

$$K_i = \frac{y_i}{x_i} = \frac{\hat{\phi}_i^l}{\hat{\phi}_i^v} \tag{3.42}$$

In this project, the Soave-Redlich-Kwong (SRK) and Peng-Robinson Stryjek-Vera (PRSV) equation of state were employed for calculating the vapour phase fugacity coefficient. However, they have been presented in Appendix B with the related equations.

## 3.5 Evaluation of Activity Coefficients

For isothermal experimentation, $x_i$, $y_i$ and P values are recorded and temperature (T) is set. The fugacity coefficient is calculated as detailed in Section 3.5.2 and the $P_i^{sat}$ values can be calculated using the common Antoine equation for vapour pressure. Using these values in equation 3.21, the activity coefficient can be calculated. Different models have been developed to account for the effect of the nonideal behaviour of a liquid solution containing hydrogen bonding on the activity coefficient. These include the Margules, Van Laar, Wilson, T-K Wilson, NRTL, and UNIQUAC amongst others. For a detailed review of each of these models, the reader is referred to the texts of Walas (1995), Raal and Mühlbauer (1998). In this project, only the NRTL excess free energy model was used primarily because the NRTL model is a flexible local composition model that can be used for the correlation of $\gamma_i$, and for representing complex VLE behaviours in multicomponent systems. Also, the work of Liu and Tan (2002) amongst others reveals that the NRTL model gave a lower average absolute deviation than the Wilson and UNIQUAC for the carboxylic-ester system measured. This is in addition to the fact that the systems measured in this study have some complexities in modeling and the additional non-random parameter is viewed as a possible improvement to the result. Hence, only the NRTL will be discussed with a comparison of the $G^E$ models thereafter.

### 3.5.1 The NRTL (Non-Random Two Liquid) Equation

Renon and Prausnitz (1968) first published the Non-Random Two Liquid (NRTL) model seen to represents an improvement over that of Wilson. Raal and Mühlbauer (1998) assert that the NRTL

equation is particularly suitable for highly non-ideal systems and is readily generalized to multicomponent systems. This model can therefore be referred to as an improved local composition model, which, unlike the Wilson equation is applicable to both partially miscible and completely miscible systems and has an additional term to account for the non-randomness in the solution.

For a binary mixture, the equations for the activity coefficients (Reid et al., 1988) are used:

$$\ln \gamma_1 = x_2^2 \left[ \tau_{21} \left( \frac{G_{21}}{x_1 + x_2 G_{21}} \right)^2 + \frac{G_{12}\tau_{12}}{(x_2 + x_1 G_{12})^2} \right] \tag{3.43}$$

$$\ln \gamma_2 = x_1^2 \left[ \tau_{12} \left( \frac{G_{12}}{x_2 + x_1 G_{12}} \right)^2 + \frac{G_{21}\tau_{21}}{(x_1 + x_2 G_{21})^2} \right] \tag{3.44}$$

where

$$G_{12} = \exp(-\alpha_{12}\tau_{12}) \tag{3.45}$$

$$G_{21} = \exp(-\alpha_{21}\tau_{21}) \tag{3.46}$$

$$\tau_{ij} = \frac{g_{ij} - g_{jj}}{RT} \tag{3.47}$$

$\tau_{12}$, $\tau_{21}$ as well as $\alpha_{12} = \alpha_{21}$ are parameters, R is the gas constant and T the absolute temperature.

According to Walas (1985) the $g_{ij}$-$g_{ii}$ parameters represent the interaction between species *i* and *j*, while the $\alpha_{12}$ parameter represents the non-randomness of the solution. Since it is believed that activity coefficients are relatively insensitive to values of $\alpha_{12}$ between -1 and 0.5, an arbitrary value is often assigned within this range. However, this parameter is adjustable and can be regressed. In addition, $\tau_{12}$ and $\tau_{21}$ are dimensionless adjustable interaction parameters, which can be expressed as a function of interaction energy parameters $\Delta g_{ij}$ as shown by equation 3.47.

The temperature dependence parameter can be introduced when VLE data are available over a wide temperature range. This is expressed in any of the forms;

$$\tau_{ij} = f(T) = a_{ij} + \frac{b_{ij}}{T} + c_{ij} \ln T + d_{ij} T \tag{3.48}$$

$$\Delta g_{ij} = f(T) = a_{ij} + b_{ij}.T + c_{ij}T^2 \tag{3.49}$$

where the format:

$$a_{ij} + \frac{b_{ij}}{T} + c_{ij} \ln T + d_{ij}T \tag{3.50}$$

is taken from the extended Antoine equation, which is also used for saturated vapour pressures.

### 3.5.2 Comparison of the $G^E$ Models

Since only the NRTL excess Gibbs free energy model was used and discussed in this project, it would be useful to present a conclusive evaluation of the efficiency and applicability of some of the common $G^E$ models.

It is important to note that the preference of one model over another is not only dictated by the fit of the experimental data to the model, but is also in practical terms influenced by the computational and mathematical aspects of the implementation of the model. In general, the models contain two or three adjustable parameters and an increase in the number of parameters gives a better fit to the data. Hence, the performance of one model over the other is often not predictable and is often obtained through a "trial and error" approach in terms of the criteria defined above.

Many researchers have attempted to compare the correlating efficiency of the more popular activity coefficient models, as observed in the works of Walas (1985), Reid et al. (1988), Gess et al. (1991) and Malanowski and Anderko (1992). Some of the findings can be summarized below as follows:

(a) The empirical models in the form of *the Margules, Van Laar and related equations* have the advantage of simplicity in their algebraic form and ease of computational and mathematical evaluation of the adjustable parameters from the experimental data. In addition, these models often surprisingly exhibit excellent correlations of experimental data obtained for fairly nonideal mixtures (including partially miscible systems), which are comparable or superior to semi theoretical models. An example of the latter can be found in the work of Chamorro et al. (2004), where those systems exhibiting moderate positive deviations were investigated. The inherent disadvantages of this approach, as mentioned previously, are that the evaluated parameters have no theoretical significance or a temperature dependence (which is crucial for the simultaneous description of $G^E$ and $H^E$) and are limited to binary systems (except for the Wohl expansion).

In terms of the computational implementation of the models, the Margules and van Laar expressions are fairly well-behaved and convergence is achieved without the need for a large number of iterations, with only the van Laar equation being slightly sensitive to the initial parameter estimates (Gess et al., 1991).

(b)The original "local composition" model *i.e. the Wilson equation* is able to correlate the vapour-liquid equilibrium of binary and multicomponent homogenous mixtures with great accuracy with only two binary parameters. With its greater simplicity when compared to the NRTL and UNIQUAC equations, it is quite clearly the most favourable amongst the local composition models for the above application. It is indeed highly recommended for strongly nonideal binary mixtures such as alcohol + hydrocarbon mixtures (Reid et al., 1987; Palmer, 1987). For the treatment of partially miscible systems, the use of the empirically-modified Wilson equation is undesirable (Reddy, 2006).

The T-K Wilson equation is more suitable for handling systems that exhibit partial miscibility, although not being directly applicable to liquid-liquid equilibria and not being widely tested as the other multicomponent models. Models such as those by Huang and Lee (1994) are directly applicable to ternary liquid-liquid equilibria, but have also not been widely tested for flexibility.(Reddy, 2006)

(c) The *NRTL equation* is recommended in many instances for the representation of vapour-liquid and liquid-liquid equilibria and in particular, is frequently superior to the other equations in representing aqueous systems. It is simpler in algebraic form than the UNIQUAC equation; however, it is a three-parameter model suffering from an increased interdependence of the three parameters. The arbitrary assignment of values to the non-randomness parameter can present many problems and can indeed affect the accuracy of the correlation (Reddy, 2006).

(d) The *UNIQUAC equation* is applicable to multicomponent vapour-liquid and liquid-liquid equilibria, just as the NRTL equation; however, the model uses only two parameters per binary interaction. It is particularly recommended for molecules with widely differing sizes and for highly nonideal systems since it incorporates actual molecular parameters such as molecular surface areas and volumes in its formulation. The UNIQUAC equation has also shown to be more readily applicable to mixtures with macromolecules such as polymers since the surface areas available for interaction *i.e.* surface fraction (as opposed to mole fractions) are the primary concentration variable (Reid et al., 1988). It is undoubtedly the most complex commonly encountered $G^E$ equation and some of the simpler empirical and semi-theoretical models when treating moderately nonideal systems (Reddy, 2006) surprisingly outperform it on some occasions.

## 3.6 Models Developed for Associating Systems

A large number of EOS's have been proposed in literatures that take into account association. Most recently developed models for associating fluids have been divided into three different categories using the principles behind model development, as well as the method employed for accounting for the extent of hydrogen bonding.

(I) Chemical theory (Heidemann and Prausnitz, 1976; Ikonomou and Donohue, 1988; Anderko, 1989a,b)

(II) Perturbation theory (Chapman et al., 1990; Huang and Radosz, 1990)

(III) Lattice/quasi-chemical theory (Panayiotou and Sanchez, 1991).

However, literature review has shown that there is yet no known model that has been developed to accurately and effectively describe the carboxylic acid and alcohol binary mixtures. As a summary of his review on the modeling of mixtures containing self-associating compounds, Scatchard (1949) concluded, "The best advice which comes from years of study of liquid mixtures is to use any model in so far as it helps, but not to believe that any moderately simple model corresponds very closely to any real mixture." (Apelblat, 2006)

Although, some work has been done and modelled for the binary mixture of carboxylic acids using the chemical theory as well as the Statistical Associating Fluid Theory (SAFT), these models still exhibit limitations when it comes to carboxylic acid-alcohol mixtures especially when the alcohols are of the ($C_3$ and higher). According to Prausnitz et al. (1980), two acid molecules have a tendency to dimerize through the formation of two stable hydrogen bonds and this may transpire even at very low pressures. Hence, modeling the binary mixtures involving associating components capable of hydrogen bonding such as alcohols remains an unsolved problem since such systems show extremely nonideal behaviour. This fact that mixtures containing self-associating compounds show strong deviations from ideal behaviour has been recognized for a long time.

Scatchard (1949) classified the associated solutions into three groups.

(1)The acid-type association: this occurs when substances have only one spot of special reactivity in each molecule (Apelblat, 2006). In this case, formation of dimers of both components and the one-to-one compound are expected, but probability of more complicated complexes is neglected since each type of molecule is assumed to have a single reactivity group. This idea supports the 1-A scheme by Huang and Radosz (1990) which allows for only one association site per molecule for acid-acid modeling in the perturbation theory. This theory is also in line with the chemical theory of dimerization of carboxylic acids.

Although, small acids like acetic acids have been known to form cyclic dimers in the vapour phase, investigations of pure-component properties of different carboxylic acids (from formic acid up to decanoic acid) showed that using a one-site association scheme gives an improved representation of liquid-density data and vapour pressure data **(**Kleiner et al., 2008).

Hence, by comparing the result of a 2-B scheme to a 1-A scheme for acids, it was seen that the effect of cross-associating interactions is of a minor influence on the phase behaviour modeling.

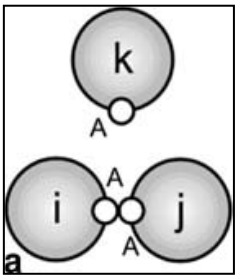


**Figure 3-1: Site-site interactions assumed by for the 1-A association scheme as suggested by Huang and Radosz (1990).**

(2)The alcohol-type association: This includes substances with two active spots on each molecule. Thus, the formation of linear chains of any length is permitted. Scatchard (1949) extended the Redlich–Kister (1947) results by taking into account deviations from the ideal behaviour resulting from different sizes of the formed associated molecules. This idea is similar to the more recent assumption of Huang and Radosz (1990) for a 2-B Scheme and Gross and Sadowski (2002) using the different association sites: a donor site at the oxygen and an acceptor site at the OH-group. Hence, figure 3.2 shows the site assumption of Huang and Radosz (1990) which was equally adopted by Gross and Sadowki (2002) for the PCSAFT model.

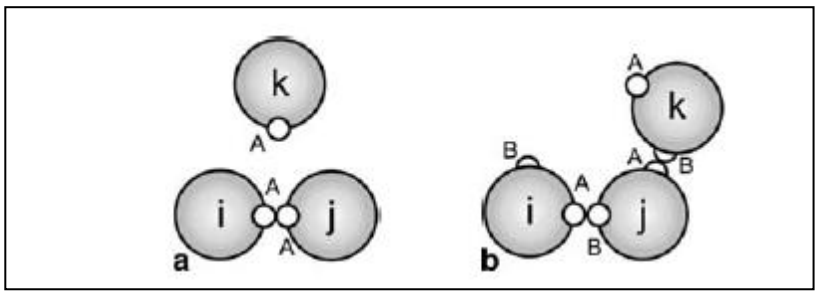


**Figure 3-2: Site-site interactions assumed for the 2-B association scheme as suggested by Huang and Radosz (1990).**

(3)The water-type association: This refers to compounds that permit the formation of a three-dimensional polymer structure due to the presence of four active spots on each molecule. Hence, the likes of Fu and Sandler, 1995, and Gross and Sadowski, 2002 adopted a 3-B or 4C association scheme for modeling.

However, attempt at accounting for the associating behaviour of alcohols in thermodynamic modeling was first made by Kretschmer and Wiebe (1954). He regarded an alcohol as a mixture of linear clusters in chemical equilibrium and attempt to explain the deviation from ideal behaviour in a mixture of these clusters and an inert compound using the combinatorial part of the Flory-Huggins model. (Apelblat, 2007)

Other researchers have made many attempts in their quest to describe the vapour-liquid equilibria (VLE) of alcohol-containing mixtures using the concept of multiscale association (Brandani and Evangelista, 1987). Theoretically- based approaches such as UNIFAC-Dortmund (Gmehling et al., 1993) group-contribution methods, NRTL and UNIQUAC activity coefficient models (Prausnitz et al., 1980) have been used. Kamlet et al.(1988) and Marcus (1991) have equally applied a generalized solvatochromic approach with linear solvation energy relationship (LSER) , and Peng-Robinson and Redlich-Kwong-Soave cubic equations of state (EOS) derived from molecular-statistical theory, have been applied. For in-depth understanding of the history of associating models, readers are referred to Apelblat (2007).

However, it is also important to mention amongst many others the Cubic Plus Association equation of state (CPA) of Kontogeorgis et al. (1996), as well as the Group Contribution with Association equation of state (GCA) by Gros and co-workers (Gros et al., 1996). The quantitative estimation of VLE behaviour of associating systems using group contribution methods has been quite helpful. However, the strong local composition effects caused by hydrogen bonding and dipole-dipole interactions are not accounted for explicitly in the models.

In summary, there is still on-going work on the development of a model to perfectly describe the associating mixtures with carboxylic acids. Hence, the PCSAFT (in the family of the Perturbation theory), the CPA, as well as the GCA (for the group-contribution purpose) will be briefly discussed. For more details, the reader is referred to the published journal articles (Chapman et. al, 1990; Kontogeorgis et al., 1996; Kontogeorgis et al., 2006; Browarzik, 2007; Ferreira et al. 2003, 2004; Sadowski and Gross, 2001, 2002).

### 3.6.1 Literature Basis for the model used in this project

The nonideality of the vapour and liquid phases is often expressed in terms of the ideal associated solution models (Apelblat, 2007). However, by analyzing the equilibrium relationship in binary systems that form dimers in both phases, Marek and Standart (1954, 1955) were able to establish that the use of a model that assume no association will lead to thermodynamically inconsistent results in mixtures such as carboxylic acids. Hence, an expression was derived to explicitly

describe the effect of dimerization in the vapour and liquid phases. This expression relates the association factors in terms of the composition, equilibrium constants and total pressure. These methods have been adopted by researchers such as Hansen et al. (1955) and Christian (1957) for the mixture of carboxylic acids (acetic acid–propionic acid). Taha and Christian (1969) successfully used similar treatment for the trifluoroacetic acid–diphenylmethane system. Ziêborak and Brzostowski (1958) also applied a similar procedure to that proposed by Marek and Standart (1954).

However, the second virial coefficients were introduced to refine these methods. Hence, small imperfection of the gas mixtures consisting of monomers, dimers and nonassociating molecules could be accounted for. Tsonopoulos and Prausnitz (1970), studied strong deviations from ideality in carboxylic acid vapours and in vapour mixtures with water and attributed the non-ideal behaviour not only to dimer formation, which is generally accepted, but also to trimer formation (Apelblat, 2007). This treatment neglected the physical contribution and only account for non-ideality of carboxylic acid vapours, which is significant even at very low pressures. Nothnagel et al. (1973) discussed this chemical theory of vapour imperfections in a general correlation applicable to binary mixtures including non-polar, polar and hydrogen-bonded components, such as alcohols, aldehydes and aliphatic acids. However, Hayden and O'Connell (1975) proposed a virial equation of state that incorporates the chemical theory to account for vapour phase nonidealities as well as the chemical interaction because of dimerization. Prausnitz et al. (1999) also included an expression that helps to correct the possible effect of dimerization on the activity coefficient in the liquid phase. Sewnarain (2002) used this model for acid-acid binary mixtures. The other models were considered as a follow up of the recommendation of Pedersen et al. (1996).

### 3.6.2 Calculating Fugacity Coefficients from Chemical Theory

The chemical theory was first developed by Dolezalek in 1908. It presumes existence of chemically distinct species in solution that are assumed to be in equilibrium. The theory assumes that these chemically distinct substances form an ideal solution. Based on these assumptions, the observed non-ideality of a solution is only an apparent one because it is established on an apparent rather than a true account of the solution's composition. Dolezalek's theory accounts for positive and negative deviations from ideality of molecules of similar size and it is applicable to mixtures containing polar and hydrogen-bonded liquids.

In the chemical theory, there are two types of reactions, association and solvation. According to Nagata et al. (1995), in an attempt to model carboxylic acid-alcohol binary mixtures, dimerization of carboxylic acid molecules and the linear association of alcohol molecules were assumed in the

liquid phase. However, this method of assuming formation of complex of carboxylic acid (A) and alcohol (B) molecules of the type (AB), gave an unsatisfactory description of the VLE. Hence, a UNIQUAC associated-solution model based on a 1:1 chemical complex-forming model was proposed which gave a good representation of the phase behaviour of carboxylic acid + alcohol mixtures. For this, they calculated the fugacity coefficients in the vapour phase according to the chemical theory of vapour imperfection (Nothnagel et al., 1973) and the free contribution of the monomer to the second virial coefficient was calculated by the method of Hayden and O'Connell (1975). This model was reported to give a good workability in the correlation and prediction of VLE and excess enthalpy data for the mixtures.

In this work, a similar chemical theory was used for calculating the fugacity coefficient in the vapour phase. The computational procedure is presented in Appendix A of Prausnitz et al. (1980) in a computer program format.

The hydrogen bonding process in carboxylic acid-alcohol is observed as a chemical reaction

$$i + j \leftrightarrow ij \tag{3.51}$$

where i and j are monomer molecules and ij is the dimer formed by hydrogen bonding. Hence, to describe the chemical reaction, the equation is given (Sewnarain, 2002):

$$K_{ij} = \frac{f_{ij}}{f_i f_j} = \frac{1}{P} \frac{z_{ij}}{z_i z_j} \frac{\phi_{ij}^*}{\phi_i^* \phi_j^*} \tag{3.52}$$

Where z is the true mole fraction of the species in equilibrium, $\phi^*$ is the fugacity coefficient of the true species, P is the system pressure and $K_{ij}$ is the reaction equilibrium constant.
To use equation (3.45), Nothnagel et al.(1973) shows that $\phi$ is expressed as :

$$\phi_i = \frac{z_i \phi_i^*}{y_i} \tag{3.53}$$

where $y_i$ is defined as the apparent mole fraction of component *i* in the vapour phase (by apparent, it means dimerization has been neglected; i.e. the experimentally measured vapour composition).

Assuming that the vapour solution behaves like an ideal solution, $\Phi^*$ is calculated by Lewis fugacity rule;

$$\ln \phi_i^* = \frac{PB_i^F}{RT} \tag{3.54}$$

where $B_i^F$ is the "free"contribution to the second virial equation calculated by Hayden and O'Connell method (1975). Hence, the chemical equilibrium constant is found from the relation:

$$K_{ij} = \frac{-(2-\delta_{ij})B_{ij}^D}{RT} \tag{3.55}$$

where $B_{ij}^D$ is the contribution of dimerization to the second virial coefficient which is also calculated by the Hayden and O'Connell method (1975). Note that $\delta_{ij}$ is set to zero for $i \neq j$ and one for $i = j$.

Thus, the calculation of the fugacity coefficient for components i and j is accomplished by solving the above equations with the restriction that the sum of $z_i$, $z_j$ and $z_{ij}$ equal to 1. By using the calculation procedure discussed by Prausnitz et al. (1980) in a Matlab programming language, the chemical theory could be incorporated to simultaneously calculate the fugacity coefficient and the liquid phase activity coefficient.

### 3.6.3 The Cubic Plus Association Equation of State (CPA)

Kontogeorgis et al. (1996) published an equation of state suitable for describing associating fluids. This is an interesting equation of state in the fact that it combines the simplicity of a cubic equation of state (the Soave-Redlich-Kwong), which is used for the physical part and the theoretical background of the perturbation theory employed for the chemical (or association) part. This conclusion according to them was reached after a careful consideration of existing models/theories for associating fluids that it was theoretically sound to combine a simple cubic equation of state like the SRK EOS (Soave, 1972) with an association term similar to that used in the SAFT EOS (Huang and Radosz, 1990).

The CPA EOS have been applied to pure components and good correlations obtained of both vapour pressures and saturated liquid volumes for primary-alcohols, phenol, tert-butyl alcohol, triethylene glycol, and water (Kontogeorgis et al. 1996). Recently, this model has been extended in a thermodynamic modeling of multicomponent mixtures containing carboxylic acids. The modeling for the methanol + propanoic acid, as well as the 2-butanol + propanoic acid reported by Kontogeorgis et al. (2007) is quite satisfactory. However, there are still some limitations that have been listed by Kontogeorgis et al. (2006). One of the unresolved challenges as relate to this project using CPA includes the different combining rules that are required for describing different types of phase equilibria (VLE, LLE, and SLE). Another limitation is the high values of the binary interaction parameters for cross-associating systems (which indicates that the model underestimates solvation), the "hard" solvating phenomena for acid-water binary systems, and finally applications in the presence of highly polar components. According to Kontogeorgis et al. (2006) , cross-associating systems i.e., solutions where both compounds are self-associating and/or when cross-

association is expected between two compounds (even if only one or none of the compounds are self-associating) represent a challenge for models such as CPA and statistical associating fluid theory (SAFT). This has been observed even for "relatively simple ideal" mixtures such as alcohol-alcohol systems or methanol-water, because all interactions must be described as accurately as possible. In most cases, there is very little room for a "cancellations of errors", unlike what can be the case for SRK or other cubic equations of state (EOS).

### 3.6.4 The Group Contribution with Association Equation of State (GCA-EOS)

In 1996, Gros and co-workers proposed a group contribution approach, combining an associating term derived from Wertheim's statistical theory with the GC-EOS (Skjold-Jorgensen, 1984, 1988) with the aim of overcoming some of the difficulties faced with the modeling of multicomponent associating mixtures. This model has been applied to the phase equilibria modeling of various binary and ternary mixtures (Gros et al., 1996). Recently, Ferreira et al. (2004) extended it like every other associating model discussed earlier to the modeling of carboxylic acid mixtures. In the extension to the modeling of carboxylic acids in associating and non-associating components, two associating groups OH and COOH were defined. Self- and cross association in these mixtures were quantified through two parallel COOH/COOH and OH/OH associations (Ferreira et al. 2003).

In order to model association using the GCA-EOS model, Ferreira et al. (2004) emphasised the importance of determining the number of associating groups, the values of the corresponding association strengths and the number of active sites in each group. It was explained that the high degree of non-ideality exhibited by carboxylic acids, even at low pressures necessitate the need to define a new associating group (COOH) as having one associating site that self-associates by double hydrogen bonding. The fraction of non-bonded molecules predicted by the SAFT equation for linear acids from propanoic to decanoic at saturated liquid conditions (Huang and Radosz, 1990) were reproduced using the procedure from Gros et al. (1996). This procedure was then further used to obtain the association parameters for the hydroxyl (OH) group. The cross-association parameters between the acid associating group and the hydroxyl associating group were calculated by a combining rule of the energy of association and volume of association. The result reported by Ferreira et al. (2004) using the GCA-EOS for the VLE of 1-Propanol+Propanoic acid at 1atm was fairly good with an average absolute deviation in temperature of 4.6 % and average absolute deviation in vapour composition of 1.1%. Overall, the result presented by Ferreira and co-workers for the GCA-EOS prediction and the GCA-EOS correlation gives an average deviation in temperature of 9.5% and 6.1% respectively with average deviation in vapour composition being 1.9% in both cases. For details into the equation for the GCA-EOS model development, the reader is referred to the published work of Gros et al. (1996) and for the extension of the model for

carboxylic mixture the work of Ferreira et al. (2004). In addition, the published work of Skjold-Jorgensen (1984, 1988) on GC-EOS can be consulted for the model development.

As previously explained, even though many models have been developed to assist in the modeling of associating binary or ternary mixtures, most of the associating systems considered have been alcohols with the hydrocarbons (e.g alkanes), as well as the carboxylic acids with the hydrocarbons (e.g alkanes). Only few works have been published that involves the modeling of two associating binary systems of carboxylic acids and alcohols. While it is important to refer to the extensive work of Ferreira et al. reported in the Journal of Chemical Thermodynamics (2004) on the modeling of phase equilibria for associating mixtures using an equation of state, it must be mentioned that none of the binary mixtures of alcohols with the carboxylic acids involve butyric acid which was used in this project. In addition, most of the measurements reported for the alcohol/carboxylic binary mixtures were at 100 kPa with the exception of methanol/acetic acid mixture, which was undertaken at both isobaric and isothermal conditions. Hence, the challenge continues in a desire to model carboxylic acid/alcohol binary mixtures successfully.

### 3.6.5 The Perturbation-Chain Statistical Associating Fluid Theory Equation of State (PC-SAFT)

The perturbed hard-chain theory (PHCT) equation of state developed by Beret and Prausnitz (1975) and Donohue and Prausnitz (1978) was the first widely applied equation of state based on molecular view. This development has revealed the potential of molecular-based theories and has been the inspiration for further developments. Recently, Wertheim's thermodynamic perturbation theory of first order (Wertheim, 1984a,b, 1986a,b) was applied by Chapman et al. (1988, 1990) in the development of the statistical associating fluid theory (SAFT) equation of state for chain molecules. There have been different modifications made to the SAFT model over the years, examples being LJ-SAFT versions,(Kraska et. al ,1996; Johnson et. al, 1994; Banaszak et. al, 1994) in which Lennard-Jones spheres served as a reference for the chain formation, and VR-SAFT, in which the attractive potentials are allowed to show variable widths ( Gil-Villegas et.al, 1997). Despite many of this theoretical improvements, one of the most successful modification remains the SAFT model suggested by Huang and Radosz (1990,1992) who applied a dispersion term developed by Chen and Kreglewski (1977) in the framework of SAFT. This dispersion term was derived by fitting a perturbation expansion to the experimental data of argon. The nonspherical shape of molecules is not accounted for in their dispersion term.

In 2001, Gross and Sadowski published a new equation of state that was concerned with developing a theory for chain molecules, applying the second-order perturbation theory of Barker

and Henderson (1967a, b). In other words, the perturbed-chain SAFT (PC-SAFT) equation of state was based on the statistical associating fluid theory (SAFT) as a reference. The PC-SAFT model has been successfully applied to a wide variety of systems, and the results from the model have a considerable improvement when compared to the original SAFT model. Recently, this model has been applied to mixtures of strongly polar and non-polar fluids (e.g. butyronitrile and *n*-heptane), mixtures of polar and associating fluids (e.g. water and acetone) and mixtures with carboxylic acids (e.g. cyclohexane and acetic acid). Although, mixtures of carboxylic acid are involved in the application, it was realized that most of the modeling involves acetic acid specifically with alkanes. One of the challenging issues is modeling with the appropriate association scheme, especially with the acids as mentioned in the introduction. The reader is referred to the published work of Gross and Sadowski (2001, 2002) for the equations explaining the model development, as well as Kontogeorgis et al. (2006) publication of capabilities, limitations and challenges of a simplified PC-SAFT equation of state.

### 3.6.6 Theoretical Comparison of the Association Models

It is important to compare the basic association theory on which the chemical theory, perturbation theory and the lattice theory correlates. The basis on which an association scheme should be employed or, in terms of perturbation theory, the number of bonding sites is still been researched into. The use of the correct association scheme depends on the associating compound (these have been elaborated on in the introduction section in this chapter). However, for multisite molecules (as in the case of Ammonia and Hydrogen Fluoride), a more advanced model is needed due to formation of branched chains, closed rings, or cyclic oligomers (Lencka and Anderko, 1993; Anderko and Prausnitz, 1994; Economou and Peters, 1995). For this, Anderko (1991) proposed an approximation equation. This seems like an advantage for the perturbation (SAFT EOS, PCSAFT) and lattice-fluid associated solutions (LFAS) model (Panayiotou and Sanchez, 1991) theories that yield explicit expressions for multisite molecules over the chemical theory that does not give explicit expressions for the association term of the compressibility factor in a multisite molecule.
Economou and Donohue (1991, 1992) revealed that chemical, perturbation, and lattice EOS's yield essentially the same expressions for the association compressibility factor ($Z^{assoc}$) for compounds which form one or two hydrogen bonds (like carboxylic acids and alcohols) and the mole fraction of monomers ($n_1/n_0$) on the basis of the superficial number of moles. Elliott et al. (1990) have also shown that the chemical and perturbation models give numerically equivalent results. Therefore, it is important to show how the association terms based on these three theories relate.

The expressions for $Z^{assoc}$ for the Associated Perturbed Anisotropic Chain Theory (APACT) and Statistical Associating Fluid Theory (SAFT) or Cubic Plus Association EOS (CPA) in the case of the linear infinite equilibria (two-site) model of the Kempter-Mecke type are:

For APACT EOS,

$$Z^{assoc} = \frac{1-\sqrt{4KRT\rho}}{1+\sqrt{4KRT\rho}} \tag{3.56}$$

and for SAFT/CPA,

$$Z^{assoc} = \left(\frac{1-\sqrt{4\Delta\rho}}{1+\sqrt{4\Delta\rho}}\right)\left(\frac{\Delta+\rho\Delta'}{\Delta}\right) \tag{3.57}$$

where $\Delta'$ is the derivative of $\Delta$ with respect to density, $\rho$ is the molar density.

In the chemical theory equations of state, the association is expressed through the equilibrium constant $K$, which is independent of density

$$\ln K = \frac{-\Delta H^{assoc}}{RT} + \frac{\Delta S^{assoc}}{R} \tag{3.58}$$

where $\Delta H^{assoc}$ and $\Delta S^{assoc}$ are respectively, the enthalpy and entropy of hydrogen-bonding formation. According to the perturbation theory EOS's (SAFT, CPA) the association strength is expressed through the $\Delta$-function

$$\Delta = \left(\frac{2-\eta}{2(1-\eta)^3}\right)\left[\exp(\varepsilon^{AB}/RT)-1\right]V^{AB} \tag{3.59}$$

Where, $\varepsilon^{AB}$ is the association energy of interaction between sites A and B and $V^{AB}$ is the molar volume. Theoretically, the only difference between CPA and SAFT lies in the definition of the reduced density $\eta$ and the association volume. It is important to note that $\Delta$ unlike K is a function of density. However, the density dependence of the association compressibility factor is much more affected by the external density dependence of the mole fraction of nonbonded molecules (first bracketed term of equation 3.57) than the density dependence of $\Delta$. Thus, if the density-dependent part of $\Delta$ is ignored, equations (3.58) and (3.59 become identical. This is observed with the expression

$$KRT = \Delta \tag{3.60}$$

Thus, an equation is given

$$\exp\left(\frac{-\Delta H^{assoc}}{RT}+\frac{\Delta S^{assoc}}{R}\right)=\exp\left(\frac{\varepsilon^{AB}}{RT}-1\right)\frac{V^{AB}}{RT} \qquad (3.61)$$

This equation (3.61) helps us identify the direct relations between the energy of association with the enthalpy of hydrogen bonding as well as of the association volume with the entropy of hydrogen bonding. (Kontogeorgis et al., 1999)

## 3.7 Data Regression and Correlation of Low Pressure VLE

There are basically three different methods for regressing low pressure VLE data. These are:

1. The combined method (The gamma-phi formulation of VLE)
2. The direct method (The phi-phi formulation of VLE, The EOS method)
3. The model-independent methods

The third method for the computation of VLE is usually used to calculate VLE from P-x data, i.e. experimental data where only the total pressure and liquid composition are measured at constant temperature. The vapour phase composition is calculated by integrating one of the many different forms of the Gibbs-Duhem equation (Sayegh and Vera, 1979). In this project, since the compositions of all the phases in equilibrium are measured, only the first two methods were used and thus the third method will not be used nor discussed any further. For the reader interested in the subject, the papers by (Ljunglin and Van Ness 1962, Mixon et al., 1965 and Sayegh and Vera, 1979) are recommended.

### 3.7.1 The Combined Method (Gamma-Phi Method)

This method is commonly used in the reduction of low-pressure data. In this method, an activity coefficient model is used to account for non-idealities in the liquid phase while an equation of state (EOS) is used to account for non-idealities in the vapour phase.

For a good VLE data reduction model, the choice of a suitable procedure or algorithm for obtaining the model parameters via regression is important. In this project, the method of least squares (Marquardt, 1963 and Gess et al., 1991) was employed. However, programmes in MATLAB have inbuilt functions (e.g fminsearch) that allow such calculations to be performed with relative ease. The regression procedure is normally conducted by minimizing the error between the experimental and model values for a particular quantity. The difference between the two values (model and experimental) is commonly termed a *residual* and is given the symbol $\delta$**.** Usually, the quantity selected for minimization is one of the following: pressure, vapour composition or excess Gibbs energy i.e. $\delta P$, $\delta y$ or $\delta g$, where $g = G^E/RT$. The regression is then run until the chosen *objective*

*function* (Van Ness and Abbott, 1982) has reached a specified, minimum value.
This objective function is usually of the form,

$$S = \sum (\delta P)^2 \tag{3.62}$$

Although certain regression programmes require that the standard deviation is used as the objective function:

$$S = \frac{1}{n} \sum \sqrt{(\delta P)^2} \tag{3.63}$$

It is important to note that unless the VLE data being analyzed are thermodynamically perfect, different objective functions will produce different parameters for a specific model. Hence, the issue of which residual results in the best fit exists and must be decided. In this project, it was observed that the $\delta P$ residual produced the best results. Van Ness and co-workers (1978) who compared all of the objective functions reported the same trend. Van Ness (1995) explains that the objective function, $\sum (\delta P)^2$ (i.e. Barker's method) is the simplest and most direct giving a result that is equally as good as any other. Figure 3.3 displays the flowchart showing the procedure for bubblepoint iteration for the combined method.

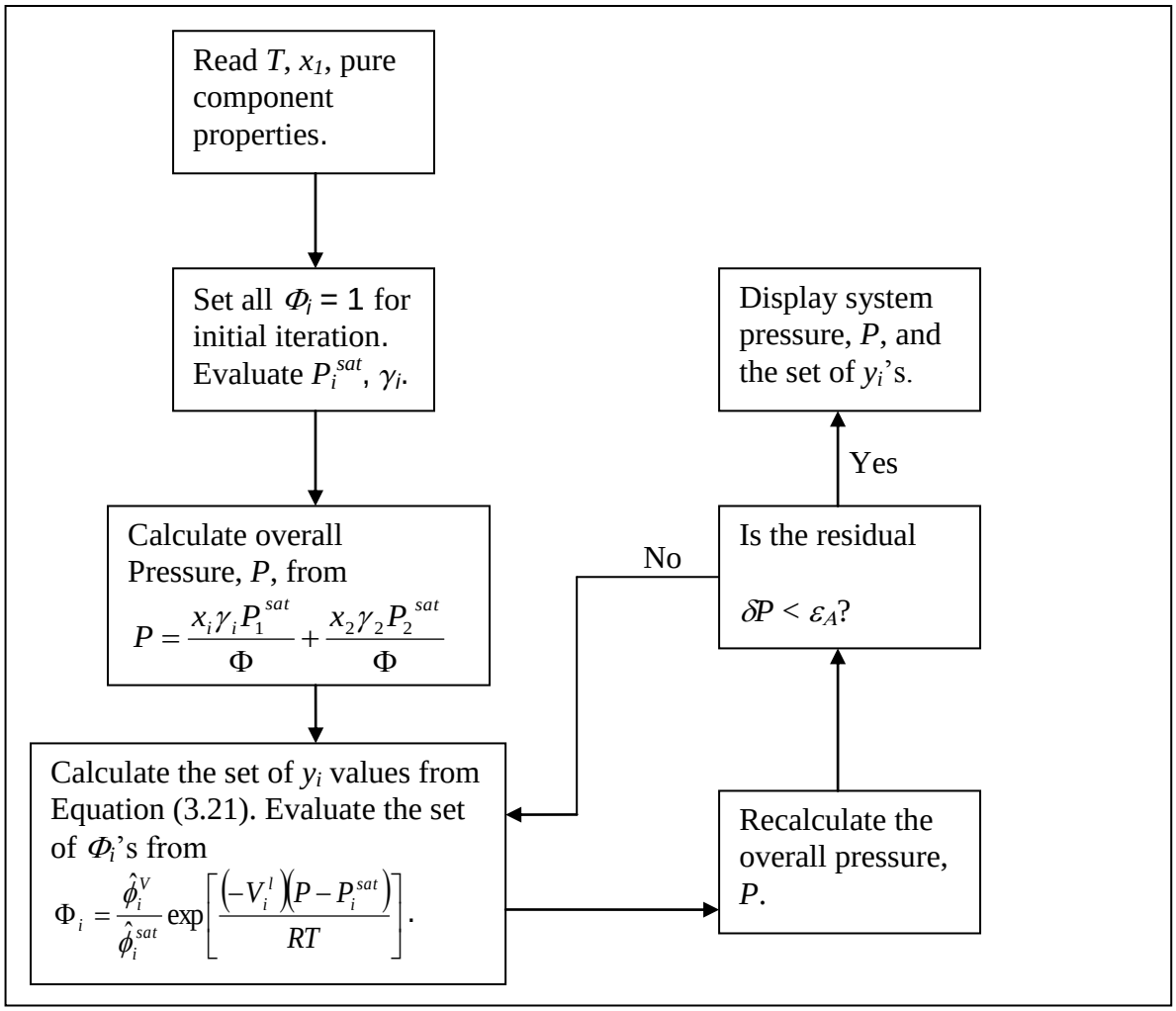


**Figure 3-3: Flow diagram for bubblepoint pressure iteration (combined method)(Clifford, 2003).**

The calculations for both isobaric and isothermal data are included. If the data are isothermal, values for the pressure and vapour composition are calculated (bubblepoint pressure iteration as in figure 3-3), whereas isobaric data necessitates calculation of the temperature and vapour composition (bubblepoint temperature iteration as shown by figure 3-4) for each experimental point.

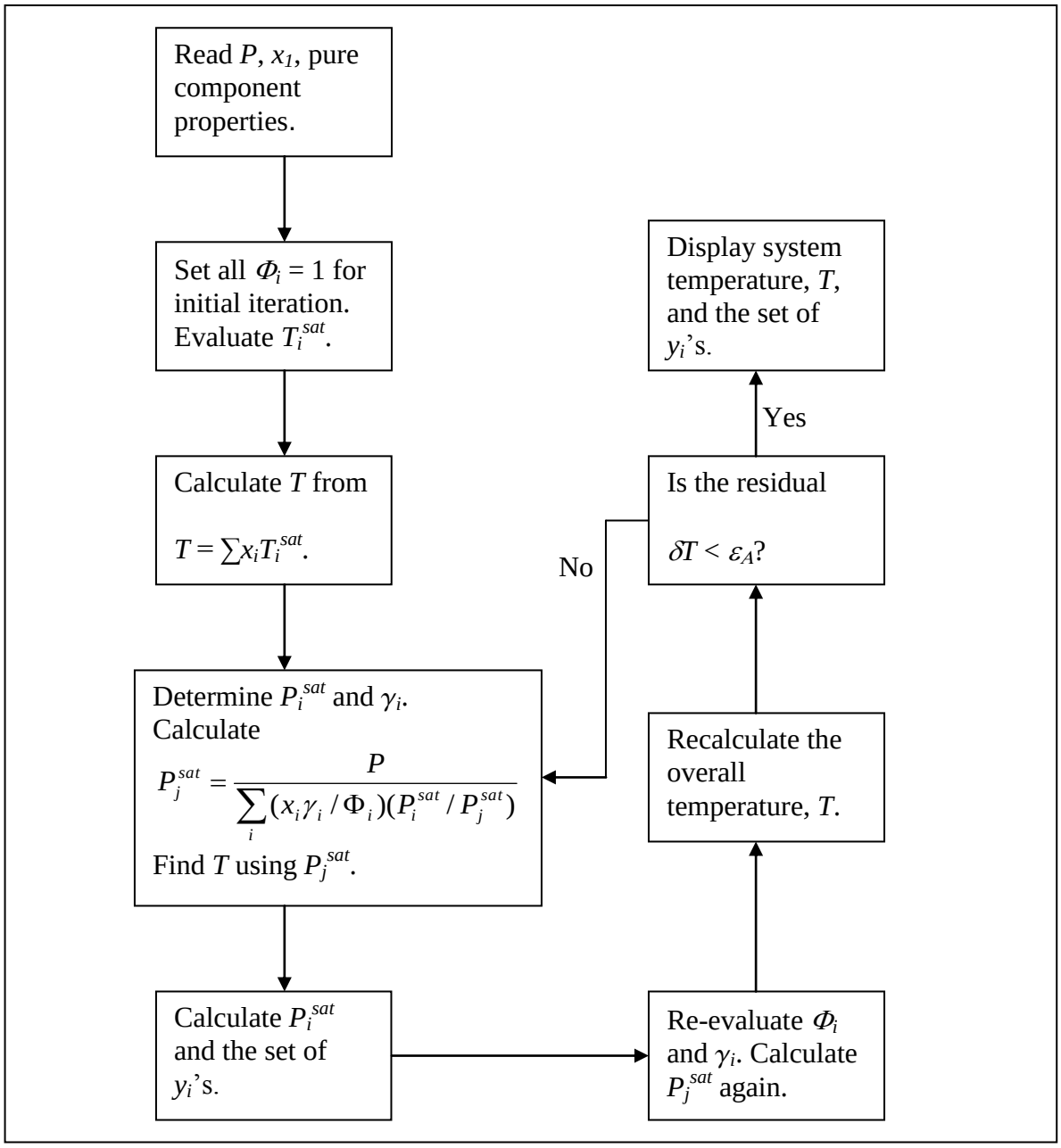


**Figure 3-4: Flow diagram for bubblepoint temperature iteration (combined method)(Clifford,2003).**

### 3.7.2 The Direct (Phi-Phi ) Method For Vapour-Liquid Equilibrium Model

Figure 3-5 and 3-6 shows a flow diagram of the procedure used for computing bubble point pressure and temperature using the direct technique.

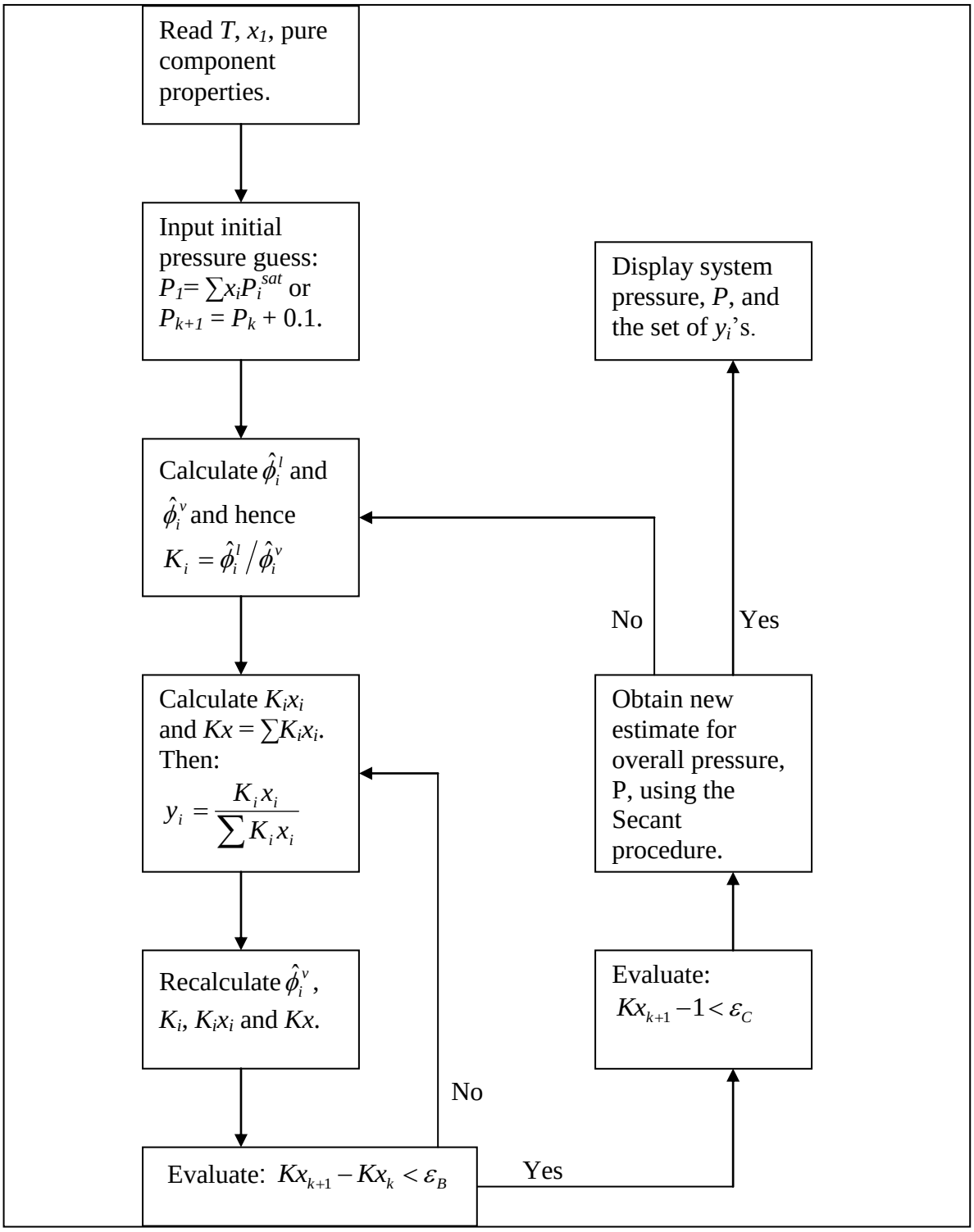


**Figure 3-5: Flow diagram for bubblepoint pressure iteration (direct method) (Clifford, 2003).**

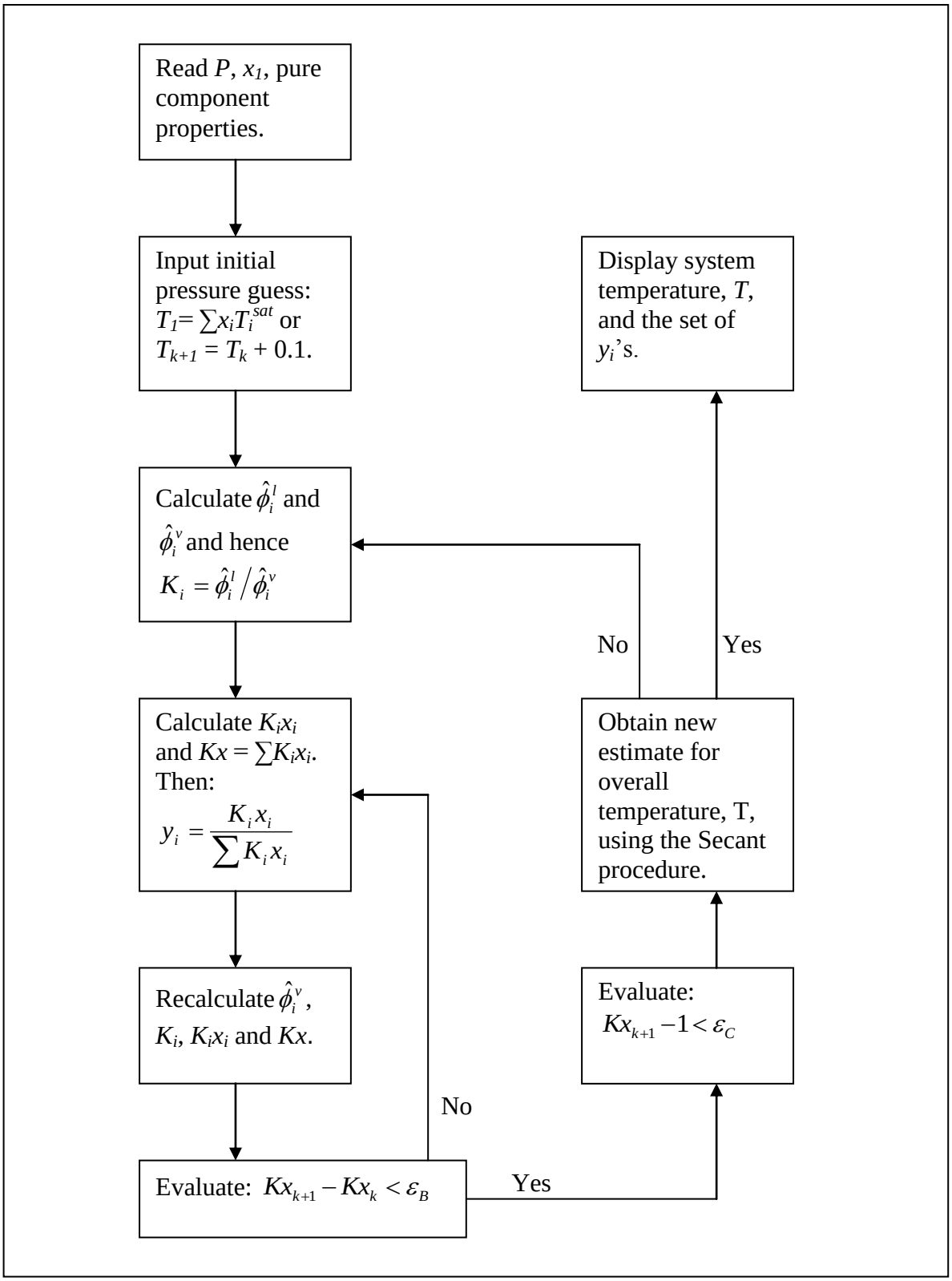


**Figure 3-6: Flow diagram for bubblepoint temperature iteration (direct method) (Clifford, 2003).**

## 3.8 Thermodynamic Consistency Testing

The Gibbs-Duhem equation is an important equation in thermodynamics on which many tests of consistency were developed. It is an important equation relating excess-properties to the activity coefficient. The different tests pertinent to this work are discussed below.

### 3.8.1 The Point Test

The recirculating equilibrium still which is used in this work allows for the measurement of temperature, pressure and both liquid and vapour compositions. This is an "*over determination"* of VLE because any one of these variables can be determined from the other three using the Gibbs-Duhem equation. In the Point Test introduced by Van Ness et al. (1973), the vapour phase composition or (pressure for isothermal data) is computed from the remaining variables and the results compared with the measured values. This comparison generates residuals $\delta$y (or $\delta$P) which for consistent data should scatter evenly about the zero axis over the full composition range. When isobaric data is to be tested, the $\delta$y and $\delta$T residuals need to be examined. Van Ness and Abbott (1982) and Hirata (1975) discuss the choice of objective functions when using this test. Fredenslund et al. (1975) and Danner and Gess (1990) provide a quantitative criterion for the acceptance of VLE data by proposing that the absolute average deviation should be less than 0.01. This criterion was used in this work.

### 3.8.2 The Direct Test

Van Ness (1995) proposed this test due to some of the inadequacies from the area test. Some of the limitations identified with the area test were that the heat of mixing data required for isobaric data is often unavailable for most systems. Hence, the right hand side of the equation describing the area test is taken to be zero, an assumption that is not valid and cannot be justified even if the $H^E$ term is divided by the square of the temperature (Raal and Mühlbauer, 1998). In addition, it was observed that the measured total pressure cancels in the ratio of the activity coefficients. This is one of the most important and accurately measured variables, but disappears in this test.

However, the formulation for the direct test is lengthy and will not be presented here and the reader interested in detail should refer to Van Ness (1995).

The formulation result for a binary system is given by the equation:

$$\delta \ln \frac{\gamma_1}{\gamma_2} = x_1 \frac{d \ln \gamma_1^{Exp}}{dx_1} + x_2 \frac{d \ln \gamma_2^{Exp}}{dx_1} - \varepsilon \qquad (3.64)$$

The superscript Exp denotes values obtained from measured experimental data and ε depends on whether the data are isothermal or isobaric. It is given by the equations*:*

$$\varepsilon_p = \frac{V^E}{RT}\frac{dP}{dx_1} \tag{3.65}$$

and

$$\varepsilon_T = \frac{-H^E}{RT^2}\frac{dT}{dx_1} \tag{3.66}$$

for the two cases respectively. When applying the test, a VLE data set is reduced using $\Sigma\ (\delta g\ )^2$ (where $g = x_1 \ln \gamma_1 + x_2 \ln \gamma_2$) as the objective function. For consistent data, the RHS of Equation (3.64) is required to be zero. The residual on the left is thus a measure of deviations from the Gibbs-Duhem equation and the extent to which the residual fails to scatter about the zero axes provides a measure of the departure of the data set from consistency (Van Ness, 1995). Van Ness (1995) also provides a quantitative criterion for the test. He gives a table of indices (see Table 3.1 below) calculated from the above mentioned residual (Equation 3.64) and they start from 1 for excellent data and go to 10 for poor data.

| Index | RMS $\delta \ln(\gamma_1/\gamma_2)$ | |
|---|---|---|
| 1 | > 0 | ≤ 0.025 |
| 2 | > 0.025 | ≤ 0.050 |
| 3 | > 0.050 | ≤ 0.075 |
| 4 | > 0.075 | ≤ 0.100 |
| 5 | > 0.100 | ≤ 0.125 |
| 6 | > 0.125 | ≤ 0.150 |
| 7 | > 0.150 | ≤ 0.175 |
| 8 | > 0.175 | ≤ 0.200 |
| 9 | > 0.200 | ≤ 0.225 |
| 10 | > 0.225 | |

**Table 3.1: Consistency table for the direct test (Van Ness, 1995)**

| Reference | Model | ($G^E$/RT) | ln$\gamma_i$ |
|---|---|---|---|
| Wilson (1964) | Wilson | $\frac{G^E}{RT} = -x_1 \ln(x_1 + x_2\Lambda_{12}) - x_2 \ln(x_2 + x_1\Lambda_{21})$ | $\ln\gamma_1 = -\ln(x_1 + x_2\Lambda_{12}) + x_2\left(\frac{\Lambda_{12}}{x_1 + x_2\Lambda_{12}} - \frac{\Lambda_{21}}{x_2 + x_1\Lambda_{21}}\right)$<br>$\ln\gamma_2 = -\ln(x_2 + x_1\Lambda_{21}) - x_1\left(\frac{\Lambda_{12}}{x_1 + x_2\Lambda_{12}} - \frac{\Lambda_{21}}{x_2 + x_1\Lambda_{21}}\right)$ |
| Renon and Prausnitz (1968) | NRTL | $\frac{G^E}{RT} = x_1x_2\left[\frac{G_{21}\tau_{21}}{x_1 + x_2G_{21}} + \frac{G_{12}\tau_{12}}{x_2 + x_1G_{12}}\right]$ | $\ln\gamma_1 = x_2^2\left[\tau_{21}\left(\frac{G_{21}}{x_1 + x_2G_{21}}\right)^2 + \frac{G_{12}\tau_{12}}{(x_2 + x_1G_{12})^2}\right]$<br>$\ln\gamma_2 = x_1^2\left[\tau_{12}\left(\frac{G_{12}}{x_2 + x_1G_{12}}\right)^2 + \frac{G_{21}\tau_{21}}{(x_1 + x_2G_{21})^2}\right]$ |
| Abrams and Prausnitz (1975) | UNIQUAC | $G^E = G^E(combinatorial) + G^E(residual)$<br>$\frac{G^E(combinatorial)}{RT} = x_1\ln\frac{\Phi_1}{x_1} + x_2\ln\frac{\Phi_2}{x_2} + \frac{z}{2}\left(q_1x_1\ln\frac{\theta_1}{\Phi_1} + q_2x_2\ln\frac{\theta_2}{\Phi_2}\right)$<br>$\frac{G^E(residual)}{RT} = -q_1x_1\ln[\theta_1 + \theta_2\tau_{21}] - q_2x_2\ln[\theta_2 + \theta_1\tau_{12}]$ | $\ln\gamma_i = \ln\gamma_i(combinatorial) + \ln\gamma_i(residual)$<br>$\ln\gamma_i = \ln\frac{\Phi_i}{x_i} + \frac{z}{2}q_i\ln\frac{\theta_i}{\Phi_i} + \Phi_j\left(l_i - \frac{r_i}{r_j}l_j\right) - q_i\ln(\theta_i + \theta_j\tau_{ji}) + \theta_jq_i\left(\frac{\tau_{ji}}{\theta_i + \theta_j\tau_{ji}} - \frac{\tau_{ij}}{\theta_j + \theta_i\tau_{ij}}\right)$ |

**Table 3.2: The excess Gibbs energy models specific to liquid phases and their expression for calculating activity coefficients.**

| Reference | Correlation for Second virial coefficients (B ) | fugacity coefficients |
|---|---|---|
| Pitzer-Curl (1957) | $\frac{BP_c}{RT_c} = f^{(0)}(T_r) + \omega f^{(1)}(T_r)$ | $\Phi_i = \exp\left[\frac{(B_{ii} - V_i^l)(P - P_i^{sat}) + Py_j^2\delta_{ij}}{RT}\right]$ |
| | $B_{ij} = \frac{RT_{cij}}{P_{cij}}(f^{(0)}(T_r) + \omega_{ij} f^{(1)}(T_r))$ | |
| Tsonopoulos (1974) | $\frac{BP_c}{RT_c} = f^{(0)}(T_r) + \omega f^{(1)}(T_r)$ | $\Phi_i = \exp\left[\frac{(B_{ii} - V_i^l)(P - P_i^{sat}) + Py_j^2\delta_{ij}}{RT}\right]$ |
| | $\frac{BP_c}{RT_c} = f^{(0)}(T_r) + \omega f^{(1)}(T_r) + f^{(2)}(T_r)$ | |
| Hayden and O'Connell (1975) + Chemical theory (Prausnitz, 1980) | $B_{ij} = B_{ij}^F + B_{ij}^D$ | $\phi_i = \frac{z_i \phi_i^*}{y_i}$ |
| | $K_{ij} = \frac{1}{P}\frac{z_{ij}}{z_i z_j}\frac{\phi_{ij}^*}{\phi_i^* \phi_j^*} = \frac{-B_{ij}^D(2-\delta_{ij})}{RT}$ | |
| | $\ln \phi_i^* = \frac{PB_i^F}{RT}$ | |

**Table 3.3: The Virial equation of state and the related evaluation of fugacity coefficients for deviation to ideal vapour phase.**

| EOS with Reference | Expressions for Z | fugacity coefficients |
|---|---|---|
| van der Waals (1873) | $Z^3 - Z^2(1+B) - ZA - AB = 0$<br>where $A = \frac{aP}{R^2T^2}$ and $B = \frac{bP}{RT}$<br>$P = \frac{RT}{V-b} - \frac{a}{V^2}$ | $\ln\phi = Z - 1 - \frac{A}{Z} - \ln(Z-B)$ |
| Redlich-Kwong (1949) | $Z^3 - Z^2 - Z(A - B - B^2) - AB = 0$<br>where $A = \frac{aP}{R^2T^{2.5}}$ and $B = \frac{bP}{RT}$<br>$P = \frac{RT}{V-b} - \frac{a}{T^{0.5}V(V+b)}$ | $\ln\phi = Z - 1 - \ln(Z-B) - \frac{A}{B}\ln\left(\frac{Z+B}{Z}\right)$ |
| Soave-Redlich-Kwong (1972) | $Z^3 - Z^2 - Z(A - B - B^2) - AB = 0$<br>where $A = \frac{aP}{R^2T^2}$ and $B = \frac{bP}{RT}$<br>$P = \frac{RT}{V-b} - \frac{a(T)}{V(V+b)}$ | $\ln\phi = Z - 1 - \ln(Z-B) - \frac{A}{B}\ln\left(\frac{Z+B}{Z}\right)$ |
| Peng-Robinson (1976) | $Z^3 - Z^2(1-B) - Z(A - 3B^2 - 2B) - (AB - B^2 - B^3) = 0$<br>where $A = \frac{aP}{R^2T^2}$ and $B = \frac{bP}{RT}$<br>$P = \frac{RT}{V-b} - \frac{a(T)}{V(V+b)+b(V-b)}$ | $\ln\phi = Z - 1 - \ln(Z-B) - \frac{A}{2B\sqrt{2}}\ln\left(\frac{Z(1+\sqrt{2})B}{Z(1-\sqrt{2})B}\right)$ |

**Table 3.4: The Cubic equation of state and the related evaluation of fugacity coefficients for deviation to ideal vapour phase.**

After the proposed equation of state of van der Waals (1873), the Redlich-Kwong (1949) became the most important model for the modification. However, Soave (1972) suggested replacing the term $a/T^{0.5}$ in RK EOS with a more general temperature-dependent term a(T). Peng and Robinson in 1976 redefined the temperature-dependent parameter a(T). A chronological order of the modification made is presented in Table 3.5. These variations of the van der Waals equations such as, RK, SRK and PR EOS are widely used in industrial and engineering applications.

| Reference | Attraction term | Values assigned to the constants |
|---|---|---|
| Redlich-Kwong (1949) | $\frac{a}{T^{0.5}V(V+b)}$ | $a=\frac{0.42748R^2T_c^{2.5}}{P_c}$<br>$b=\frac{0.08664RT_c}{P_c}$ |
| Soave-Redlich-Kwong (1972) | $\frac{a(T)}{V(V+b)}$ | $a=\frac{0.42747R^2T_c^{2}}{P_c}$<br>$b=\frac{0.08664RT_c}{P_c}$ |
| Peng-Robinson (1976) | $\frac{a(T)}{V(V+b)+b(V-b)}$ | $a=\frac{0.45724R^2T_c^{2}}{P_c}$<br>$b=\frac{0.07780RT_c}{P_c}$ |
| Stryjek-Vera (1986a) | $\frac{a(T)}{(V^2+2bV-b^2)}$ | |

**Table 3.5: Modification of the attractive term in the van der Waals equation of state and values of the attractive term (a) and repulsive term (b)**

| mixture | component 1 | component 2 | association type | cross-association parameters |
|---|---|---|---|---|
| acid−acid | 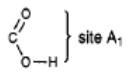 | 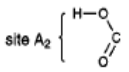 | $\epsilon^{A_1A_1}\neq 0$<br>$\epsilon^{A_2A_2}\neq 0$<br>$\epsilon^{A_1A_2}\neq 0$ | $\epsilon^{A_1A_2}=\sqrt{\epsilon^{A_1A_1}\epsilon^{A_2A_2}}$<br>$\kappa^{A_1A_2}=(\kappa^{A_1A_1}+\kappa^{A_2A_2})/2$ |
| alcohol−alcohol | 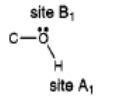 | 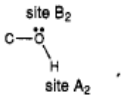 | $\epsilon^{A_1B_1}\neq 0,\ \epsilon^{A_2B_2}\neq 0$<br>$\epsilon^{A_1B_2}=\epsilon^{A_2B_1}\neq 0$<br>$\epsilon^{A_1A_1}=\epsilon^{A_2A_2}=\epsilon^{A_1A_2}=\epsilon^{A_2A_1}=0$<br>$\epsilon^{B_1B_1}=\epsilon^{B_2B_2}=\epsilon^{B_1B_2}=\epsilon^{B_2B_1}=0$ | $\epsilon^{A_1B_2}=\epsilon^{A_2B_1}=\sqrt{\epsilon^{A_1B_1}\epsilon^{A_2B_2}}$<br>$\kappa^{A_1B_2}=\kappa^{A_2B_1}=(\kappa^{A_1B_1}+\kappa^{A_2B_2})/2$ |
| acid−alcohol | 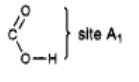 | 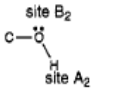 | $\epsilon^{A_1A_1}\neq 0,\ \epsilon^{A_2B_2}\neq 0$<br>$\epsilon^{A_1A_2}=\epsilon^{A_1B_2}\neq 0$<br>$\epsilon^{A_2A_2}=\epsilon^{B_2B_2}=0$ | $\epsilon^{A_1A_2}=\epsilon^{A_1B_2}=\sqrt{\epsilon^{A_1A_1}\epsilon^{A_2B_2}}$<br>$\kappa^{A_1A_2}=\kappa^{A_1B_2}=(\kappa^{A_2A_1}+\kappa^{A_2B_2})/2$ |
| water−acid | 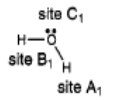 | 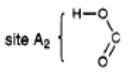 | $\epsilon^{A_1C_1}=\epsilon^{B_1C_1}\neq 0,\ \epsilon^{A_2A_2}\neq 0$<br>$\epsilon^{A_1A_2}=\epsilon^{B_1A_2}=\epsilon^{C_1A_2}\neq 0$<br>$\epsilon^{A_2A_1}=\epsilon^{B_1B_1}=\epsilon^{C_1C_1}=\epsilon^{A_1B_1}=0$ | $\epsilon^{A_2A_2}=\epsilon^{B_1A_2}=\epsilon^{C_1A_2}=\sqrt{\epsilon^{A_1C_1}\epsilon^{A_2A_2}}$<br>$\kappa^{A_1A_2}=\kappa^{B_1A_2}=\kappa^{C_1A_2}=(\kappa^{A_1C_1}+\kappa^{A_2A_2})/2$ |
| water−alcohol | 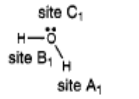 | 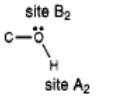 | $\epsilon^{A_1C_1}=\epsilon^{B_1C_1}\neq 0,\ \epsilon^{A_2B_2}\neq 0$<br>$\epsilon^{A_2B_2}=\epsilon^{B_1B_2}=\epsilon^{C_1A_2}\neq 0$<br>$\epsilon^{A_2A_1}=\epsilon^{B_1B_1}=\epsilon^{C_1C_1}=\epsilon^{A_1B_1}=0$<br>$\epsilon^{A_2A_2}=\epsilon^{B_2B_2}=0$<br>$\epsilon^{A_1A_2}=\epsilon^{B_1A_2}=\epsilon^{C_1B_2}=0$ | $\epsilon^{A_1B_2}=\epsilon^{B_1B_2}=\epsilon^{C_1A_2}=\sqrt{\epsilon^{A_1C_1}\epsilon^{A_2B_2}}$<br>$\kappa^{A_1B_2}=\kappa^{B_1B_2}=\kappa^{C_1A_2}=(\kappa^{A_1C_1}+\kappa^{A_2B_2})/2$ |

**Table 3.6: Type of Associations and Cross-Associations Parameters for Cross-Associating Mixtures (Fu and Sandler, 1995)**

CHAPTER
**4**

# EQUIPMENT DESCRIPTION

Measurements for this project were undertaken on a glass recirculating VLE still designed by Raal (Raal and Mühlbauer, 1998) and a stainless still VLE apparatus of Reddy (2006). The equipment was discussed in detail by Joseph et al. (2001) and Sewnarain et al. (2002). An excellent review on the history of the circulating VLE stills in addition to this glass still is available in Raal and Mühlbauer (1998). For the purpose of reference, the schematic diagram of the VLE still is presented in figure 4.1

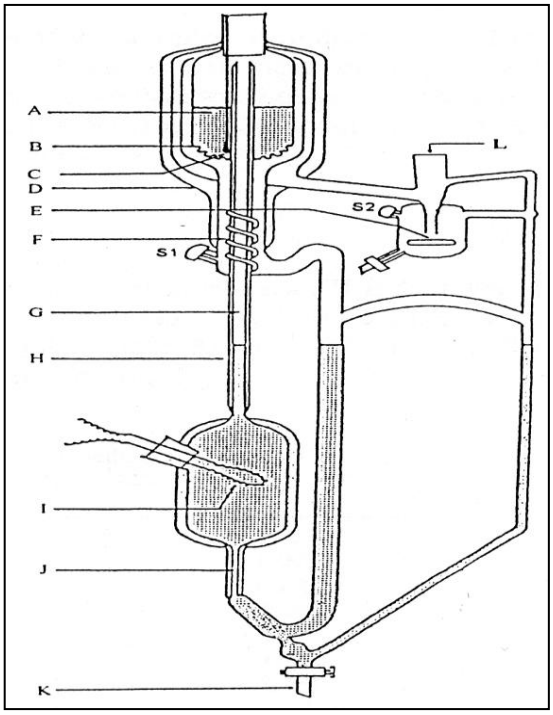


**Figure 4-1: Schematic diagram of the VLE Still (Clifford, 2003).**

A: stainless steel wire mesh packing; B: drainage holes; C: PT-100 sensor; D: vacuum jacket; E: magnetic stirrer; F: stainless steel mixing spiral; G: insulated Cottrell pump; H: vacuum jacket; I: internal heater; J: capillary leg; K: drainage valve; L: condenser attachment; S1: liquid sampling septum; S2: vapour sampling septum.

The VLE apparatus of Reddy (2006) which was also used for this project consists of the following equipment:

- The VLE still
- A 113.4 liter ballast tank
- A Grant CZ2 refrigeration apparatus
- An Edwards Speedivac vacuum pump
- A Nitrogen gas cylinder
- Pressure sensors *i.e.* the Sensotec Super TJE pressure transducer and the Wika P-10 transmitter
- Agilent model 34401A 6 ½ digit multimeter for reading temperature in resistance of the sensor in the equilibrium chamber
- Pt-100 temperature sensors.
- A Labotech water bath complete with ethylene glycol solution as the cooling medium and a pump.
- 3 Chuan Hsin (Model: SRV-10) variable-voltage transformers (0 - 240 V)
- Power supply unit.
- A Shinko pressure controller to control pressure from the two solenoid valves
- RKC temperature controller display (Model: CB-40)
- A multi-channel TCL Pt-100 selector switch box (allows for switching between the sensors of the equilibrium chamber and that of the reboiler)
- A solenoid valve (Clippard valve).
- A Shimadzu GC2010 for chromatograph analysis

The apparatus was constructed from machined 316 stainless steel and features sight glasses to allow for observation of the fluid behaviour in the Cottrell tube and in the liquid and vapour condensate sampling traps, Reddy (2006).

## 4.1. The Vapour-Liquid Equilibrium Apparatus

Figures 4-1 and 4-2 give a schematic diagram of the vapour-liquid equilibrium stills used for this project. For the purpose of clarity the data acquisition/control, pressure stabilization and cooling/condensing systems have been shown separately as the auxiliary features in Figure 4-3 for the stainless steel apparatus.

A main feature of the stainless steel apparatus design is the equilibrium chamber (C). A liquid mixture is charged into the reboiler (A) and brought to a boil by internal and external heaters (H1

and H2 respectively). The internal heater consists of a heater cartridge that provides the actual drive for boiling. It also provides nucleation sites for smooth boiling and allows precise control of the circulation rate. The external heater consists of nichrome wire that is wrapped around the reboiler, which compensates for the heat losses to the environment.

The boiling generates a vapour-liquid mixture that is forced upward through the vacuum insulated Cottrell tube (B) and then into the equilibrium chamber (C) which also has a Platinum temperature sensor (Pt2) that is connected to a multi-channel TCL Pt-100 selector switch box. This multi-channel TCL Pt-100 selector switch box allows for switching between the sensors of the equilibrium chamber (Pt2) and that of the reboiler (Pt1), as well as display the temperature in the equilibrium chamber in relation to that in the reboiler in order to reduce heat loss. The equilibrium chamber is packed with 3 mm rolled 316 stainless-steel wire mesh cylinders in order to provide a large interfacial area that ensures significant contact between the vapour and liquid phases. This arrangement has an advantage of achieving equilibrium rapidly, even for species with a high relative volatility. A Pt-100 temperature sensor is situated within the packing (Pt3) to provide an accurate measurement of the system's equilibrium temperature. The right hand side and bottom of the equilibrium chamber consists of holes to allow disengagement of the liquid and vapour phases. The liquid flows into a liquid trap (G) to allow sampling for composition analysis, while the vapour flows upward around the equilibrium chamber providing an important thermal lag.

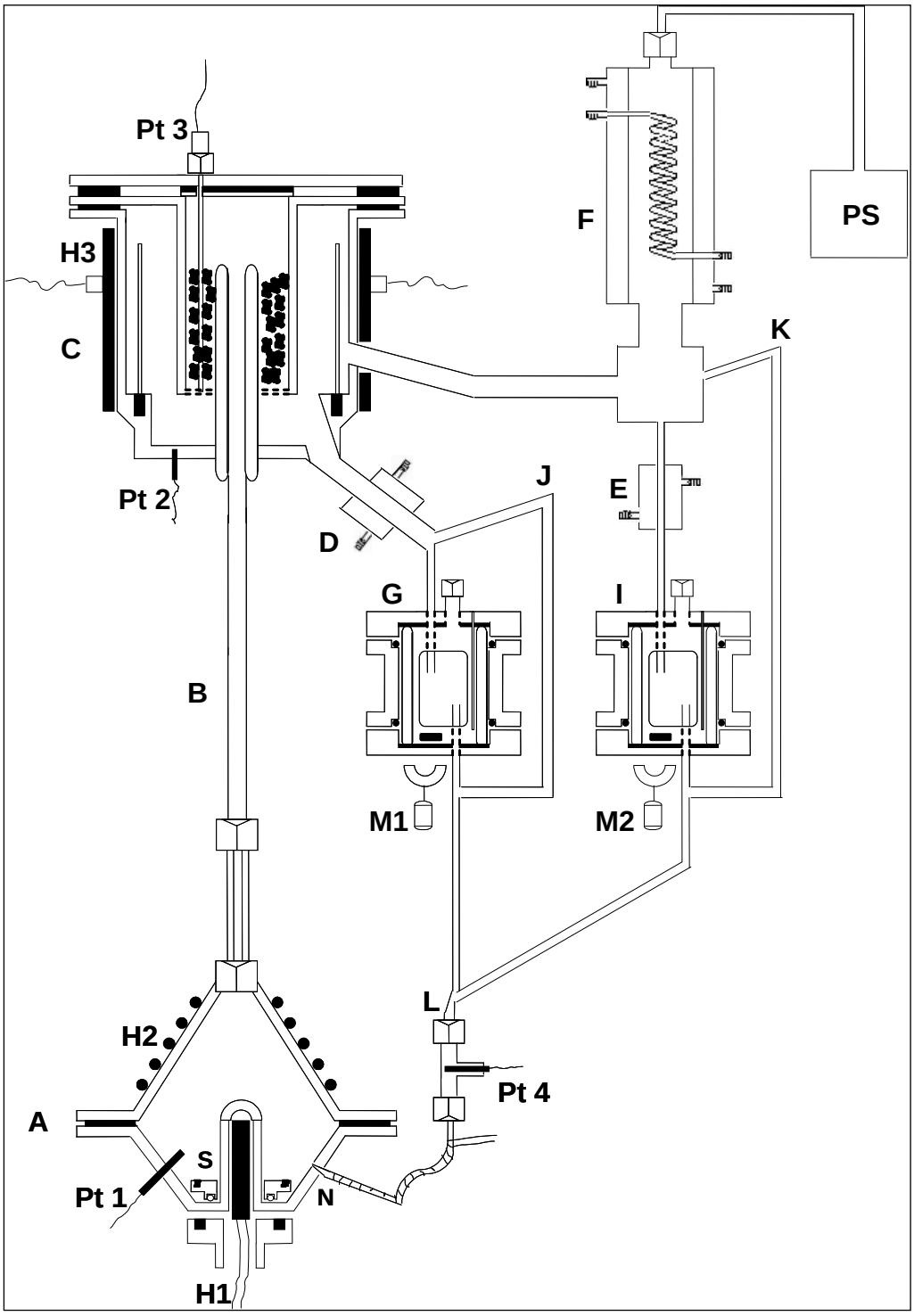


**Figure 4-2: Schematic diagram of the stainless steel VLE still taken from Reddy (2006).**

**A:** reboiler; **B:** Cottrell tube; **C:** equilibrium chamber; **D:** liquid cooler; **E:** vapour condensate cooler; **F:** condenser; **G:** liquid sample trap; **H1**, **H2**, **H3:** heaters; **I:** vapour condensate sample trap; **J:** liquid trap pressure equalizer tube; **K:** vapour condensate sample trap equalizer tube; **L:** return line union; **M1**,**M2:** motor-shaft mounted magnets; **N:** capillary; **PS:** pressure stabilization system; **Pt1**, **Pt2**, **Pt3**, **Pt4:** platinum temperature resistors; **S:** reboiler stirrer.

The vapour then flows to a condenser (F) where the condensate collects in a vapour condensate sample trap (I) before overflowing to the reboiler via a return line union where the vapour condensate sample trap equalizer tube (K) meet with the liquid trap pressure equalizer tube (J).

## 4.2 Temperature Measurement and Control

A Pt-100 temperature sensor connected to a temperature display was used to measure the equilibrium temperature. The Wika Pt-100 had an accuracy of ± 0.005 K. Other Pt-100 temperatures sensors were also used for the measurement of the temperature of the equilibrium chamber wall, the vapour sample loop and the vapour take-off stream and were all connected to a single temperature display via a multi-channel TCL Pt-100 selector switch box which allows for switching between the sensors of the equilibrium chamber and that of the reboiler. These temperatures were important for the composition analysis of a vapour sample to avoid partial condensation of the vapour phase. The Pt-100 temperature sensors were calibrated before use to obtain accurate temperature readings (refer to Chapter 5 for the calibration procedure). The accuracy of the measured temperature was estimated to be within ±0.02 K for both the glass still and the stainless steel apparatus and the accuracy of the temperature control varied between 0.01 and 0.05 K.

## 4.3 Pressure Measurement and Control

The system pressure was measured using a WIKA model P10 pressure transmitter and effectively controlled with a Shinko SWS-ACS01M pressure controller that utilised a two-way solenoid valve connected to a vacuum pump and a vent to the atmosphere. The accuracy of both the Sensotec pressure transducer and that of the Wika pressure transmitter was 0.05 % for the full span of the range of operation. The pressure controller actuates a two-way control valve and leads to a vacuum pump, allowing precise control of the pressure at desired values. The calibration procedure is discussed in Chapter 5. The pressure accuracy was estimated as ±0.02 kPa and ±0.03 kPa for the stainless steel and glass still respectively and controlled to within 0.01 kPa for isobaric operation.

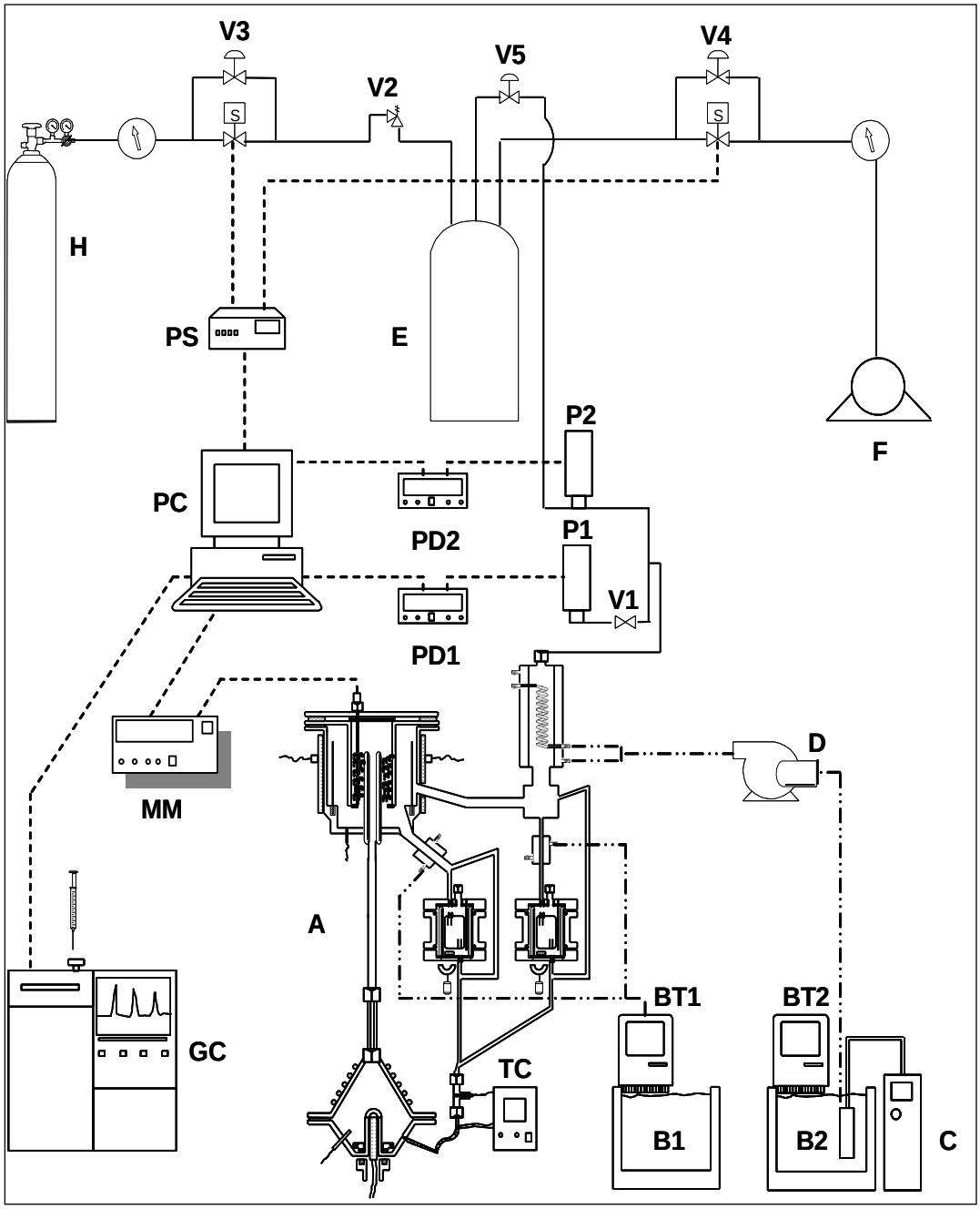


**Figure 4-3: Schematic diagram of the equipment layout of the steel apparatus taken from Reddy (2006)**

**A:** VLE still; **B1,B2:** water baths; **BT1**, **BT2:** thermostats/circulator pumps; **C:** refrigeration apparatus; **D**: coolant fluid pump; **E**: ballast tank; **F**: vacuum pump; **GC**: gas chromatograph; **H**: gas cylinder; **MM**: multimeter; **P1**: pressure transducer (Sensotec); **P2**: pressure transmitter (Wika); **PC**: personal computer; **PD1**, **PD2**: pressure displays; **PS**: power supply unit; **TC**: temperature controller; **V1**: shut-off valve; **V2**: safety relief valve; **V3**,**V4**,**V5**: control valves; electronic lines; water lines; pneumatic lines.

## 4.4 Sampling

The vapour phase and liquid samples were withdrawn directly from the sample trap using a gas-tight syringe through a chemically resistant septum. The gas-tight syringe ensured that no sample was lost during the sampling process. The samples were then analysed using a gas chromatograph (GC). The accuracy of the equilibrium composition measurement was estimated to be ±0.002 of a mole fraction.

## 4.5 Composition Analysis

The equilibrium liquid and vapour samples were accurately analysed by gas chromatography using the Shimadzu GC2010 with a thermal conductivity detector, which used helium as the carrier gas. A Cwax20M 1.0 micron Film Bonded capillary column of 30 metre in length with inner diameter of 0.53 mm was used for component separation in the GC. The operation and sampling procedures of the GC are discussed in Chapter 5, while the calibration result is discussed in Chapter 6.

CHAPTER
5

# EXPERIMENTAL PROCEDURE

A careful and detailed execution of an experimental procedure in the acquisition of phase equilibrium data is necessary for accurate VLE measurement. Researchers in the field of thermodynamics have been confronted with an abundance of experimental difficulties and uncertainties. This was exemplified in the uncertainties that characterized the operating procedure for the vapour condensate recirculating apparatus of Jones and Colburn (1943), where a slight incorrect input of energy in the nichrome windings around the crucial sections of the apparatus had compromised the operational efficiency of the apparatus and the quality of data acquired. Consequently, a systematic and careful approach is necessary for the attainment of precise phase equilibrium data, where the experimental procedure includes everything from the procurement of the chemical systems from a supplier to the actual measurements conducted in the laboratory.

The successful design of an analytical VLE experiment requires, in addition to the identification of the key system variables, a formulation of strategies to address existing or potential challenges that might be experienced during the course of the experiment. The relative difficulty in the design of VLE experiments, in addition to phenomenological occurrences such as azeotropic behaviour, chemical association in the vapour phase, phase splitting, thermally-induced polymerization and decomposition, is dependent upon the operating conditions (temperature, pressure). It also depends on nature of the chemical systems under study, measurements to be undertaken (P-T-x-y), number of components in the system (binary or multi-component) and the composition range to be studied (dilute or finite composition ranges) (Reddy 2006).

The nature of the chemical components to be studied should be investigated thoroughly beforehand from both a safety and practical standpoint. The health and the safety of the experimenter is their first personal responsibility. It is also important to minimize hazards to the immediate environment. Material and safety data sheets (MSDS) are an important source of information on the potential hazards in the handling of chemicals with regards to acute and chronic toxicity, corrosiveness, flammability and permissible exposure limits to laboratory and research chemicals, etc. In terms of

the actual measurement procedure for chemicals, the thermal sensitivity, hygroscopic nature, photostability, oxidative stability, etc. of the chemical components can compromise the accuracy of the VLE measurements. Measurements on n-alkanes (Morgan and Kobayashi, 1994), alkenes (Joyce at al., 1991), polynuclear aromatic hydrocarbons (Sivaraman and Kobayashi, 1982; Gupta et al., 1991) and chemically associating oxygenates such as carboxylic acids (Prausnitz et al., 1980; Gess et al., 1991), together with the highly non-ideal alkane and alcohol mixtures (Oh et al., 2004) have traditionally been classes of compounds for which difficulty has been experienced in obtaining reliable phase equilibrium data. Measurements on the high molecular weight aliphatic and aromatic compounds have been plagued by thermal decomposition and polymerization while hydrogen bonding and association in the vapour phase have equally affected those of oxygenated organic compounds (Reddy, 2006).

## 5.1 Preparation of the experimental apparatus and the chemical systems

The preparation of the apparatus for vapour pressure or VLE measurements is a crucial exercise to ensure the efficient operation of the VLE still during the experimental run, upon which the accuracy of the measured thermodynamic variables for the system hinges. Leaks have become a concern during experimental data measurement, the effect which is not only limited to uncertainties in the measured temperatures and pressures, but the loss of material from the system through a leak (especially in the equilibrium chamber or sample traps) can adversely affect the phase composition measurements.

In the leak-testing procedure, the apparatus is pressurized (up to about 0.6 MPa) and a surfactant-based liquid leak detector, such as the commercially available formulation, Snoop®, is applied to the various tube fittings, gaskets and other seals in the apparatus. The existence of a leak can be easily detected in the form of the bubbling of the surfactant as a result of a leak in the fitting. After the leak test, a low-boiling solvent, pentane, was run through the system to remove contaminants since the commonly used solvent acetone is incompatible with the o-rings in the sample traps. The most volatile of the components under study in the binary VLE mixture was used as the “cleaning” solvent. After the solvent is circulated throughout the apparatus for approximately 10 hours, the still is drained to remove most of the effluent. The VLE apparatus is then evacuated to about 1kPa, heated slightly (~323.15K) and left overnight to remove trace amounts of the solvent (Reddy 2006).

The chemical systems under study in this work were non-acid chemicals (alcohols) and carboxylic acids (butyric acid to be precise). The refractive index of the components were measured at 293.15

K on an ATAGO® 7000 α refractometer and then compared with literature, after which the purities of the compounds were analyzed by gas chromatography analysis to ensure that the purity was in accordance with that stated by the supplier. In the event that the substance was not obtainable in sufficient purity or found to contain significant impurities, purification procedures were necessitated.

With the removal of contaminants and the elimination of system leaks, the apparatus was then deemed fit to be employed for the measurement of vapour pressures or vapour-liquid equilibria. The validation of the purity of the chemicals and the necessity of the purification steps ensured that erroneous phase equilibrium measurements would not be obtained as result of questionable purities of the substances investigated for the experimental determinations in the study (Reddy, 2006).

## 5.2 Calibration of the pressure and temperature sensors

For any measurement and possible designs to be effected using VLE data set, accurate measurement of the system pressure and temperature is important and since the equilibrium temperature sensor calibration is dependent on the system pressure, the pressure calibration had to be done first. Also, the calibration of the system variables in the VLE apparatus is equally important since the accuracy of the measured data depends directly on the precision of the various calibrations. The accuracies of the pressure transducer were estimated as ±0.02 kPa and ±0.03 kPa for the stainless steel and glass still respectively. It was controlled to within 0.01 kPa for isobaric operation while the accuracy of the measured temperature was estimated to be within ±0.02 K for both the glass still and the stainless steel apparatus and the accuracy of the temperature control varied between 0.01 and 0.05 K.

The electronic pressure sensors used are calibrated by comparing the pressure readings from the Sensotec Super TJE pressure transducer with those displayed on the CPH6000 with an accuracy of ±0.001 kPa with that of the WIKA pressure transducer to be calibrated. This was achieved by connecting both sensors to a common pressure manifold in a leak-free system and varying the system pressure until the calibration has been achieved for the desired pressure range through a comparison of the two readings. A linear plot of “actual pressure” versus “displayed pressure” completed the calibration.

The “in-situ” technique for temperature calibration was employed where the Pt-100 temperature sensor was used to measure the system. The Pt-100 resistance was displayed on an Agilent model 34401A 6 ½ digit multimeter, with the graphical user interface reflecting the true temperature

calculated from the Pt-100 resistance using the temperature versus resistance calibration curve. For the temperature calibration, the still was operated isobarically over a range of pressure using a pure component. At each pressure setting, the equilibrium (plateau) region was obtained and the resistance of the sensor was recorded. The actual temperature corresponding to that predicted from the Antoine equation (for the test chemicals with coefficients obtained from Dortmund Data Bank Software 2009) was then compared to the temperature output. This temperature reading (Kelvin) was obtained using a calibration equation on the multimeter to convert the temperature in ohms to Kelvin.

Calibration charts of the temperature versus resistance relationship for a Pt-100 sensor were used for the remaining temperature sensors in the apparatus since these were qualitative measurements.

The calibration of the sensor was carried out using two pure components, one low boiling and the other high boiling for the stainless steel apparatus. The use of the two chemicals (ethanol and n-heptane) was to ensure that a large range of temperatures in which the experiment will be performed was covered. Also, the temperature calibration for the glass still was carried out using 2-butanol and 2-methyl-1-propanol. As in the case above for the pressure transmitter calibration, a plot of the resistance against the actual temperature gave the desired relationship.

## 5.3 Operating procedure

In the operating procedure, the ballast tank was isolated from the high-pressure source and the vacuum pump was switched on. The control valve on the by-pass loop on the vacuum line was then opened to allow for the rapid evacuation of the ballast and the VLE still. The pressure control system was not employed so the "normally closed" solenoid valves had not been activated yet. After evacuation of the ballast had been achieved by monitoring the pressure readings from the respective displays, the vacuum line was isolated from the ballast.

Nitrogen gas was then fed slowly, using the by-pass loop control valve into the VLE still via the ballast. The valve is turned off when the nitrogen supply reached the desired sub-atmospheric pressure and the vacuum pump is switched on in order to draw the liquid mixture into the still via the drain/fill valve on the reboiler. It is important that the vacuum used be higher than the vapour pressure of the components at the temperature of the still to prevent the occurrence of the flashing during the introduction of the material into the still (Reddy 2006).

The capacity of the VLE still is approximately 170- 180 ml and this is slightly varied with regards to the pressure and temperature range (as affecting the density of the vapour phase), the thermophysical properties of the chemical components (thermal expansivities, volatilities, etc.) and the circulation rate as controlled by the heat input into the still. The material was fed slowly into

the reboiler until the liquid level was just above the glass insert in the Cottrell tube. After the liquid mixture had been charged to the still, the power supply for the stirrer was switched on and a suitable current input determined an optimal stirring rate for the reboiler contents. The internal and external heaters for the reboiler and the external heater of the equilibrium chamber were then turned on and initial heating was at a low voltage input (usually 20V) which was read from a multimeter connected to the respective Chuan Hsin (Model: SRV-10) variable-voltage transformers (0 - 240 V)(Reddy, 2006). The desired pressure was manually set with the by-pass loop control valves on both the low-pressure and the high- pressure input sides. With the pressure controlled, the temperature of the contents of the reboiler and the boiling characteristics of the mixture were monitored as a function of heat input in the form of small (~10V) energy increments into the VLE still heaters from the variable- voltage resistors. The Pt-100 sensor in the reboiler was used to monitor the temperature and was read off a RKC temperature controller display (Model: CB-40). At the same time, the temperature of the equilibrium chamber was monitored on the same display as the reboiler temperature sensor to ensure it was not heated too rapidly. When continuous boiling of the mixture was observed in the Cottrell tube, coupled with a steady flow of the liquid and vapour condensate phases in the respective traps, the heat input was maintained and the system was left to stabilize.

One of the aims of this project was to be able to measure the VLE data for the carboxylic acid-alcohol binary mixture with the possibility of avoiding the ester and water formation. This was actually a challenge on the course of this research as the reaction was observed to take a longer time to form at temperatures of 333.15 and 353.15 K, but much quicker at temperatures above 373.15 K. During the project, the VLE apparatus had to be drained several times for the carboxylic acid-alcohol mixtures and fresh chemical used due to such formations observed in the vapour phase. Effort was also made to monitor the systems overnight while liquid and vapour compositions withdrawn are analysed on the gas chromatograph whenever the system is believed to be at equilibrium without allowing the mixtures to stay too long together at equilibrium. Hence, through this method, the measurements could be achieved at the various isotherms without the formation of esters and water.

### 5.3.1 Isobaric Operation

The cooling coil unit and the pump for the Labotech water bath were first switched on to allow the ethylene glycol solution to reach a sufficiently low temperature (about 268.15 K). It is important to mention that the ethylene glycol/water mixture should be mixed in the correct ratio in order to achieve the desired cooling capacity and not to waste the chemical as the ethylene glycol is an expensive chemical compared to water. Once this temperature was achieved, the power supply to the temperature and pressure displays, the pressure controller were then switched on. The clean still

was then charged with only one of the pure components, until the liquid filled was visible to a level ± 4 cm in the Cottrell tube. The vacuum pump was then switched on for operations below atmospheric pressure and the pressure controller was set to the desired operating pressure. At this point, the pressure in the still decreased towards the set-point pressure.

The internal and external heaters, as well as the motors for the stirrers were then switched on to bring the liquid in the reboiler to a boil, where the internal heater provided the principal heating and the external heater for the reboiler and equilibrium chamber compensated for heat losses to the environment. It is important that adequate heat be applied to achieve a vigorous pumping action in the Cottrell tube and a good circulation rate, where the circulation rate is determined by observing the drop rate in the condenser. The power supplied from the internal heater to the still was then increased until the plateau region was found. According to Kneisl et al. (1989), this is the region where the boiling temperature does not change for a slight increase in the power input. Kneisl et al. (1989) also found the boiling temperature to be a function of the power input. Thus, operation in the plateau region is critical, as operation outside this region gives rise to incorrect boiling point temperatures. Once operation in the plateau region was achieved, the system was allowed to reach equilibrium, at which point the temperature and composition are constant. For most systems, equilibrium is attained within thirty minutes. However, for the systems measured in this work, an equilibration time as long as five hours was found to be required for measurement with the stainless still, but the equilibrium is achieved within 45 minutes for the glass still. Investigation is still being made as to why such a long equilibration time is required for the stainless still.

Once equilibrium had been established, the temperature was then noted. For VLE systems, the liquid and vapour samples were then withdrawn through the sample septa using a gas-tight liquid syringe and analysed by gas chromatography. Sample injections for each phase were made into the GC to obtain the compositions, were an average deviation for the area ratios within a tolerance of 0.001 was used.

To determine the VLE curves, the following steps were followed:

1. Drain off the condensed vapour (about 2 ml) and enough liquid from the liquid trap such that the total volume removed is about 4 ml. Condensate and liquid trap samples are collected in separate vial for GC analysis.
2. Add about 4 ml of the higher boiling compound to the still via the liquid sample trap, and let the system come to a new equilibrium as evidenced by a stable temperature and a continuous recirculation of the condensed vapour to the reboiler.

3. The new mixture was allowed to reach equilibrium and the liquid and vapour samples is withdrawn for GC analysis thereafter. The criteria discussed for establishing equilibrium are applied. It is critical that the system be at equilibrium for data to be valid. One cannot rush through the experiment – this will lead to invalid data points.
4. The samples were analyzed using the Gas chromatograph.

This procedure was repeated for steps 1 - 4 until sufficient data was measured to cover the entire composition range.

At high pressures, the vacuum pump was disconnected from the low-pressure side and atmospheric pressure was used to correct the system pressure fluctuations by serving as a vent.

### 5.3.2 Isothermal Operation

Isothermal operation of the still was dependant on the successful operation of the still under isobaric mode, as the isothermal operation was manually controlled. Therefore, the operating procedure is the same as for isobaric operation. The pressure in the still was first set to a value such that when equilibrium was reached, the equilibrium temperature was close to the desired set-point temperature. The isobaric operation was then stopped and the temperature was manually adjusted to its desired value, where increasing or decreasing the pressure had the effect of increasing or decreasing the temperature respectively. Once the desired temperature was found, the plateau was then found and the pressure corresponding to the desired temperature was noted. Liquid and vapour samples were then withdrawn and analysed in the same manner as for the isobaric operation.

## 5.4 Determination of equilibrium

The most frequently used criterion for judging the equilibrium condition is that of stability of the equilibrium temperature (in isobaric operation) or system pressure (in isothermal operation) as a function of time and heat input. The attainment of a “plateau region” corresponds to the drop rate (Rogalski and Malanowski, 1980) or heat input (Kneisl et al., 1989) which results in the flattening of the curve of the variation of the pressure or temperature of the system as a function of heat input into the reboiler.

The typical system behaviour for the VLE of a mixture as a function of temperature in an isobaric determination is shown in Figure 5.1, where the region A-B corresponds to the “plateau region”. The sensitivity of the sensors and the analytical technique is crucial in ascertaining the “plateau region”.

The determination of the equilibrium condition in this study was based on the satisfaction of two criteria in the form of the following:

(a) The attainment of a *plateau region* for the system temperature (isobaric mode) or pressure (isothermal mode) as a function of small voltage increments (~ 5 V) from the variac into the reboiler internal heater. With each voltage increment, the system was allowed a response time of 10 to 15 minutes before the next voltage increment. When a stable pressure or temperature reading was recorded as a function of energy input for a satisfactory time or voltage increment period, the first of the two principle criteria for the determination of the equilibrium condition was satisfied (Reddy 2006).

(b) The observation of the *fluid flow* characteristics of the system was used as a purely qualitative criterion. With the initiation of steady state boiling, the fluid flow dynamics of the phases in the Cottrell tube and the sample traps was observed as a function of energy input into the still. The Cottrell tube was observed to ensure that there was a continuous and steady "pumping" of slugs of vapour and liquid up the Cottrell tube. The drop rate and flow patterns of the equilibrium phases were monitored. It is imperative that the equilibrium temperature be independent of the circulation rate (as a function of heat input) for internal consistency in the apparatus (Yerazunis et al., 1964). This was constantly monitored throughout the run.

For the determination of the vapour pressure measurements for the pure components, the two points are important. Equilibrium times of around 20 - 30 minutes were typically achieved for the operation of the apparatus.

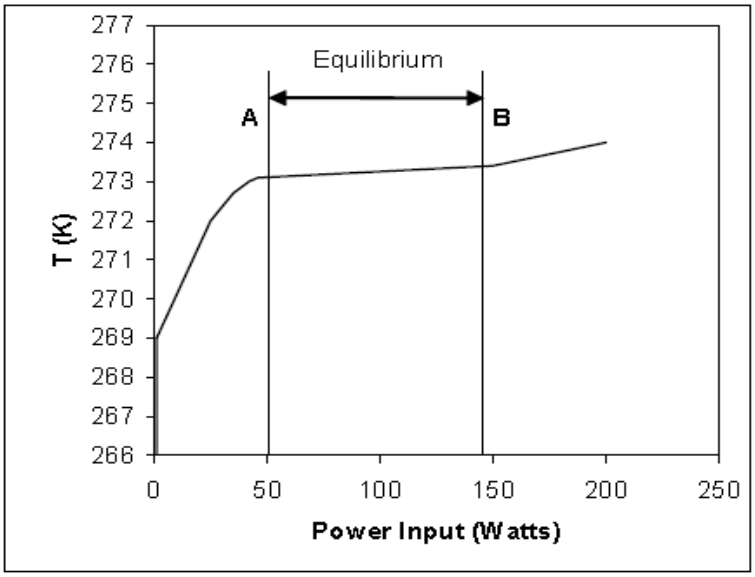


**Figure 5-1: Plot of the temperature as a function of power input to indicate the attainment of the plateau region for the system temperature (isobaric mode) (Reddy 2006).**

## 5.5 Analytical technique for the phase composition determinations

The analysis of the phases was performed using a Shimadzu GC-2010 gas chromatograph, which was equipped with capillary column injection ports and thermal conductivity detector. The data acquisition and control of the gas chromatograph parameters were achieved with a Shimadzu GCsolution® software interface on a Proline personal computer. This was linked to the inbuilt communications bus module in the Shimadzu gas chromatograph via serial port communication. The software interface is shown in Figure 5.2. The use of the interface allowed for the development of methods by programming the injector, column and detector temperatures, setting the column flow rate, setting experimental run times, etc. The data acquisition system allowed for the real time logging of the data, which could be stored as an output file for post-run analysis, as shown in Figure 5.3.

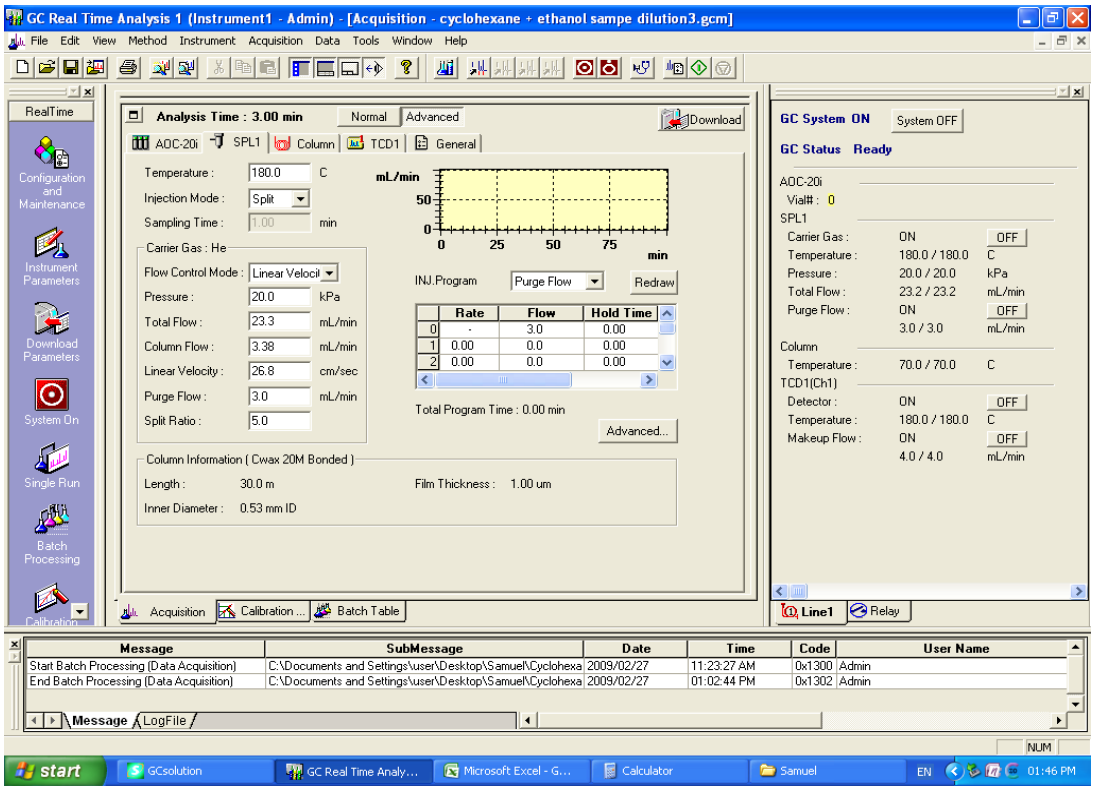


**Figure 5-2: Control interface for the Shimadzu GC 2010 solution® software.**

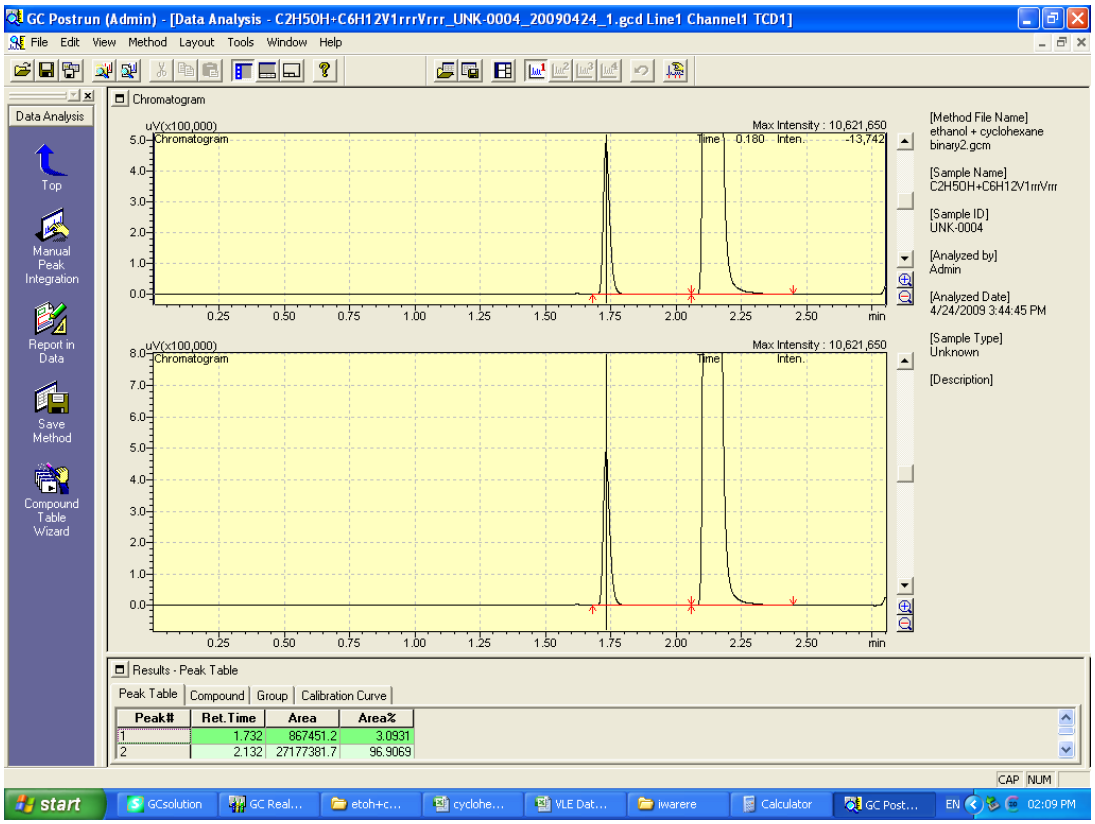


**Figure 5-3: Post-run analysis of the chromatograms.**

The column was preconditioned prior to use to remove any traces of solvents or any other contaminants as the latter can contribute to "ghost peaks" appearing in the chromatograms and affect the column performance. The presence of "ghost peaks" can adversely affect the quantitative analysis, especially when these peaks overlap with those for solutes that are to be determined. The conditioning procedure was conducted by heating the column to a temperature 10 $^{o}$C below that of the column maximum temperature and leaving the gas chromatograph to run overnight with a steady flow of helium gas flowing through the column. The column fitting on the detector port was disconnected during this procedure to prevent the contamination of the detector.

The calibration procedure used for the gas chromatographic detector was the chromatogram area ratio method described by Raal and Mühlbauer (1998). The method describes the use of area ratios for the determination of the response factors, which can then be used for a quantitative analysis.

The response factor is the proportionality constant for the relationship between the mole fractions of a component injected in the column and the corresponding response of the detector in the form of an area on a chromatogram.

For a binary mixture, the response factor can be represented as follows:

$$\frac{n_1}{n_2} = \left(\frac{A_1}{A_2}\right)\left(\frac{F_1}{F_2}\right) = \frac{x_1}{x_2} \tag{5.1}$$

The response factor ratio, $F_1/F_2$, is obtained from the plot of $A_1 / A_2$ versus $x_1 / x_2$ over the full composition range and should extrapolate through the origin. A refers to the area of component 1 or 2 and x to the composition (mole) of component 1 or 2.

Equation (5.1), indicates that the response factor ratio, $F_1/F_2$, is necessarily constant for a linear plot of $A_1 / A_2$ versus $x_1 / x_2$ and is obtained as the slope of this plot. Furthermore, the inverse of the slope for the linear plot of $A_2/A_1$ versus $x_2 / x_1$ should equal to $F_1/F_2$ (i.e. $F_1/F_2$ should equal the inverse of $F_2/F_1$ and vice versa. The shape of the calibration plots depend on the detector type and the system under investigation. Therefore, non-linear plots are not uncommon, especially for thermal conductivity detectors. However, these plots should also pass through the origin.

After the analysis has been concluded, the Shimadzu GC-2010 gas chromatograph unit, the injector, column and detector were cooled to approximately 303.15 K with a constant flow of helium carrier gas. The gas flows from the respective cylinders were turned off, the GCsolution® program was closed and the gas chromatograph was turned off.

## 5.6 Shut-down procedure

To ensure that the VLE apparatus and the auxiliary equipment are properly shut down, it is important to discuss the systematic approach used to effect these.

The Shinko pressure control program interface was closed and the system was maintained at the current pressure value whilst the mixture cooled. This was achieved by terminating the heat input into the still by switching the variacs off. For sub -atmospheric operation, the polyflow tubing was removed from the quick connect fitting on the vacuum side. The vacuum pump was turned off after being opened to atmosphere to prevent a build-up of an internal vacuum in the pump causing the pump oil to be sucked into the gauge.

After sufficient cooling of the reboiler and the equilibrium chamber had occurred, (from the temperature readings of the respective Pt-100 sensors), the VLE apparatus was then depressurized (if $P_{system}$ was greater than 150 kPa ) or pressurized (if $P_{system}$ was less than 90 kPa). For the former, this was achieved by bleeding through one of the by-pass loop control valves from the ballast. In the case of the latter, nitrogen gas was supplied to equalize the pressure with that of atmospheric

pressure. The contents of the still were then drained using the drain/fill valve of the reboiler and safely disposed off in designated waste bottles (Reddy 2006).

## 5.7 Operation of the glass VLE Still

The experimental procedure stated by Clifford (2003) in his thesis was adopted for the VLE glass apparatus. This is similar to the operation of the stainless steel recirculating cell.

CHAPTER
6

# EXPERIMENTAL RESULTS

The experimental procedure presented in Chapter 5 was derived after numerous runs were carried out on two test systems. The test systems were measured to ensure that the VLE still was operating correctly and that the method used for obtaining the experimental data was satisfactory. These test systems consisted of the cyclohexane (1) + ethanol (2) system at 40 kPa and 150 kPa which was measured on the stainless steel apparatus. While the cyclohexane (1) + ethanol (2) system at 40 kPa has reliable literature data against which data can be compared, the test system at 150 kPa has no published literature data that could be used as a reference. The systems were measured below atmospheric pressure (40 kPa) and above (150 kPa) because the new systems in this study were measured at a similar pressure and temperature range. The systems are completely miscible across the entire VLE composition range and also include an azeotrope.

Equilibrium data were measured for the two test systems mentioned above and the results obtained were compared to literature data. This chapter presents the results for the test systems and new systems measured during this project. The analysis and discussion of the data will be dealt with in Chapter 7. In order to satisfactorily confirm the accuracy of the measured data, the purities of the components must be determined (Section 6.1), after which the components vapour pressure measurements are presented. Vapour-liquid equilibrium data were obtained for three binary systems: 2-Propanol (1) +Butyric acid (2), 2-Butanol (1) + Butyric acid (2) and 2-Methyl-1-propanol (1) + Butyric acid (2) which has not been previously measured.

## 6.1 Chemical Purity

All the chemicals used in the test systems were liquids at room temperature and pressure. They were all purchased from Merck and purity was verified by GC analysis, following the method of Raal and Mühlbauer (1998) and refractive index measurements. The GC analysis gave no

significant impurities and the chemicals were thus used without further purification. Table 6-1 gives the nominal purities of the test chemicals as well as the chemicals for the new systems together with literature values of the refractive indices. The refractive index of the systems used was measured on an ATAGO ® Refractometer RX-7000 α at a target temperature of 293.15K. The accuracy of the refractometer is ±0.01. The literature refractive index is reported for temperature at 293.15 K.

| **Reagent** | **Refractive Index** | | **G C Analysis (Peak Area %)** | **Min. Purity specified by Supplier(Mass %)** [b] |
|---|---|---|---|---|
| | *Exp* | *Ref** | | |
| **Ethanol** | 1.3613 | 1.3611 | 100 | ≥ 99.5 |
| **Cyclohexane** | 1.4267 | 1.4266 | 100 | ≥ 99.5 |
| **2-Propanol** | 1.3774 | 1.3776 | 100 | ≥ 99.8 |
| **2-Butanol** | 1.3973 | 1.3975 | 100 | ≥ 99.5 |
| **2-Methyl-1-Propanol** | 1.3958 | 1.3955 | 100 | ≥ 99.0 |
| **Butyric Acid** | 1.3982 | 1.3980 | 100 | ≥ 99.5 |

**Table 6-1: Chemical purities and Refractive indices**

[*] Weast et al., (1984) [b] As stated by the supplier

## 6.2 Calibration of sensors

The calibration of the temperature sensors, as well as the pressure transducers was undertaken and the procedure discussed in section 5.2 under the experimental procedure in chapter 5. The plots of the pressure and temperature calibration are presented below in Figure 6-1 to 6-5 respectively. The plots presented in Figure 6-6 to 6-7 represent the deviation between the measured actual pressure of the transducer and the calculated pressure. For the temperature sensor, the actual temperature value was found to be approximately the same with the calculated. Thus, a deviation plot is not presented.

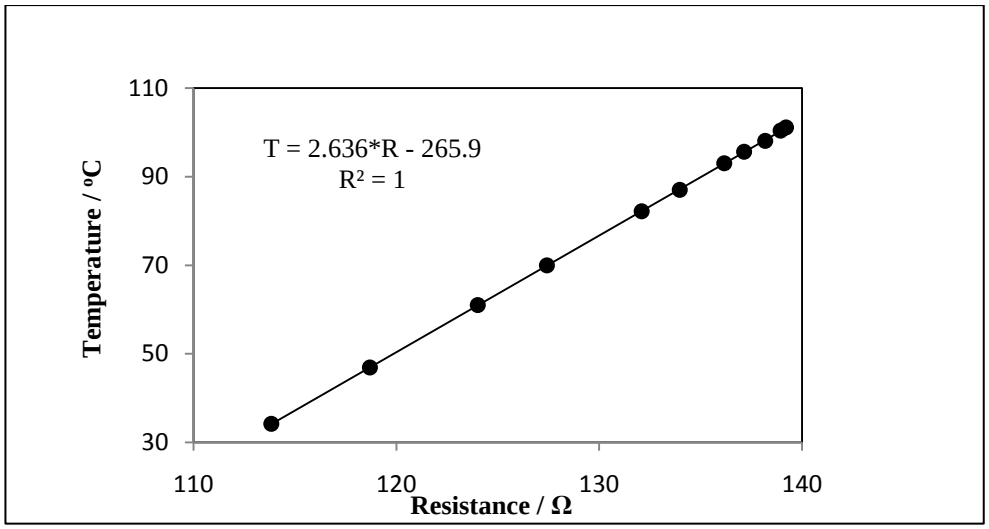


**Figure 6-1: Temperature calibration of the temperature sensor (Pt100) for the stainless steel VLE apparatus**

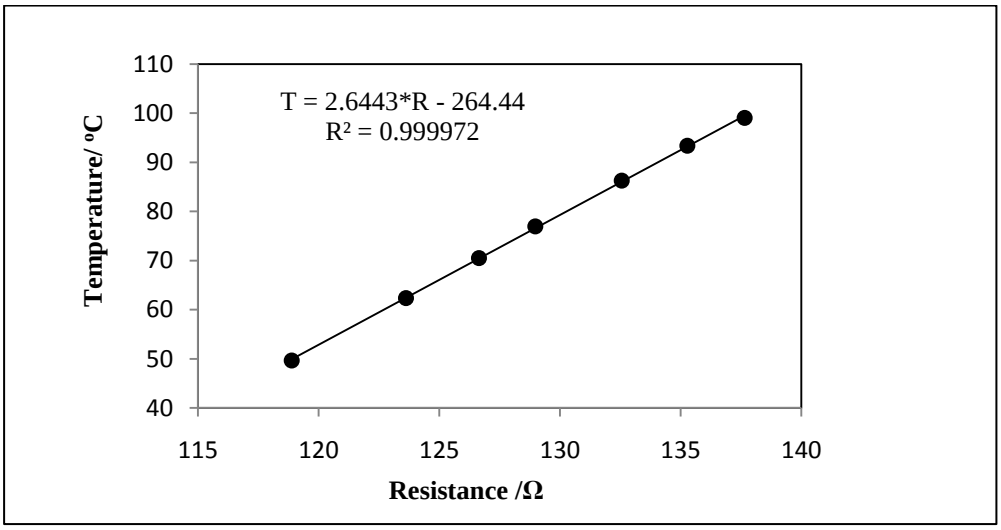


**Figure 6-2: Temperature calibration of the temperature sensor (Pt100) for the glass VLE apparatus.**

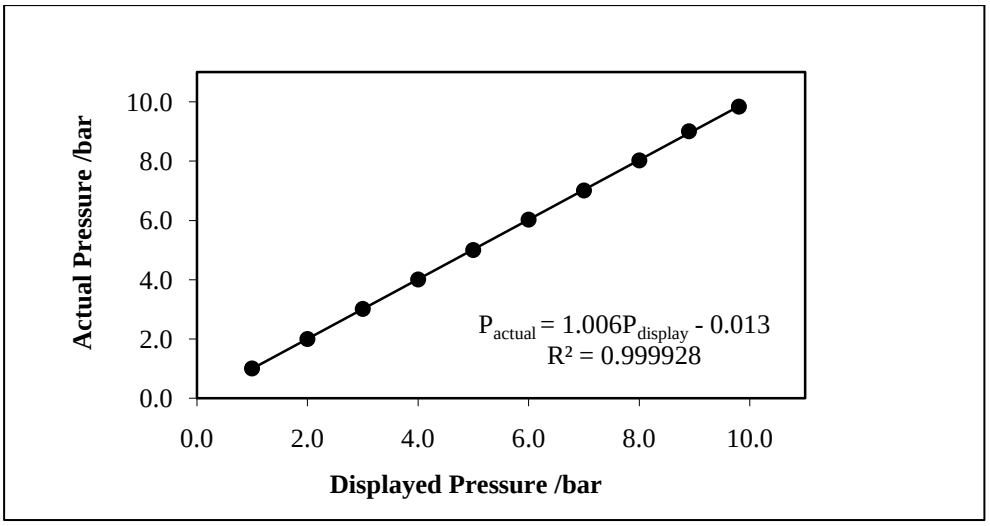


**Figure 6-3: Pressure calibration of the transducer for the stainless steel VLE apparatus.**

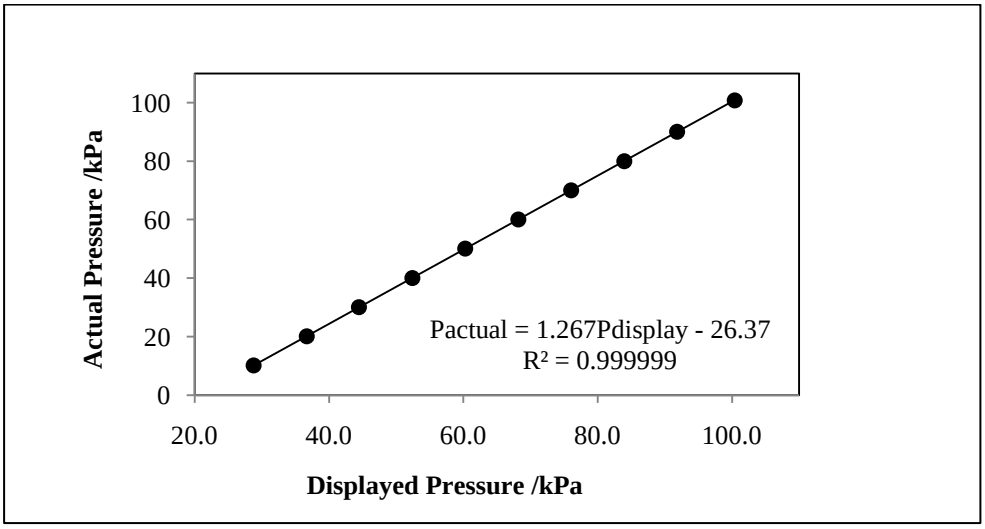


**Figure 6-4: Pressure calibration of the transducer for the glass VLE apparatus**

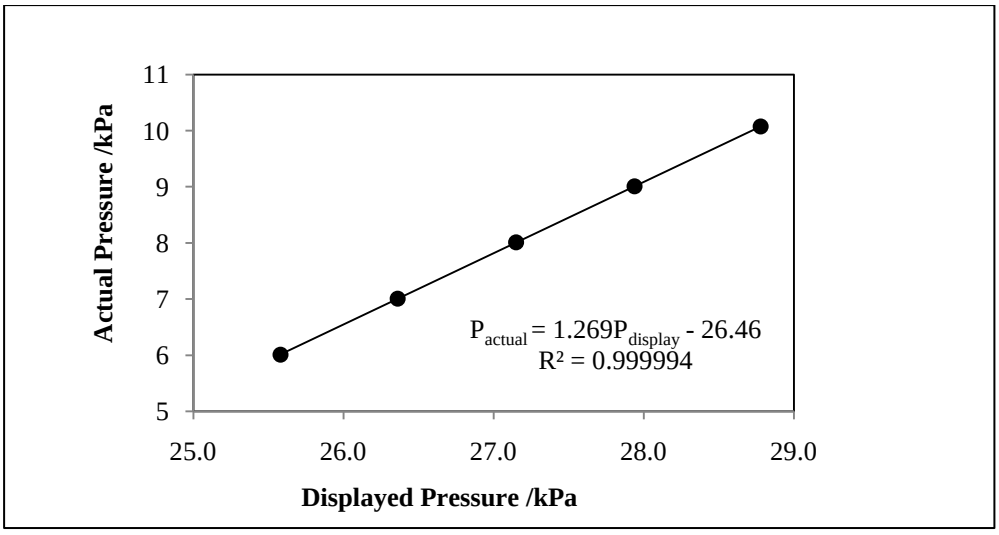


**Figure 6-5: Pressure calibration of the transducer for the glass VLE apparatus**

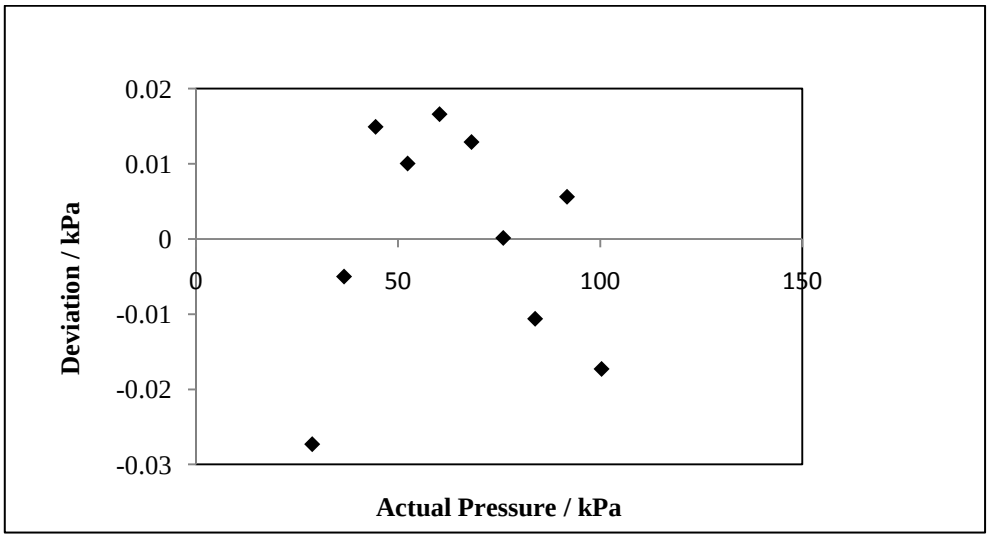


**Figure 6-6: Plot of the deviation between the actual and calculated pressure versus the actual pressure calibration of the Transducer for the glass VLE apparatus.**

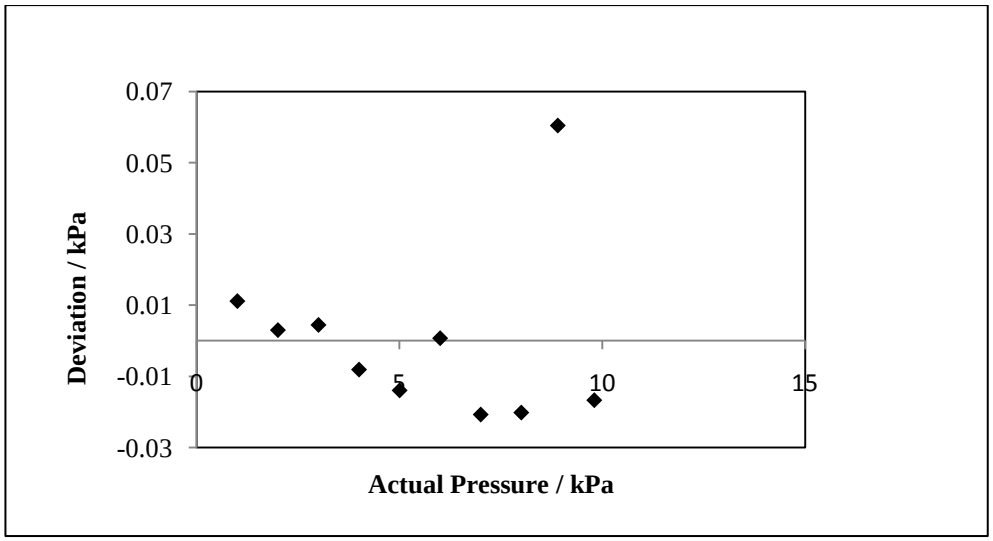


**Figure 6-7: Plot of the deviation between the actual and calculated pressure versus the actual pressure calibration of the Transducer for the stainless-steel VLE apparatus.**

## 6.3 Vapour pressures

The vapour pressures were the first to be measured for all the chemicals used. These are presented in Tables 6-2 to 6-7 and plotted as a residual plot in Figures 6-10 to 6.17. The vapour pressure data were regressed to obtain parameters for both the Antoine and Wagner (1988) equations. The differences between the experimentally measured pressures and the predicted pressures are given by

$$\left|\Delta P_i\right| = P_{experimental} - P_{calculated} \tag{6.1}$$

while the deviation between the experimental and calculated pressure is in the form of average absolute relative deviation (AARD).

$$\Delta P_{avg} = \frac{1}{n}\sum_{i}^{n}\frac{\left|P_{\exp} - P_{calc}\right|}{P_{\exp}} \tag{6.2}$$

| T /K | P/ kPa | $\Delta P_{Wagner}$/kPa | $\Delta P_{Antoine}$/kPa | $\Delta T_{Antione}$/K |
|---|---|---|---|---|
| 315.78 | 20.12 | 0.0014 | 0.0089 | 0.0002 |
| 323.74 | 30.19 | 0.0019 | 0.0028 | 0.0000 |
| 329.68 | 40.26 | 0.0000 | 0.0047 | 0.0002 |
| 338.55 | 60.39 | 0.0013 | 0.0004 | 0.0003 |
| 345.32 | 80.53 | 0.0009 | 0.0035 | 0.0000 |
| 351.10 | 100.7 | 0.0002 | 0.0014 | 0.0011 |
| **AAD** | | **0.0010** | **0.0036** | **0.0003** |

**Table 6-2: Vapour Pressure data for Ethanol**

| T /K | P/ kPa | $\Delta P_{Wagner}$/kPa | $\Delta P_{Antoine}$/kPa | $\Delta T_{Antione}$/K |
|---|---|---|---|---|
| 308.91 | 20.39 | 0.0015 | 0.0083 | 0.0016 |
| 325.75 | 40.39 | 0.0033 | 0.0058 | 0.0000 |
| 337.17 | 60.36 | 0.0037 | 0.0031 | 0.0001 |
| 346.07 | 80.43 | 0.0021 | 0.0061 | 0.0000 |
| 354.13 | 100.4 | 0.0004 | 0.0021 | 0.0022 |
| **AAD** | | **0.0022** | **0.0051** | **0.0008** |

**Table 6-3: Vapour pressure data for Cyclohexane**

| T /K | P/ kPa | $\Delta P_{Wagner}$/kPa | $\Delta P_{Antoine}$/kPa | $\Delta T_{Antione}$/K |
|---|---|---|---|---|
| 307.48 | 10.07 | 0.0186 | 0.0032 | 0.0000 |
| 320.29 | 20.13 | 0.0070 | 0.0086 | 0.0003 |
| 334.30 | 40.27 | 0.0044 | 0.0010 | 0.0001 |
| 343.26 | 60.41 | 0.0009 | 0.0032 | 0.0003 |
| 355.56 | 100.7 | 0.0047 | 0.0047 | 0.0003 |
| 360.48 | 120.8 | 0.0040 | 0.0045 | 0.0004 |
| 366.27 | 151.0 | 0.0021 | 0.0014 | 0.0000 |
| 368.85 | 166.1 | 0.0032 | 0.0027 | 0.0001 |
| 371.60 | 181.2 | 0.0087 | 0.0088 | 0.0008 |
| 373.56 | 196.3 | 0.0020 | 0.0022 | 0.0000 |
| 374.27 | 201.4 | 0.0023 | 0.0028 | 0.0000 |
| **AAD** | | **0.0052** | **0.0039** | **0.0002** |

**Table 6-4: Vapour pressure data for 2-Propanol**

| T /K | P/ kPa | $\Delta P_{Wagner}$/kPa | $\Delta P_{Antoine}$/kPa | $\Delta T_{Antione}$/K |
|---|---|---|---|---|
| 322.66 | 10.40 | 0.0082 | 0.0268 | 0.0000 |
| 335.50 | 20.67 | 0.0113 | 0.0048 | 0.0000 |
| 343.81 | 30.62 | 0.0030 | 0.0112 | 0.0006 |
| 349.93 | 40.64 | 0.0028 | 0.0070 | 0.0002 |
| 354.89 | 50.47 | 0.0037 | 0.0042 | 0.0000 |
| 359.07 | 60.61 | 0.0047 | 0.0066 | 0.0007 |
| 363.03 | 70.63 | 0.0001 | 0.0028 | 0.0003 |
| 366.43 | 80.54 | 0.0016 | 0.0040 | 0.0003 |
| 369.81 | 90.66 | 0.0033 | 0.0029 | 0.0004 |
| 372.54 | 100.2 | 0.0013 | 0.0011 | 0.0004 |
| **AAD** | | **0.0040** | **0.0071** | **0.0003** |

**Table 6-5: Vapour pressure data for 2-Butanol**

| T /K | P/ kPa | $\Delta P_{Wagner}$/kPa | $\Delta P_{Antoine}$/kPa | $\Delta T_{Antione}$/K |
|---|---|---|---|---|
| 319.63 | 5.85 | 0.0314 | 0.0429 | 0.0000 |
| 329.84 | 10.59 | 0.0253 | 0.0337 | 0.0007 |
| 343.29 | 20.57 | 0.0071 | 0.0063 | 0.0007 |
| 352.12 | 30.57 | 0.0168 | 0.0261 | 0.0016 |
| 357.80 | 40.20 | 0.0021 | 0.0019 | 0.0000 |
| 363.20 | 50.69 | 0.0034 | 0.0038 | 0.0004 |
| 367.65 | 60.66 | 0.0021 | 0.0048 | 0.0005 |
| 371.52 | 70.52 | 0.0022 | 0.0056 | 0.0005 |
| 375.25 | 80.54 | 0.0039 | 0.0014 | 0.0000 |
| 378.28 | 90.08 | 0.0004 | 0.0000 | 0.0000 |
| 381.46 | 100.7 | 0.0010 | 0.0020 | 0.0002 |
| **AAD** | | **0.0087** | **0.0117** | **0.0004** |

**Table 6-6: Vapour pressure data for 2-Methyl-1-Propanol**

| T /K | P/ kPa | $\Delta P_{Wagner}$/kPa | $\Delta P_{Antoine}$/kPa | $\Delta T_{Antione}$/K |
|---|---|---|---|---|
| 375.60 | 10.51 | 0.0176 | 0.0296 | 0.0000 |
| 390.60 | 20.46 | 0.0036 | 0.0045 | 0.0016 |
| 401.32 | 30.34 | 0.0281 | 0.0168 | 0.0002 |
| 408.30 | 40.63 | 0.0129 | 0.0191 | 0.0020 |
| 414.54 | 50.71 | 0.0195 | 0.0207 | 0.0019 |
| 420.07 | 59.52 | 0.0051 | 0.0077 | 0.0003 |
| 425.54 | 70.67 | 0.0128 | 0.0163 | 0.0011 |
| 429.08 | 80.57 | 0.0037 | 0.0008 | 0.0000 |
| 432.79 | 90.57 | 0.0015 | 0.0010 | 0.0001 |
| 436.03 | 100.4 | 0.0003 | 0.0035 | 0.0000 |
| **AAD** | | **0.0105** | **0.0120** | **0.0007** |

**Table 6-7: Vapour pressure data for Butyric Acid**

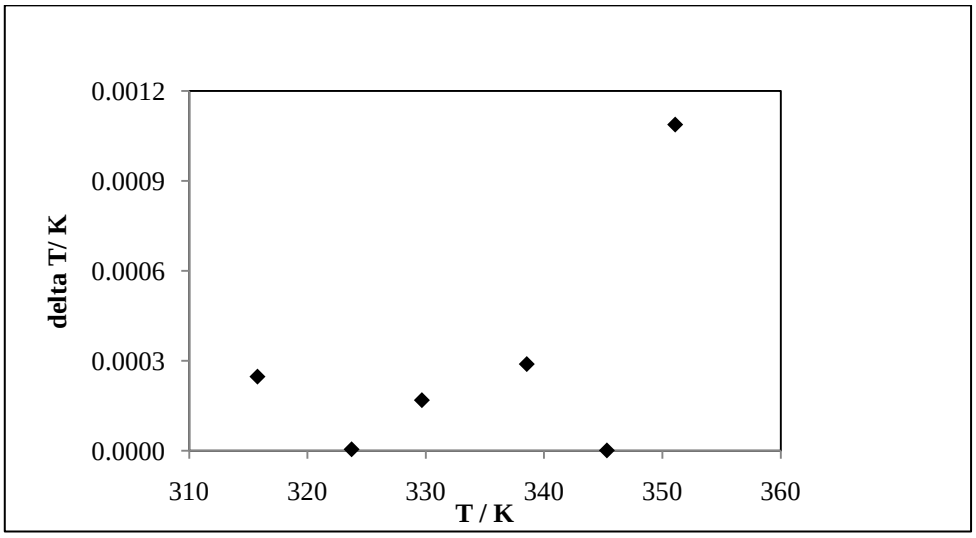


**Figure 6-8: Plot of the average absolute deviation between experimental and calculated temperature (delta T) versus the experimental temperature (T/ K) for Vapour pressure data of Ethanol**

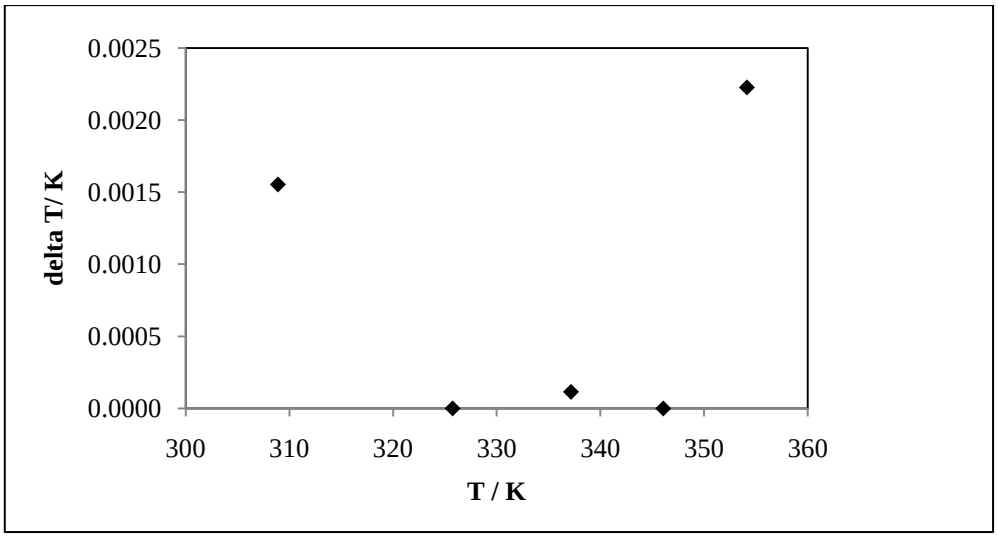


**Figure 6-9: Plot of the average absolute deviation between experimental and calculated temperature (delta T) versus the experimental temperature (T/ K) for Vapour pressure data of Cyclohexane.**

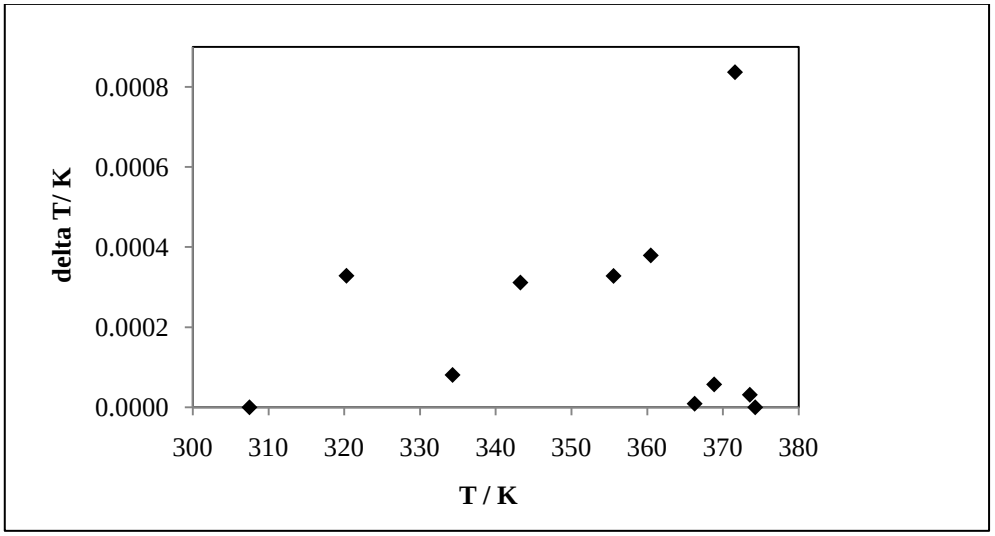


**Figure 6-10: Plot of the average absolute deviation between experimental and calculated temperature (delta T) versus the experimental temperature (T/ K) for Vapour pressure data of 2-Propanol.**

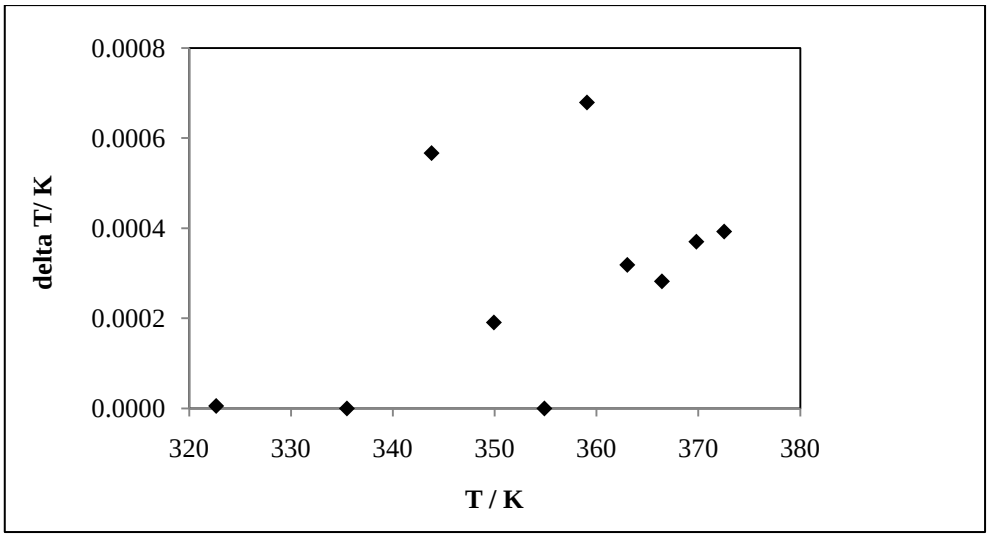


**Figure 6-11: Plot of the average absolute deviation between experimental and calculated temperature (delta T) versus the experimental temperature (T/ K) for Vapour pressure data of 2-Butanol.**

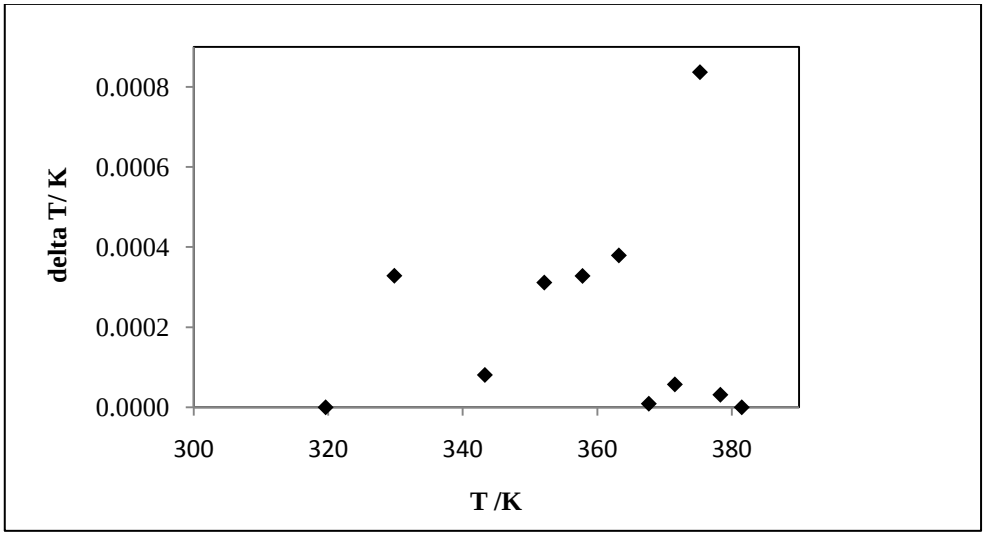


**Figure 6-12: Plot of the average absolute deviation between experimental and calculated temperature (delta T) versus the experimental temperature (T/ K) for Vapour pressure data of 2-Methyl-1-Propanol.**

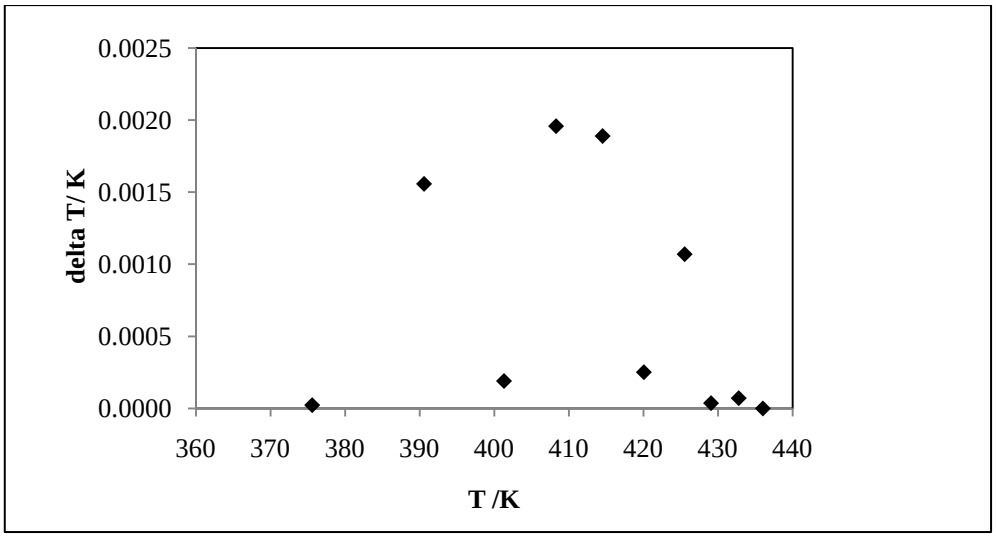


**Figure 6-13: Plot of the average absolute deviation between experimental and calculated temperature (delta T) versus the experimental temperature (T/ K) for Vapour pressure data of Butyric acid.**

## 6.4 Gas chromatograph operating conditions and detector calibrations

A Shimadzu GC-2010 gas chromatograph unit with a C20MWax capillary column, injection ports and thermal conductivity detector was employed for all the qualitative chemical purity determinations, as well as the quantitative sample analyses conducted in this study.

### 6.4.1 Operating conditions

The gas chromatograph operating conditions for the cyclohexane (1) + ethanol (2) test system is presented in Table 6-8, while the operating conditions for the new systems measured (2-propanol, 2-butanol, 2-methyl-1-propanol and butyric acid) are presented in Table 6-9.

| Operating conditions | Cyclohexane and Ethanol test system |
|---|---|
| Carrier gas | Helium |
| Carrier gas flow (ml.min-1) | 30 |
| Temperature control mode | Isothermal |
| Injector temperature ($^{o}$ C) | 180 |
| Column temperature ($^{o}$C | 70 |
| Detector temperature ($^{o}$C) | 180 |
| Flow control mode | Linear velocity |
| Pressure | 20 kPa |
| Total flow | 23.3 mL/min |
| Experimental run times(min) | 3 |

**Table 6-8. Gas chromatograph operating conditions for the Test systems**

| Operating conditions | |
|---|---|
| Carrier gas | Helium |
| Carrier gas flow (ml.min-1) | 30 |
| Temperature control mode | Isothermal |
| Injector temperature ($^{o}$ C) | 220 |
| Column temperature ($^{o}$C) | 160 |
| Detector temperature ($^{o}$C) | 220 |
| Flow control mode | Linear velocity |
| Pressure | 23.3 kPa |
| Total flow | 19.3 mL/min |
| Experimental run times(min) | 3 |

**Table 6-9. Gas chromatograph operating conditions for the new systems**

### 6.4.2 Detector calibrations

The thermal conductivity detector was calibrated for all the systems using the area ratio method of Raal and Mühlbauer (1998).

## 6.5 Vapour-Liquid Equilibrium Results

### 6.5.1 Cyclohexane (1) + Ethanol (2) System at 40 kPa

VLE data for the cyclohexane (1) + ethanol (2) system were measured at 40 kPa and 150 kPa to serve as a test system. The data obtained by Joseph (2001) at 40 kPa were used for the purpose of comparison.

The GC calibration curves, experimental data, x-*y* and *T*-*x*-*y* plots are presented below.

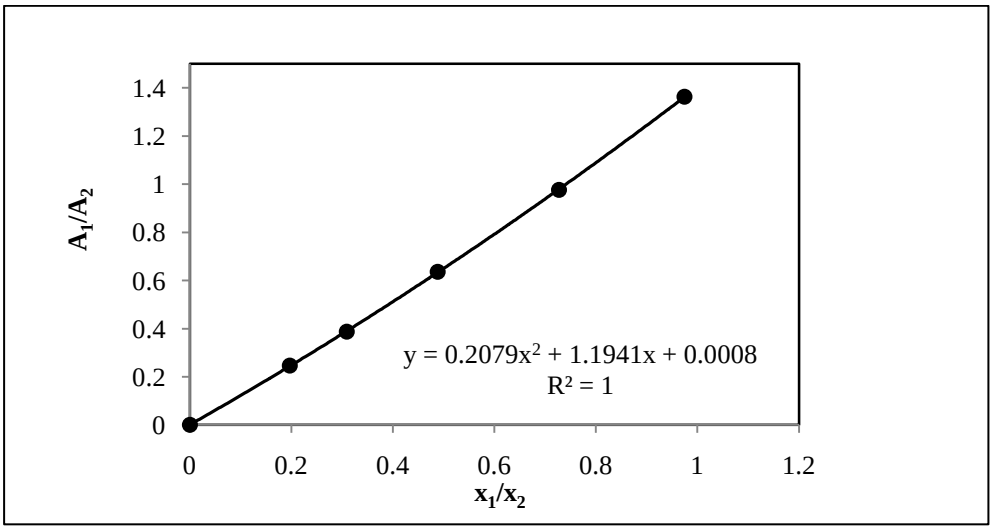


**Figure 6-14: $A_1/A_2$ versus $x_1/x_2$ for the cyclohexane (1) + ethanol (2) system. (Cyclohexane dilute region)**

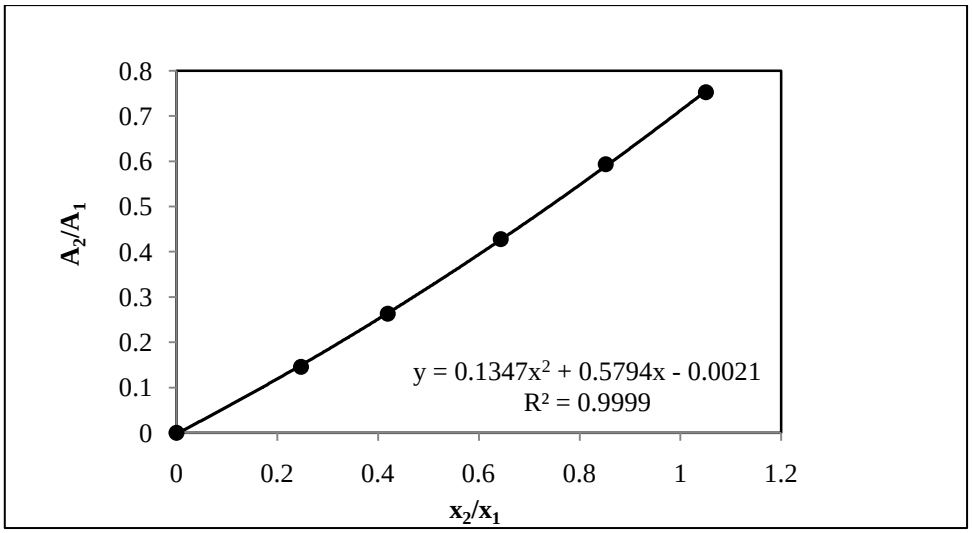


**Figure 6-15: $A_2/A_1$ versus $x_2/x_1$ for the cyclohexane (1) + ethanol (2) system (Cyclohexane rich region)**

| T /K | $x_1$ | $y_1$ | T /K | $x_1$ | $y_1$ |
|---|---|---|---|---|---|
| 329.45 | 0.0000 | 0.0000 | 315.30 | 0.8940 | 0.6716 |
| 324.89 | 0.0269 | 0.1792 | 315.72 | 0.9041 | 0.6817 |
| 323.03 | 0.0439 | 0.2748 | 316.53 | 0.9250 | 0.6920 |
| 322.93 | 0.0444 | 0.2955 | 317.54 | 0.9653 | 0.7385 |
| 321.54 | 0.0665 | 0.3317 | 319.47 | 0.9676 | 0.8082 |
| 320.87 | 0.0777 | 0.3467 | 320.78 | 0.9741 | 0.8608 |
| 314.59 | 0.5840 | 0.5890 | 322.77 | 0.9782 | 0.9349 |
| 314.57 | 0.7732 | 0.6284 | 324.38 | 0.9851 | 0.9555 |
| 314.68 | 0.8098 | 0.6307 | 325.64 | 1.0000 | 1.0000 |
| 314.98 | 0.8559 | 0.6372 | | | |

**Table 6-10: Vapour-liquid equilibrium data for the cyclohexane (1) + ethanol (2) system at 40 kPa.**

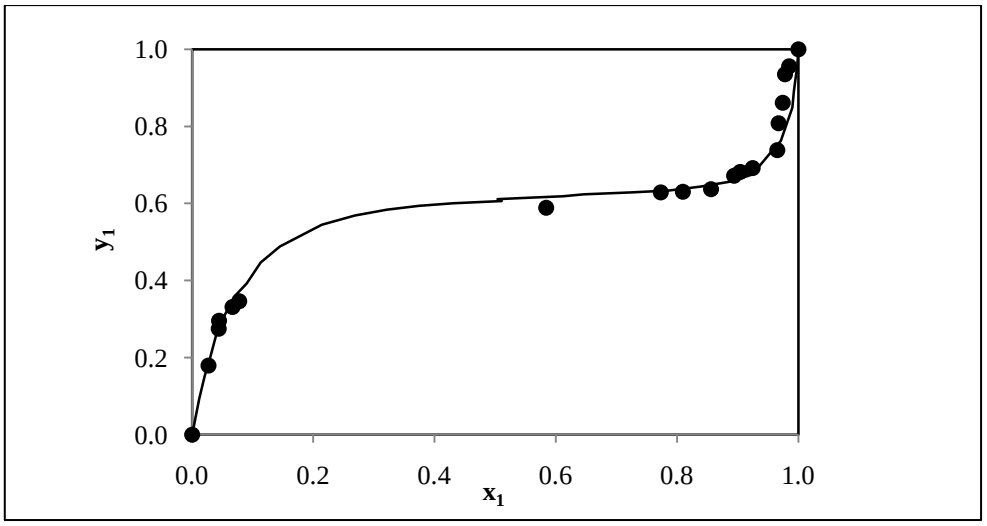


**Figure 6-16: Experimental x-y curve for the cyclohexane (1) + ethanol (2) system at 40 kPa; (—**), Joseph (2001) ;(•), this work

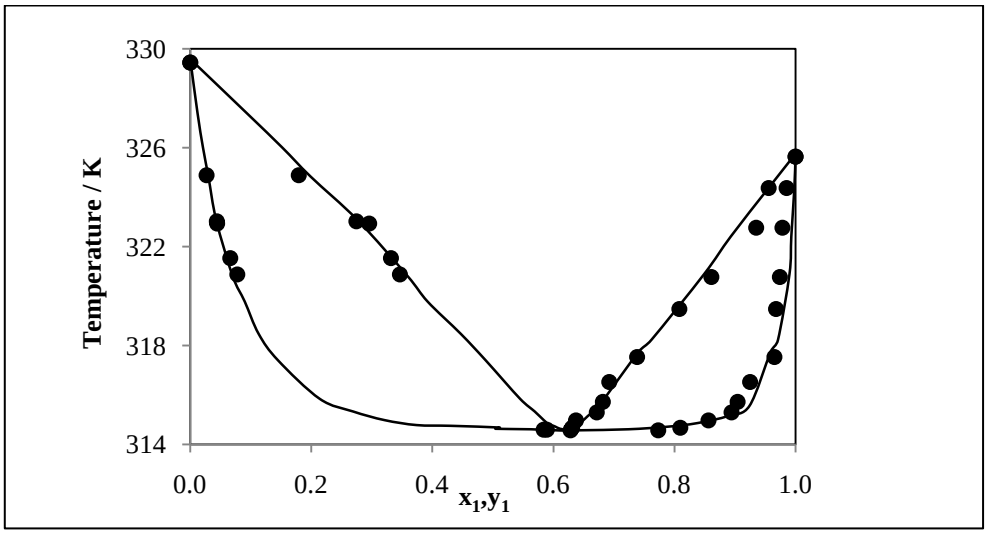


**Figure 6-17: T-x-y curve for the cyclohexane (1) + ethanol (2) system at 40 kPa;** (—), Joseph (2001); (•), this work

### 6.5.2 Cyclohexane (1) + Ethanol (2) System at 150 kPa

| T /K | $x_1$ | $y_1$ | T /K | $x_1$ | $y_1$ |
|---|---|---|---|---|---|
| 361.83 | 0.0000 | 0.0000 | 349.63 | 0.5444 | 0.5120 |
| 357.24 | 0.0517 | 0.1998 | 349.73 | 0.5564 | 0.5251 |
| 355.61 | 0.0711 | 0.2564 | 352.61 | 0.8904 | 0.6294 |
| 351.89 | 0.1577 | 0.3811 | 361.10 | 0.9765 | 0.8326 |
| 350.68 | 0.2512 | 0.4499 | 367.87 | 1.0000 | 1.0000 |
| 349.69 | 0.4203 | 0.5045 | | | |

**Table 6-11: Vapour-liquid equilibrium data for the cyclohexane (1) + ethanol (2) system at 150 kPa.**

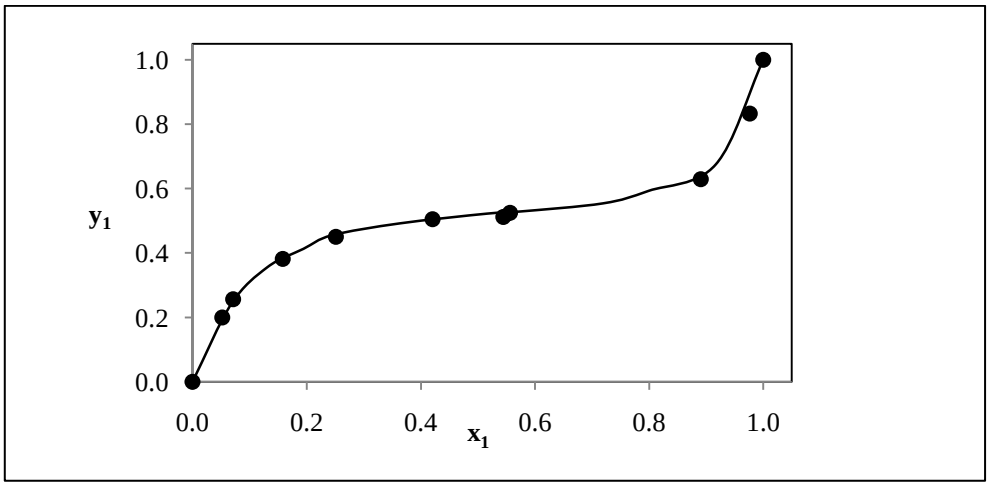


**Figure 6-18: Experimental x-y curve for the cyclohexane (1) + ethanol (2) system at 150 kPa; (•)**, this work; (—), Reddy (2006).

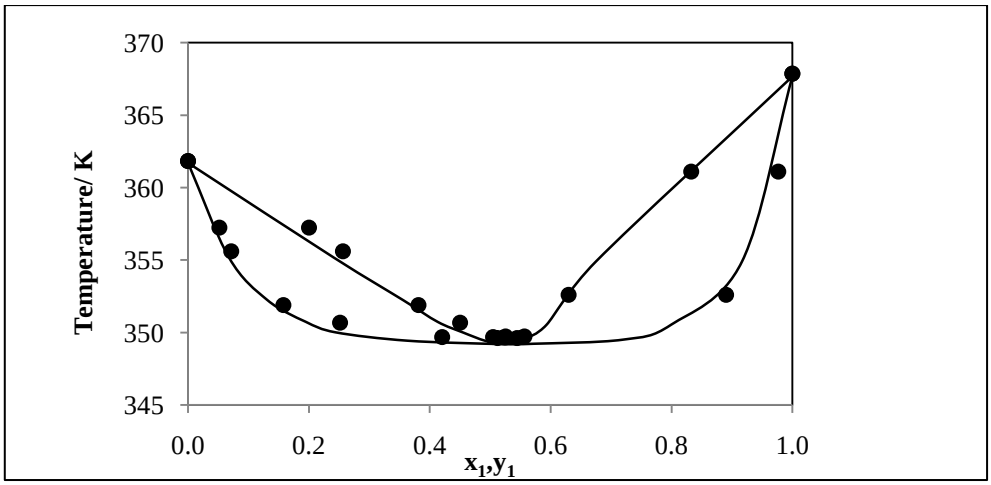


**Figure 6-19: T-x-y curve for the cyclohexane (1) + ethanol (2) system at 150 kPa; (•** ), this work; (—), Reddy (2006).

### 6.5.3 2-Propanol (1) + Butyric Acid (2) System

This data represents new VLE data as this system has not been measured before. The GC calibration plots, experimental data, *x-y* and *P-x-y* plots are presented below.

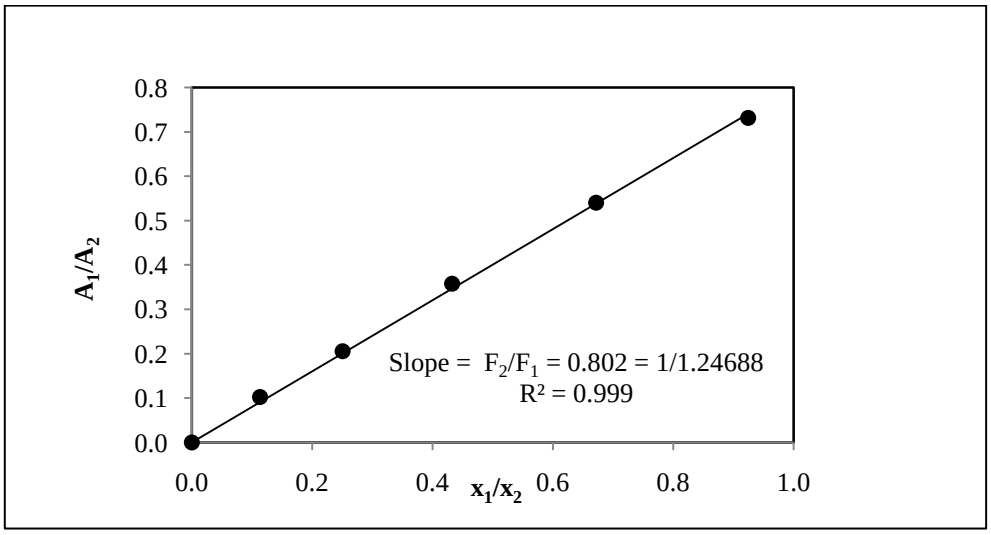


**Figure 6-20: Calibration curve for the 2-propanol (1) + butyric acid (2) system (2- Propanol dilute region).**

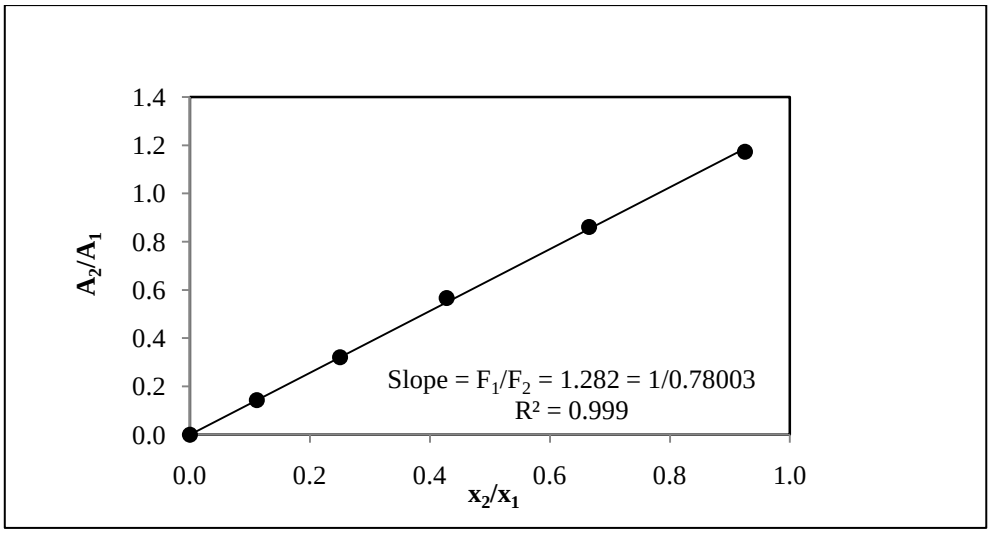


**Figure 6-21: Calibration curve for the 2-propanol (1) +butyric acid (2) system (2- Propanol rich region).**

| T = 333.15 K | | | T = 353.15 K | | | T = 373.15 K | | |
|---|---|---|---|---|---|---|---|---|
| **P/kPa** | **$x_1$** | **$y_1$** | **P/kPa** | **$x_1$** | **$y_1$** | **P/kPa** | **$x_1$** | **$y_1$** |
| 1.29 | 0.0000 | 0.0000 | 3.86 | 0.0000 | 0.0000 | 9.94 | 0.0000 | 0.0000 |
| 1.82 | 0.0242 | 0.2656 | 4.86 | 0.0100 | 0.1579 | 10.85 | 0.0085 | 0.1255 |
| 3.51 | 0.0738 | 0.5705 | 6.34 | 0.0329 | 0.2558 | 14.85 | 0.0330 | 0.2876 |
| 6.38 | 0.1467 | 0.7704 | 7.98 | 0.0455 | 0.3682 | 21.07 | 0.0728 | 0.4970 |
| 8.13 | 0.1851 | 0.8197 | 10.78 | 0.0763 | 0.5298 | 30.06 | 0.1261 | 0.6483 |
| 10.80 | 0.2631 | 0.8766 | 11.60 | 0.0877 | 0.5817 | 41.22 | 0.1908 | 0.7454 |
| 11.67 | 0.2858 | 0.8903 | 13.96 | 0.1113 | 0.6397 | 47.46 | 0.2320 | 0.7846 |
| 14.66 | 0.3812 | 0.9298 | 15.29 | 0.1244 | 0.6682 | 60.77 | 0.3039 | 0.8381 |
| 17.19 | 0.4479 | 0.9553 | 21.13 | 0.1918 | 0.7669 | 71.76 | 0.3673 | 0.8806 |
| 19.19 | 0.5022 | 0.9665 | 25.42 | 0.2503 | 0.8402 | 79.96 | 0.4116 | 0.9013 |
| 21.28 | 0.5531 | 0.9736 | 29.20 | 0.2884 | 0.8755 | 90.23 | 0.4576 | 0.9151 |
| 23.02 | 0.6005 | 0.9768 | 49.79 | 0.5161 | 0.9590 | 101.7* | 0.5149 | 0.9297 |
| 24.74 | 0.6501 | 0.9852 | 53.43 | 0.5673 | 0.9677 | 103.0* | 0.5207 | 0.9340 |
| 27.64 | 0.7318 | 0.9905 | 60.62 | 0.6471 | 0.9775 | 109.4* | 0.5644 | 0.9436 |
| 31.32 | 0.8278 | 0.9909 | 80.55 | 0.8889 | 1.0000 | 151.1* | 0.7795 | 0.9812 |
| 35.69 | 0.9544 | 0.9941 | 86.85 | 0.9682 | 1.0000 | 171.1* | 0.8880 | 0.9925 |
| 37.39 | 1.0000 | 1.0000 | 88.46 | 0.9924 | 1.0000 | 194.4* | 1.0000 | 1.0000 |
| | | | 90.36 | 1.0000 | 1.0000 | | | |

* Data measured on the stainless steel apparatus

**Table 6-12: Vapour-liquid equilibrium data for the 2-propanol (1) + butyric acid (2) system at 333.15, 353.15 and 373.15 K**

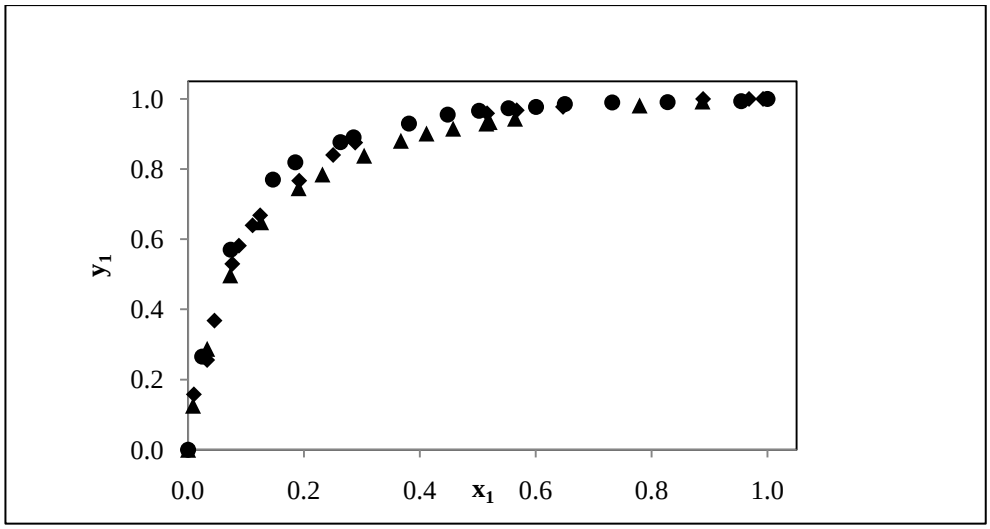


**Figure 6-22: Experimental x-y curve for the 2-propanol (1) +butyric acid (2) system at 333.15 (•), 353.15 (♦) and 373.15 (▲) K**

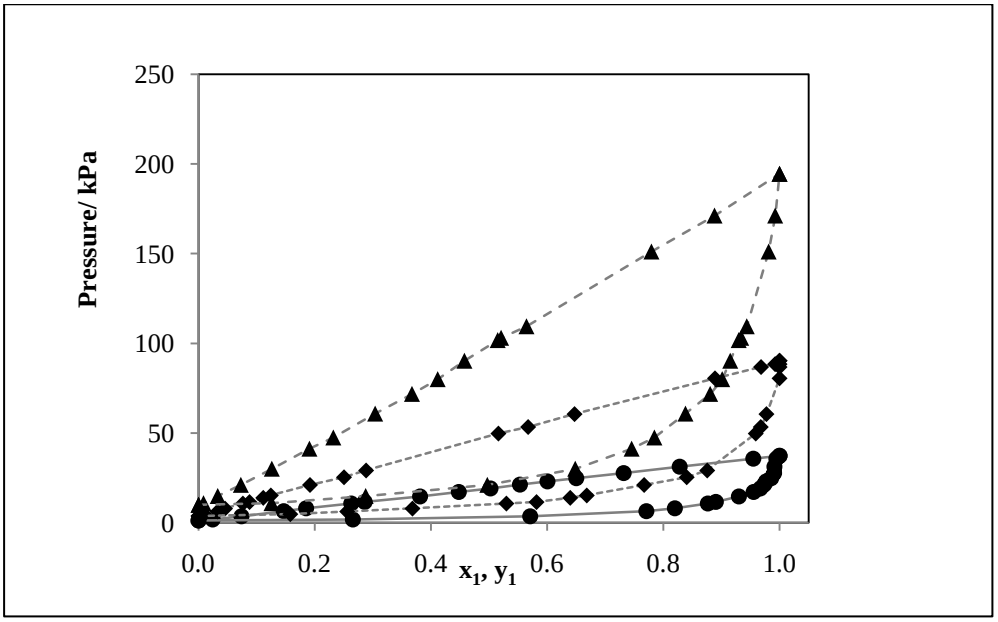


**Figure 6-23: P-x-y curve for the 2-propanol (1) + butyric acid (2) system at 333.15 (•), 353.15 (♦) and 373.15 (▲) K**. The dash represent a fitted experimental line.

### 6.5.4 2-Butanol (1) + Butyric Acid (2) System

The composition analysis of this system was analysed using the Shimadzu GC2010 gas chromatograph. The data obtained represents new VLE data. The GC calibration plots, experimental data, *x-y*, and *P-x-y* plots are presented below.

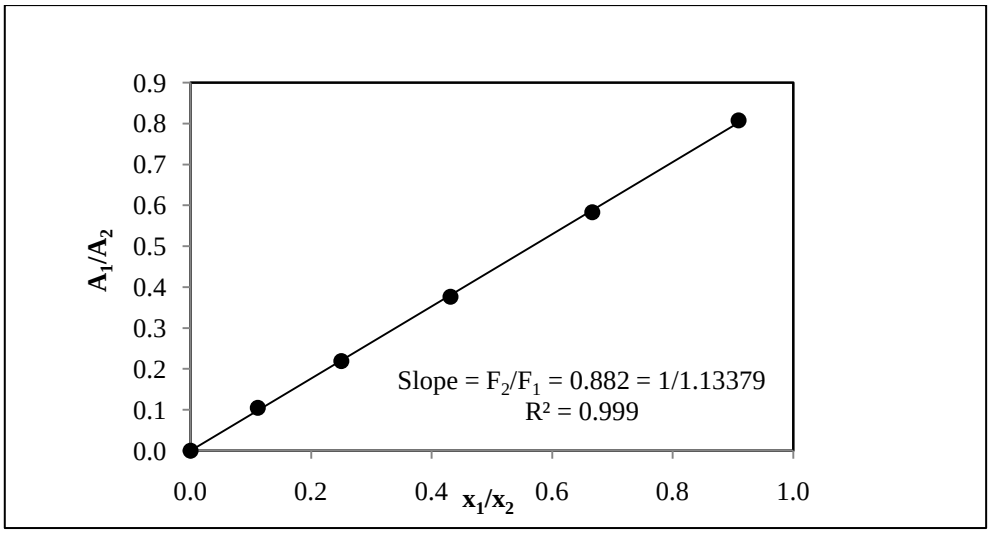


**Figure 6-24: Calibration curve for the 2-butanol (1) + butyric acid (2) system (2-Butanol dilute region).**

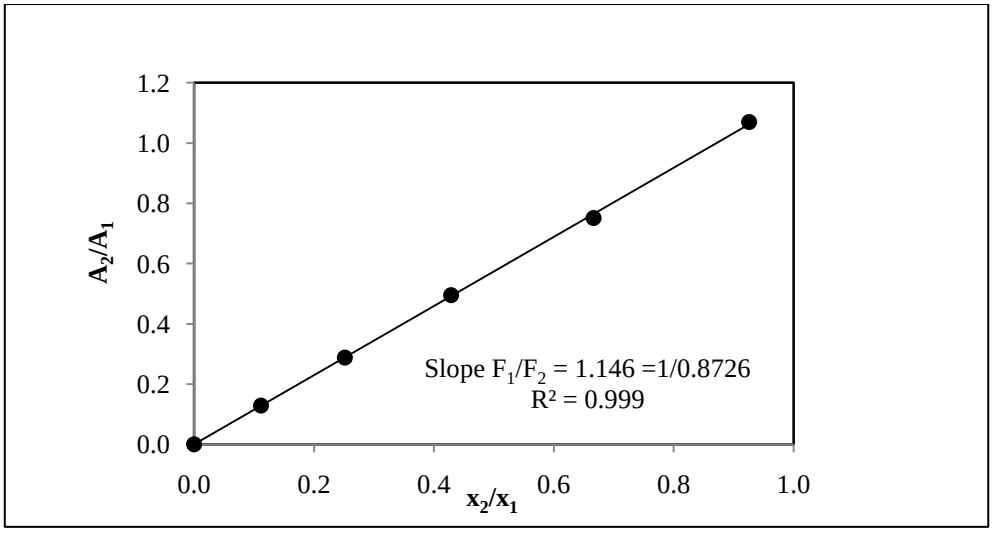


**Figure 6-25: Calibration curve for the 2-butanol (1) + butyric acid (2) system (2-Butanol rich region).**

| T = 333.15 K | | | T = 353.15 K | | | T = 373.15 K | | |
|---|---|---|---|---|---|---|---|---|
| **P/kPa** | **$x_1$** | **$y_1$** | **P /kPa** | **$x_1$** | **$y_1$** | **P/kPa** | **$x_1$** | **$y_1$** |
| 1.29 | 0.0000 | 0.0000 | 3.82 | 0.0000 | 0.0000 | 10.16 | 0.0000 | 0.0000 |
| 1.68 | 0.0325 | 0.2199 | 5.04 | 0.0429 | 0.2791 | 14.60 | 0.0511 | 0.3035 |
| 2.21 | 0.0588 | 0.4268 | 6.28 | 0.0701 | 0.4363 | 15.33 | 0.0596 | 0.3518 |
| 3.06 | 0.1192 | 0.5703 | 7.59 | 0.0948 | 0.4998 | 20.61 | 0.1033 | 0.5259 |
| 4.47 | 0.2032 | 0.7285 | 7.74 | 0.1052 | 0.5266 | 24.79 | 0.1521 | 0.6223 |
| 5.84 | 0.2725 | 0.8343 | 8.40 | 0.1238 | 0.5671 | 27.36 | 0.1961 | 0.6857 |
| 5.66 | 0.2567 | 0.8242 | 14.59 | 0.2653 | 0.7702 | 33.60 | 0.2528 | 0.7559 |
| 6.56 | 0.3071 | 0.8710 | 17.30 | 0.3179 | 0.8294 | 39.34 | 0.3350 | 0.8135 |
| 7.86 | 0.3946 | 0.9056 | 20.74 | 0.4007 | 0.8667 | 44.51 | 0.3791 | 0.8549 |
| 9.98 | 0.5028 | 0.9393 | 22.76 | 0.4630 | 0.9049 | 50.03 | 0.4489 | 0.8917 |
| 11.82 | 0.6300 | 0.9673 | 26.48 | 0.5225 | 0.9332 | 53.92 | 0.4839 | 0.8941 |
| 11.92 | 0.6383 | 0.9690 | 29.25 | 0.5982 | 0.9542 | 58.90 | 0.5284 | 0.9287 |
| 14.20 | 0.7695 | 0.9774 | 34.40 | 0.7005 | 0.9746 | 68.25 | 0.6166 | 0.9502 |
| 14.67 | 0.7936 | 0.9837 | 36.14 | 0.7450 | 0.9818 | 68.53 | 0.6199 | 0.9517 |
| 17.14 | 0.9226 | 1.0000 | 39.63 | 0.8158 | 0.9830 | 74.96 | 0.6999 | 0.9722 |
| 18.70 | 1.0000 | 1.0000 | 46.38 | 0.9689 | 1.0000 | 82.58 | 0.7856 | 0.9866 |
| | | | 48.05 | 1.0000 | 1.0000 | 92.56* | 0.8853 | 0.9934 |
| | | | | | | 102.6* | 0.9866 | 1.0000 |
| | | | | | | 104.6* | 1.0000 | 1.0000 |

* Data measured on the stainless steel apparatus

**Table 6-13: Vapour-liquid equilibrium data for the 2-butanol (1) + butyric acid (2) system.**

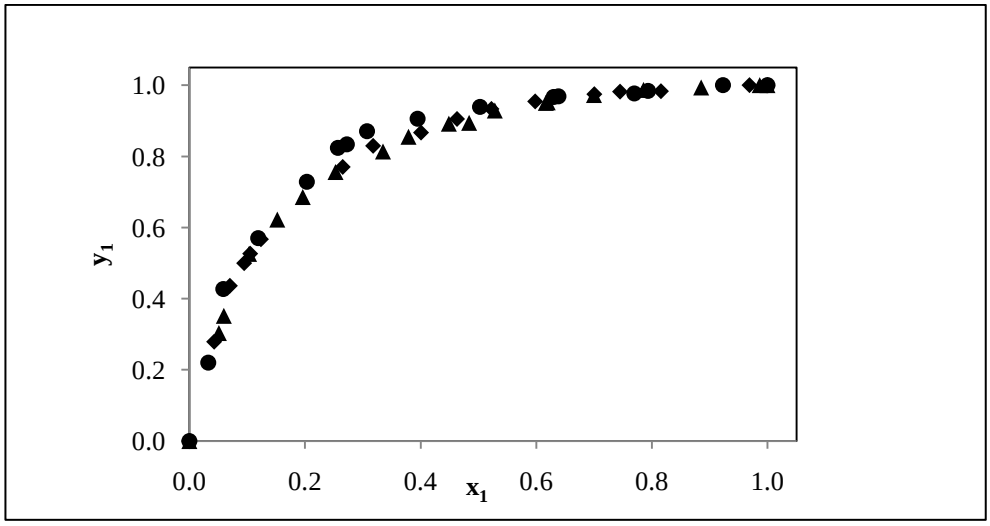


**Figure 6-26: Experimental x-y curve for the 2-butanol (1) + butyric acid (2) system at 333.15 (•), 353.15 (♦) and 373.15 (▲) K**

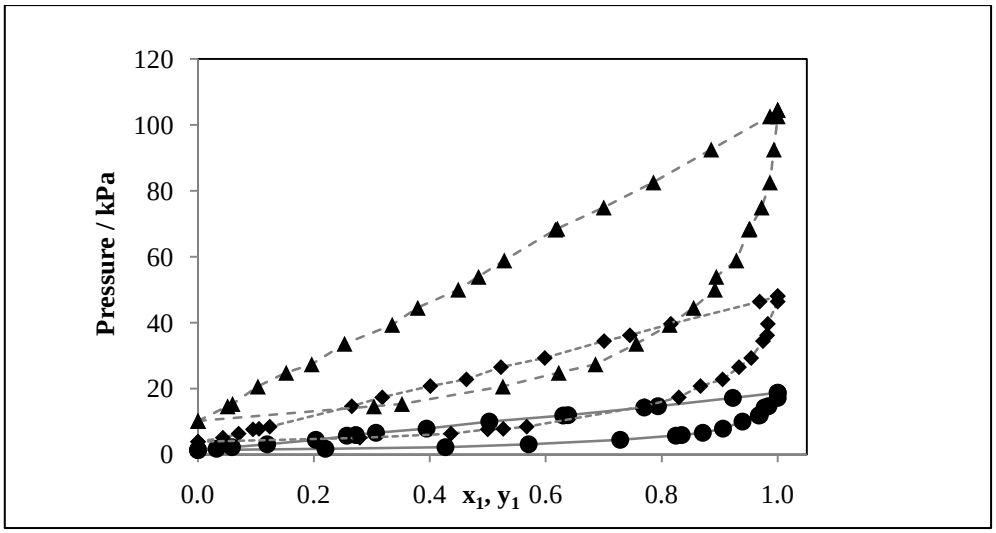


**Figure 6-27: P-x-y curve for the 2-butanol (1) +butyric acid (2) system at 333.15 (•), 353.15(♦) and 373.15 (▲) K** The dash represent a fitted experimental line.

### 6.5.5 2-Methyl-1-Propanol (1) + Butyric Acid (2) System

The composition analysis of this system was analysed using the Shimadzu GC2010 gas chromatograph, similar to all the other systems measured previously. The data obtained represents new VLE data. The GC calibration plots, experimental data, *x-y* and *P-x-y* plots are presented below.

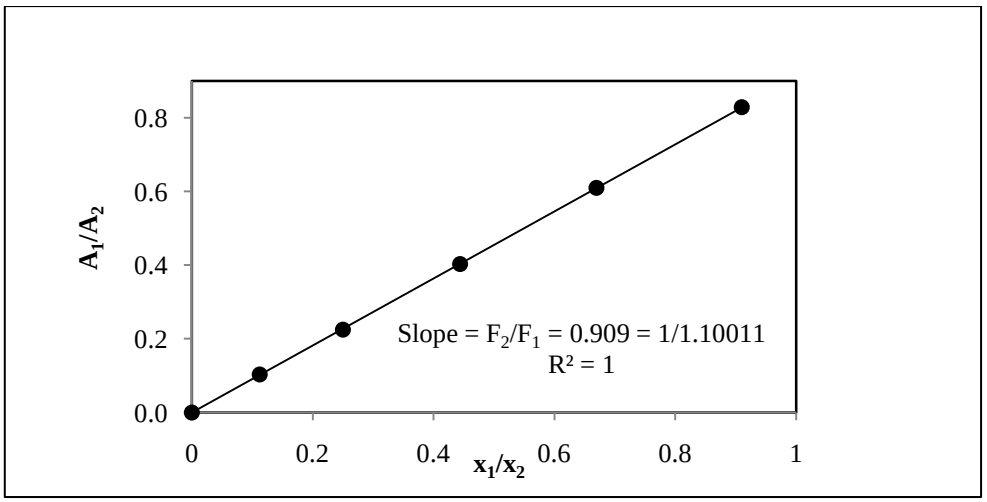


**Figure 6-28: Calibration curve for the 2-methyl-1-propanol (1) + butyric acid (2) system (2- methyl-1-propanol dilute region).**

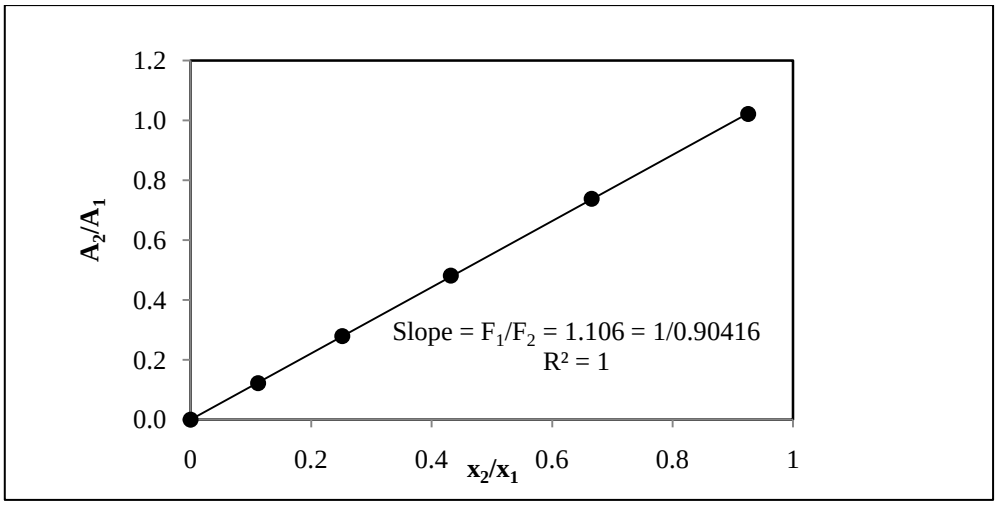


**Figure 6-29: Calibration curve for the 2-methyl-1-propanol (1) + butyric acid (2) system (2- methyl-1-propanol rich region).**

| T = 333.15 K | | | T = 353.15 K | | | T = 373.15 K | | |
|---|---|---|---|---|---|---|---|---|
| **P/kPa** | **$x_1$** | **$y_1$** | **P/kPa** | **$x_1$** | **$y_1$** | **P/kPa** | **$x_1$** | **$y_1$** |
| 1.29 | 0.0000 | 0.0000 | 3.86 | 0.0000 | 0.0000 | 9.94 | 0.0000 | 0.0000 |
| 1.95 | 0.0816 | 0.3946 | 5.53 | 0.0705 | 0.3288 | 13.68 | 0.0567 | 0.2420 |
| 2.10 | 0.0932 | 0.4323 | 7.56 | 0.1424 | 0.5212 | 15.47 | 0.0948 | 0.3631 |
| 2.49 | 0.1259 | 0.5096 | 9.55 | 0.2107 | 0.6336 | 19.10 | 0.1600 | 0.5156 |
| 2.83 | 0.1659 | 0.6009 | 10.44 | 0.2423 | 0.6818 | 29.31 | 0.3251 | 0.7247 |
| 3.38 | 0.2118 | 0.6693 | 11.32 | 0.2813 | 0.7217 | 33.34 | 0.3860 | 0.7745 |
| 4.03 | 0.2651 | 0.7359 | 13.06 | 0.3461 | 0.7743 | 38.27 | 0.4520 | 0.8321 |
| 4.58 | 0.3211 | 0.7927 | 14.59 | 0.3930 | 0.8168 | 40.90 | 0.4883 | 0.8530 |
| 5.34 | 0.3812 | 0.8411 | 15.77 | 0.4305 | 0.8478 | 43.58 | 0.5309 | 0.8751 |
| 6.30 | 0.4758 | 0.8908 | 17.38 | 0.4903 | 0.8857 | 47.71 | 0.5788 | 0.9033 |
| 6.93 | 0.5195 | 0.9187 | 19.32 | 0.5524 | 0.9157 | 50.52 | 0.6257 | 0.9232 |
| 8.23 | 0.6472 | 0.9546 | 20.99 | 0.6107 | 0.9382 | 53.73 | 0.6756 | 0.9479 |
| 9.04 | 0.7185 | 0.9712 | 23.14 | 0.6616 | 0.9536 | 55.28 | 0.6969 | 0.9528 |
| 9.81 | 0.7699 | 0.9789 | 24.93 | 0.7278 | 0.9699 | 59.49 | 0.7518 | 0.9680 |
| 11.02 | 0.8788 | 0.9925 | 27.76 | 0.8256 | 0.9861 | 63.33 | 0.8118 | 0.9814 |
| 11.93 | 0.9684 | 1.0000 | 33.22 | 1.0000 | 1.0000 | 66.21 | 0.8612 | 0.9858 |
| 12.36 | 1.0000 | 1.0000 | | | | 71.97 | 0.9349 | 1.0000 |
| | | | | | | 76.32 | 1.0000 | 1.0000 |

**Table 6-14: Vapour-liquid equilibrium data for the 2-methyl-1-propanol (1) + butyric acid (2) system.**

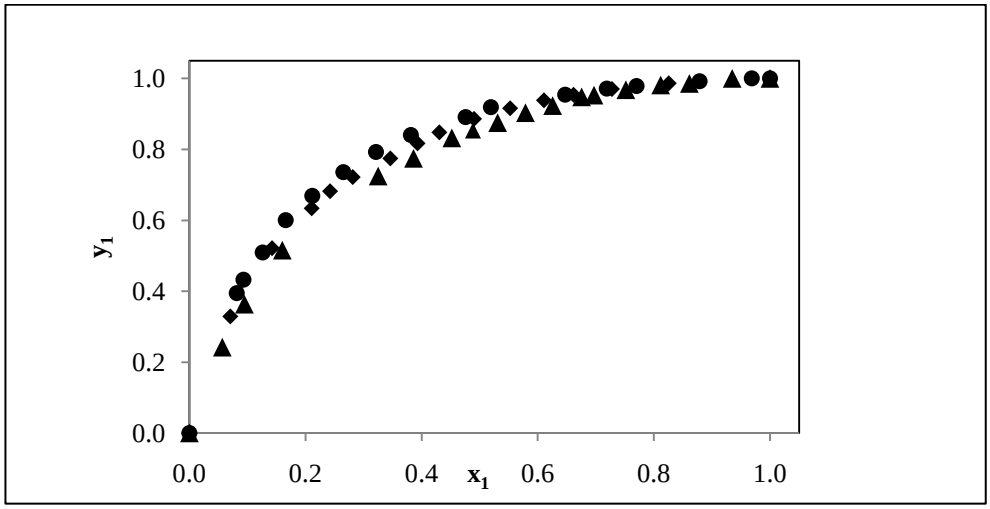


**Figure 6-30: Experimental x-y curve for the 2-methyl-1-propanol (1) + butyric acid (2) system at 333.15 (•), 353.15 (♦) and 373.15 (▲) K**

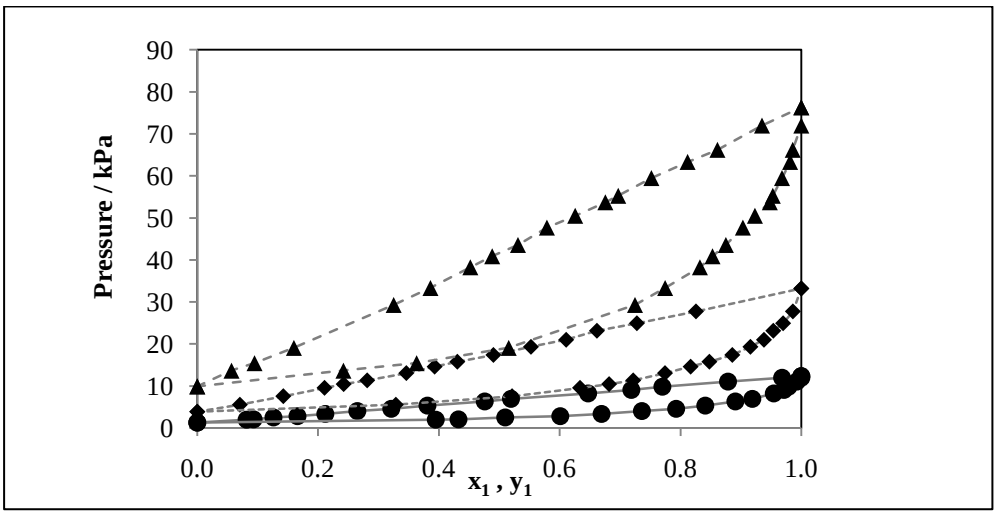


**Figure 6-31: P-x-y curve for the 2-methyl-1-propanol (1) +butyric acid (2) system at 333.15 (•), 353.15 (♦) and 373.15 (▲) K** The dash represent a fitted experimental line.

CHAPTER
7

# DATA ANALYSIS AND DISCUSSION

This chapter includes the regression of the data using both the combined and direct methods for the isothermal data, as well as a discussion of the results presented in this work. The vapour pressure curves measured are also discussed since the data were fitted to both the Wagner (Reid et al., 1988) equation and the Antoine equation.

## 7.1 Regression of the Vapour Pressure Data

The vapour pressure data were regressed to find parameters for both the Antoine equation:

$$\ln(P)/kPa = A - \frac{B}{T/^{o}C + C} \tag{7.1}$$

and the Wagner (Reid et al, 1988) equation:

$$\ln\left(\frac{P}{P_c}\right)/kPa = [A\tau + B\tau^{1.5} + C\tau^{3} + D\tau^{6}] \tag{7.2}$$

where

$$\tau = 1 - \frac{T}{T_c} \tag{7.3}$$

The parameters obtained are given in Tables 7-1 and 7-2 below.

| | A | B | C | $\Sigma(\Delta P^2)$ |
|---|---|---|---|---|
| Ethanol | 13.00 | 1833.2 | 140.35 | 0.175 |
| Cyclohexane | 10.00 | 1078.0 | 117.45 | 0.407 |
| 2-Propanol | 15.80 | 3164.4 | 200.25 | 3.870 |
| 2-Butanol | 12.50 | 1732.2 | 121.25 | 0.712 |
| 2-Methyl-1-Propanol | 13.30 | 2156.8 | 139.55 | 1.178 |
| Butyric Acid | 15.60 | 3972.9 | 197.35 | 3.744 |

**Table 7-1: Parameters for the Antoine equation**

| | A | B | C | D | $\Sigma(\Delta P^2)$ |
|---|---|---|---|---|---|
| Ethanol | -51.65 | 107.3 | -191.3 | 519.65 | 0.016 |
| Cyclohexane | -54.75 | 111.5 | -157.0 | 275.97 | 0.098 |
| 2-Propanol | -4.246 | -10.94 | 16.40 | -93.50 | 3.755 |
| 2-Butanol | -38.01 | 75.55 | -142.4 | 383.87 | 0.323 |
| 2-Methyl-1-Propanol | -33.90 | 64.90 | -122.9 | 328.88 | 0.577 |
| Butyric Acid | 24.84 | -83.70 | 153.0 | -527.25 | 3.035 |

**Table 7-2: Parameters for the Wagner (Reid et al., 1988) equation. The critical properties were taken from DDB, 2009 and Prausnitz et al. (1980)**

For all the pure component vapour pressure data measured, the Wagner (Reid et al., 1988) equation (Equation 7-2) was found to give a superior correlation of the vapour pressure data when compared to the simpler Antoine equation (Equation 7-1). This is evident by the significantly lower $\sum(\Delta P^2)$ values for the Wagner equation presented in Table 7-2. The fact that the Wagner equation provides a better fit to the vapour pressure data is not unexpected since this equation has four adjustable parameters in comparison to three parameters of the Antoine equation. Both equations, however, fitted the data exceedingly well.

The vapour pressures were regressed using the objective function of Barker's method (which minimizes the sum of the squares of the pressure residual) with the built-in function (fminsearch) in MATLAB used in solving for an optimal parameter solution. The sum of the squares of the pressure difference per point was determined using the following equation:

$$\Delta P = \sum_{i}^{n} \left( P_i^{\exp} - P_i^{calc} \right)^2 \tag{7.4}$$

where *n* stands for the number of experimental points measured.

The average pressure differences (given in kPa) were small for all the pure components measured as shown by Tables 6-2 to 6-7 in the result on section 6-3. The percentage differences for each component were generally small. In all cases, however, the percentage difference between the measured data and the literature data was less than 0.1%.

### 7.2 Gas Chromatograph Calibration

The Shimadzu gas chromatograph (GC2010) was used to determine the compositions for both the test systems and new systems measured. The gas chromatograph calibration plots were generally observed to be linear. However, the calibration graphs for the cyclohexane + ethanol system displayed a slight curve and the best fit through the points was obtained using a quadratic equation. This meant that the calibration could not be generalized to apply to the entire composition range by inverting the slopes of the curves; therefore, an average response factor ratio was not calculated. Alternatively, caution had to be taken to ensure that the correct calibration plots were employed. This depends on whether the samples were being taken in the dilute ethanol region or the dilute cyclohexane region.

The 2-propanol (1) + butyric acid (2) calibration plots are presented in Figures 6-20 and 6-21, while Figures 6-24 and 6-25 apply to the 2-butanol (1) – butyric acid (2) system and Figures 6-28 and 6-29 represent the 2-methyl-1-propanol (1) – butyric acid (2) system . The inverses of the response factor ratios were not equal for the three systems; although the differences were small (the percentage difference in each case was less than 1%). Hence, the correct calibration curve was applied in the correct region. For the 2-propanol + butyric acid system, Figure 6-20 was employed in the butyric acid-rich (or 2-propanol dilute) region and Figure 6-21 in the 2-propanol-rich region. A similar procedure was followed for the 2-butanol + butyric acid system and 2-methyl-1-propanol + butyric acid system.

Following this method ensured the accuracy of the composition measurements in the dilute regions on either side of the *x-y* and *P-x-y* curves. The accuracy of the composition was ± 0.005 mole fraction for the 2-Propanol + Butyric acid, ± 0.004 mole fraction for the 2-Butanol + Butyric acid, and ± 0.001 mole fraction for the 2-Methyl-1-Propanol + Butyric acid system calibrations for the GC.

## 7.3 Experimental VLE Binary system

### 7.3.1 Cyclohexane (1) + Ethanol (2) system

The measured data for the cyclohexane + ethanol test system at 40 kPa were compared to the literature data of Joseph (2001), while the experimental data for the same test system at 150 kPa were compared to the work of Reddy (2006). This comparison is presented in Figures 6-16 to 6-19 and it can be seen that the experimental data matches the literature data well. Thus, it was concluded that both the experimental setup and procedure were operating as desired.

### 7.3.2 New systems

No literature data could be found for comparison of the data measured for the following systems:

- 2-Butanol (1) + Butyric Acid (2): 333.15, 353.15 and 373.15 K isotherms.
- 2-Propanol (1) + Butyric acid (2) system: 333.15, 353.15 and 373.15 K isotherms
- 2-Methyl-1-Propanol (1) + Butyric acid (2) system: 333.15, 353.15and 373.15 K

These systems at the various isotherms therefore constitute new data.

## 7.4 Physical Properties

The physical properties of the pure components that were required for the theoretical treatment of the experimental VLE data on this project were obtained from the Dortmund Data Bank (DDB, 2009) and Prausnitz et al (1980). These properties such as critical pressure, critical temperature, critical volume, acentric factors, and critical compressibility, as well as the correlations used to estimate certain properties are compiled in Appendix A. Other properties and parameters such as $\kappa_1$ (kappa) used in the alpha correlation (α-function in the Stryjek-Vera form of Peng-Robinson EOS) were derived during modeling of the experimental data and are presented in the relevant sections of this chapter.

## 7.5 Data Regression of experimental VLE binary system

### 7.5.1 Direct Method

The direct (phi-phi) method uses an EOS to describe both liquid and vapour phases. The equation describing the fugacity coefficients is:

$$\widehat{f}_i^{\,L} = x_i \widehat{\phi}_i^{\,L} = \widehat{f}_i^{\,V} = y_i^V \widehat{\phi}_i^{\,V} \tag{7.5}$$

#### 7.5.1.1 Models used

The following thermodynamic models were used to correlate the measured VLE data using the direct method:

PR-SV-WS(NRTL) & SRK-WS(NRTL )

The expression representing the combination of the EOS, combined with the alpha correlation, using a mixing rule that incorporates a $G^E$ model in its fugacity coefficient expression is in the order:

*EOS – α Correlation - Mixing rule* (*$G^E$ Model*)

Hence, PR-SV-WS (NRTL) refers to the Peng-Robinson EOS, with the Stryjek-Vera α correlation. WS refers to the Wong-Sandler mixing rule that incorporates the NRTL activity coefficient model. While SRK-WS (NRTL) refers to the Soave-Redlich-Kwong EOS and the other abbreviations remains the same as defined earlier on.

### 7.5.2 Combined method

In this project, a virial equation of state was employed using the Tsonopoulos (1974) correlation in describing the vapour phase, as well as the Hayden and O'Connell (1975) with Chemical theory to explicitly account for the vapour phase imperfection, while the NRTL activity coefficient model was used for the calculation of the liquid phase activity coefficient ($\gamma_i$). This is described with the equation:

$$y_i \Phi_i P = x_i \gamma_i P_i^{sat} \tag{3.21}$$

where the expression $\Phi_i$ represents the fugacity coefficient calculated by the Virial EOS (Tsonopoulos) as well as Hayden and O' Connell, $\gamma_i$ represent the activity coefficient for NRTL, and $P_i^{sat}$ the saturated vapour pressure calculated by a vapour pressure correlation equation (e.g. Antoine equation).

The Tsonopoulos coefficient ($B_{11}$, $B_{22}$, $B_{12}$) are calculated as explained in Section 3.4.1.1 and the phi calculated from the equation:

$$\Phi_i = \frac{\hat{\phi}_i}{\phi_i^{sat}} \exp\left[\frac{-V_i^l (P - P_i^{sat})}{RT}\right] \tag{3.22}$$

### 7.5.3 Parameter estimation for the fitting of experimental VLE data

The techniques used in the reduction of the measured binary VLE data involved determining the optimal parameters for each of the thermodynamic models used. These involve the bubble pressure calculations based on both the combined and direct methods as discussed in detail in Section 3.7.1 and 3.7.2 respectively. The model parameters were optimized by minimizing the pressure and vapour composition deviations between the experimental data and those calculated by the model. The difference between these values was minimized by solving for the optimal parameter solutions of each thermodynamic model which was achieved using a least-square estimation of nonlinear parameters.

The Peng-Robinson EOS and Soave-Redlich-Kwong EOS, was combined with the α-correlation of Stryjek-Vera (1986)(SV) with the Wong-Sandler (1992) mixing rule together with the NRTL excess Gibbs free energy model for the direct method, while the Virial EOS using the Tsonopoulos (1974) correlation together with the NRTL excess Gibbs free energy model employed for the combined method. The Hayden and O'Connell with the chemical theory was employed to account for both chemical interactions in the vapour phase, as well as vapour-phase nonidealities. These methods were discussed in detail in Section 7.7 and 7.8.

It is important to mention that for a binary mixture, while the three (NRTL model) parameters $\tau_{12}$, $\tau_{21}$ and $\alpha_{12}$ are adjustable; several authors have suggested that it is better for it to be fixed between 0.2 and 0.47. It is necessary to point out that parameter estimation for VLE modeling using local composition models is a difficult global optimization problem, and their characteristics pose a challenge to any optimization technique (Gutiérrez-Antonio et al, 2009). For parameter estimation on this project, the $\alpha_{12}$ was fixed at 0.3 for the Peng-Robinson with Stryjek –Vera equation of state, but regressed for the Soave-Redlich-Kwong equation of state and the virial equation of state, as well as in the Hayden O'Connell with chemical theory. This was decided after a rigorous test on the model showed a much better deviation when the $\alpha_{12}$ is regressed for the Virial EOS and the chemical theory.

The second virial coefficients were evaluated using the correlations discussed in Section 3.4.1 and the liquid molar volumes were obtained through application of the modified Rackett (1970) equation.

### 7.5.4 Computational Procedure

A flow diagram for the bubble pressure computation via the combined and direct method is presented in Figure 3-1 and 3-2 respectively.
The inputs used for the regression of the VLE data in the direct method are listed below:
- pure component properties, such as, critical temperatures and pressures, acentric factors
- alpha correlation parameter ($\kappa_1$)
- *ZRA* values to estimate molar volumes used in the activity coefficient models
- system temperature and liquid compositions of the measured data
- initial estimates for the binary interaction ($k_{ij}$) and $G^E$ model parameters ($\alpha_{ij}$, $\tau_{12}$ ,$\tau_{21}$ in the NRTL model)

The optimized binary interaction and $G^E$ model parameter values were used to predict the entire P-x-y diagram for that specific isotherm using the objective function in equation 7.6 and 7.7. The experimental data measured in this project was then compared to those correlated via the direct method using a combination of models.

The inputs used for the regression of the VLE data in the combined method are listed below:
- pure component properties, such as, critical temperatures and pressures, acentric factors
- alpha correlation parameter ($\kappa_1$)
- vapour-phase standard-state fugacity constants, $\Phi_i$
- *ZRA* values to estimate molar volumes used in the activity coefficient models ( modified Rackett equation)
- system temperature and liquid compositions of the measured data
- initial estimates for the binary interaction and $G^E$ model parameters.

### 7.5.5 Generalized parameter optimization routine

The Marquardt (1963) method was used for solving for an optimal parameter solution in the regression models. This procedure performs an optimum interpolation between the Taylor series and the gradient methods. The Marquardt method compares the calculated outputs from a thermodynamic computation such as vapour compositions and/or pressures to the experimentally measured values. The difference between the two data sets (experimental and calculated) is minimized using certain objective functions thereby providing a set of optimized parameters.

### 7.5.6 Objective functions

According to Van Ness (1995), minimizing the pressure residuals ($\Delta P$) provides a fit that is at least as good as any other that might be obtained by minimizing a different residual (e.g. $\Delta y$). In this work, two residuals were used in modeling each set of data; namely pressure and vapour composition. The results from the regression of vapour pressure confirmed that the objective function based on the average absolute deviation in pressure provided a fit that was at least as good as any other. However, the optimal parameters were obtained by minimizing the sum of the average absolute deviations of the errors between the calculated and experimental values of the pressure and vapour composition.

For the pure component properties, the $\kappa_1$ (kappa) parameter found in the Stryjek and Vera (1986) α-correlations respectively were regressed using experimental vapour pressure data measured for that component. The computational procedure in obtaining the calculated pressure is similar to that discussed by Naidoo (2004). The objective function used in these computations was:

$$S = \frac{1}{n}\sum_{i}^{n}\left(\frac{\left|P_i^{\exp} - P_i^{calc}\right|}{P_i^{\exp}}\right) \tag{7.6}$$

For the chemical theory, the objective function finds the minimum deviation between the calculated vapour composition and the experimental vapour composition as given below:

$$S = \frac{1}{n}\sqrt{\sum_{i}^{n}\left(y_i^{\exp} - y_i^{calc}\right)^2} \tag{7.7}$$

The binary interaction and $G^E$ model parameters in the binary VLE computations were determined by least squares regression of the experimental P-T-x-y data. The objective function employed for the least squares regression was:

$$S = \frac{1}{n}\sum_{i}^{n}\left(\frac{\left|P_i^{\exp} - P_i^{calc}\right|}{P_i^{\exp}}\right) + \left(\left|y_i^{\exp} - y_i^{calc}\right|\right) \tag{7.8}$$

### 7.5.7 Regressed pure component parameters

For the pure component properties, the $\kappa_1$ (kappa) parameter found in the Stryjek and Vera (1986) α-correlations respectively were regressed from pure component vapour pressure data. Table 7-3 presents the kappa values.

| Components | $\kappa_1$ | AAD %(ΔP) |
|---|---|---|
| 2-Propanol | 0.2038 | 0.0441 |
| 2-Butanol | 0.3968 | 0.0470 |
| 2-Methyl-1-Propanol | 0.4556 | 0.0874 |
| Butyric Acid | 0.1422 | 0.0768 |

**Table 7-3: Pure component $\kappa_1$(kappa) values in the PR-SV EOS**

## 7.6 Phase Equilibrium Results

### 7.6.1 Cyclohexane (1) + Ethanol (2)

The cyclohexane + ethanol test system data were regressed using one of the liquid-phase activity coefficient models, NRTL in conjunction with the Hayden and O'Connell (1975) method for determining the second virial coefficients (used in determining the fugacity coefficients for the vapour phase correction term). The model parameters obtained from this regression are provided in Table 7-4.

The NRTL equation fit the experimental data well. A similar trend was found by Joseph et al. (2002) for the cyclohexane (1) + ethanol (2) system. He used three liquid-phase activity coefficient models (Wilson, NRTL and UNIQUAC), but observed the UNIQUAC to give the worst performance of the liquid-phase activity coefficient models. Therefore, it was not necessary to use multiple models, hence the reason for the NRTL used. The experimental data are presented, along with the fit provided by the model, in Figures 7-8 through 7-11.

| **Parameters** | **P = 40 kPa** | **P = 150 kPa** |
|---|---|---|
| $\alpha_{ij}$ | 0.4655 | 0.4655 |
| $\tau_{12}$ | 2.2706 | 1.7706 |
| $\tau_{21}$ | 1.6090 | 1.0590 |
| AAD(ΔT) | 0.0020 | 0.0003 |
| AAD(Δy) | 0.0218 | 0.0036 |
| AE% | 0.0479 | 0.0013 |

**Table 7-4: Model parameters and deviations from experimental values for the cyclohexane (1) + ethanol (2) system at 40 and 150 kPa.**

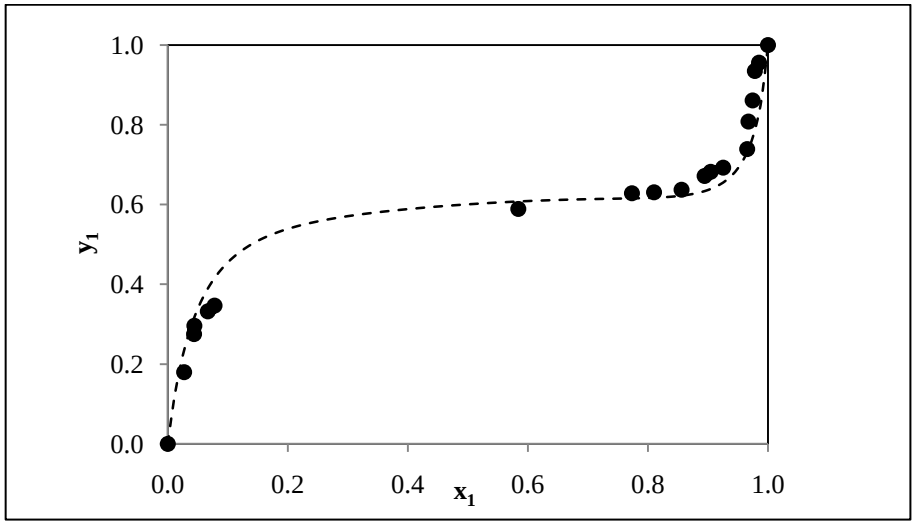


**Figure 7-1: NRTL model fitted to x-y data for cyclohexane (1) + ethanol (2) system at 40 kPa. Experimental data (●); Model (- - -)**

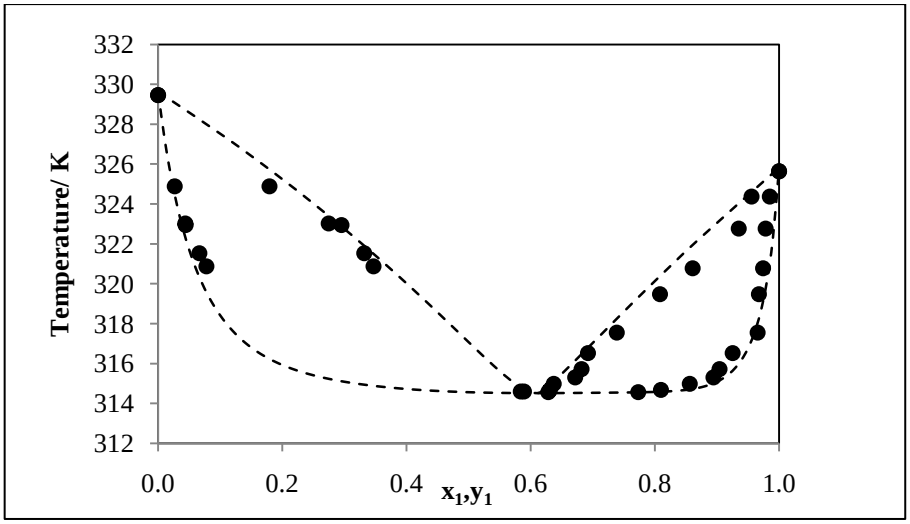


**Figure 7-2: NRTL model fitted to T-x-y data for cyclohexane (1) + ethanol (2) system at 40 kPa. Experimental data (●); Model (- - -)**

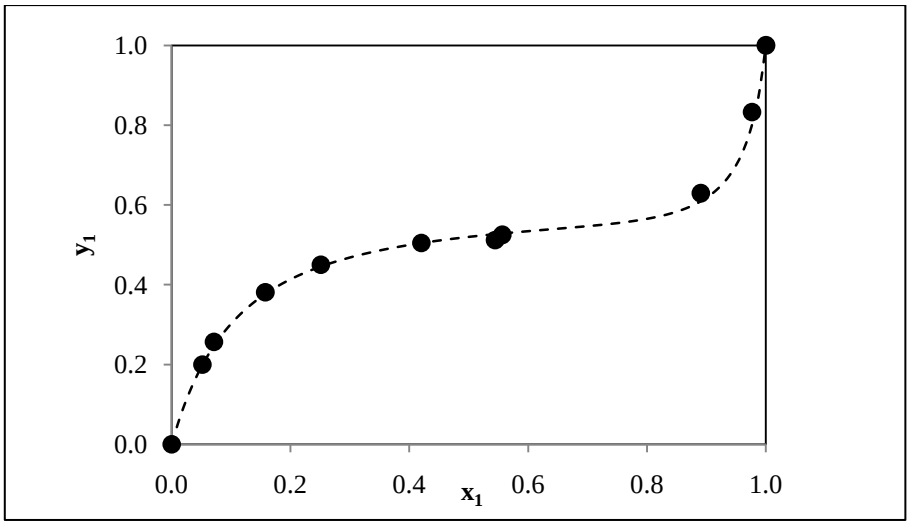


**Figure 7-3: NRTL model fitted to x-y data for cyclohexane (1) + ethanol (2) system at 150 kPa. Experimental data (●); Model (- - -)**

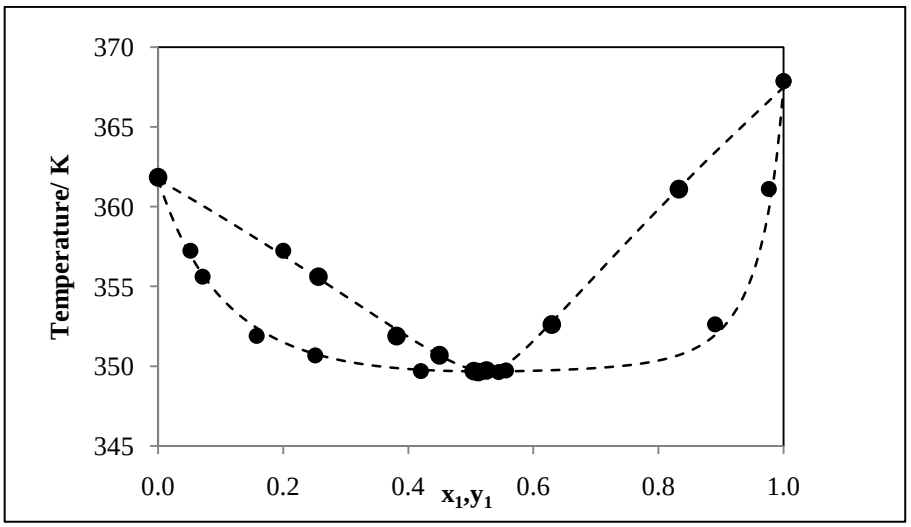


**Figure 7-4: NRTL model fitted to T-x-y data for cyclohexane (1) + ethanol (2) system at 150 kPa. Experimental data (●); Model (- - -)**

## 7.7 Analysis of modelling and data for new systems

### 7.7.1 Experimental Activity coefficients

This section is introduced in order to observe the plots of gamma with respect to composition for a non-associating and associating model. The experimental liquid-phase activity coefficient was first

calculated by evaluating the vapour phase correction factor from a second virial coefficient as given by equation (3.22). This was then used in the equation (3.21) by rearranging the equation to evaluate the activity coefficient.

The method is outlined and discussed in section 3.5.2 using the Chemical theory approach for evaluating the activity coefficients for an associating model.

However, equations 7.9 and 7.10 taken from Prausnitz et al. (1999) were included in the calculations.

$$\gamma_i = \frac{2k_i}{(2k_i - 1)x_i + k_i x_j + (x_i^2 + 2k_i x_i x_j + k_i x_j^2)^{1/2}} \qquad (7.9)$$

where

$$k_i = 4K_{ij} + 1 \qquad (7.10)$$

The equation (3.52) for calculating $K_{ij}$ is given in Section 3.6.2.

For the carboxylic acid-alcohol binary mixture, it was observed that the non-associating method produces poor values (refer to Plot 7.5). This behaviour is attributed to the association effect of the systems measured, especially at low pressure and moderate temperatures.

By applying the equations (7.9 and 7.10) to evaluate the experimental activity coefficients, significant improvement was observed. This trend was observed to be the same for all the systems measured.

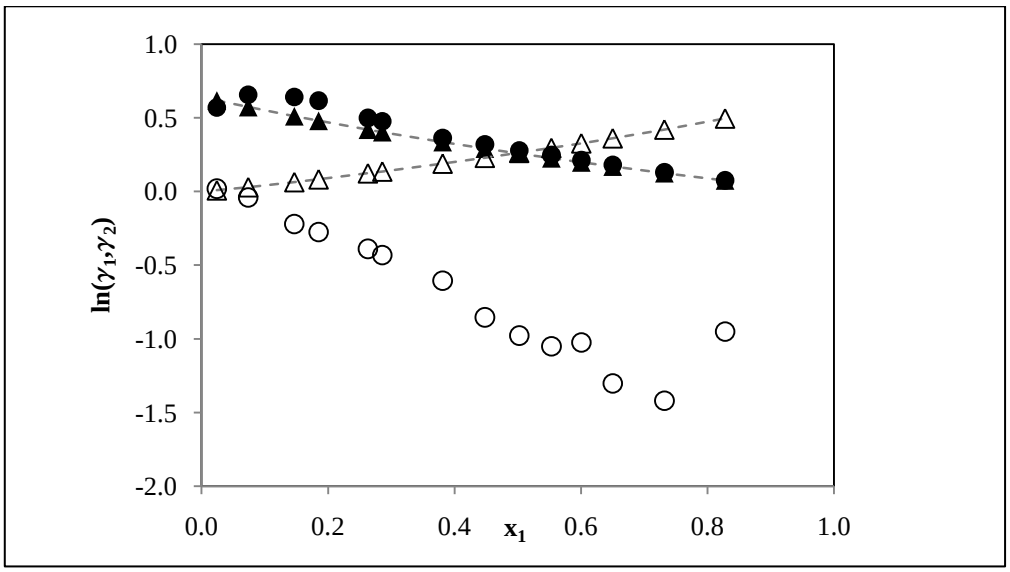


**Figure 7-5: Experimental liquid-phase activity coefficients calculated for the 2-propanol (1) +butyric acid (2) system at 333.15 K using the Non-associating models and the chemical theory approach for the liquid phase. (●), ln$\gamma_1$, (○), ln$\gamma_2$ for non-associating model, (▲), ln$\gamma_1$ ,(Δ), ln$\gamma_2$ for the chemical theory.**

## 7.7.2 Phase behaviour of the new Systems

### 7.7.2.1 Alcohol + Carboxylic Acid mixtures

Choosing the correct association model is the first important step in the modeling of the new systems measured. It has become a practice to use an equation of state together with an equilibrium equation for dimerization in order to represent the vapour-phase behaviour of carboxylic acid binary mixtures. This practice is based on the assumption that dimers are the only or predominant oligomer formed by carboxylic acid in vapour phase. Some researchers who suggest that formation of higher-order oligomers may also play a significant role in the vapour-phase behaviour of the acids do not generally accept this assumption. However, butyric acid, which is a carboxylic acid used in this project was assumed after the review of Vawdrey et al.(2004) on the vapour phase association of *n*-aliphatic carboxylic acids (C4 to C10) to be the only oligomer formed in the vapour-phase. The possible formation of dimers in the liquid phase was not taken into account in this model. However, an equation proposed by Prausnitz et al. (1999) was used in the chemical theory to correct the liquid phase activity coefficient using the equilibrium constants for the species formed. In order to validate their calculation methods, acetic acid with data already reported in literature was used. Vawdrey et al. (2004) used the ab-initio and density functional theory (DFT) as a method to study the vapour-phase association (Prausnitz et al., 1969) of carboxylic acids. These methods were used in evaluating the relative stability of various oligomers, the enthalpies and entropies of association as well as the equilibrium constants for the interconversion between the stable molecules formed.

The equilibrium constant for the dimer for acetic acid at 400 K and 100 kPa shows the dimer mole fraction ($y_d$ ) to be 0.5. This high value indicates that the dimer should be considered as a significant species in the vapour-phase even at modest temperatures and pressures.
Vawdrey et al. (2004) also examined the association enthalpies of the oligomers in order to determine the oligomer structures. The magnitude of the enthalpy for the trimers formed in the acetic acid used as the reference acid was small, indicating that the hydrogen bonds in the trimer are weaker than those in the dimer. Based on this study of acetic acid oligomers, the trimer as well as tetramer (for acids longer than C2) fractions were considered insignificant in calculating carboxylic acid vapour properties, while dimers were considered the only important oligomers in the vapour-phase of the carboxylic acids. In addition, dimerization constants have been observed to decrease with increasing carbon-number indicating less association with larger acids. Using the chemical theory in this project, the association constant was observed to decrease as temperature increases. This is in agreement with the observation of Prausnitz et al. (1999).

Also, all cross association constants are assumed to be equal and independent of *i*, thus an association constant $K_{(AB)}$ is assigned to the reaction for the dimer formation for simplicity. For this project using the chemical theory approach, the cross association coefficient as well as the fugacity coefficient in vapour phase was calculated using the Hayden and O'Connell method. The Hayden and O'Connell (1975) method was also employed to determine the dimerization equilibrium constant as well as the effective enthalpy of formation of the physically bound pairs. The second virial coefficient for dimerization was also calculated from Hayden and O'Connell (1975) method and the liquid molar volumes were evaluated using the modified Rackett equation.

### 7.7.3 Discussion of phase equilibrium result for the new systems

The 2-propanol (1) + butyric acid (2), 2-butanol (1) + butyric acid (2) and 2-methyl-1-propanol (1) + butyric acid (2) systems were measured at three isotherms viz. 333.15, 353.15 and 373.15 K respectively in order to determine the temperature dependence of the model parameter used.

In this project, with regards to the VLE data reduction, the models provided a better fit to all the systems measured at 373.15 K. This is quite understandable, since the association seems to disappear at higher temperature and dimers are much more formed at moderate temperature (e.g 333.15 K) and lower pressure (about 20 kPa and below). This also explains why the chemical theory gave the highest percentage error at 373.15 K for all the systems since it was taking into account the formation of dimers which probably have been broken due to the high temperature and pressure (since the boiling point of the 2-propanol and 2-butanol were less than 373.15 K). These agree with the discussion of Prausnitz et al. (1980) that dimerization decreases as pressure falls as a direct consequence of Le Chatelier's principle. Hence, it can be said that the degree to which dimerization will take place is influenced by the system pressure which explains why the plots at 373.15 K is seen to be more ideal. This also explains why the models do not often accurately fit the experimental data in the carboxylic acid dilute regions except for the Hayden and O'Connell with Chemical theory that accounts for the non-ideality and chemical interactions in the vapour phase.

As was mentioned in Section 7.5 and 7.6, the data reduction was conducted by minimizing the pressure and composition. Therefore, in the discussions of the individual systems that follow, the best fit model is judged based on the model that exhibited the least error, which is the sum of the square of the absolute average deviation of the calculated pressures from the experimental pressures and the square of the average deviation for the composition.

### 7.7.3.1 2-Propanol (1) + Butyric Acid (2) System

The result shown in Table 7-6 indicate that all the models give a low average absolute deviation value and these differences are so small that when the results are viewed graphically it is difficult to tell which model performed better. The direct method modeling performed fair in this work. For the direct method, SRK-WS-NRTL $G^E$ model gives an overall reduced deviation. This could be explained in line with the suggestion by Pedersen et al. (1996) that a comparison of association models such as CPA against state-of-the-art local composition models such as the SRK-Huron Vidal/NRTL model could help to establish the actual improvement gained by the Wertheim theory over the local composition principle, which indirectly also accounts for the hydrogen bonding/polar phenomena. Hence, it could be suggested that the good fit provided by the SRK-WS/NRTL in this project is an indication that this combination could in some cases of associating mixtures give a better fit especially at moderate pressure and temperature. This is also supported by the reported of Soo et al. (2009) for n-butane + ethanol binary mixtures at 323 to 423 K where the PR/WS/NRTL equation of state shows good correlation with the results, while the PC-SAFT is slightly less accurate.

From Table 7-5, it can be observed that the activity coefficients for the 2-propanol (1) + butyric acid (2) deviates a little from unity. Thus, the system shows a practically ideal behaviour in the liquid-phase. However, a large deviation from ideality was reported for the vapour phase. Although, this can be seen to move closer to unity as the temperature increases. The results from the regression of the VLE data along with the deviations in vapour composition , pressure and the overall percentage error showing the performance of each model used for the 2-propanol (1) + butyric acid (2) system are presented in Table 7-6.

| P/kPa | $x_1$ | $y_1$ | $z_1$ | $z_2$ | $\gamma_1$ | $\gamma_2$ | $\Phi_1$ | $\Phi_2$ |
|---|---|---|---|---|---|---|---|---|
| | | | | **T=333.15 K** | | | | |
| 1.82 | 0.0242 | 0.2656 | 0.1447 | 0.3745 | 1.8542 | 1.0078 | 0.5446 | 0.5099 |
| 3.51 | 0.0738 | 0.5705 | 0.2492 | 0.1737 | 1.7732 | 1.0295 | 0.4369 | 0.4043 |
| 6.38 | 0.1467 | 0.7704 | 0.2686 | 0.0735 | 1.6664 | 1.0656 | 0.3487 | 0.3199 |
| 8.13 | 0.1851 | 0.8197 | 0.2594 | 0.0522 | 1.6154 | 1.0861 | 0.3165 | 0.2895 |
| 10.80 | 0.2631 | 0.8766 | 0.2468 | 0.0317 | 1.5210 | 1.1310 | 0.2815 | 0.2568 |
| 11.67 | 0.2858 | 0.8903 | 0.2426 | 0.0273 | 1.4957 | 1.1449 | 0.2725 | 0.2484 |
| 14.66 | 0.3812 | 0.9298 | 0.2300 | 0.0158 | 1.3981 | 1.2078 | 0.2474 | 0.2249 |
| 17.19 | 0.4479 | 0.9553 | 0.2206 | 0.0094 | 1.3375 | 1.2565 | 0.2309 | 0.2097 |

| P/kPa | $x_1$ | $y_1$ | $z_1$ | $z_2$ | $\gamma_1$ | $\gamma_2$ | $\Phi_1$ | $\Phi_2$ |
|---|---|---|---|---|---|---|---|---|
| 19.19 | 0.5022 | 0.9665 | 0.2127 | 0.0067 | 1.2921 | 1.2994 | 0.2201 | 0.1997 |
| 21.28 | 0.5531 | 0.9736 | 0.2047 | 0.0050 | 1.2524 | 1.3425 | 0.2103 | 0.1907 |
| 23.02 | 0.6005 | 0.9768 | 0.1984 | 0.0043 | 1.2178 | 1.3855 | 0.2031 | 0.1841 |
| 24.74 | 0.6501 | 0.9852 | 0.1938 | 0.0026 | 1.1837 | 1.4336 | 0.1967 | 0.1782 |
| 27.64 | 0.7318 | 0.9905 | 0.1854 | 0.0016 | 1.1320 | 1.5211 | 0.1872 | 0.1694 |
| 31.32 | 0.8278 | 0.9909 | 0.1754 | 0.0015 | 1.0776 | 1.6392 | 0.1770 | 0.1600 |
| | | | | **353.15 K** | | | | |
| 4.86 | 0.0100 | 0.1579 | 0.0920 | 0.4613 | 1.8032 | 1.0015 | 0.5826 | 0.5477 |
| 6.34 | 0.0329 | 0.2558 | 0.1375 | 0.3742 | 1.7672 | 1.0084 | 0.5374 | 0.5027 |
| 7.98 | 0.0455 | 0.3682 | 0.1837 | 0.2937 | 1.7480 | 1.0129 | 0.4989 | 0.4647 |
| 10.78 | 0.0763 | 0.5298 | 0.2384 | 0.1961 | 1.7028 | 1.0249 | 0.4501 | 0.4170 |
| 11.60 | 0.0877 | 0.5817 | 0.2550 | 0.1698 | 1.6868 | 1.0297 | 0.4385 | 0.4057 |
| 13.96 | 0.1113 | 0.6397 | 0.2622 | 0.1363 | 1.6545 | 1.0399 | 0.4099 | 0.3782 |
| 15.29 | 0.1244 | 0.6682 | 0.2647 | 0.1212 | 1.6371 | 1.0458 | 0.3962 | 0.3651 |
| 21.13 | 0.1918 | 0.7669 | 0.2682 | 0.0748 | 1.5536 | 1.0783 | 0.3498 | 0.3209 |
| 25.42 | 0.2503 | 0.8402 | 0.2730 | 0.0475 | 1.4882 | 1.1091 | 0.325 | 0.2974 |
| 29.20 | 0.2884 | 0.8755 | 0.2689 | 0.0350 | 1.4486 | 1.1306 | 0.3073 | 0.2806 |
| 49.79 | 0.5161 | 0.9590 | 0.2354 | 0.0092 | 1.2530 | 1.2834 | 0.2456 | 0.2231 |
| 53.43 | 0.5673 | 0.9677 | 0.2304 | 0.0070 | 1.2168 | 1.3246 | 0.2382 | 0.2163 |
| 60.62 | 0.6471 | 0.9775 | 0.2203 | 0.0046 | 1.1651 | 1.3949 | 0.2255 | 0.2045 |
| 80.55 | 0.8889 | 0.9999 | 0.1992 | 0.0000 | 1.0382 | 1.6679 | 0.1994 | 0.1803 |
| | | | | **373.15 K** | | | | |
| 10.85 | 0.0085 | 0.1255 | 0.0773 | 0.5203 | 1.7080 | 1.0006 | 0.6160 | 0.5948 |
| 14.85 | 0.0330 | 0.2876 | 0.1619 | 0.3854 | 1.6740 | 1.0053 | 0.5631 | 0.5409 |
| 21.07 | 0.0728 | 0.4970 | 0.2507 | 0.2424 | 1.6218 | 1.0170 | 0.5046 | 0.4817 |
| 30.06 | 0.1261 | 0.6483 | 0.2896 | 0.1493 | 1.5574 | 1.0361 | 0.4470 | 0.4243 |
| 41.22 | 0.1908 | 0.7454 | 0.2968 | 0.0959 | 1.4864 | 1.0628 | 0.3984 | 0.3765 |
| 47.46 | 0.2320 | 0.7846 | 0.2961 | 0.0768 | 1.4448 | 1.0815 | 0.3778 | 0.3563 |
| 60.77 | 0.3039 | 0.8381 | 0.2872 | 0.0523 | 1.3783 | 1.1171 | 0.3431 | 0.3227 |
| 71.76 | 0.3673 | 0.8806 | 0.2824 | 0.0360 | 1.3252 | 1.1515 | 0.3211 | 0.3014 |
| 79.96 | 0.4116 | 0.9013 | 0.2765 | 0.0285 | 1.2908 | 1.1775 | 0.3073 | 0.2881 |
| 90.23 | 0.4576 | 0.9151 | 0.2671 | 0.0233 | 1.2573 | 1.2061 | 0.2924 | 0.2738 |
| 101.74 | 0.5149 | 0.9297 | 0.2581 | 0.0183 | 1.2185 | 1.2442 | 0.2782 | 0.2602 |
| 103.02 | 0.5207 | 0.9340 | 0.2579 | 0.0171 | 1.2147 | 1.2483 | 0.2767 | 0.2588 |
| 109.44 | 0.5644 | 0.9436 | 0.2540 | 0.0142 | 1.1872 | 1.2797 | 0.2698 | 0.2522 |
| 151.10 | 0.7795 | 0.9812 | 0.2300 | 0.0041 | 1.0736 | 1.4664 | 0.2351 | 0.2191 |
| 171.14 | 0.8880 | 0.9925 | 0.2204 | 0.0016 | 1.0294 | 1.5865 | 0.2228 | 0.2074 |

**Table 7-5: Vapour-liquid equilibrium data for the 2-propanol (1) +butyric acid (2) system at 333.15K, 353.15K and 373.15K taking chemical theory into account for the experimental liquid-phase activity coefficients and vapour-phase correction for non-ideality.**

PRSV = Peng-Robinson Stryjek-Vera equation of state, SRK = Soave-Redlich-Kwong equation of state, WS = Wong-Sandler mixing rule, VEOS = Virial equation of state, HOC = Hayden and O'Connell, CT = Chemical Theory and TsC = Tsonopoulos Correlation

| Model | T/ K | $k_{ij}$ | $\alpha_{12}$ | $\Delta g_{12}$* | $\Delta g_{21}$* | AAD (ΔP) | AAD (Δy) | AE% |
|---|---|---|---|---|---|---|---|---|
| SRK-WS | 333.15 | -0.0686 | -0.2918 | 2621.47 | -5539.88 | 0.0914 | 0.0065 | 0.8394 |
| | 353.15 | 0.0528 | -0.1952 | 4387.61 | -8808.69 | 0.1324 | 0.0164 | 1.7808 |
| | 373.15 | 0.0376 | -0.2482 | 3504.91 | -6205.04 | 0.0247 | 0.0244 | 0.1203 |
| PRSV-WS | 333.15 | -1.0440 | 0.3000 | 12851.42 | -689.99 | 0.1235 | 0.0082 | 1.5326 |
| | 353.15 | -0.8478 | 0.3000 | 14199.90 | -1125.75 | 0.1677 | 0.0174 | 2.8431 |
| | 373.15 | -0.7821 | 0.3000 | 12412.56 | -345.93 | 0.0326 | 0.0259 | 0.1733 |
| VEOS(TsC) | 333.15 | | -0.2234 | 2519.38 | -5539.88 | 0.1102 | 0.0087 | 1.2214 |
| | 353.15 | | -0.3508 | 2368.79 | -5872.46 | 0.1536 | 0.0186 | 2.3941 |
| | 373.15 | | -0.9231 | 608.46 | -2286.16 | 0.0367 | 0.0288 | 0.2178 |
| HOC -CT | 333.15 | | 0.7475 | 3092.42 | 757.29 | 0.0549 | 0.0137 | 0.3202 |
| | 353.15 | | 0.7767 | 3535.59 | 740.32 | 0.0458 | 0.0158 | 0.2347 |
| | 373.15 | | 1.2356 | 4472.91 | 1408.73 | 0.0449 | 0.0060 | 0.2052 |

**Table 7-6: Modeling results for the 2-Propanol+Butyric Acid system at 333.15, 353.15 and 373.15 K with NRTL $G^E$ model (*, J/mol)**

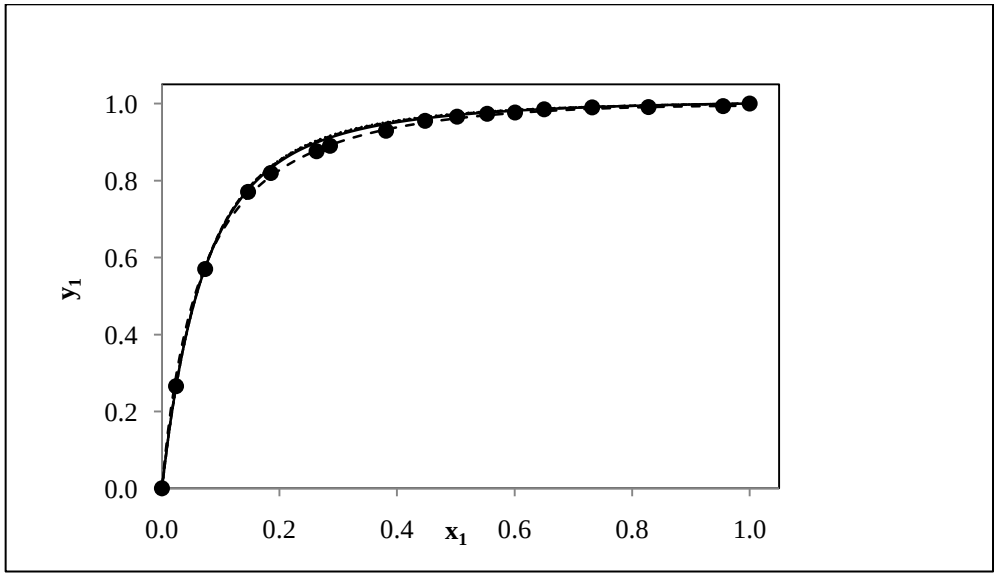


**Figure 7-6: x-y plot for the 2-propanol (1) + butyric acid (2) system at 333.15 K (● ), this work; (—), SRK-WS; (---), PRSV-WS; (---), VEOS; (- - -), HOC-CT**

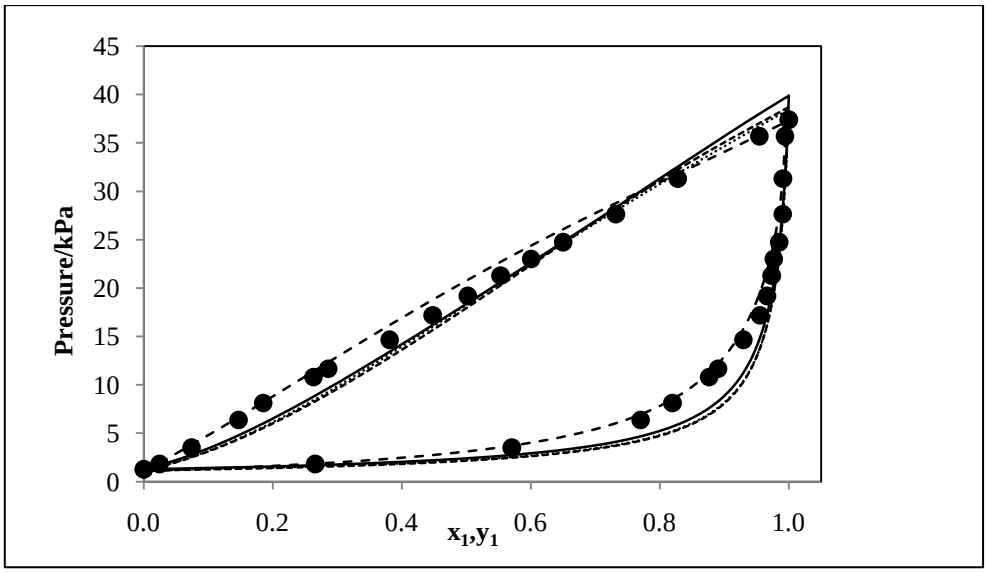


**Figure 7-7: P-x-y VLE plot for the 2-propanol (1) + butyric acid (2) system at 333.15 K (● ), this work; (—), SRK-WS;( ---), PRSV-WS; (---), VEOS; (- - -), HOC-CT**

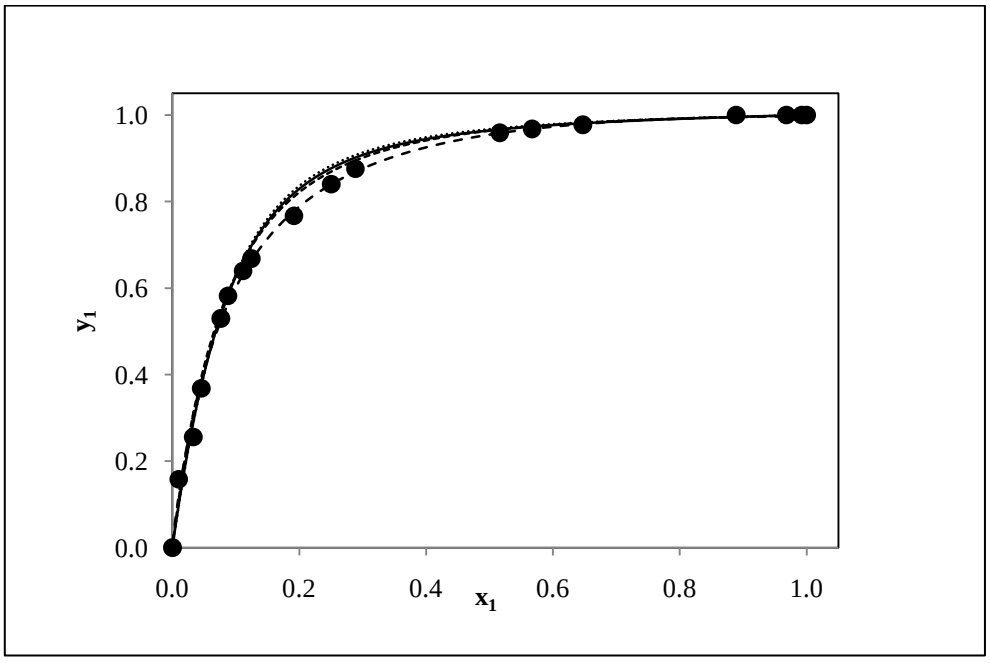


**Figure 7-8: x-y VLE plot for the 2-propanol (1)-butyric acid (2) system at 353.15 K ( ●) , this work; (—), SRK-WS; (---), PRSV-WS; (---), VEOS; (- - -), HOC-CT**

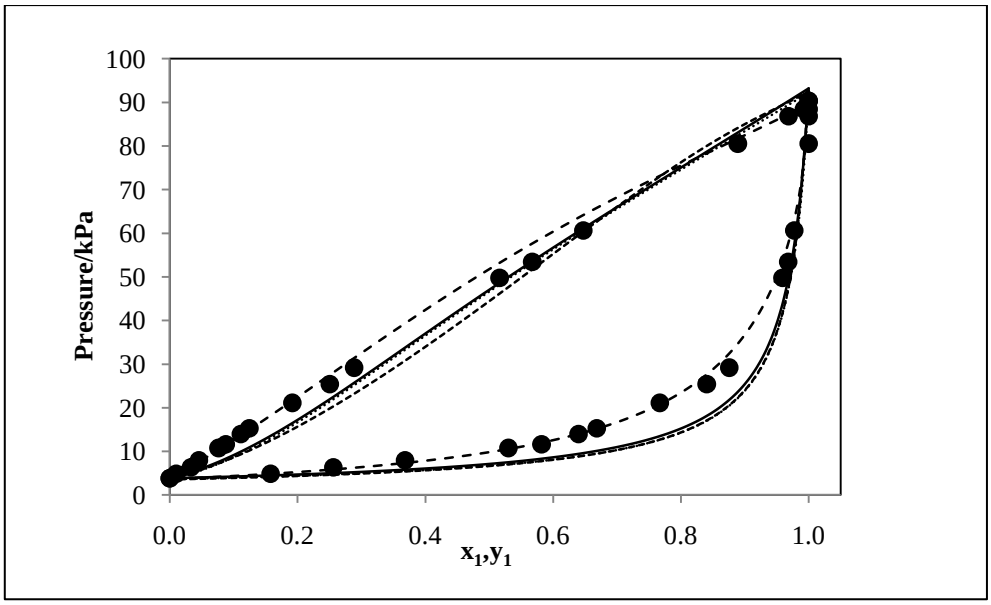


**Figure 7-9: P-x-y VLE plot for the 2-propanol (1)-butyric acid (2) system at 353.15 K (• ), this work; (—), SRK-WS; (---), PRSV-WS; (---), VEOS; (- - -), HOC-CT**

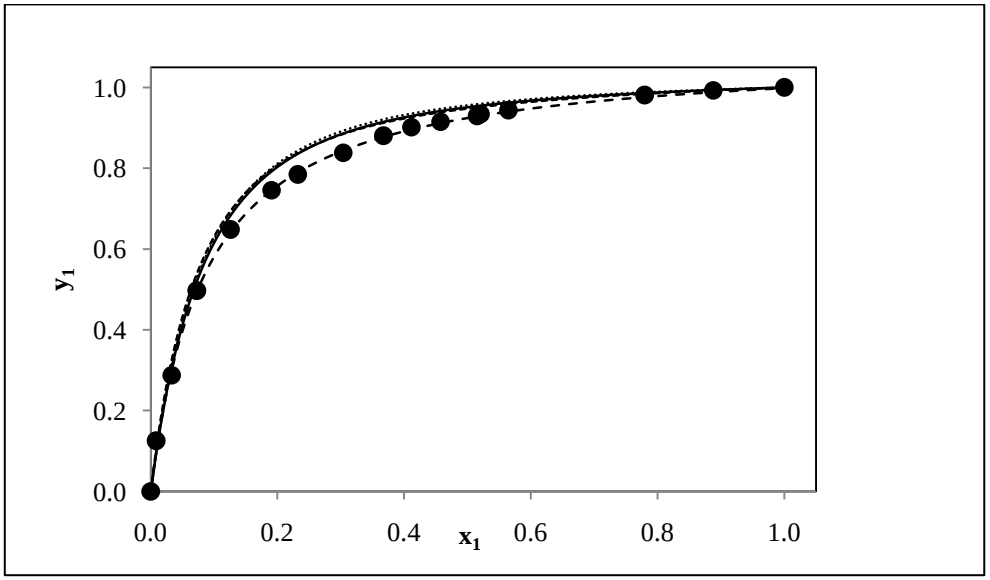


**Figure 7-10: x-y VLE plot for the 2-propanol (1)-butyric acid (2) system at 373.15 K (• ), this work; (—), SRK-WS;(---), PRSV-WS; (---), VEOS; (- - -), HOC-CT**

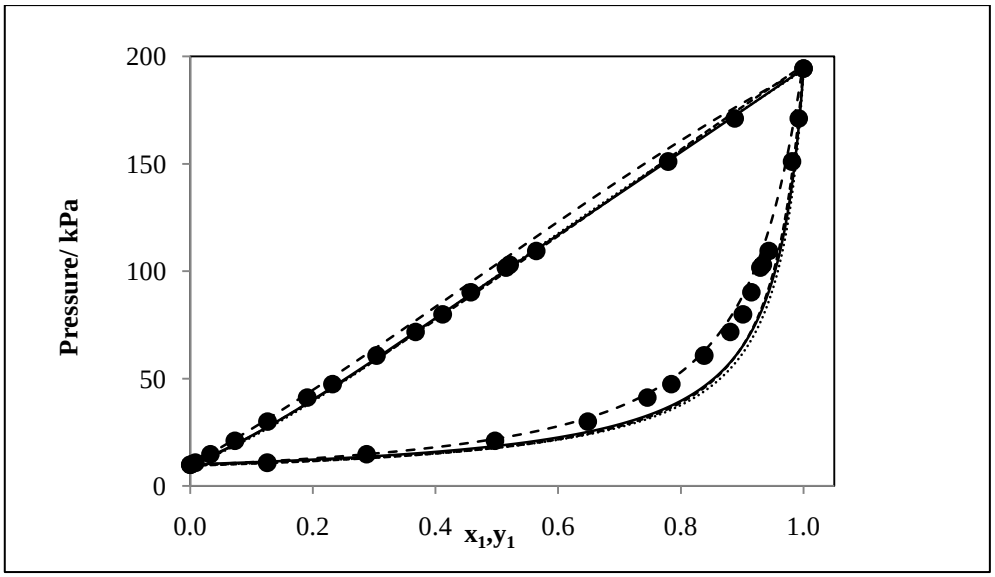


**Figure 7-11: P-x-y VLE plot for the 2-propanol (1)-butyric acid (2) system at 373.15 K ( •) , this work;( —), SRK-WS; (---), PRSV-WS; (---), VEOS;( - - -), HOC-CT**

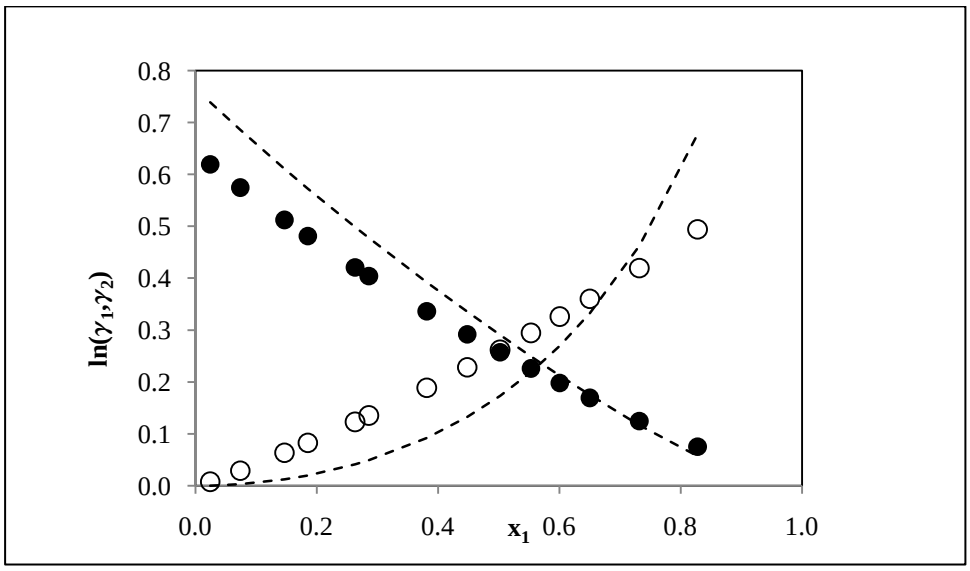


**Figure 7-12: Comparison between the experimentally determined liquid-phase activity coefficients and those calculated from the NRTL model with chemical theory for 2-propanol (1) + butyric acid (2) system at 333.15 K.**
**(• ), experimental activity coefficient; (- - -), NRTL model**

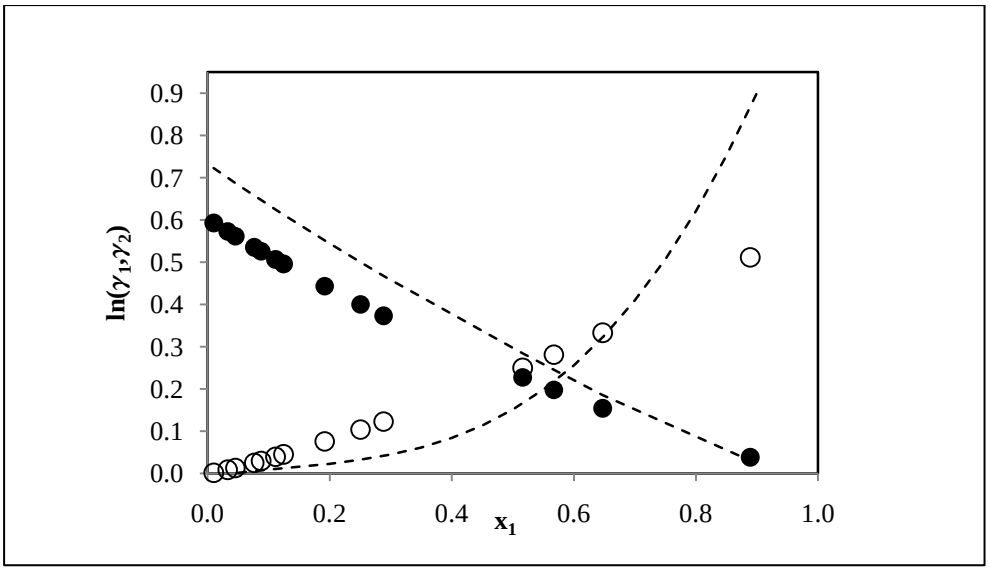


**Figure 7-13: Comparison between the experimentally determined liquid-phase activity coefficients and those calculated from the NRTL model with chemical theory for 2-propanol (1) + butyric acid (2) system at 353.15 K.**
**(• ), experimental activity coefficient; (- - -), NRTL model**

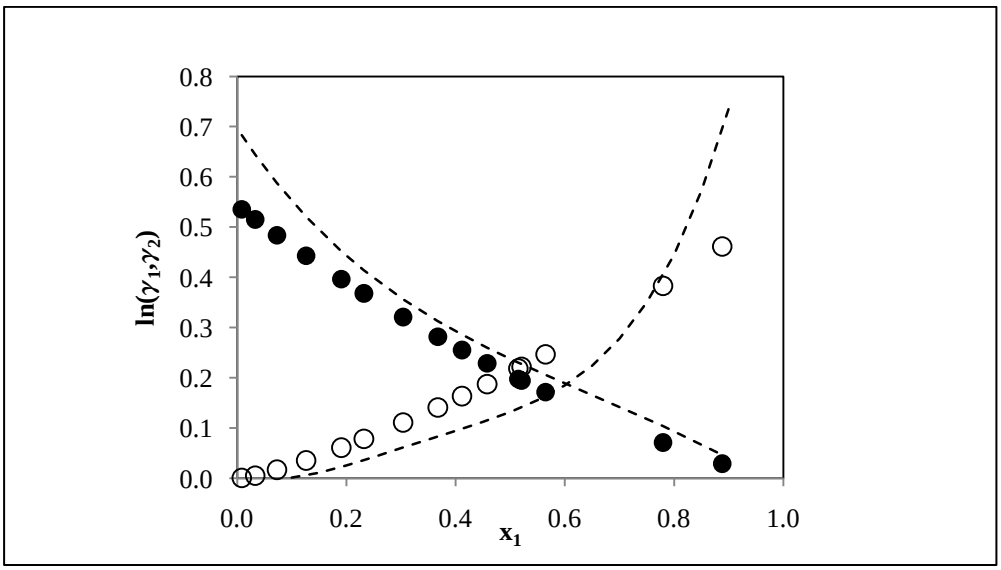


**Figure 7-14: Comparison between the experimentally determined liquid-phase activity coefficients and those calculated from the NRTL model with chemical theory for 2-propanol (1) + butyric acid (2) system at 373.15 K.**
**( •) , experimental activity coefficient; (- - -), NRTL model**

It is important to mention that the activity coefficients were not determined during the direct method regressions, since the direct method is based on fugacity coefficients in both the vapour and liquid phases. Thus, there are no model activity coefficients to which the experimental values may be compared. Due to this reason, the direct test could not be performed for the Soave-Redlich-

Kwong and Peng-Robinson EOS data reductions (the direct test is based on the deviations between the experimental and the model activity coefficients). However, the thermodynamic consistency was checked via the point test.

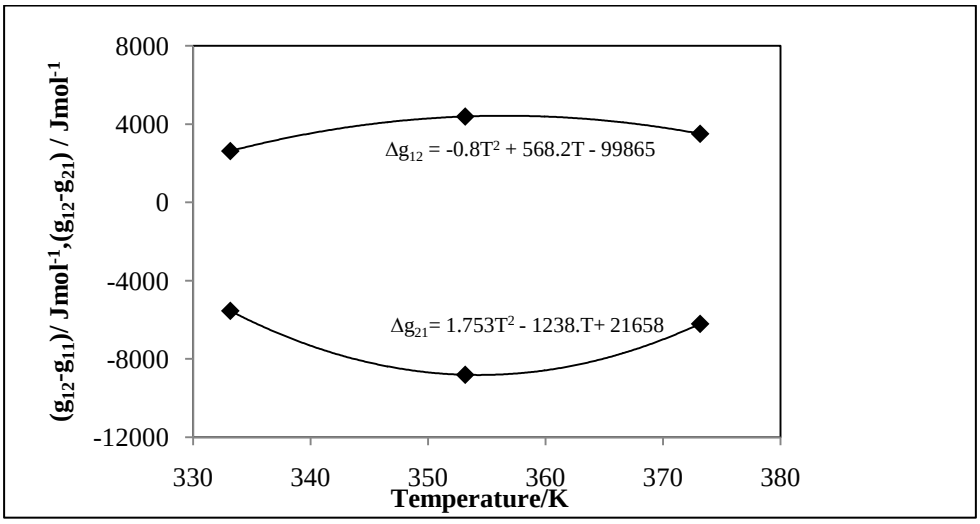


**Figure 7-15 : Temperature dependence of the NRTL model parameters for 2-propanol (1) + butyric acid (2) using the SRK-WS model**

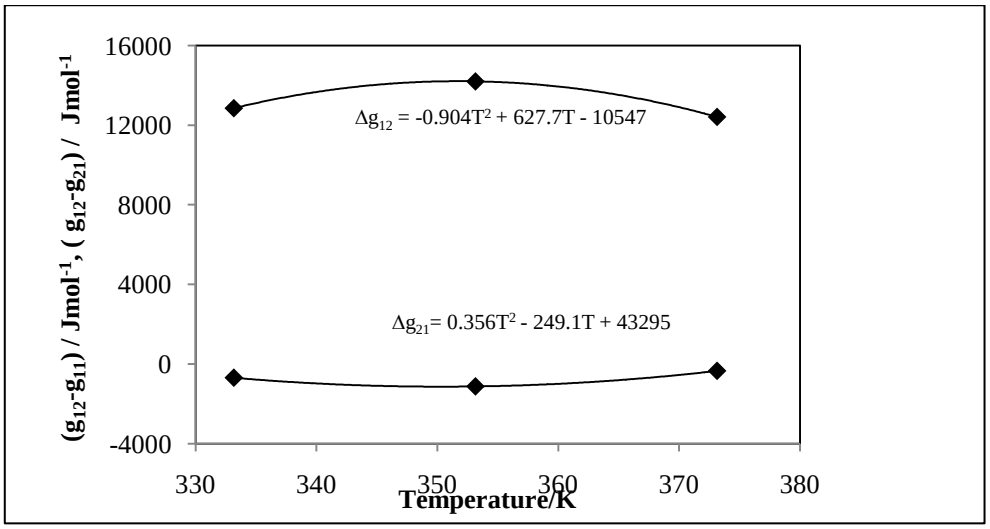


**Figure 7-16 : Temperature dependence of the NRTL model parameters for 2-propanol (1) + butyric acid (2) using PRSV-WS model**

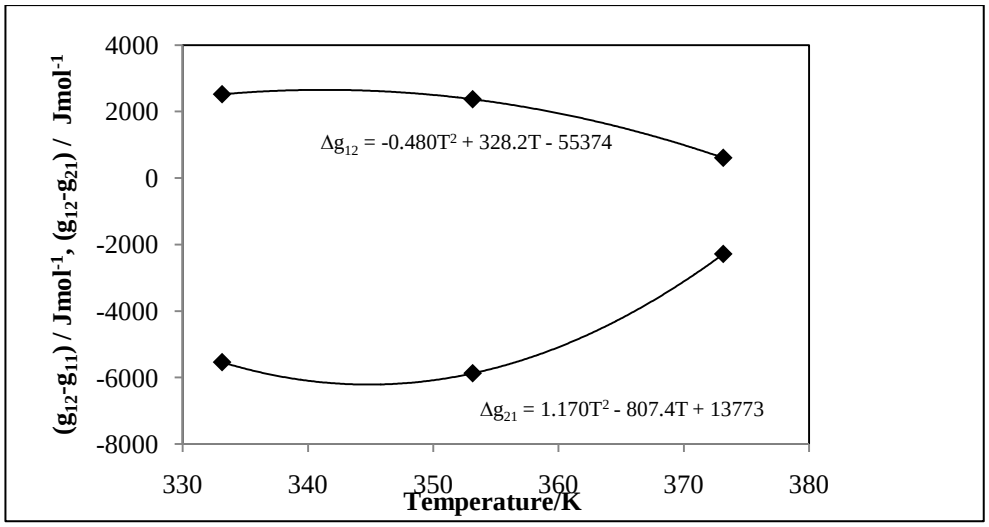


**Figure 7-17 : Temperature dependence of the NRTL model parameters for 2-propanol (1) + butyric acid (2) using Virial EOS (Tsonopoulos)**

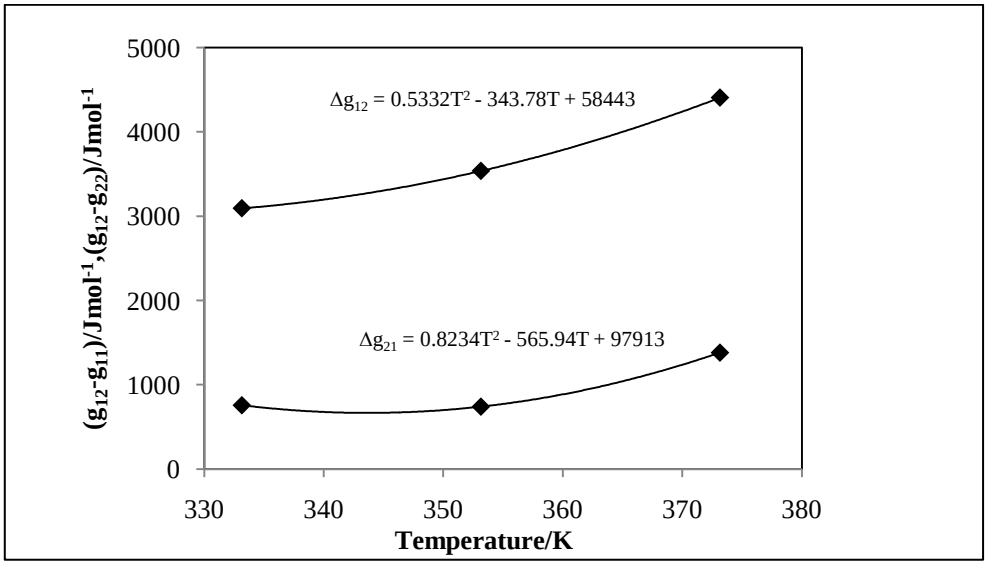


**Figure 7-18 : Temperature dependence of the NRTL model parameters for 2-propanol (1) + butyric acid (2) using Hayden O'Connell with Chemical theory**

### 7.7.3.2 2-Butanol (1) + Butyric Acid (2) System

All of the models were fitted to the 2-butanol + butyric acid system and, in general, the models performed better for this system than they did for the 2-propanol + butyric acid system. This is self-evident when the deviations from the experimental data are considered. For the 2-butanol + butyric acid system, all the isotherms have a $\Delta y$ value within 0.01; whilst for the 2-propanol-butyric acid system each model gave a $\Delta y$ greater than 0.01 at 353.15 K and 373.15 K with an exception observed only at 333.15K for the same system.

It is important to point out that as in the case of the 2-propanol + butyric acid system, the models could not effectively fit the experimental data in the 2-butanol dilute regions. The regressed experimental data using chemical theory are presented in Table 7-7 along with the calculated activity coefficient (γ) and the vapour-phase correction term (Φ). In addition, the parameters obtained through regression of the experimental VLE data for the 2- butanol (1) + butyric acid (2) system are presented on Table 7-8.

| P/kPa | $x_1$ | $y_1$ | $z_1$ | $z_2$ | $\gamma_1$ | $\gamma_2$ | $\Phi_1$ | $\Phi_2$ |
|---|---|---|---|---|---|---|---|---|
| | | | | **T = 333.15 K** | | | | |
| 1.68 | 0.0325 | 0.2199 | 0.1192 | 0.4084 | 1.8445 | 1.0112 | 0.5422 | 0.5235 |
| 2.21 | 0.0588 | 0.4268 | 0.2118 | 0.2738 | 1.8010 | 1.0227 | 0.4961 | 0.4777 |
| 3.06 | 0.1192 | 0.5703 | 0.2528 | 0.1829 | 1.7088 | 1.0515 | 0.4433 | 0.4256 |
| 4.47 | 0.2032 | 0.7285 | 0.2808 | 0.1002 | 1.5956 | 1.0961 | 0.3854 | 0.3690 |
| 5.84 | 0.2725 | 0.8343 | 0.2900 | 0.0591 | 1.5312 | 1.1271 | 0.3518 | 0.3362 |
| 5.66 | 0.2567 | 0.8242 | 0.2899 | 0.0550 | 1.5132 | 1.1367 | 0.3475 | 0.3320 |
| 6.56 | 0.3071 | 0.8710 | 0.2890 | 0.0409 | 1.4753 | 1.1583 | 0.3318 | 0.3168 |
| 7.86 | 0.3946 | 0.9056 | 0.2793 | 0.0278 | 1.3877 | 1.2173 | 0.3084 | 0.2941 |
| 9.98 | 0.5028 | 0.9393 | 0.2624 | 0.0162 | 1.2934 | 1.2999 | 0.2794 | 0.2661 |
| 11.82 | 0.6300 | 0.9673 | 0.2516 | 0.0081 | 1.1986 | 1.4137 | 0.2601 | 0.2475 |
| 11.92 | 0.6383 | 0.9690 | 0.2512 | 0.0076 | 1.1929 | 1.4219 | 0.2592 | 0.2466 |
| 14.20 | 0.7695 | 0.9774 | 0.2350 | 0.0052 | 1.1107 | 1.5653 | 0.2404 | 0.2286 |
| 14.67 | 0.7936 | 0.9837 | 0.2332 | 0.0037 | 1.0970 | 1.5950 | 0.2371 | 0.2254 |
| | | | | **353.15 K** | | | | |
| 5.039 | 0.0429 | 0.2791 | 0.1564 | 0.3904 | 1.7590 | 1.0119 | 0.5605 | 0.5415 |
| 6.281 | 0.0701 | 0.4363 | 0.2283 | 0.2843 | 1.7185 | 1.0224 | 0.5231 | 0.5043 |
| 7.586 | 0.0948 | 0.4998 | 0.2456 | 0.2366 | 1.6834 | 1.0327 | 0.4915 | 0.4730 |
| 7.738 | 0.1052 | 0.5266 | 0.2572 | 0.2224 | 1.6690 | 1.0372 | 0.4882 | 0.4698 |
| 8.396 | 0.1238 | 0.5671 | 0.2693 | 0.1976 | 1.6440 | 1.0456 | 0.4748 | 0.4565 |
| 14.592 | 0.2653 | 0.7702 | 0.2994 | 0.0855 | 1.4770 | 1.1175 | 0.3888 | 0.3721 |
| 17.303 | 0.3179 | 0.8294 | 0.3020 | 0.0594 | 1.4237 | 1.1479 | 0.3641 | 0.3481 |
| 20.737 | 0.4007 | 0.8667 | 0.2939 | 0.0432 | 1.3479 | 1.2003 | 0.3391 | 0.3237 |
| 22.764 | 0.4630 | 0.9049 | 0.2956 | 0.0297 | 1.2964 | 1.2436 | 0.3267 | 0.3117 |
| 26.477 | 0.5225 | 0.9332 | 0.2867 | 0.0196 | 1.2511 | 1.2884 | 0.3072 | 0.2929 |
| 29.251 | 0.5982 | 0.9542 | 0.2814 | 0.0129 | 1.1985 | 1.3509 | 0.2949 | 0.2810 |
| 34.395 | 0.7005 | 0.9746 | 0.2687 | 0.0067 | 1.1351 | 1.4467 | 0.2756 | 0.2624 |
| 36.144 | 0.7450 | 0.9818 | 0.2651 | 0.0047 | 1.1100 | 1.4931 | 0.2700 | 0.2569 |
| 39.628 | 0.8158 | 0.9830 | 0.2552 | 0.0042 | 1.0731 | 1.5740 | 0.2596 | 0.2470 |

| P/kPa | $x_1$ | $y_1$ | $z_1$ | $z_2$ | $\gamma_1$ | $\gamma_2$ | $\Phi_1$ | $\Phi_2$ |
|---|---|---|---|---|---|---|---|---|
| | | | | **373.15 K** | | | | |
| 14.60 | 0.0511 | 0.3035 | 0.1709 | 0.3790 | 1.6524 | 1.0102 | 0.5631 | 0.5440 |
| 15.33 | 0.0596 | 0.3518 | 0.1952 | 0.3473 | 1.6413 | 1.0128 | 0.5548 | 0.5357 |
| 20.61 | 0.1033 | 0.5259 | 0.2655 | 0.2305 | 1.5866 | 1.0275 | 0.5048 | 0.4859 |
| 24.79 | 0.1521 | 0.6223 | 0.2952 | 0.1722 | 1.5301 | 1.0464 | 0.4743 | 0.4558 |
| 27.36 | 0.1961 | 0.6857 | 0.3143 | 0.1384 | 1.4828 | 1.0651 | 0.4583 | 0.4400 |
| 33.60 | 0.2528 | 0.7559 | 0.3219 | 0.0997 | 1.4266 | 1.0914 | 0.4259 | 0.4081 |
| 39.34 | 0.3350 | 0.8135 | 0.3268 | 0.0718 | 1.3531 | 1.1336 | 0.4018 | 0.3845 |
| 44.51 | 0.3791 | 0.8549 | 0.3278 | 0.0532 | 1.3172 | 1.1583 | 0.3834 | 0.3666 |
| 50.03 | 0.4489 | 0.8917 | 0.3269 | 0.0380 | 1.2647 | 1.2005 | 0.3666 | 0.3502 |
| 53.92 | 0.4839 | 0.8941 | 0.3183 | 0.0360 | 1.2402 | 1.2232 | 0.3561 | 0.3400 |
| 58.90 | 0.5284 | 0.9287 | 0.3193 | 0.0234 | 1.2107 | 1.2537 | 0.3439 | 0.3281 |
| 68.25 | 0.6166 | 0.9502 | 0.3080 | 0.0154 | 1.1573 | 1.3198 | 0.3242 | 0.3091 |
| 68.53 | 0.6199 | 0.9517 | 0.3080 | 0.0149 | 1.1554 | 1.3225 | 0.3237 | 0.3086 |
| 74.96 | 0.6999 | 0.9722 | 0.3034 | 0.0083 | 1.1123 | 1.3904 | 0.3121 | 0.2974 |
| 82.58 | 0.7856 | 0.9866 | 0.2959 | 0.0038 | 1.0713 | 1.4726 | 0.3000 | 0.2856 |
| 92.56 | 0.8853 | 0.9934 | 0.2842 | 0.0018 | 1.0306 | 1.5832 | 0.2862 | 0.2723 |

**Table 7-7: Vapour-liquid equilibrium data for the 2-butanol (1) +butyric acid (2) system at 333.15K, 353.15K and 373.15K taking chemical theory into account for the experimental liquid-phase activity coefficients and vapour-phase correction for non-ideality.**

| Model | T /K | $k_{ij}$ | $\alpha_{12}$ | $\Delta g_{12}$* | $\Delta g_{21}$* | AAD ($\Delta$P) | AAD ($\Delta$y) | AE% |
|---|---|---|---|---|---|---|---|---|
| SRK-WS | 333.15 | -0.7323 | 0.0768 | 10070.68 | -5539.33 | 0.0702 | 0.0110 | 0.5042 |
| | 353.15 | -0.7409 | 0.6617 | 6158.45 | 1572.06 | 0.0368 | 0.0076 | 0.1412 |
| | 373.15 | -0.3805 | 0.0768 | 5459.81 | -535.80 | 0.0247 | 0.0085 | 0.0685 |
| PRSV-WS | 333.15 | -0.2278 | 0.3000 | 8097.65 | -3803.68 | 0.1003 | 0.0115 | 1.0201 |
| | 353.15 | -0.0328 | 0.3000 | 8550.60 | -4661.85 | 0.0598 | 0.0098 | 0.3675 |
| | 373.15 | -0.2278 | 0.3000 | 7826.41 | -1345.25 | 0.0370 | 0.0103 | 0.1472 |
| VEOS | 333.15 | | -0.1685 | 2192.92 | -3957.09 | 0.0924 | 0.0102 | 0.8639 |
| | 353.15 | | -0.2845 | 1527.43 | -2936.23 | 0.0624 | 0.0098 | 0.3987 |
| | 373.15 | | -0.3508 | 1499.17 | -2629.43 | 0.0364 | 0.0103 | 0.1434 |
| HOC -CT | 333.15 | | 0.5213 | 3863.67 | -167.87 | 0.0668 | 0.0169 | 0.4743 |
| | 353.15 | | 1.0923 | 4988.62 | 1089.19 | 0.0667 | 0.0086 | 0.4523 |
| | 373.15 | | 1.2092 | 4892.12 | 1542.37 | 0.0714 | 0.0114 | 0.5227 |

**Table 7-8: Modeling results for the 2-Butanol+Butyric Acid system at 333.15, 353.15 and 373.15K with NRTL $G^E$ model (*, J/mol)**

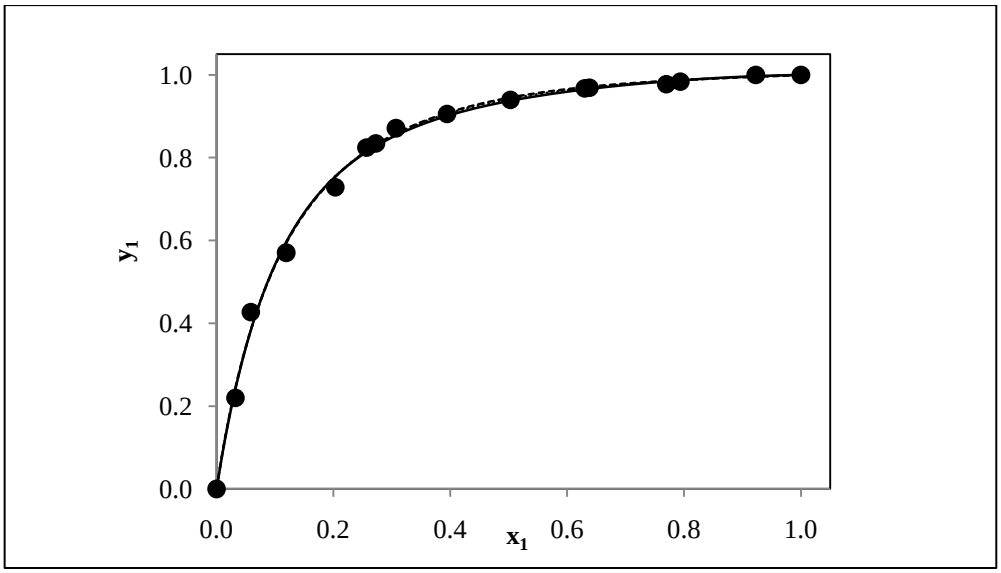


**Figure 7-19: x-y VLE plot for the 2-butanol (1) + butyric acid (2) system at 333.15 K ( •) , this work; (—), SRK-WS; (---), PRSV-WS; (---), VEOS; (- - -), HOC-CT**

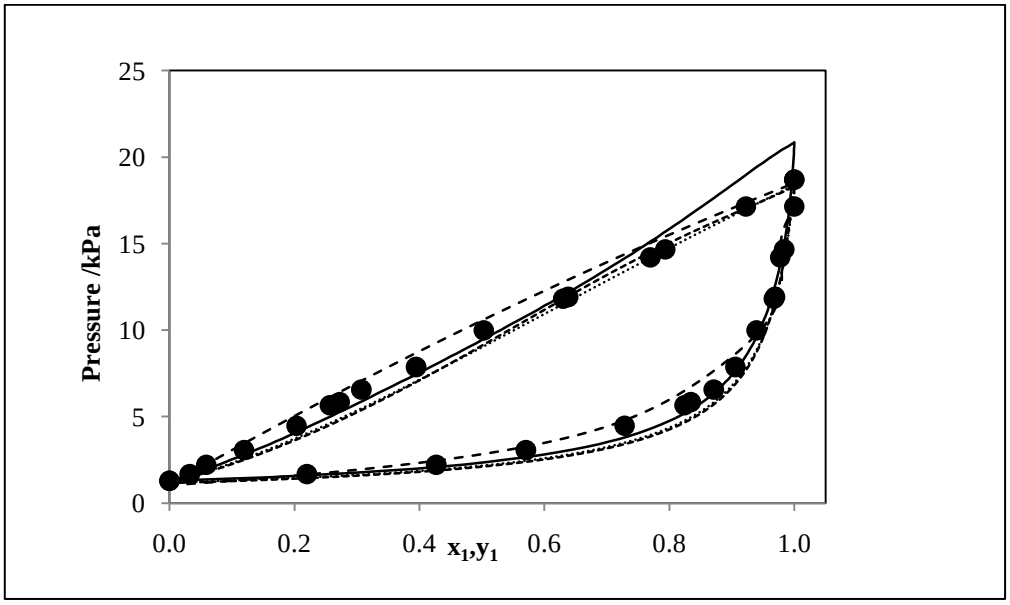


**Figure 7-20: P-x-y VLE plot for the 2-butanol (1) + butyric acid (2) system at 333.15 K ( • ), this work; (—), SRK-WS; (---), PRSV-WS; (---), VEOS; (- - -), HOC-CT**

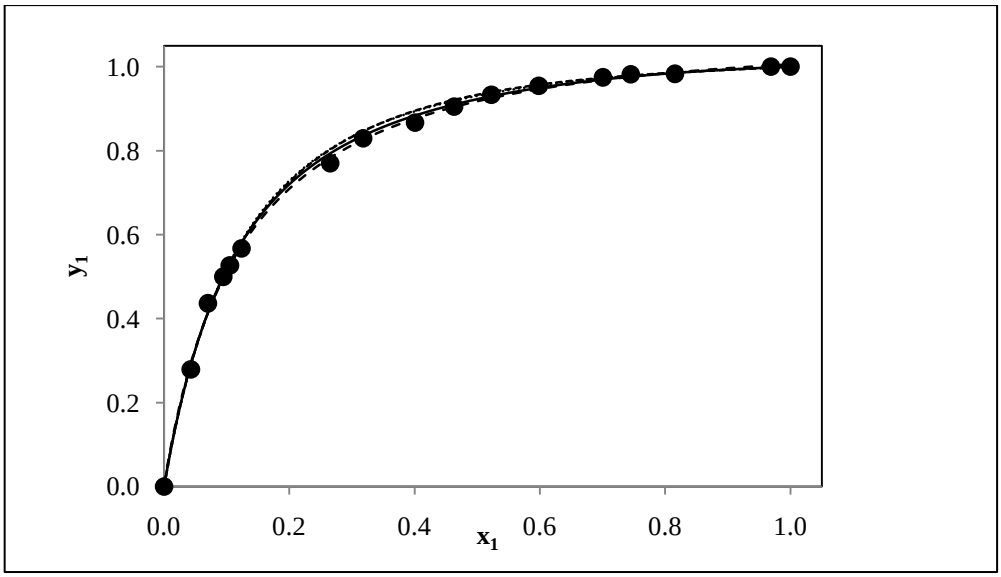


**Figure 7-21: x-y VLE plot for the 2-butanol (1) + butyric acid (2) system at 353.15 K (● ), this work;( —), SRK-WS;( ---), PRSV-WS;( ---), VEOS; (- - -), HOC-CT**

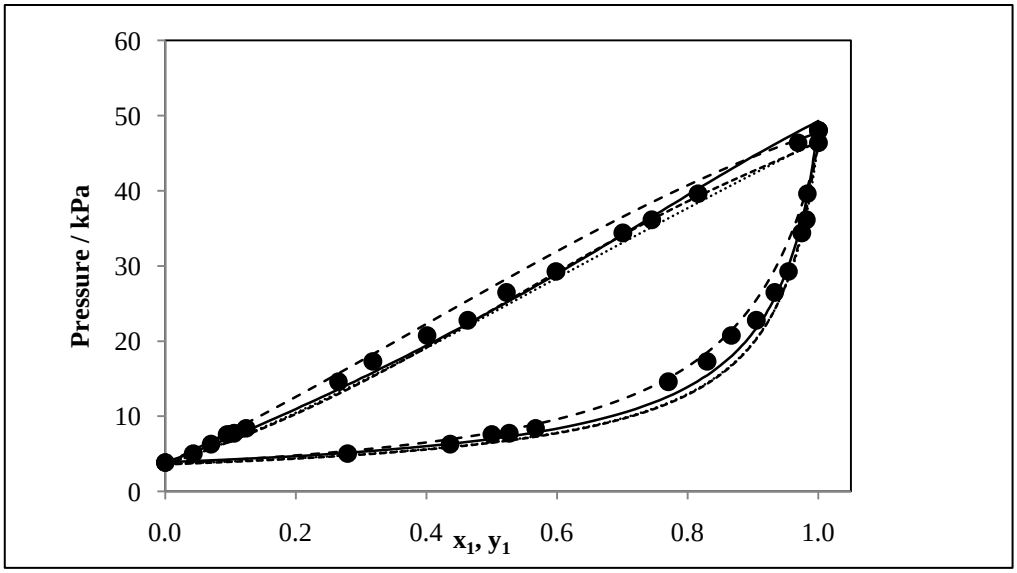


**Figure 7-22:P-x-y VLE plot for the 2-butanol (1) + butyric acid (2) system at 353.15K ( • ), this work; (—), SRK-WS;( ---), PRSV-WS; (---), VEOS; (- - -), HOC-CT**

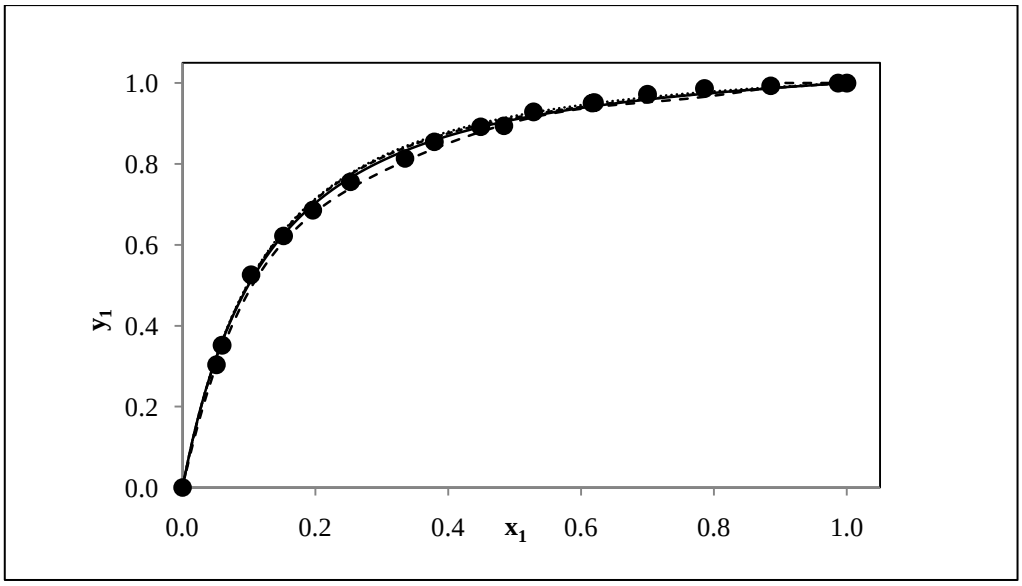


**Figure 7-23: x-y VLE plot for the 2-butanol (1) + butyric acid (2) system at 373.15 K (● ), this work; (—), SRK-WS; (---), PRSV-WS;( ---), VEOS; (- - -), HOC-CT**

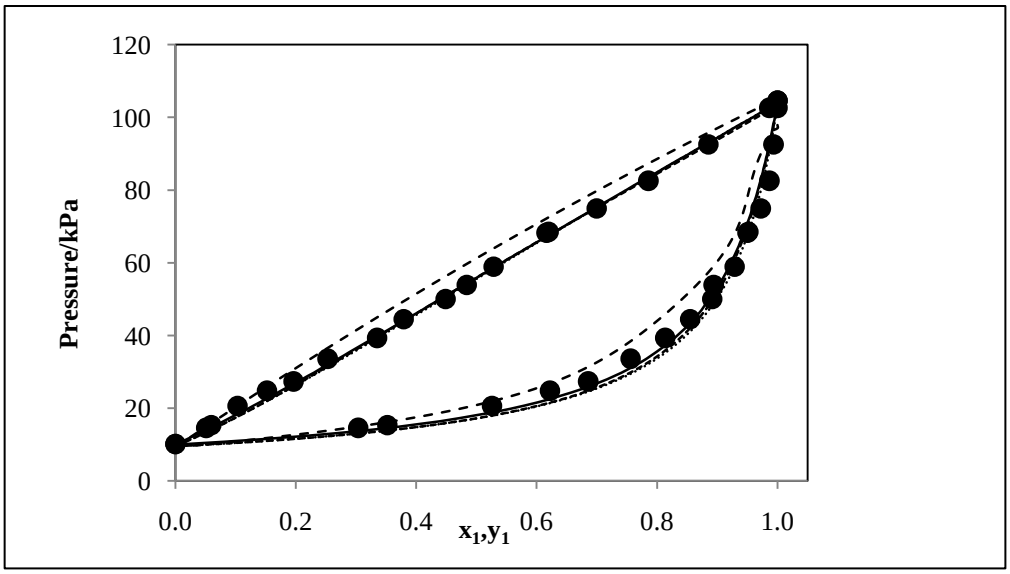


**Figure 7-24: P-x-y VLE plot for the 2-butanol (1) + butyric acid (2) system at 373.15 K (● ), this work;( —), SRK-WS; (---), PRSV-WS; (---), VEOS;(- - -), HOC-CT**

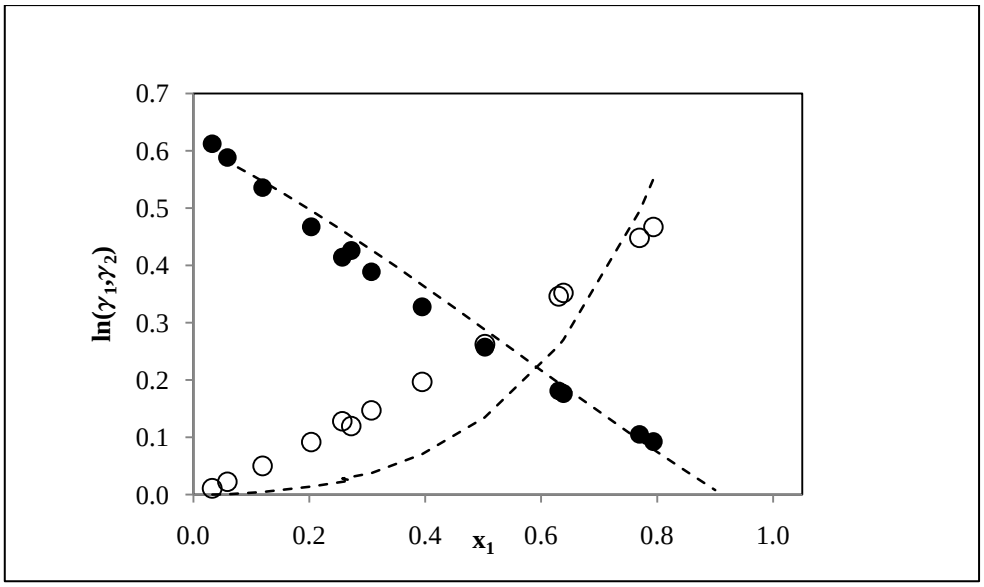


**Figure 7-25: Comparison between the experimentally determined liquid-phase activity coefficients and those calculated from the NRTL model with chemical theory for 2-butanol (1) + butyric acid (2) system at 333.15 K.**

**( •) , experimental activity coefficient; (- - -), NRTL model**

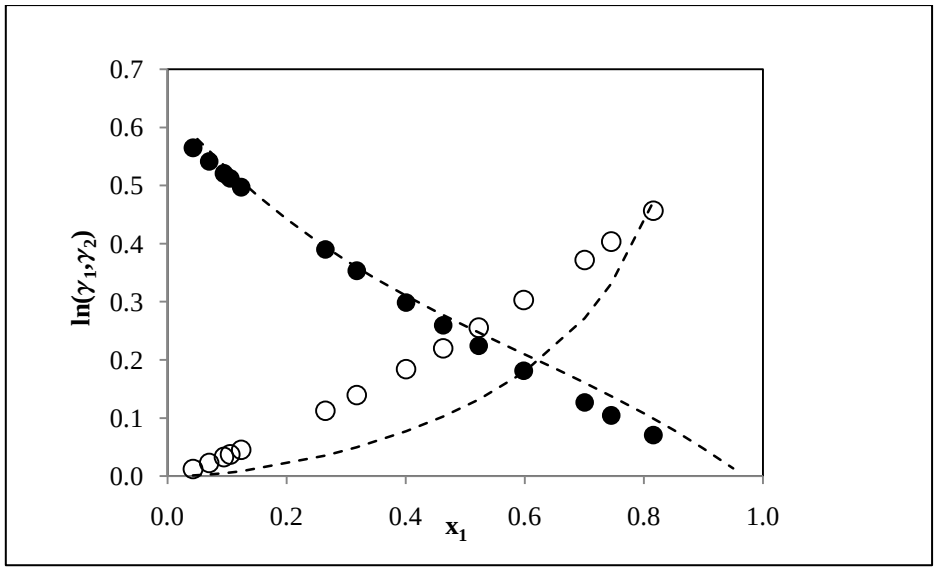


**Figure 7-26: Comparison between the experimentally determined liquid-phase activity coefficients and those calculated from the NRTL model with chemical theory for 2-butanol (1) + butyric acid (2) system at 353.15 K.**

**( •) , experimental activity coefficient; (- - -), NRTL model**

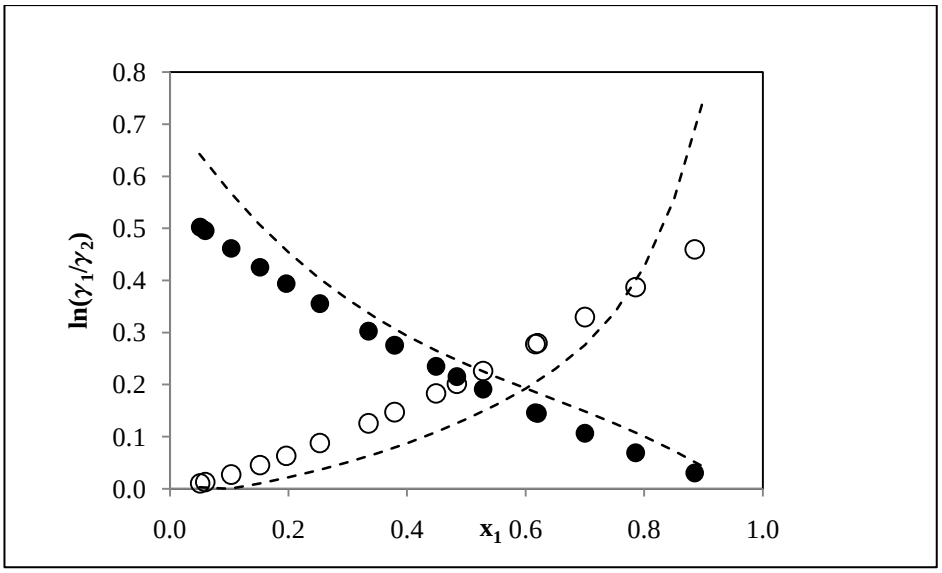


**Figure 7-27: Comparison between the experimentally determined liquid-phase activity coefficients and those calculated from the NRTL model with chemical theory for 2-butanol (1) + butyric acid (2) system at 373.15 K**

**( •) , experimental activity coefficient; (- - -), NRTL model**

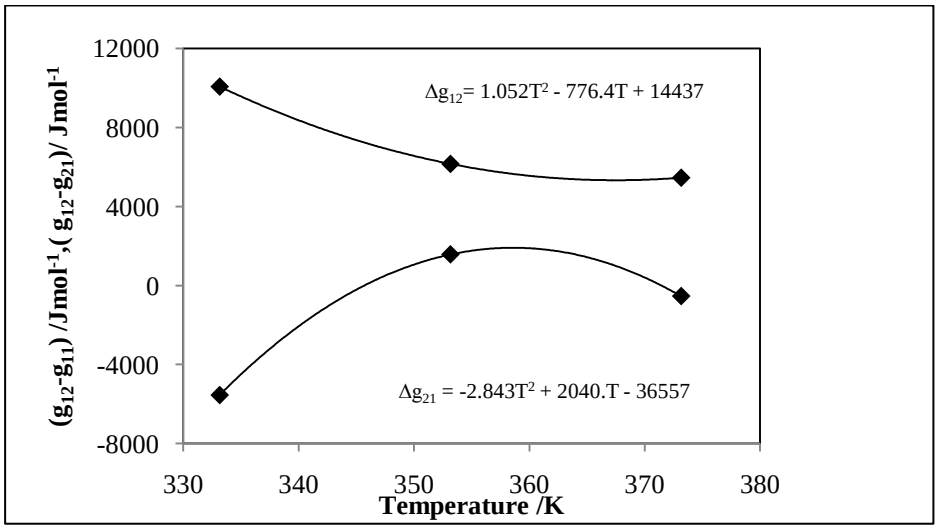


**Figure 7-28 : Temperature dependence of the NRTL model parameters for 2-butanol (1) + butyric acid (2) using SRK-WS model**

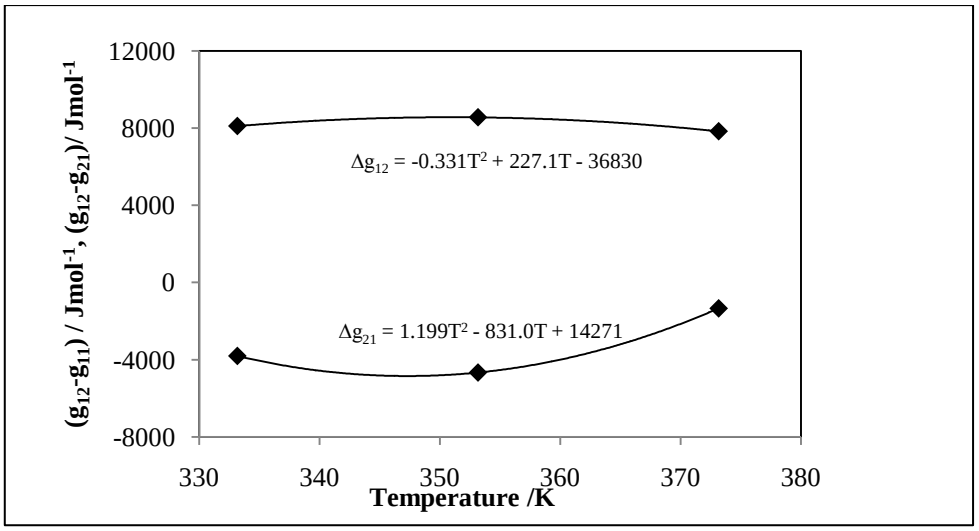


**Figure 7-29 : Temperature dependence of the NRTL model parameters for 2-butanol (1) + butyric acid (2) using PRSV-WS model**

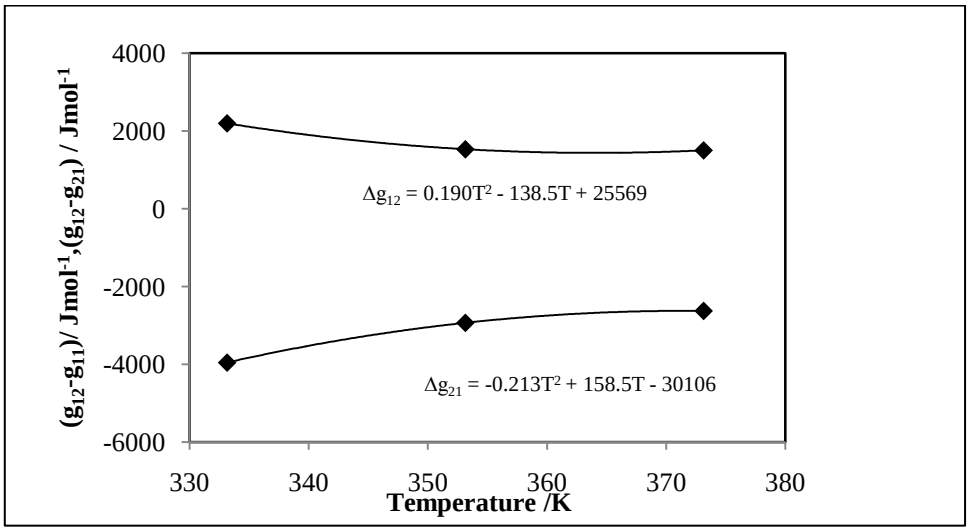


**Figure 7-30 : Temperature dependence of the NRTL model parameters for 2-butanol (1) + butyric acid (2) using Virial EOS (Tsonopoulos)**

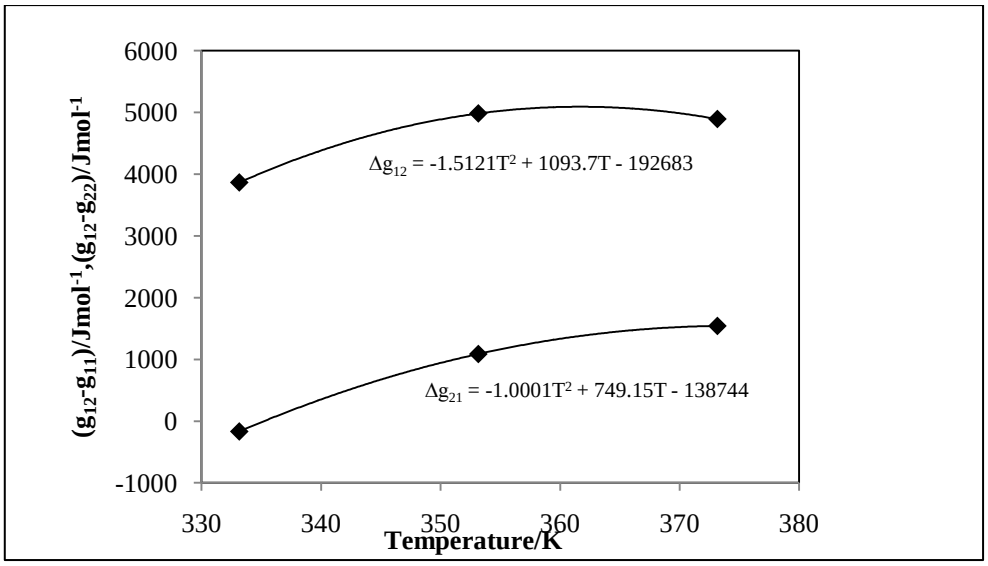


**Figure 7-31 : Temperature dependence of the NRTL model parameters for 2-butanol (1) + butyric acid (2) using Hayden O'Connell with Chemical theory**

### 7.7.3.3 2-Methyl-1-propanol (1) + Butyric Acid (2) System

All of the models were fitted to the 2-methyl-1-propanol + butyric acid system. Even though the models did not fit this system well graphically, the deviations ($\Delta y$) from the experimental data are less than 0.01 at 333.15 K and 353.15K while the Hayden and O'Connell with chemical theory gives average absolute deviations from experimental data less than 0.01 for all the systems. The chemical theory can be seen graphically to fit the vapour phase accurately. Hence, the P-x-y plots reveal the impact of the chemical interactions that occurred in the liquid phases which the other models used did not account for. However, the chemical theory does not present a good deviation in terms of pressure. The average absolute deviation values for pressure are higher than the rest system since chemical theory does not regression for pressure directly but instead calculates the vapour pressure of the apparent (monomer). Hence, it could be assumed that there are some possible chemical interactions in the liquid phase that is not totally accounted for using this model. However, in terms of the overall error, the chemical theory can be said to be the best model. In addition, the chemical theory was able to evaluate the liquid activity coefficient in the liquid phase taking into account possible associations.

It is important to mention that the results modelled for the new systems shows that $\Delta y$ for this work is better than that reported by Ferreira et al. (2004). According to Ferreira et al. (2004), only the table for the results for VLE of alcohols and acids were reported with the average percentage deviation in pressure and composition. For all the systems reported with the GCA-EOS prediction,

GCA-EOS correlation and MHV2, the overall average deviations reported were 9.5 , 1.9 , 6.1, 1.9 , 14 and 4.1 respectively while on this project using the SRK-WS, VEOS ,PRSV-WS and HOC-CT, the overall average percentage deviations are 6.09 , 1.05 , 8.15 , 1.23 ,8.9 , 1.22 , 5.89, and 0.95 respectively. Hence, it could be said that the results obtained so far give a better average deviation for the vapour composition, but the GCA-EOS correlation gives a lower average deviation in the pressure than the PRSV-WS and VEOS models.

Also, a comparison of individual models used in this work is made with that from Pillay (2009) who modelled 1-propanol+butyric acid mixtures at 333.15 and 353.15K using the NRTL-Hayden O'Connell (NRTL-HOC), Wilson-Hayden O'Connell (WILS-HOC), Uniquac-Hayden O'Connell (UNIQ-HOC), NRTL-Nothnagel (NRTL-NTH) and NRTL-VPA/IK-CAPE EOS(NRTL-VPA). It could be observed, that all the models in this work gave an individual deviation better than those reported by Pillay except in the case of 2-propanol+butyric acid at 373.15K. In this case, only chemical theory gave a value below 0.01. Although, the Nothnagel (1973) correlation included the chemical theory of vapour imperfection, it must be said that a little modification has been made on this chemical theory by including the equation by Prausnitz et al.(1999) to correct the liquid phase activity coefficient.

Table 7-9 presents the regressed VLE data regressed with the Chemical theory along with the activity coefficient ($\gamma$) and the vapour-phase correction term ($\Phi$) as well as the true mole fractions of the components in the vapour phase. The values from Table 7-9 indicated that there is a little deviation from unity in the liquid phase as opposed to the strong deviation from unity observed for the vapour phase. However, it could be noticed from Table 7-9 that the fugacity coefficient moves towards unity as the temperature increases. A plot of the fugacity coefficient against the mole fraction of the alcohol showing the extent of vapour-phase deviation form ideality is presented in Appendix C. A plot of the dimerization contribution to the second virial coefficient as a function of temperature is also presented in Appendix C. The parameters obtained through regression of the experimental VLE data for the 2- methyl-1-propanol (1) + butyric acid (2) system using all the models employed on this project is presented on Tables 7-10.

| **P/kPa** | $x_1$ | $y_1$ | $z_1$ | $z_2$ | $\gamma_1$ | $\gamma_2$ | $\Phi_1$ | $\Phi_2$ |
|---|---|---|---|---|---|---|---|---|
| | | | | **T=333.15** | | | | |
| 1.95 | 0.0816 | 0.3946 | 0.2039 | 0.3018 | 1.7651 | 1.0332 | 0.5168 | 0.4984 |
| 2.10 | 0.0932 | 0.4323 | 0.2181 | 0.2760 | 1.7473 | 1.0387 | 0.5044 | 0.4861 |
| 2.49 | 0.1259 | 0.5096 | 0.2427 | 0.2248 | 1.6992 | 1.0549 | 0.4763 | 0.4583 |
| 2.83 | 0.1659 | 0.6009 | 0.2737 | 0.1748 | 1.6439 | 1.0757 | 0.4555 | 0.4378 |
| 3.38 | 0.2118 | 0.6693 | 0.2861 | 0.1357 | 1.5849 | 1.101 | 0.4275 | 0.4103 |
| 4.03 | 0.2651 | 0.7359 | 0.2948 | 0.1014 | 1.5216 | 1.1322 | 0.4006 | 0.3840 |
| 4.58 | 0.3211 | 0.7927 | 0.3026 | 0.0758 | 1.4605 | 1.1673 | 0.3817 | 0.3655 |

| P/ kPa | $x_1$ | $y_1$ | $z_1$ | $z_2$ | $\gamma_1$ | $\gamma_2$ | $\Phi_1$ | $\Phi_2$ |
|---|---|---|---|---|---|---|---|---|
| 5.34 | 0.3812 | 0.8411 | 0.3026 | 0.0547 | 1.4004 | 1.2078 | 0.3597 | 0.3441 |
| 6.30 | 0.4758 | 0.8908 | 0.3002 | 0.0352 | 1.3156 | 1.2782 | 0.3370 | 0.3220 |
| 6.93 | 0.5195 | 0.9187 | 0.2980 | 0.0252 | 1.2800 | 1.3137 | 0.3244 | 0.3098 |
| 8.23 | 0.6472 | 0.9546 | 0.2887 | 0.0131 | 1.1869 | 1.4307 | 0.3024 | 0.2885 |
| 9.04 | 0.7185 | 0.9712 | 0.2826 | 0.0080 | 1.1411 | 1.5061 | 0.2909 | 0.2774 |
| 9.81 | 0.7699 | 0.9789 | 0.2753 | 0.0057 | 1.1105 | 1.5658 | 0.2812 | 0.2680 |
| 11.02 | 0.8788 | 0.9925 | 0.2658 | 0.0019 | 1.0519 | 1.7099 | 0.2678 | 0.2551 |
| | | | | **353.15 K** | | | | |
| 5.53 | 0.0705 | 0.3288 | 0.1790 | 0.3529 | 1.7180 | 1.0226 | 0.5444 | 0.5258 |
| 7.56 | 0.1424 | 0.5212 | 0.2564 | 0.2268 | 1.6199 | 1.0542 | 0.4919 | 0.4736 |
| 9.55 | 0.2107 | 0.6336 | 0.2876 | 0.1598 | 1.5370 | 1.0880 | 0.4538 | 0.4360 |
| 10.44 | 0.2423 | 0.6818 | 0.2998 | 0.1343 | 1.5017 | 1.1048 | 0.4397 | 0.4221 |
| 11.32 | 0.2813 | 0.7217 | 0.3082 | 0.1140 | 1.4604 | 1.1265 | 0.4270 | 0.4097 |
| 13.06 | 0.3461 | 0.7743 | 0.3137 | 0.0876 | 1.3969 | 1.1651 | 0.4051 | 0.3882 |
| 14.59 | 0.3930 | 0.8168 | 0.3174 | 0.0682 | 1.3546 | 1.1952 | 0.3885 | 0.3721 |
| 15.77 | 0.4305 | 0.8478 | 0.3198 | 0.0550 | 1.3227 | 1.2206 | 0.3772 | 0.3610 |
| 17.38 | 0.4903 | 0.8857 | 0.3218 | 0.0397 | 1.2752 | 1.2637 | 0.3633 | 0.3474 |
| 19.32 | 0.5524 | 0.9157 | 0.3192 | 0.0281 | 1.2297 | 1.3123 | 0.3485 | 0.3331 |
| 20.99 | 0.6107 | 0.9382 | 0.3164 | 0.0199 | 1.1903 | 1.3618 | 0.3373 | 0.3221 |
| 23.14 | 0.6616 | 0.9536 | 0.3093 | 0.0144 | 1.1582 | 1.4086 | 0.3243 | 0.3096 |
| 24.93 | 0.7278 | 0.9699 | 0.3052 | 0.0090 | 1.1196 | 1.4748 | 0.3147 | 0.3003 |
| 27.76 | 0.8256 | 0.9861 | 0.2970 | 0.0040 | 1.0683 | 1.5859 | 0.3011 | 0.2872 |
| | | | | **373.15 K** | | | | |
| 13.68 | 0.0567 | 0.2420 | 0.1389 | 0.4209 | 1.6452 | 1.0119 | 0.5740 | 0.5551 |
| 15.47 | 0.0948 | 0.3631 | 0.2008 | 0.3403 | 1.5971 | 1.0245 | 0.5530 | 0.5341 |
| 19.10 | 0.1600 | 0.5156 | 0.2667 | 0.2416 | 1.5215 | 1.0497 | 0.5173 | 0.4986 |
| 29.31 | 0.3251 | 0.7247 | 0.3240 | 0.1182 | 1.3616 | 1.1283 | 0.4471 | 0.4292 |
| 33.34 | 0.3860 | 0.7745 | 0.3306 | 0.0923 | 1.3118 | 1.1623 | 0.4268 | 0.4093 |
| 38.27 | 0.4520 | 0.8321 | 0.3375 | 0.0653 | 1.2625 | 1.2025 | 0.4057 | 0.3886 |
| 40.90 | 0.4883 | 0.8530 | 0.3375 | 0.0557 | 1.2373 | 1.2261 | 0.3957 | 0.3788 |
| 43.58 | 0.5309 | 0.8751 | 0.3380 | 0.0462 | 1.2092 | 1.2554 | 0.3863 | 0.3697 |
| 47.71 | 0.5788 | 0.9033 | 0.3370 | 0.0345 | 1.1794 | 1.2905 | 0.3731 | 0.3568 |
| 50.52 | 0.6257 | 0.9232 | 0.3369 | 0.0268 | 1.1521 | 1.3271 | 0.3650 | 0.3489 |
| 53.73 | 0.6756 | 0.9479 | 0.3377 | 0.0178 | 1.1249 | 1.3689 | 0.3563 | 0.3404 |
| 55.28 | 0.6969 | 0.9528 | 0.3357 | 0.0159 | 1.1139 | 1.3877 | 0.3524 | 0.3366 |
| 59.49 | 0.7518 | 0.9680 | 0.3313 | 0.0105 | 1.0869 | 1.4389 | 0.3423 | 0.3268 |
| 63.33 | 0.8118 | 0.9814 | 0.3276 | 0.0059 | 1.0599 | 1.5000 | 0.3339 | 0.3187 |
| 66.21 | 0.8612 | 0.9858 | 0.3233 | 0.0044 | 1.0397 | 1.5548 | 0.3280 | 0.3129 |

**Table 7-9: Vapour-liquid equilibrium data for the 2-methyl-1-propanol (1) +butyric acid (2) system at 333.15, 353.15 and 373.15K taking chemical theory into account for the experimental liquid-phase activity coefficients and vapour-phase correction for non-ideality.**

| Model | T/ K | $k_{ij}$ | $\alpha_{12}$ | $\Delta g_{12}$* | $\Delta g_{21}$* | AAD (ΔP) | AAD (Δy) | AE% |
|---|---|---|---|---|---|---|---|---|
| SRK-WS | 333.15 | -0.5900 | -0.574 | 2578.54 | -2545.58 | 0.0744 | 0.0019 | 0.5541 |
| | 353.15 | -0.3422 | -5.000 | 587.83 | -478.31 | 0.0637 | 0.0046 | 0.4083 |
| | 373.15 | -0.0715 | -0.096 | 4747.47 | -6205.04 | 0.0298 | 0.0137 | 0.1073 |
| PRSV-WS | 333.15 | 0.1001 | 0.3000 | 2889.88 | -3908.94 | 0.1193 | 0.0033 | 1.4235 |
| | 353.15 | 0.0041 | 0.3000 | 1339.80 | -2474.65 | 0.1040 | 0.0084 | 1.0882 |
| | 373.15 | 0.0451 | 0.3000 | 10284.30 | -5945.98 | 0.0565 | 0.0153 | 0.3427 |
| VEOS(TsC) | 333.15 | | 0.8651 | 689.54 | -1676.53 | 0.0994 | 0.0027 | 0.9886 |
| | 353.15 | | 0.2865 | 1071.82 | -2068.87 | 0.1000 | 0.0082 | 1.0058 |
| | 373.15 | | -0.143 | 4066.10 | -6205.04 | 0.0425 | 0.0178 | 0.2120 |
| HOC -CT | 333.15 | | 1.1627 | 3782.33 | 631.53 | 0.0660 | 0.0049 | 0.4389 |
| | 353.15 | | 1.1011 | 6147.05 | 883.56 | 0.0634 | 0.0044 | 0.4040 |
| | 373.15 | | 1.1871 | 6273.93 | 626.59 | 0.0499 | 0.0042 | 0.2513 |

**Table 7-10: Modeling results for the 2-methyl-1-propanol (1) + butyric acid system at 333.15, 353.15 and 373.15K with NRTL $G^E$ model (*, J/mol)**

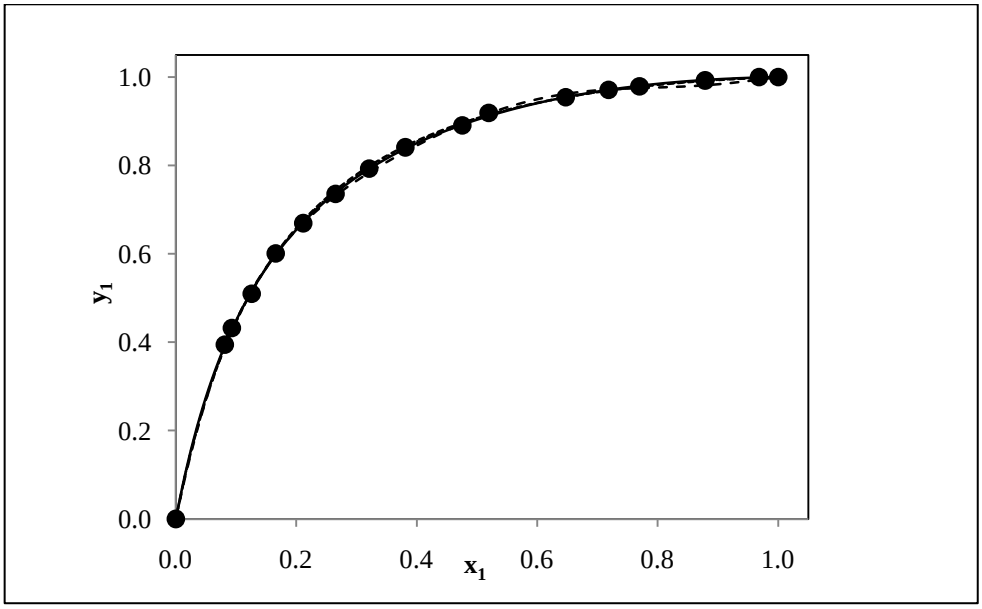


**Figure 7-32: x-y VLE plot for the 2-methyl-1-propanol (1) + butyric acid (2) system at 333.15K (•) , this work;( —), SRK-WS; (---), PRSV-WS; (---), VEOS;( - - -) , HOC-CT**

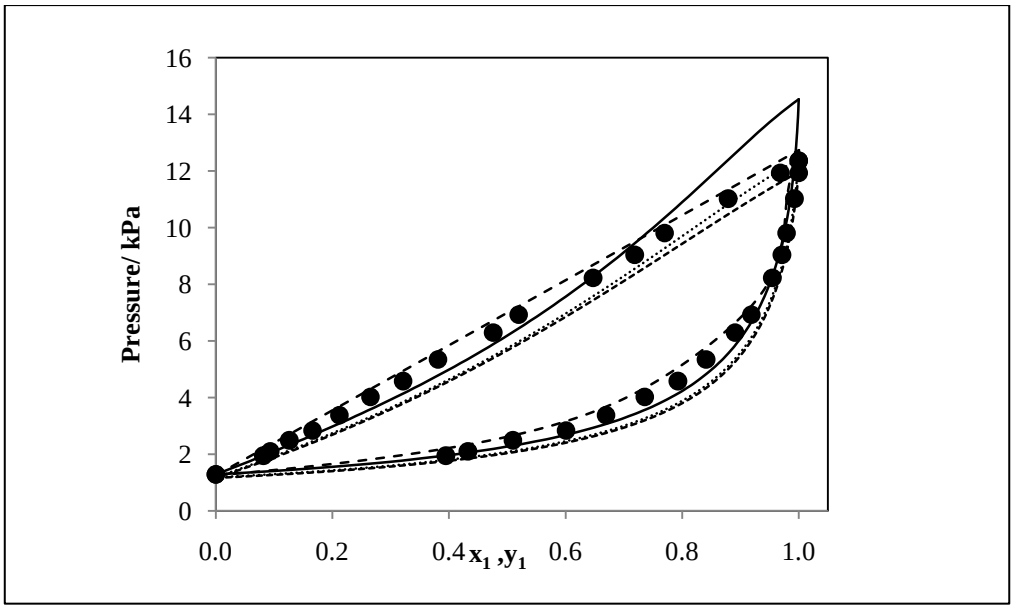


**Figure 7-33: P-x-y VLE plot for the 2-methyl-1-propanol (1) + butyric acid (2) system at 333.15 K (•) , this work; (—), SRK-WS; (---), PRSV-WS;( ---), VEOS; (- - -) , HOC-CT**

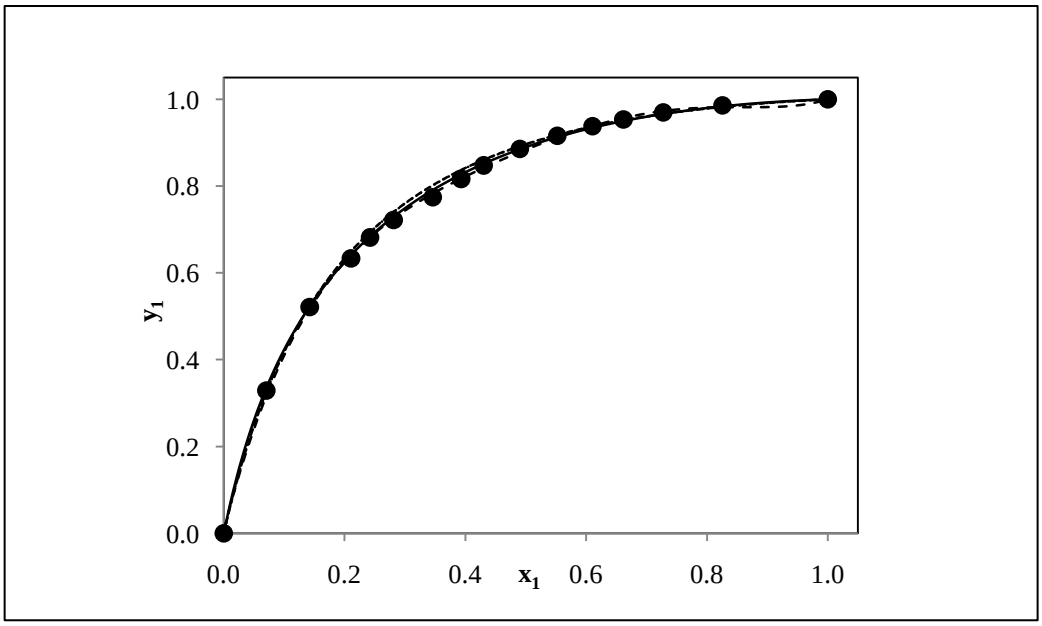


**Figure 7-34: x-y VLE plot for the 2-methyl-1-propanol (1) + butyric acid (2) system at 353.15 K (•) , this work; (—), SRK-WS; (---), PRSV-WS; (---), VEOS; (- - -) , HOC-CT**

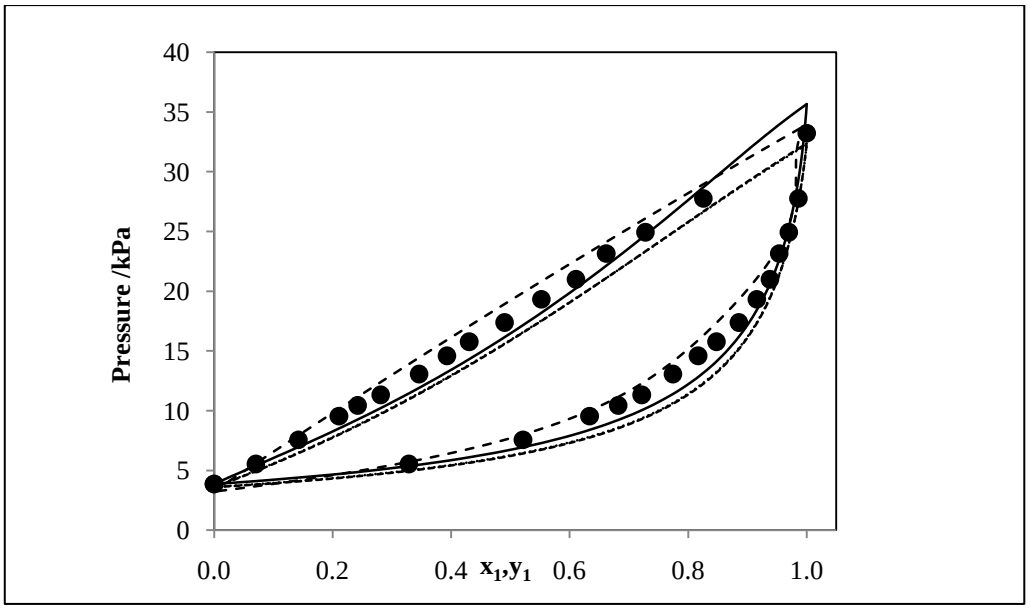


**Figure 7-35: P-x-y VLE plot for the 2-methyl-1-propanol (1) + butyric acid (2) system at 353.15 K (•) , this work; (—), SRK-WS; (---), PRSV-WS; (---), VEOS; (- - -) , HOC-CT**

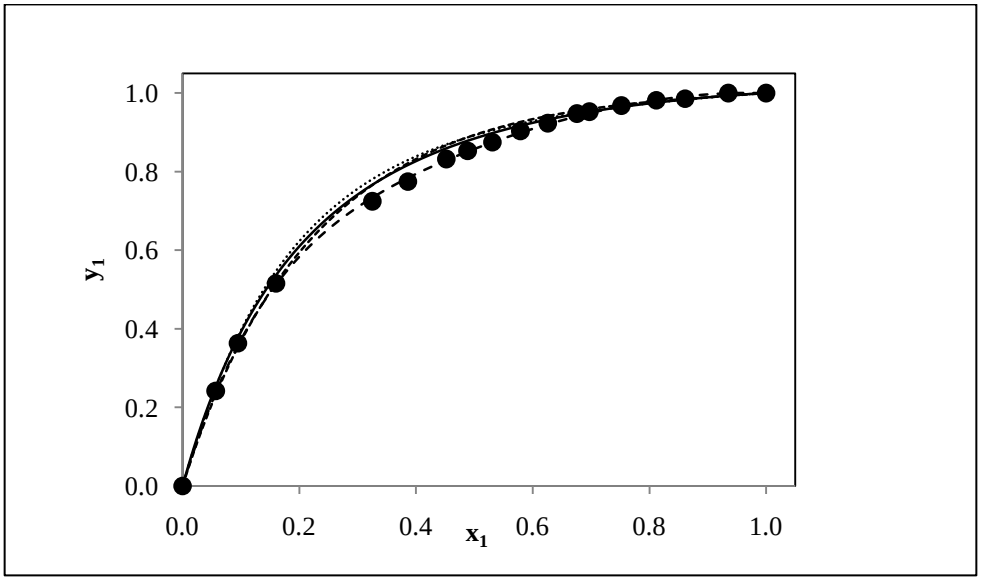


**Figure 7-36: x-y VLE plot for the 2-methyl-1-propanol (1) + butyric acid (2) system at 373.15 K (•) , this work; (—), SRK-WS; (---), PRSV-WS; (---), VEOS; (- - -) , HOC-CT**

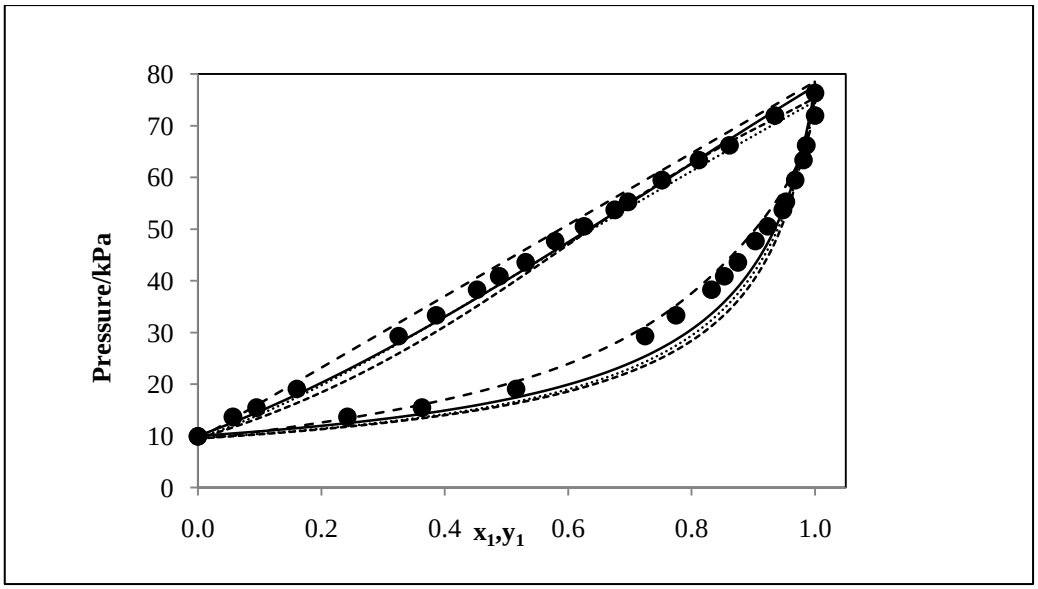


**Figure 7-37: P-x-y VLE plot for the 2-methyl-1-propanol (1)-butyric acid (2) system at 373.15 K (•) , this work; (—), SRK-WS; (---), PRSV-WS; (---), VEOS; (- - -) , HOC-CT**

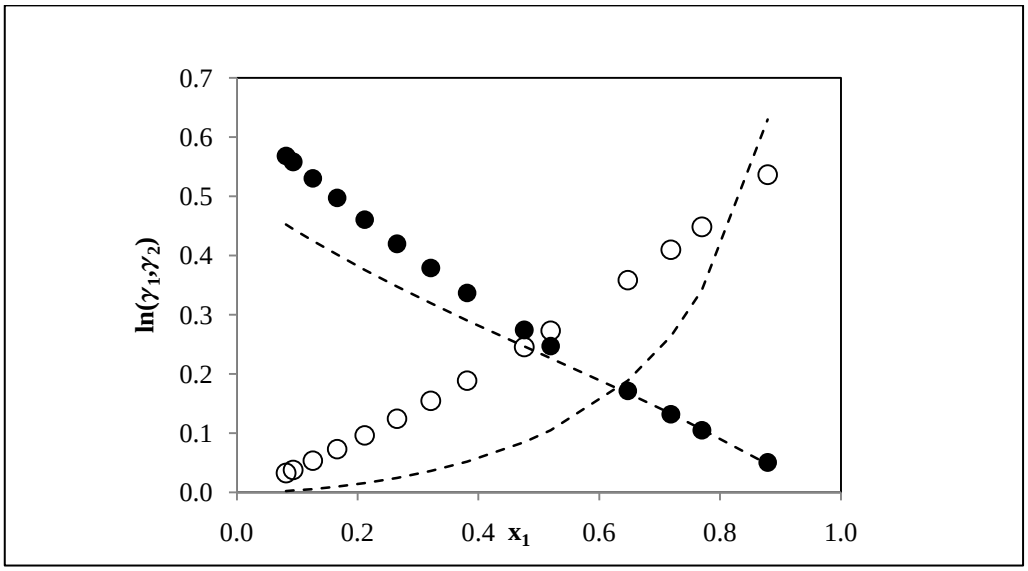


**Figure 7-38: Comparison between the experimentally determined liquid-phase activity coefficients and those calculated from the NRTL model with chemical theory for 2-methyl-1-propanol (1) + butyric acid (2) system at 333.15 K. (•) , experimental activity coefficient; (- - -), NRTL model**

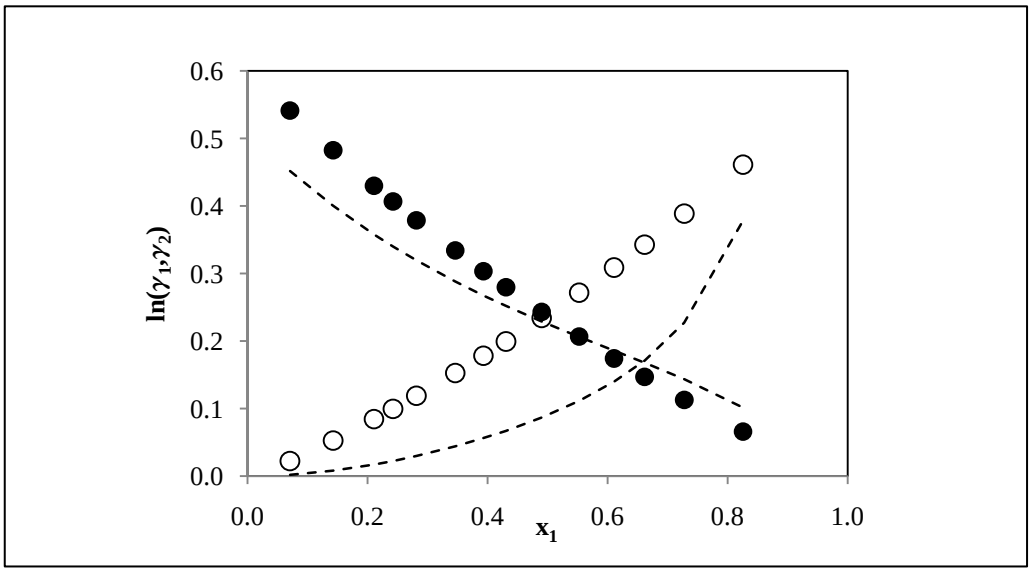


**Figure 7-39: Comparison between the experimentally determined liquid-phase activity coefficients and those calculated from the NRTL model with chemical theory for 2-methyl-1-propanol (1) + butyric acid (2) system at 353.15 K. (•) , experimental activity coefficient; (- - -), NRTL model**

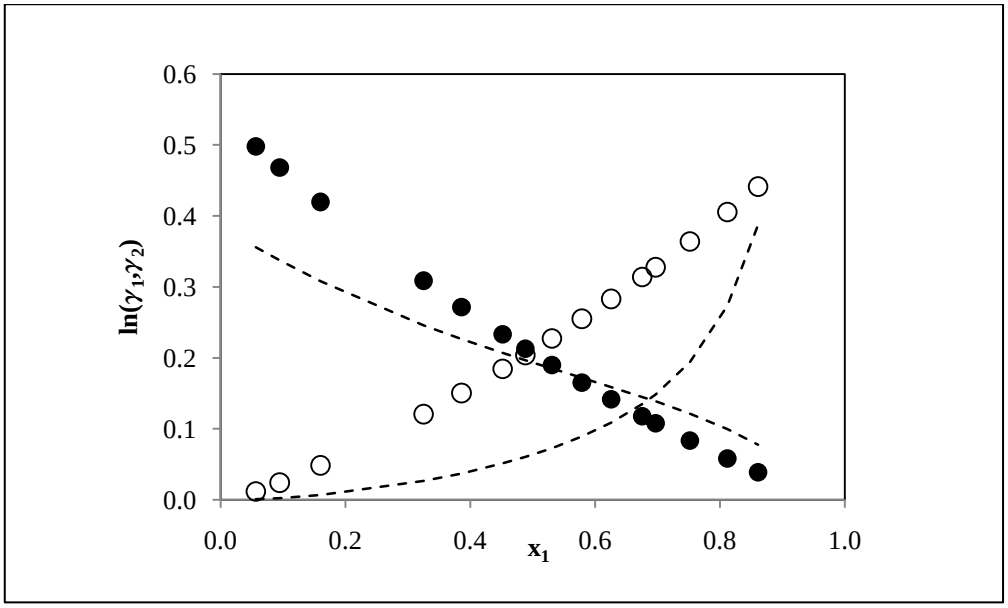


**Figure 7-40: Comparison between the experimentally determined liquid-phase activity coefficients and those calculated from the NRTL model with chemical theory for 2-methyl-1-propanol (1) + butyric acid (2) system at 373.15 K. (•) , experimental activity coefficient; (- - -), NRTL model**

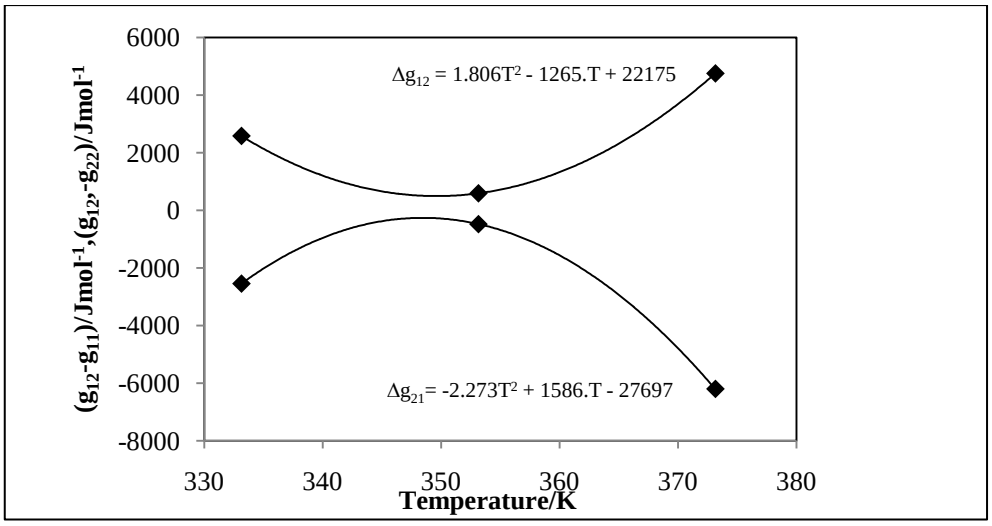


**Figure 7-41 : Temperature dependence of the NRTL model parameters for 2-methyl-1-propanol (1) + butyric acid (2) using SRK-WS model**

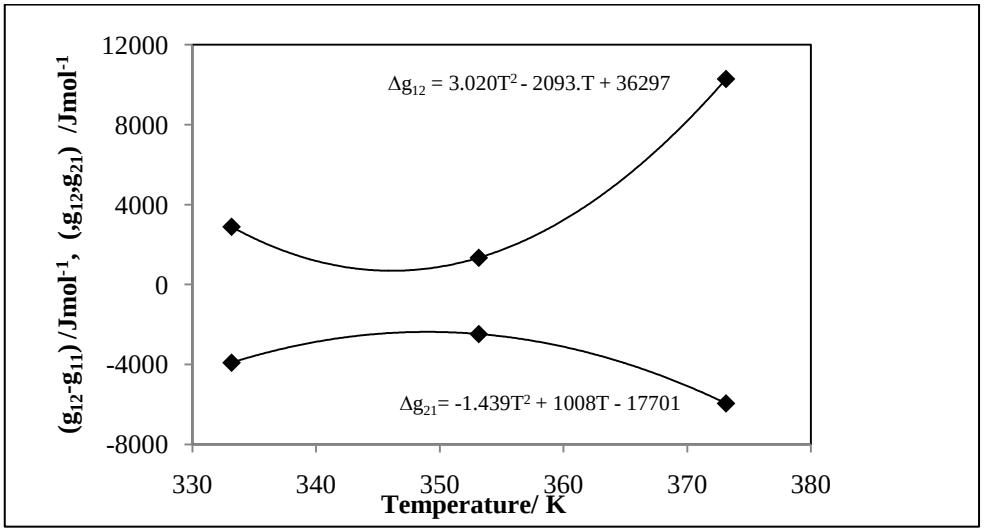


**Figure 7-42 : Temperature dependence of the NRTL model parameters for 2-methyl-1-propanol (1) + butyric acid (2) using PRSV-WS model**

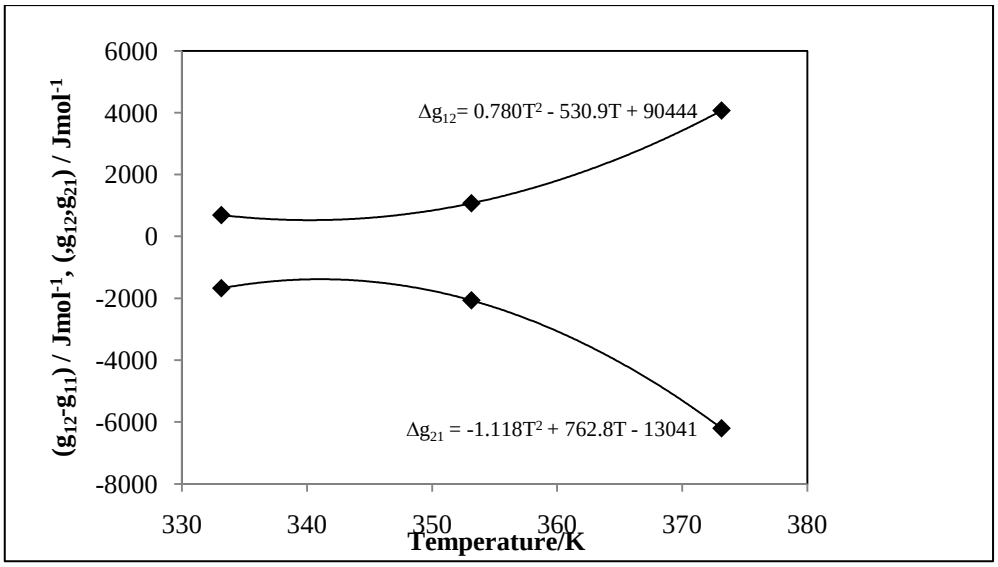


**Figure 7-43 : Temperature dependence of the NRTL model parameters for 2-methyl-1-propanol (1) + butyric acid (2) using Virial EOS (Tsonopoulos)**

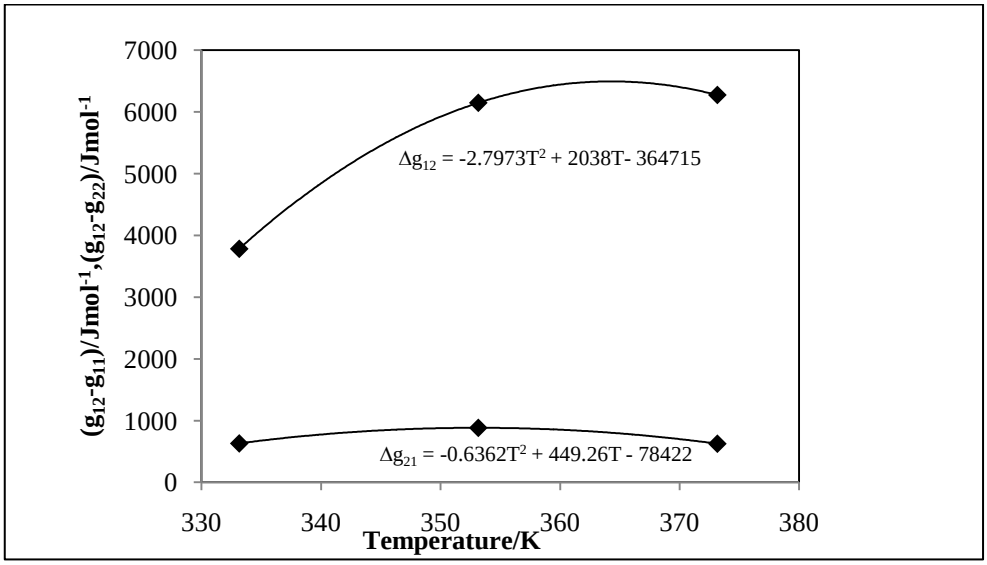


**Figure 7-44 : Temperature dependence of the NRTL model parameters for 2-methyl-1-propanol (1) + butyric acid (2) using Hayden O'Connell with Chemical theory**

## 7.8 Thermodynamic Consistency Testing

### 7.8.1 2-Propanol (1) + Butyric Acid (2) System

The $\Delta y$ values obtained for the 2-propanol + butyric acid system are given in Tables 7-7. As was noted in Section 7.3.3.2, the average absolute deviations of the vapour compositions were adversely influenced by the association effects exhibited in the dilute regions of the carboxylic acid systems. Thus, the $\Delta y$ residuals were (for the most part) greater than 0.01 for the 2-propanol + butyric acid system. The root mean square (RMS $\delta \ln (\gamma_1/\gamma_2)$) deviation of the model activity coefficient from the experimental data using the chemical theory approach also gave a fair value for the same system above. However, Clifford (2003) in his model of carboxylic acids reported high RMS values with a comment that the association effect must have been accountable for such high values. Hence, he further comments that in the case of carboxylic acid binary VLE systems, the point test apparently provides a far better indication of thermodynamic consistency than the highly recommended direct test.

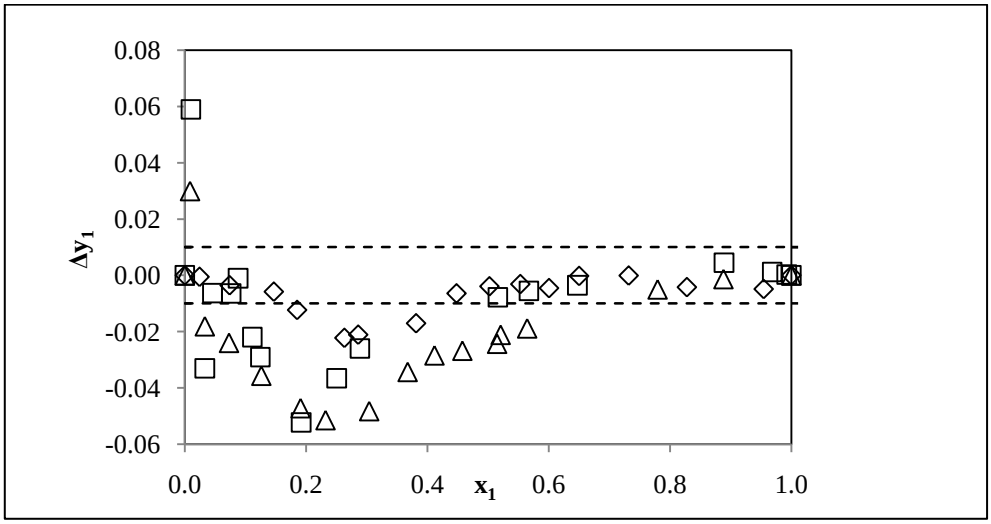


**Figure 7-45: Deviation of the SRK-WS-NRTL model vapour compositions from the experimental values for the 2-propanol (1) + butyric acid (2) system.**

(◊),T = 333.15 K ; (□) ,T = 353.15 K; (Δ) , T = 373.15 K ; ---- 0.01

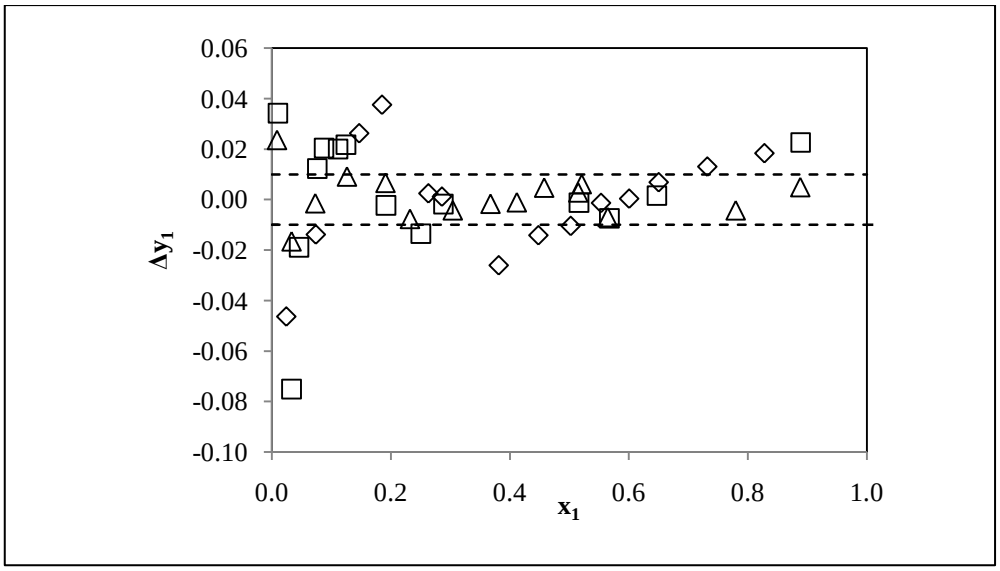


**Figure 7-46: Deviation of the HOC-CT model vapour compositions from the experimental values for the 2-propanol (1) + butyric acid (2) system.**

(◊),T = 333.15 K ; (□) ,T = 353.15 K; (Δ) , T = 373.15 K ; ---- 0.01

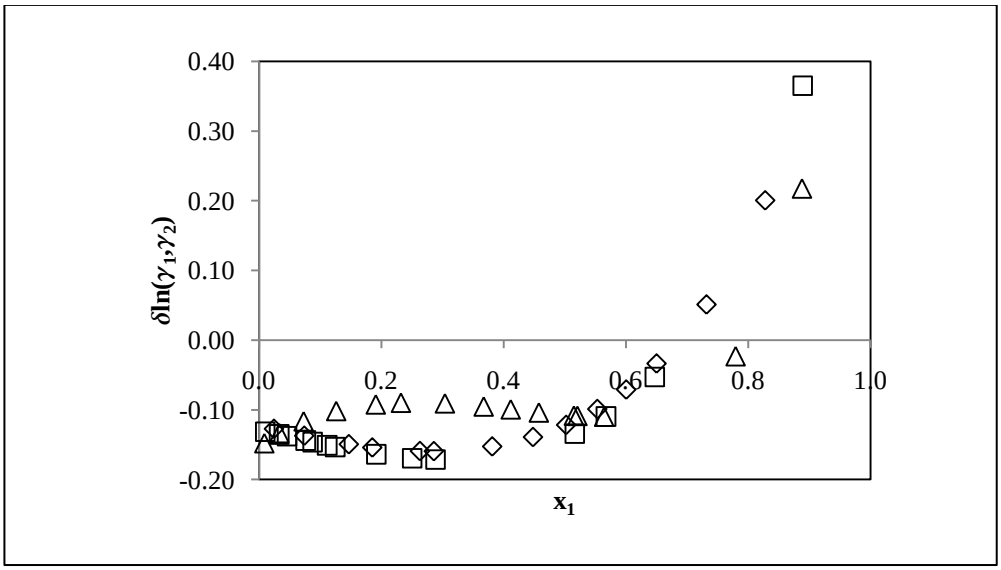


**Figure 7-47: Deviation of the HOC-CT model activity coefficients from the experimental values for the 2-propanol (1) + butyric acid (2) system.**

(◊),T = 333.15 K ; (□) ,T = 353.15 K; (Δ) , T = 373.15 K

### 7.8.2 2-Butanol (1) + Butyric Acid (2) System

The models provided a far better fit to the 2-butanol + butyric acid system than the 2-propanol–butyric acid system. Thus, the $\Delta y$ values for the 2-butanol + butyric acid system are good. All the experimental data sets passed the point test, in most cases. The only data set that struggled was the isotherm at 333.15 K, which only achieved an average absolute vapour phase deviation within 0.01 and 0.0103.

The direct test using the chemical theory was observed to give a good value for this system than for the 2-propanol + butyric acid system. However, the point test is still preferred in this case as mentioned earlier as a means of determining thermodynamic consistency for carboxylic acids binary mixtures.

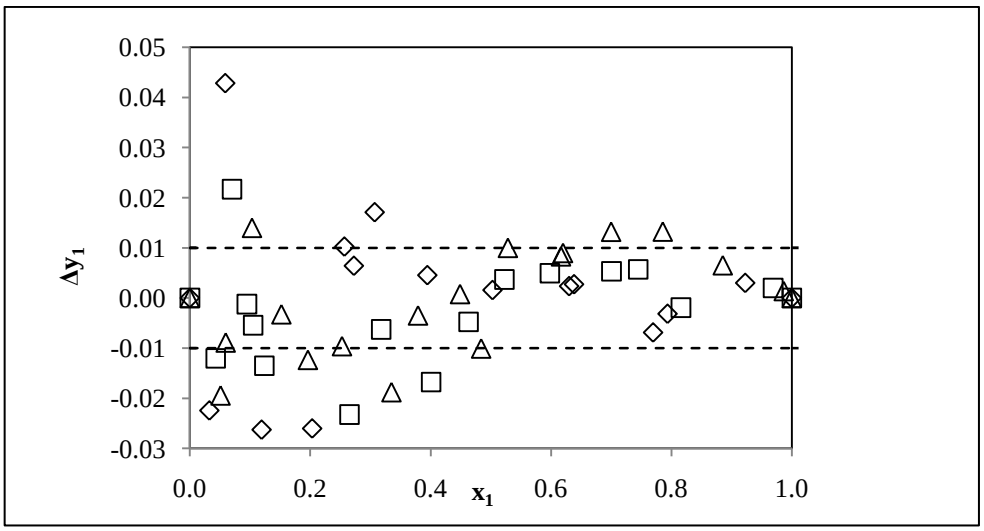


**Figure 7-48: Graph of the deviation of the SRK-WS-NRTL model vapour compositions from the experimental values for the 2-butanol (1) + butyric acid (2) system.**

(◊),T = 333.15 K ; (□) ,T = 353.15 K; (Δ) , T = 373.15 K ; ----- 0.01 line

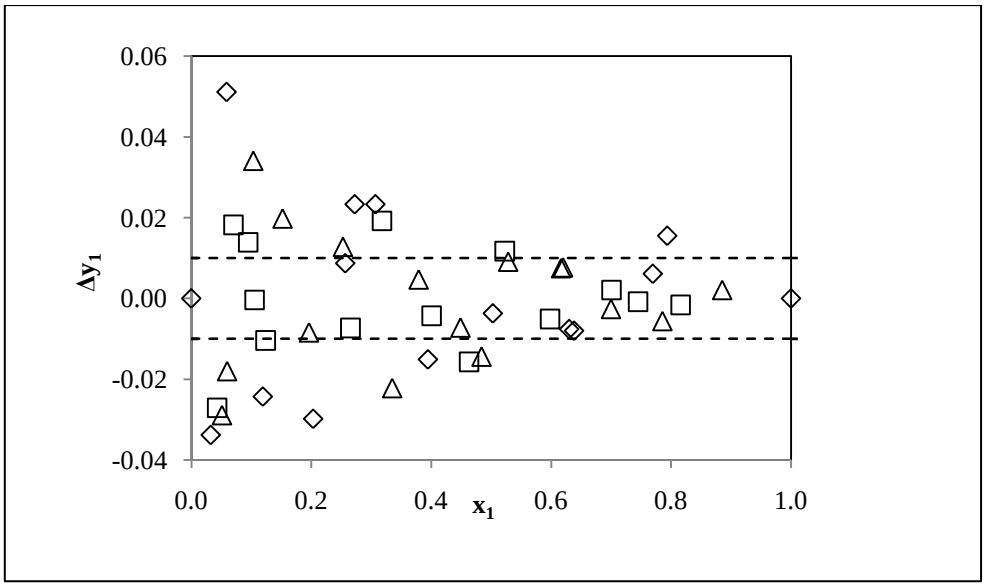


**Figure 7-49: Graph of the deviation of the HOC-CT model vapour compositions from the experimental values for the 2-butanol (1) + butyric acid (2) system.**

(◊),T = 333.15 K ; (□) ,T = 353.15 K; (Δ) , T = 373.15 K ; ----- 0.01 line

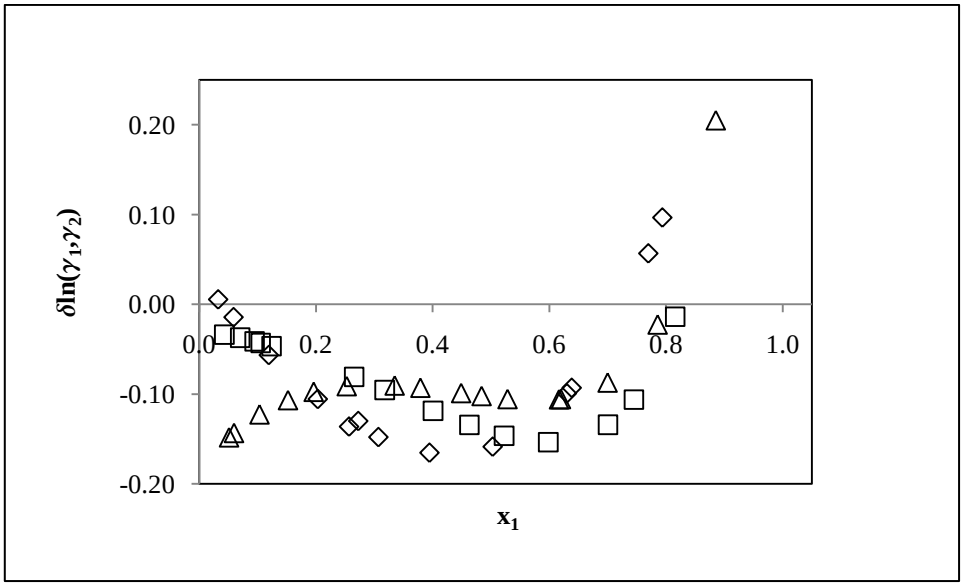


**Figure 7-50: Graph showing the deviation of the HOC-CT model activity coefficients from the experimental values for the 2-butanol (1) + butyric acid (2) system.**

(◊), T = 333.15 K ; ; (□), T = 353.15 K ; (Δ),T = 373.15 K

### 7.8.3 2-Methyl-1-propanol (1) + Butyric Acid (2) System

The models provided a fit as good as the 2-butanol + butyric acid system in comparison to the 2-propanol + butyric acid system. Hence, the $\Delta y$ values for the 2-methyl-1-propanol + butyric acid system are good. All the experimental data sets passed the point test as in case of the 2-butanol + butyric acid system. The only data set that struggled was the isotherm at 373.15 K, which only achieved an average absolute vapour phase deviation within 0.01 and 0.017. However, the chemical theory passed the point test for the entire isotherm measured for this system.

The direct test gave a fair result as mentioned for all the systems measured in this project.

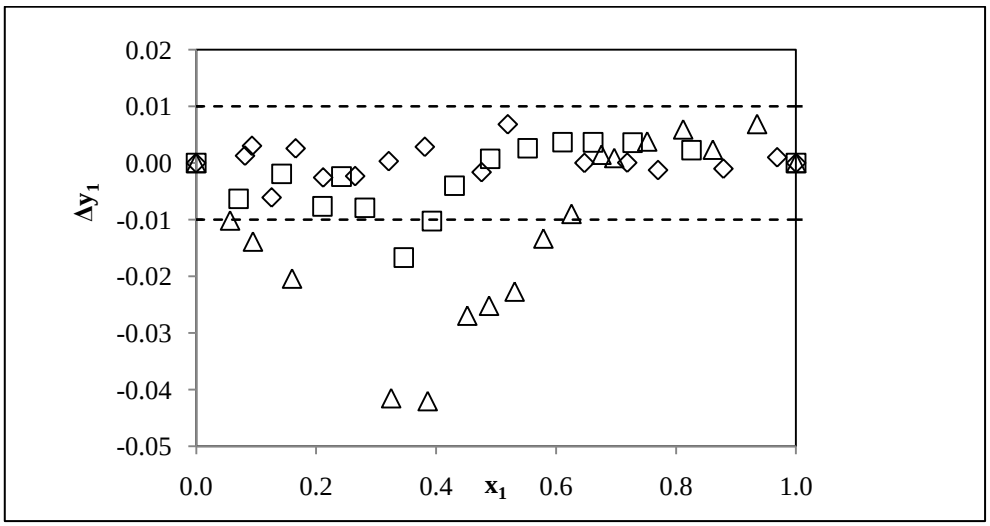


**Figure 7-51: Graph of the deviation of the SRK-WS-NRTL model vapour compositions from the experimental values for the 2-methyl-1-propanol (1) + butyric acid (2) system.**

(◊),T = 333.15 K ; (□) ,T = 353.15 K; (Δ) , T = 373.15 K ; ----- 0.01 line

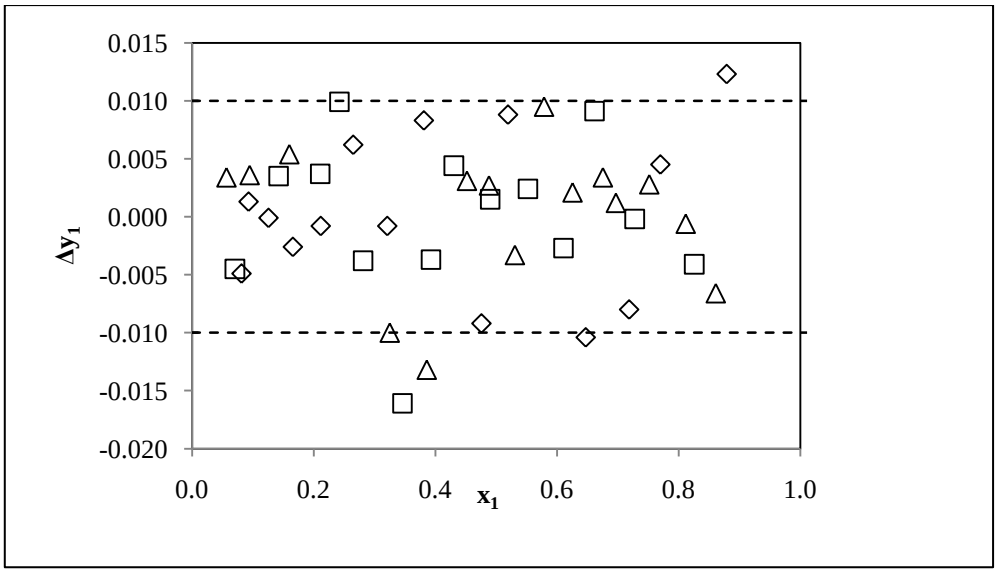


**Figure 7-52: Graph of the deviation of the HOC-CT model vapour compositions from the experimental values for the 2-methyl-1-propanol (1) + butyric acid (2) system.**

(◊),T = 333.15 K ; (□) ,T = 353.15 K; (Δ) , T = 373.15 K ; ----- 0.01 line

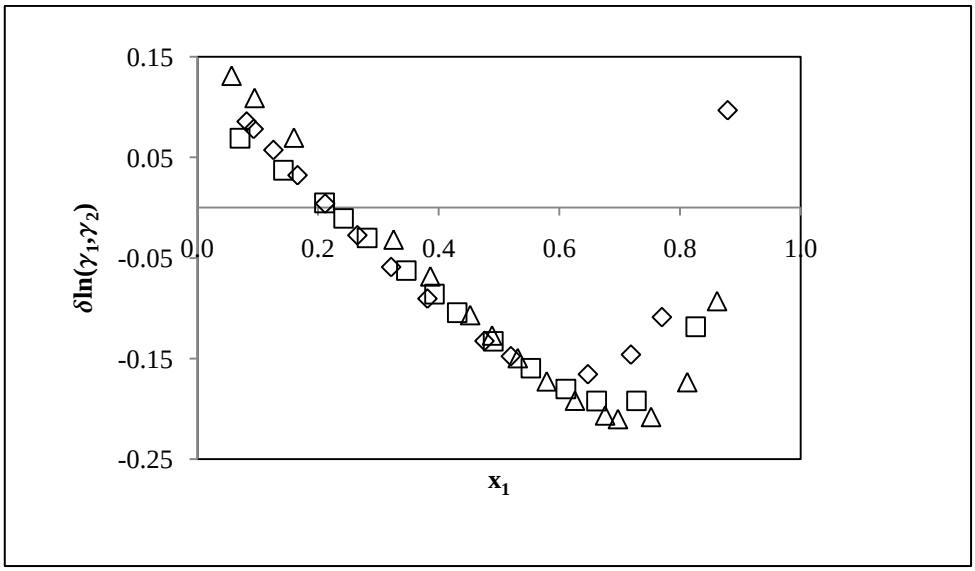


**Figure 7-53: Graph showing the deviation of the HOC-CT model activity coefficients from the experimental values for the 2-butanol (1) + butyric acid (2) system.**

(◊),T = 333.15 K ; (□) ,T = 353.15 K; (Δ) , T = 373.15 K

### 7.8.4 Root Mean Square deviation between model and experimental activity coefficient – Van Ness (1995) direct test

**Table 7-10: Root mean square value for the direct test using chemical theory**

| Binary system | 333.15K | 353.15 K | 373.15 K |
|---|---|---|---|
| 2-Propanol+Butyric Acid | 0.1319 | 0.1657 | 0.1152 |
| 2-Butanol+ Butyric Acid | 0.1094 | 0.095 | 0.114 |
| 2-Methyl-1-Propanol+ Butyric Acid | 0.0999 | 0.1174 | 0.1472 |

## 7.9 Relative Volatility

Generally, distillation is a technique to separate components according to their relative volatility. Thus, relative volatility can be expressed as a measure comparing the vapour pressures of the components in a liquid mixture of chemicals. In order to separate a binary mixture using distillation process, there must be differences in volatilities of the components. Hence, the ease of separating two components in a binary mixture is a function of the difference in their relative volatility.
The vapour-liquid equilibrium curve line which is generally referred to as the equilibrium line also provides information on how easy or difficult it would be to separate a binary mixture.

Relative volatility can be expressed mathematically as:

$$\alpha = \left( y_i / x_i \right) \div \left( y_j / x_j \right) = K_i / K_j \qquad (7.11)$$

where, α is the relative volatility, $x_i$ and $y_i$ are the respective liquid and vapour compositions for component *i* ,while $x_j$ and $y_j$ are the liquid and vapour compositions for component *j*.
The ratio of the vapour composition to the liquid composition is referred to as the K-factor or the vapour-liquid distribution ratio.

When a component has a larger K-factor than the other does in a binary mixture, the latter is said to be the less volatile and the former is the more volatile component. In such case, the relative volatility will be greater than one, which is good for separation. Thus, the greater the value of α above 1.0, the easier the separation. However, in a case where α is 1.0, no separation is possible in a normal distillation since this means that both components are equally volatile. Thus, they will vapourise together when heat is applied to the system.

It is important to remember that no further separation can take place for a system in equilibrium since the net transfer rate from liquid to vapour is exactly balanced by the transfer rate from vapour to liquid. From the equilibrium curve for the systems measured on this project, it can be observed that there is a relative distance between the diagonal line and the equilibrium curve (where y = x). When their liquid concentrations are equal, components that are more volatile have higher vapour pressures than less volatile components. However, it is important to note that in general, relative volatility of a mixture changes with the mixture composition.

### 7.9.1 2-Propanol (1) + Butyric Acid (2) System

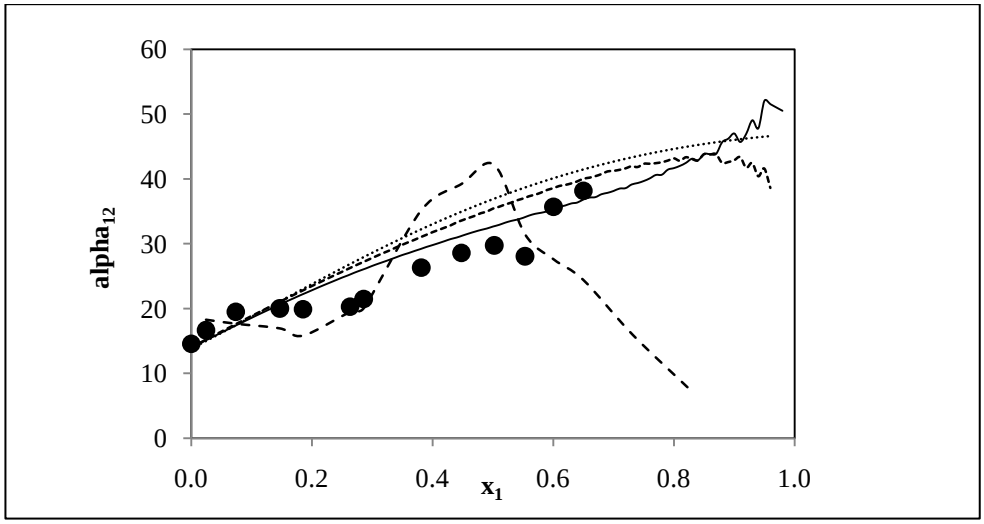


**Figure 7-54 : Plot of Relative volatilty against the mole fraction more volatile Component (2-propanol) in liquid x at 333.15 K (•) , this work; (—), SRK-WS; (---), PRSV-WS; (- - -), VEOS(TsC) ; (- - - -), HOC-CT**

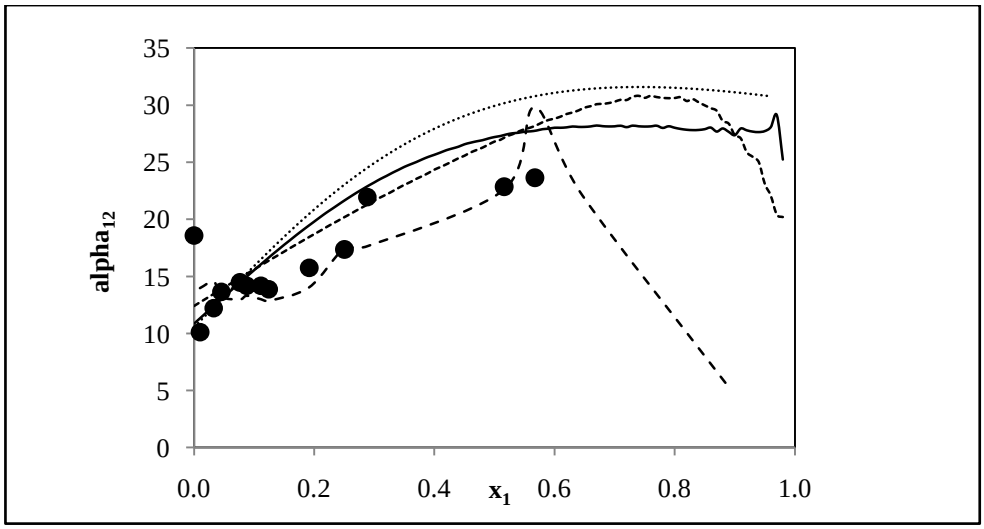


**Figure 7-55 : Plot of Relative volatilty against the mole fraction more volatile component (2-propanol) in liquid x at 353.15 K (•) , this work; (—), SRK-WS; (---), PRSV-WS; (- - -), VEOS(TsC) ; (- - - -), HOC-CT**

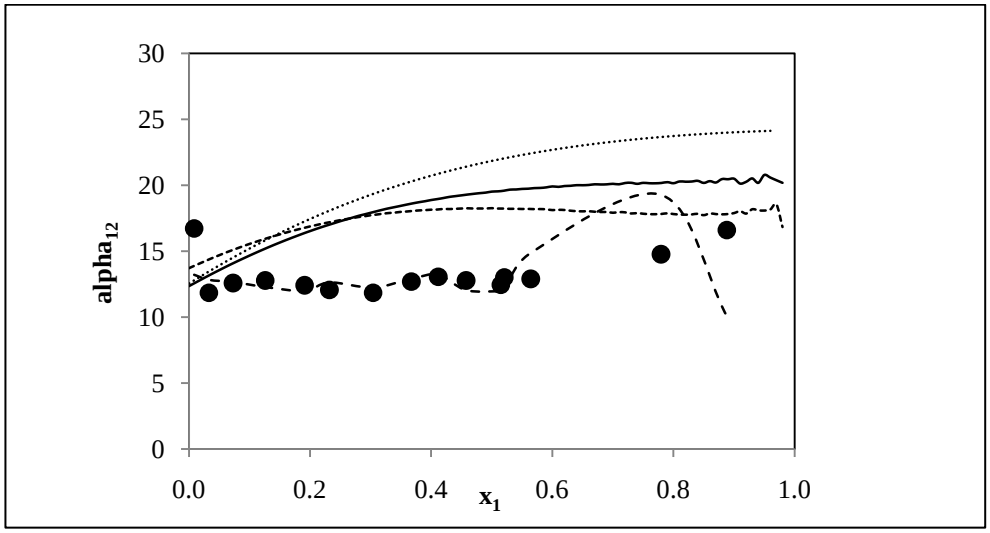


**Figure 7-56 : Plot of Relative volatilty against the mole fraction more volatile component (2-propanol) in liquid x at 373.15 K**
**(•) , this work; (—), SRK-WS; (---), PRSV-WS; (- - -), VEOS(TsC) ; (- - - -), HOC-CT**

### 7.9.2 2-Butanol (1) + Butyric Acid (2) System

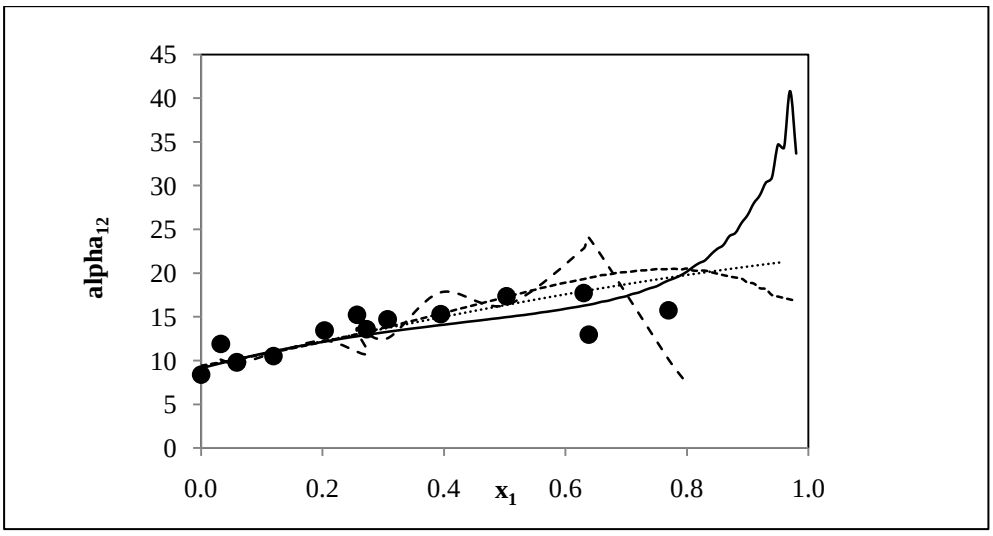


**Figure 7-57 : Plot of Relative volatilty against the mole fraction more volatile component (2-butanol) in liquid x at 333.15 K**
**(•) , this work; (—), SRK-WS; (---), PRSV-WS; (- - -), VEOS(TsC) ; (- - - -), HOC-CT**

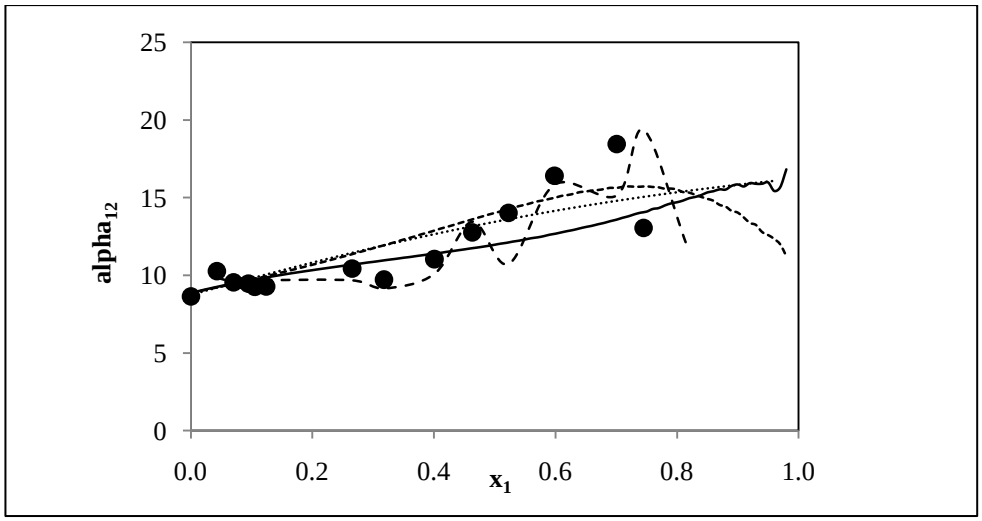


**Figure 7-58 : Plot of Relative volatilty against the mole fraction more volatile component (2-butanol) in liquid x at 353.15 K (•) , this work; (—), SRK-WS; (---), PRSV-WS; (- - -), VEOS(TsC; (- - - -), HOC-CT**

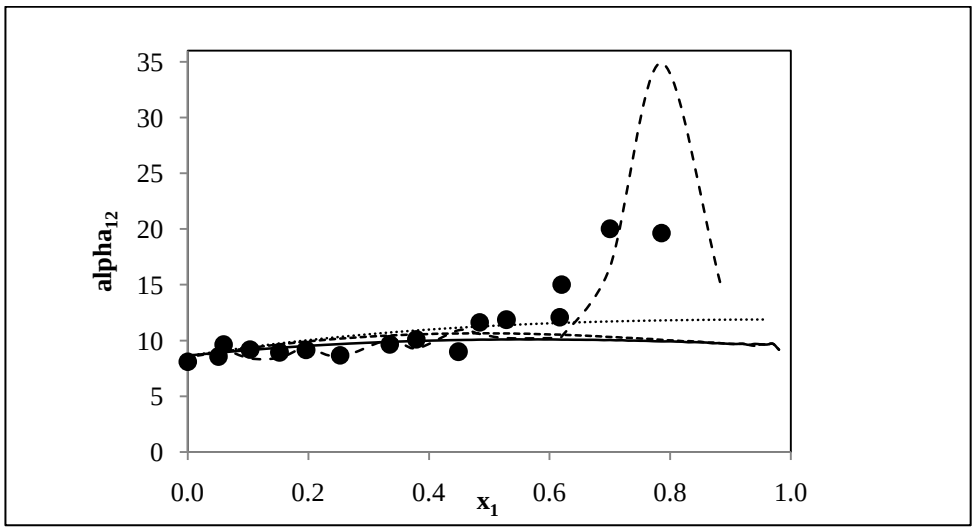


**Figure 7-59 : Plot of Relative volatilty against the mole fraction more volatile component (2-butanol) in liquid x at 373.15 K (•) , this work; (—), SRK-WS; (---), PRSV-WS; (- - -), VEOS(TsC) ; (- - - -), HOC-CT**

### 7.9.3 2-Methyl-1-propanol (1) + Butyric Acid (2) System

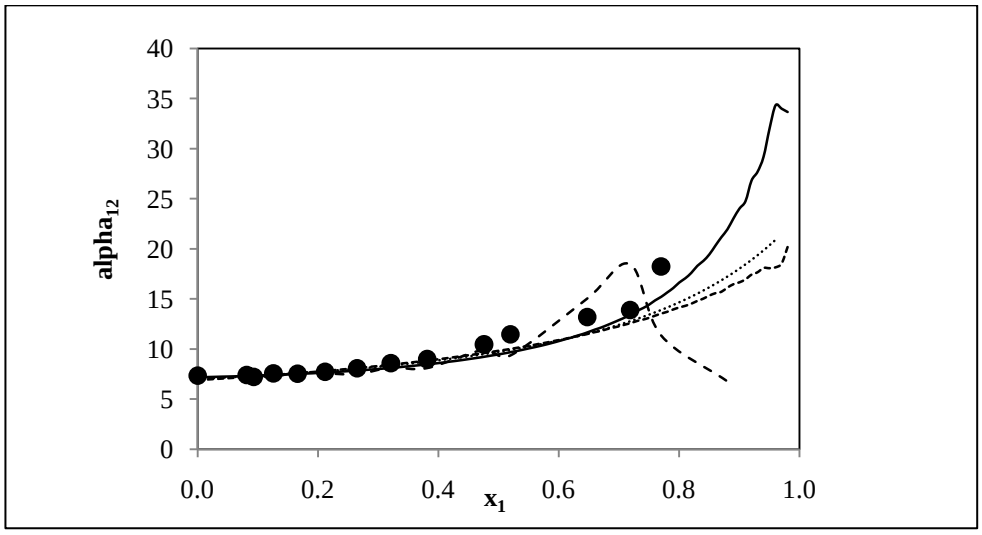


**Figure 7-60 : Plot of Relative volatilty against the mole fraction more volatile component (2-methyl-1-propanol) in liquid x at 333.15 K (•) , this work; (—), SRK-WS; (---), PRSV-WS; (- - -), VEOS(TsC); (- - - -), HOC-CT**

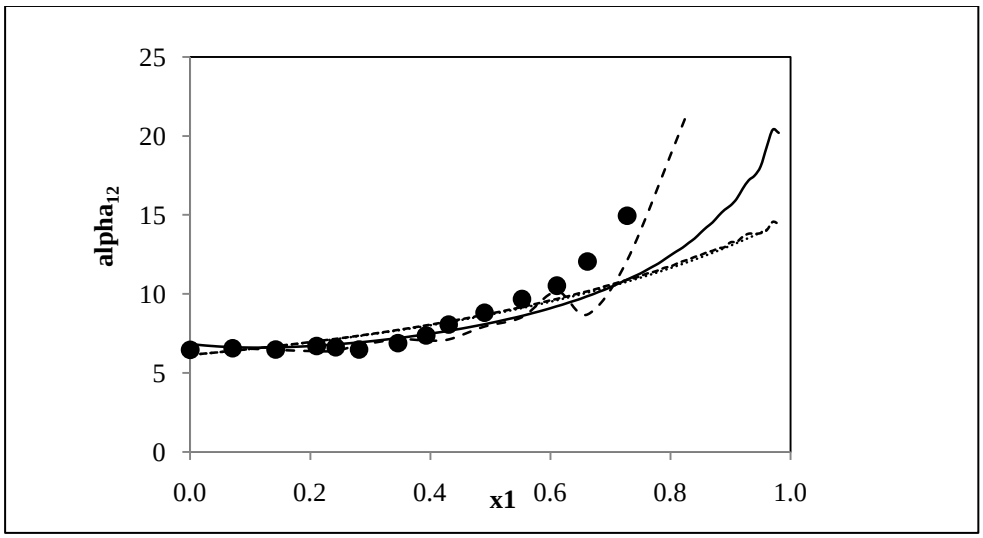


**Figure 7-61 : Plot of Relative volatilty against the mole fraction more volatile component (2-methyl-1-propanol) in liquid x at 353.15 K (•) , this work; (—), SRK-WS; (---), PRSV-WS; (- - -), VEOS(TsC);( - - - -), HOC-CT**

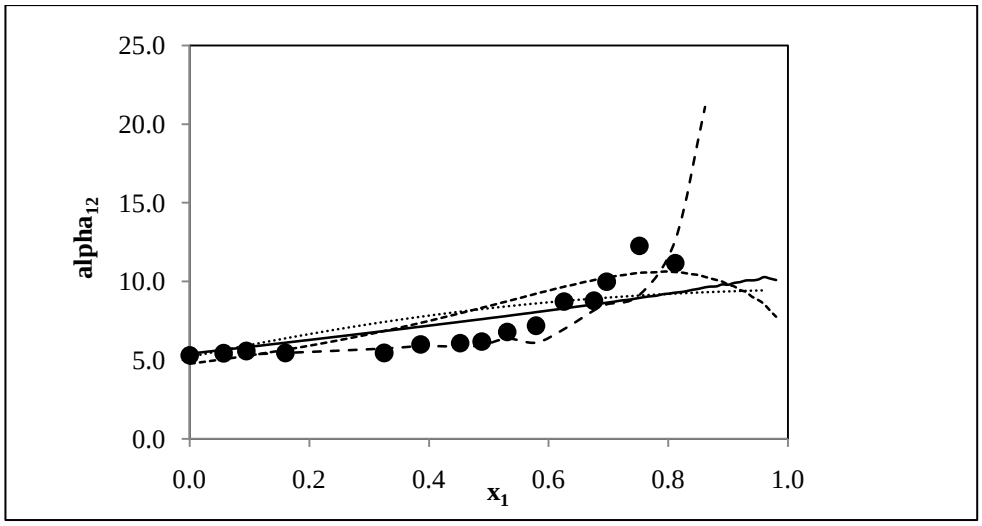


**Figure 7-62 : Plot of Relative volatilty against the mole fraction more volatile component (2-methyl-1-propanol) in liquid x at 373.15 K (● ), this work; (—), SRK-WS; (---), PRSV-WS; (- - -), VEOS(TsC); ( - - - -), HOC-CT**

It can be observed that all the models do not accurately fit the experimental relative volatility. However, the difference in the relative volatility is greater than one (1); indicating that the systems measured in this project can be easily separated in a distillation column under similar operating conditions of temperature.

CHAPTER
8

# CONCLUSION

In order to separate some oxygenated hydrocarbon (specifically carboxylic acid-alcohol binary mixtures) that are part of the industrial waste from the Sasol streams a stainless steel (Reddy, 2006) and a glass re-circulating vapour-liquid equilibrium (VLE) apparatus by Joseph et al. (2001) and Clifford (2003) was utilized for the project.

Three previously unmeasured systems: 2-propanol, 2-butanol and 2-methyl-1-propanol were measured with butyric acid as the second component at three isotherms at 333.15, 353.15 and 373.15 K respectively. The formation of dimers had an effect on the thermodynamic modeling. Hence, two common equation of state namely; Soave-Redlich-Kwong (1972) and Stryjek- Vera (1986) form of Peng- Robinson (1976) that accounts for non-idealities but assume no association was employed. The Virial equation of state (Tsonopoulos correlation) that account for vapour-phase non-idealities was also employed. In conclusion, the Hayden and O'Connell with chemical theory that account for vapour phase non-idealities and any possible chemical interaction in the binary systems was used.
However, some of the main conclusions are:

1.The three previously unmeasured systems (2-propanol (1) + butyric acid (2), 2-butanol (1) + butyric acid (2) and 2-methyl-1-propanol (1) + butyric acid (2) ) at all the isotherms 333.15, 353.15 and 373.15 K showed practically ideal behaviour.

2. The vapour-phase fugacity coefficient showed a wide negative deviation from ideality while the liquid phase activity coefficient could be notice to be closer to unity. However, the liquid phase activity coefficient showed a positive deviation from Raoult's law.
3. The Hayden and O'Connell (1975) with the chemical theory approach was found to give a better fit for the vapour phase and a true representation of the effect of chemical interaction on the newly

measured systems. This can be observed when the results and plots are compared to the Soave-Redlich-Kwong (1972) +NRTL excess Gibbs free energy and Wong Sandler , The Stryjek-Vera (1986) form of Peng-Robinson (1976) + NRTL excess Gibbs free energy and Wong-Sandler equation of state as well as the virial equation of state using the Tsonopoulos correlation.

4. By evaluating the liquid-phase activity coefficient using equation (7.9) and (7.10) proposed by Prausnitz et al. (1999) in the chemical theory, the activity coefficient plots were observed to improve significantly more than when a model that account for no association was used.

5. The chemical theory model was observed to give a higher percentage error than the other models at 373.15 K. This was attributed to the fact that cross-association constants $K_{(AB)}$ decreases with increasing chain length of the alcohol molecules as well as an increase in temperature.

6. The newly measured system was found to be thermodynamically consistent when the point test (Van Ness at al., 1973) and the direct test were applied. This conclusion was reached since the average absolute deviation in the vapour composition for most of the data agreed with the suggested value of 0.01 by Gess et al. (1991). Also, the calculated root mean square (RMS) value from the regression were less than 0.2, a value regarded to imply inconsistent data according to Van Ness (1995) using the direct test for consistency.

CHAPTER
9

# RECOMMENDATIONS

The work completed in this project has revealed several areas that need further development. These areas primarily have to do more with the modeling of carboxylic acid-alcohol mixtures. In addition, included are some recommendations pertaining to the study of oxygenated hydrocarbon systems:

1. The modeling of the carboxylic acid and alcohol systems needs to be improved. Several cubic equations of state exist that incorporate association but the result from all of these models shows that there is still some improvement that needs to be made. In addition, more complicated equations of state such as SAFT (statistical associated fluid theory, developed by Chapman et al. (1989, 1990), the PCSAFT (perturbed chain statistical associating fluid theory) model developed by Sadowski and co-workers (2001) , the CPA(cubic plus association equation of state) model presented by Kontogeogis at al. and GCA (group contribution association equation of state) model of Gros et al.(1996) have been used (amongst others) to obtain good agreement between calculated and measured data for systems containing highly polar compounds. The equation of state modeling carried out in this project serves as a step to these more complicated equations of state, which should be used in future work.

2. Crucial stages in the model development are the careful estimation of pure compound parameters from extensive and reliable vapour pressure and liquid density data. The assessment of the physical significance of the parameters for the final selection of the parameters, as well as the careful selection of the association scheme for the associating compounds involved and the combining rules for the cross-associating systems are important.

Major future challenges should consider the following:

(i) The addition of an association term to Peng-Robinson equation of state may also help to give a good fit.

(ii) The understanding of the importance of cooperativity phenomena and the other limitations of Wertheim theory in taking into account the intramolecular association as well as ring structures (Gupta, and Brinkley, 1998).

(iii) The study of the relative importance of the various terms (attractive, repulsive, association) of models like CPA and PC-SAFT.

(iv) The role/necessity of additional contributions (polar, quadrupolar) to describe effects that are not explicitly taken into consideration with the Wertheim theory.

(v) The comparison of CPA, PC-SAFT and GCA against state-of-the-art local composition models such as the SRK-Huron Vidal/NRTL model (from Pedersen et al.1996), which can help to establish the actual improvement gained by the Wertheim theory over the local composition principle, which indirectly also accounts for the hydrogen bonding/polar phenomena.

3. In the area of the possible reaction that can result in the formation of water and esters in the vapour phase, it was observed that the reaction should not be allowed to stand at equilibrium for too long, and a TCD detector must be used for the vapour composition sample analysis (which is able to detect the presence of water in the sample) on a gas chromatograph. It is also recommended where any physical change because of a chemical reaction is observed in the vapour or liquid phase, the entire systems must be drained and a fresh sample used. The area ratio of the composition analysed on the gas chromatograph must be below 1% at all times. Although, this may become a challenge at the very dilute regions of the mixtures, caution must be taken to successfully achieve this. Following this way, it is possible to conveniently separate the carboxylic acid-alcohols binary mixtures in the laboratory taking both the liquid and vapour phase samples without contamination of the samples.

4. In order to be able to successfully measure the other reacting mixtures in the remaining 10 components matrix (namely the aldehydes; Ethanal and Propanal) with the alcohols and carboxylic acids, the ethanol should be put in a cylinder and feed like a gas. This is because the boiling point is around 293.15 K at atmospheric pressure and because of the health hazard (since it is carcinogenic). The measurement should be considered at temperatures range of 373.15 to 413.15 K to ensure good separation as well as prevent the spontaneous rate of reaction, which easily occur at higher temperature.

5. Apelblat (2007) reviews the historical development and challenges in modeling association systems especially carboxylic acid-alcohol. Although, a brief summary was made in the literature review of this write-up, it is recommended that readers should get the journal for proper understanding of the current modeling challenges in the carboxylic acid-alcohol systems.
In addition, it has been observed over the long period of investigation (1884 to date) of associated mixtures, that there is no systematic and consistent presentation of results as different molecular models have been proposed for the same system. This trend is equally observed in the carboxylic acid mixtures previously measured in our research laboratory at the University of KwaZulu-Natal. Thus, there is need for consistency in modeling.

6. For future modeling of acid-acid mixtures, the 1A scheme of PCSAFT or Simplified SAFT should be used and the result compared with the chemical theory model used on this project.
For the modeling of carboxylic acids-ketones/aldehydes mixtures, the 2B scheme of PCSAFT and the virial equation of state with any of Pitzer-Curl (1957) correlation or Tsonopoulos (1974) correlation should be considered along with the Hayden and O'Connell using chemical theory to account for simple association. While for the carboxylic acids and alcohol mixture (with research on-going), the PCSAFT or Simplified SAFT (using 1A scheme for the acids and 2B or 3B scheme for the alcohol) should be considered with the chemical theory rather than the non-associating cubic equation of states. However, since the focus should be directed to simple models with a few parameters, the use of the SRK/WS/NRTL combination, which was used in this project is recommended.

# REFERENCES


Abbott, M M, and Van Ness, H, C. (1975), "Vapour Liquid Equilibrium: Part III- Data Reduction with Precise Expressions for $G^E$", American Institute of Chemical Engineers Journal, 21, 1 62 – 71.

Abbott, M., M., (1986), "Low pressure phase equilibria: Measurement of VLE", Fluid Phase Equilibria, 29,193-207.

Abrams, D S, and Prausnitz, J M, (1975), "Statistical Thermodynamics of Liquid Mixtures: A New Expression for the Excess Gibbs Energy of Partly or Completely Miscible Systems", American Institute of Chemical Engineers Journal, 21 , 116 -128.

Ahlers J., (2003),"Entwicklung einer universellen Gruppenbeitragszustandsgleichung", Thesis, Carl-von-Ossietzky-Universität Oldenburg, 1-144.

Anderko, A., (1989a), "A simple equation of state incorporating association", Fluid Phase Equilibria, 45, 39.

Anderko, A., (1989b), "Extension of AEOS model to systems containing any number of associating and inert compounds", Fluid Phase Equilibria, 50, 21.

Anderko, A., (1991), "Phase equilibria in aqueous systems from an equation of state based on the chemical approach", Fluid Phase Equilibria, 65, 89.

Anderson, T F and Prausnitz, J M, (1978), "Application of the UNIQUAC Equation to Calculation of Multicomponent Phase Equilibria. 1: Vapour-Liquid Equilibria; 2: Liquid-Liquid Equilibria", Industrial and Engineering Chemistry. Process Design and Development, Vol. 17, pp. 552-567.

Andreas, K., Gerard J. P. Krooshof, R.T., (2004), "COSMOSPACE: Alternative to conventional activity-coefficient models", AIChE J., 48(10), 2332-2349.

Apelblat, A, (2007) Erratum to "The concept of associated solutions in historical development: Part 1. The 1884–1984 period" [J. Mol. Liq. 128 (2006) 1–31] Journal of Molecular Liquids 130 (2007) 133–162.

Banaszak, M., Chiew, Y. C., O'Lenick, R., Radosz, M., (1994), "Thermodynamic Perturbation Theory: Lennard-Jones Chains", Journal of Chemical Physics, 100, 3803.

Barker, J A, (1953), "Determination of Activity Coefficients from Total Pressure Measurements", Australian Journal of Chemistry, Vol. 6, pp. 207-210.

Beret, S., Prausnitz, J. M., (1975), "Perturbed Hard-Chain Theory: An Equation of State for Fluids Containing Small or Large Molecules", American International Chemical Eng. Journal, 21, 1123.

Black, C, (1958), "Vapour Phase Imperfections in Vapour-Liquid Equilibria", Industrial and Engineering Chemistry, Vol. 50, pp. 391-402

Browarzik, D., (2007), "Continuous thermodynamics of binary associating systems", Fluid Phase Equilibria, 254,174–187.

Brandani, V (1983), "A continuous linear association model for determining the enthalpy of hydrogen-bond formation and the equilibrium association constant for pure hydrogen-bonded liquids", Fluid Phase Equilibria, 12, 87-104.

Brandani, V., and Evangelista, F.,(1987), "Correlation and Prediction of Enthalpies of Mixing for Systems Containing Alcohols with the UNIQUAC Associated- Solution Theory", Ind. Eng. Chem. Res., 26, 2423-2430.

Carlson, E. C., (1996), "Don't Gamble with Physical Properties for Simulation", Chem. Eng. Progress. 92 no. 10, 35-46.

Chapman, W. G., Jackson, G., Gubbins, K. E., (1988), "Phase equilibria of associating fluids. Chain molecules with multiple bonding sites", Molecular Physics, 65, 1057.

Chapman, W.G, Gubbins, K.E, Jackson, G and Radosz, M., (1989), "SAFT: Equation-of-State Solution Model for Associating Fluids", Fluid Phase Equilibria, 52, 31-38.

Chapman, W.G, Gubbins, K.E, Jackson, G and Radosz, M., (1990), "New Reference Equation of State for Associating Fluids", Industrial and Engineering Chemistry Research, 29, 1709-1721.

Chen, S. S.; Kreglewski, A., (1977), "Applications of the Augmented van der Waals Theory of Fluids. I. Pure Fluids", Ber. Bunsenges Physical Chemistry, 81 (10), 1049-1057.

Christian, S. D , J. Phys. Chem. 61 (1957) 1441 (as in Apelblat, A, (2007) Erratum to "The concept of associated solutions in historical development: Part 1. The 1884–1984 period" [J. Mol. Liq. 128 (2006) 1–31] Journal of Molecular Liquids 130 (2007) 133–162).

Cholinski, J., Szafranski, A and Wyrzykowska –Stankiewicz, D, (1986), "Computer Aided Second Virial Coefficient Data for Organic Individual Compounds and Binary Systems", PWN Polish Scientific Publishers, Warsaw.

Clifford, S.L, (2003) "Low-Pressure Vapour-Liquid Equilibrium and Molecular Simulation of Carboxylic acids", MSc Thesis, University of Natal, Durban, South Africa.

Clifford, S.L, Ramjugernath, D and Raal,J.D.,(2004), "Sub-atmospheric Vapor Pressure Curves for Propionic Acid, Butyric Acid, Isobutyric Acid, Valeric Acid, Isovaleric Acid, Hexanoic Acid, and Heptanoic Acid", Journal of Chemical Eng. Data, 49, 1189-1192.

Clifford, S.L, Ramjugernath, D and Raal,J.D.,(2005), ""Vapour-liquid equilibrium of carboxylic acid systems: Propionic acid+valeric acid and isobutyric acid+valeric acid", Fluid Phase Equilibria,237, 89-99.

Coon, J.E., J.E. Auwaerter and E. McLaughlin,(1989), "A comparison of solid-liquid equilibrium with vapor-liquid equilibrium for prediction of activity coefficients in systems containing polynuclear aromatics", Fluid Phase Equilibria, 44 ,305-345.

Danner, R P and Gess, M A, (1990), "A Data Base Standard for the Evaluation of Vapour-Liquid Equilibrium Models", Fluid Phase Equilibria, Vol. 56, pp. 285-301.

Deiters, U.K. and G.M. Schneider, (1986), "High pressure phase equilibria: experimental methods", Fluid Phase Equilibria, 29, 145-160.

Dohrn, R. and G. Brunner, (1995), "High-Pressure Fluid-Phase Equilibria: Experimental Methods and Systems Investigated (1988-1993)", Fluid Phase Equilibria, 106, 214.

Dortmund Data Bank,(2009), DDBST Software and Separation Technology GmbH, DDB Software Package Version 2009, Oldenburg.

Dvorak, K.; Boublik, T., (1963), “Liquid-Vapor Equilibria. XXIX. Measurement of Equilibrium Data in the Systems with high Equilibrium Ratio of the Components”, Collect. Czech. Chem. Commun. , 28, 1249-1255.

Dymond, J H, and Smith, E B (1980), “The Virial Coefficients of Gases and Gaseous Mixtures”, Clarendon Press, Oxford.

Economou, I. G., and Donohue, M. D.,(1992), “Equation of State with Multiple Associating Sites for Water and Water-Hydrocarbon Mixtures", Ind. Eng. Chem. Res., 31, 2388-2394.

Eubank, P. T. and Xiaonian W., (2004),“Characteristics of activity coefficient models for liquid solutions”, American Institute of Chemical Engineers Journal, 50,854-861.

Flory, P J, (1942) Journal of Physical Chemistry, 10, 51 as in Prausnitz (1969)

Fredenslund A., Jones R.L. and Prausnitz J.M. (1975) Group-Contribution Estimation of Activity Coefficients in Nonideal Liquid Mixtures, American Institute of Chemical Engineers Journal, Vol. 21, No. 6, November 1975 pp. 1086-1099.

Fredenslund, A, Gmehling, J, and Rasmussen, P, (1977), “Vapour Liquid Equilibrium using UNIFAC”, Elsevier Scientific Publishing Company, New York.

Fredenslund Aage, Jürgen Gmehling and Peter Rasmussen, (1979) “Vapor-liquid equilibria using UNIFAC: a group contribution method” , Elsevier Scientific New York

Freeman, J.R. and G.M. Wilson, (1985), “High Temperature Vapour-Liquid Equilibrium Measurements on Acetic Acid/Water Mixtures” in: M.S. Benson and D. Zudkevitch (Eds.), Experimental Results from the Design Institute for Physical Property Data I: Phase Equilibria, AIChE Symposium Series No.244, Volume 81, pp.14**.**

Ferreira, O., T. Fornari, E .A. Brignole, and S.B. Bottini, (2003), “Modelling of association effects in mixtures of Carboxylic acids with associating and non-associating components”, Latin American Applied Research, 33, 307–312.

Ferreira, O., E .A. Brignole , Eugénia A. Macedo, (2004), “Modelling of phase equilibria for associating mixtures using an equation of state”, Journal of Chemical Thermodynamics, 36 ,1105–1117.

Gess, M A, Danner, R P, and Nagvekar, M (1991), "Thermodynamic Analysis of Vapour Liquid Equilibria: Recommended Models and Standard Data base", Design Institute for Physical Property Data, American Institute of Chemical Engineers.

Gil-Villegas, A., Galindo, A., Whitehead, P. J., Mills, S. J.; Jackson, G., Burgess, A. N.,(1997), "Statistical associating fluid theory for chain molecules with attractive potentials of variable range", Journal of Chemical Physics, 106, 4168.

Gmehling, J and Onken, U, (1977-1982), "Vapour-Liquid Equilibrium Data Collection", DECHEMA Chemistry Data Series, Frankurt/Main.

Gmehling, J., Li, J., and Schiller, M., (1993),"A Modified UNIFAC Model 2. Present Parameter Matrix and Results for Different Thermodynamic Properties", Ind. Eng. Chem. Res., 32, 178-193.

Griswold, J., Andres, D. and Klien, V.A., (1943), "Determination of high pressure vapor-liquid equilibria. The vapor-liquid equilibrium of benzene-toluene", Transactions of the American Institute of Chemical Engineers, 39,223-240.

Gros, H.P, Bottini, S., Brignole, E.A., (1996), "A Group contribution equation of state for associating mixtures", Fluid Phase Equilibria, 116,537-544.

Gross, J.; Sadowski, G.,(2001), "Perturbed-Chain SAFT: An Equation of State Based on a Perturbation Theory for Chain Molecules", Ind. Eng. Chem. Res., 40, 1244.

Gross, J.; Sadowski, G.,(2002), "Modeling Polymer Systems Using the Perturbed-Chain Statistical Associating Fluid Theory Equation of State", Ind. Eng. Chem. Res., 41, 1084-1093.

Gross, J., Sadowski, G.,(2002), "Application of the perturbed-chain SAFT equation of state to associating systems", Ind. Eng. Chem. Res., 41,5510-5515.

Gupta, S K and Rawat, B S, (1991), "Isothermal Vapor-Liquid Equilibria of Tetralin and 1-Methylnaphthalene with Triethylene Gylcol and N-Methylpyrrolidone at $160^0$C", Fluid Phase Equilibria, Vol. 63, pp. 211-217.

Gutiérrez-Antonio, C; Bonilla-Petriciolet, A.; Segovia-Hernández, J.G; Briones-Ramírez, A. (2009) "Effect of adjusted parameters of NRTL model in design, optimization, and control of homogeneous azeotropic distillation columns", ESAT 2009, PA-3

Hala, E., J. Pick, V. Fried and O. Vilim, (1967), "Vapour-Liquid Equilibrium", second edition, Pergamon Press, Oxford.

Harris, R.A., (2001), Master of Science in Chemical Engineering Thesis, University of Natal, Durban, South Africa.

Harris, R.A., (2004), PhD Thesis, University of KwaZulu-Natal, Durban, South Africa.

Hiaki, T..(1996), "Isothermal vapor-liquid equilibria for 2-propanol + octane and 2-propanol + 2,2,4-trimethylpentane at 348.15 K", Fluid Phase Equilibria, 1015

Hayden, J G, and O'Connell, J P, (1975), "A Generalised Method for Predicting Second Virial Coefficients", Industrial and Engineering Chemistry. Process Design and Development, Vol. 14, pp 209 – 216.

Heidemann, R A and Prausnitz, J M, (1976), "A van der Waals-type Equation of State for Fluids with Associating Molecules", Proc. Natl. Acad. Sci.,. 73, 1773-1776.

Herington, E F G, (1947), "A Thermodynamic Consistency Test for the Internal Consistency of Experimental Data on Volatility Ratios", Nature, 60, 610 -611

Hiaki, T..(1996), "Isothermal vapor-liquid equilibria for 2-propanol + octane and 2-propanol + 2,2,4-trimethylpentane at 348.15 K", Fluid Phase Equilibria, 1015.

Hirata, M, Ohe, S, and Nagahama, K, (1975), "Computer Aided Data Book of Vapour Liquid Equilibria: Kodasha Limited, Elsevier Publishing Company, Tokyo.

Holderbaum T.,(1991),"Die Vorausberechnung von Dampf-Flüssig-Gleichgewichten mit einer Gruppenbeitragszustandsgleichung", Fortschrittsber. VDI Reihe 3, 243, 1-154.

Huggins, M L, (1942), Journal of Physical Chemistry, 9, 440 as in Prausnitz (1969).

International Union of Pure and Applied Chemistry, (1993), "Quantities, Units and Symbols in Physical Chemistry", 2nd edition, Oxford: Blackwell Science. ISBN 0-632-03583-8. p. 50. Electronic version.

Huang, S. H.; Radosz, M.,(1990), "Equation of state for small, large, polydisperse and associating molecules", Ind. Eng. Chem. Res., 29, 2284.

Huang, S. H.; Radosz, M., (1991), "Equation of State for Small, Large, Polydisperse, and Associating Molecules: Extensions to Fluid Mixtures", Ind. Eng. Chem. Res., 30, 1994.

Ikonomou, G. D.; Donohue, M. D.,(1988), "Extension of the associated perturbed anisotropic chain theory to mixtures with more than one associating component", Fluid Phase Equilibria, 39, 129.

Ioannis G. Economou, (2002), Statistical Associating Fluid Theory: A Successful Model for the Calculation of Thermodynamic and Phase Equilibrium Properties of Complex Fluid Mixtures, Ind. Eng. Chem. Res., 41, 953-962.

J. Li, C. Chen and J. Wang, (2000), "Vapor-liquid equilibrium data and their correlation for binary systems consisting of ethanol, 2-propanol, 1, 2-ethanediol and methyl benzoate", Fluid Phase Equilibria, 169, 75-84.

Johnson, J. K.; Müller, E. A.; Gubbins, K. E., (1994), "Equation of State for Lennard-Jones Chains", Journal of Physical Chemistry, 98, 6413.

Jones, C. A.; Schoenborn, E. M.; Colburn, A. P., (1943), "Equilibrium Still for miscible mixtures - Data on Ethylene dichloride-Toluene and Ethanol-Water", Industrial Engineering Chemistry, 35, 666-672.

Jørgensen, W L, (1986), "Optimized Intermolecular Potential Functions for Liquid Alcohols", Journal of Physical Chemistry, Vol. 90, pp. 1276-1284.

Joseph, M A, (2001), Master of Science in Chemical Engineering Thesis, University of Natal, Durban, South Africa.

Joseph, M. A., Raal, .J .D and Ramjugernath, .D, (2001), "Phase Equilibrium Properties of Binary Systems with Diacetyl from a Computer Controlled Vapour-Liquid Equilibrium Still", Fluid Phase Equilibria, 182, 157-176.

Joseph, M A, Raal, J D and Ramjugernath, D, (2002), “Computer-aided Measurement of Vapour-Liquid Equilibria in a Dynamic Still at Sub-Atmospheric Pressures”, Developments in Chemical Engineering Mineral Processes, 10, 615-637.

Joyce, P. C., Leggett, B. E., Thies, M. C., (1999), "Vapor-liquid equilibrium for model Fischer-Tropsch waxes (hexadecane, 1-hexadecene, and 1-hexadecanol) in supercritical hexane", Fluid Phase Equilibria, 158-160(1-2), 723-731.

Junyang , Z., and Ying, H., (1990), “Thermodynamics of associated solutions: excess properties of alcohol-alkane and alcohol-carboxylic acid mixtures” , Fluid Phase Equilibria, 57, 89-104

Kato, M, Yoshikawa, H and Yamaguchi, M, (1990), “Vapour-Liquid Equilibrium Measurements of Three Binary Systems Made of Formic Acid, Acetic Acid and Propionic Acid by the Dew-Point Temperature Method”, Fluid Phase Equilibria, 54, 47-56.

Kamlet, M. J., Doherty, R. M., Abraham, M. H., Marcus, Y., and Taft, R. W.,(1988), “Linear Solvation Energy Relationships. 46. An Improved Equation for Correlation and Prediction of Octanol/Water Partition Coefficients of Organic Nonelectrolytes (Including Strong Hydrogen Bond Donor Solutes)", J.Phys. Chem., 92, 5244-5255.

Karre, L., Gaube, J., (1988), “Determination of ternary VLLE by $P(X_1,X_2)$ measurements, Fluid Phase Equilibria”, 42, 195-207.

Klekers, A J and Scheller, W A, (1968), “Isothermal Vapour-Liquid Equilibrium Data for the System Formic Acid – Valeric Acid at 50°, 75°, and 100°C”, Journal of Chemical Engineering Data, 13, 480-482.

Kneisl, P, Zondlo, J W and Wallace, B W, (1989), “The Effect of Fluid Properties on Ebulliometer Operation”, Fluid Phase Equilibria, 46, 85-94.

Kraska, T.; Gubbins, K. E., (1996), “Phase Equilibria Calculations with a Modified SAFT Equation of State. 1. Pure Alkanes, Alkanols, and Water”, Ind. Eng. Chem. Res., 35, 4727.

Kontogeorgis, G. M., E. C. Voutsas, I. V. Yakoumis, and D.P. Tassios , (1996),“An Equation of State for Associating Fluids” Ind. Eng. Chem. Res., 35, 4310-4318.

Kontogeorgis, G.M, Samer O.D., Zeuthen, J., Michelsen, M., Stenby, E.H., (2004), “Application of the CPA equation of state to organic acids”, Fluid Phase Equilibria, 225,107–113.

Kontogeorgis, G.M., Michelsen, M.L., Folas, G.K., Samer Derawi, Nicolas von Solms, and Stenby ,E.H.,(2006), “Ten Years with the CPA (Cubic-Plus-Association) Equation of State. Part 2. Cross-Associating and Multicomponent Systems”, Ind. Eng. Chem. Res., 45, 4869-4878.

Lewis, Gilbert N. (1908), "The osmotic pressure of concentrated solutions, and the laws of the perfect solution," Journal of American Chemical Society, 30, 668-683.

Ljunglin, JJ, and Van Ness, H C, (1962), “Calculation of Vapour Liquid Equilibria from Vapour Pressure Data”, Chemical Engineering Science 17, 531 – 539.

Malanowski S., (1982), “Experimental methods for vapour-liquid equilibria. II. Dew- and bubble-point method”, Fluid Phase Equilibria, 9, 311-317.

Malanowski, S and Anderko, A, (1992) “Modelling Phase Equilibrium: Thermodynamic Background and Practical Tools, John Wiley and Sons, Inc, New York, USA.

Marquadt, D W, (1963), “An Algorithm for Least-Squares Estimation of Non-Linear Parameters”, Journal. Society of Industrial and Applied Mathematics, 11, 431-441.

Matthias Kleiner.(2009), "Thermodynamic Modeling of Complex Systems", Structure and Bonding.

Mathias P.M., Copeman T.W.,(1983), “Extension of the Peng-Robinson Equation of State to Complex Mixtures: Evaluation of the Various Forms of the Local Composition Concept”, Fluid Phase Equilibria, 13, 91-108, 1983.,

Marsh, K., N., (1989), “New methods for vapour-liquid-equilibria measurements”, Fluid Phase Equilibria, 52, 169-180.

McClellan, A L, (1963 -1974), “Tables of Experimental Dipole Moments”, W. H Freeman, San Francisco.

Meng, L and Duan, Y., (2007) "An extended correlation for second virial coefficients of associated and quantum fluids", Fluid Phase Equilibria, 258, 29-33

Mixon, F.C, Gumowski, B., and Carpenter, B.H, (1965), "Computation of Vapour Liquid Equilibrium Data from Solution Vapour Pressure Measurements", Industrial and Engineering Chemistry, Fundamentals, 4, No 4 pp 455 – 459.

Miyamoto, S, Nakamura, S, Iwai, Y and Arai, Y, (2001), "Measurement of Isothermal Vapour-Liquid Equilibria for Monocarboxylic Acid + Monocarboxylic Acid Binary Systems with a Flow-Type Apparatus", Journal of Chemical Engineering Data, 46, 405-409.

Morachevsky, A G and Zharov, V T, (1963), Zhurnal Prikladnoi Khimii, Vol. 36, pp 2771 as reported by Gmehling, J and Onken, U, (1977), "Vapour Liquid Equilibrium Data Collection, Organic Hydroxy Compounds:Alcohols", 1, Part 2a, 429, DECHEMA, Frankfurt/Main.

Morgan, D. L., Kobayashi, R., (1994), "Direct vapor pressure measurements of ten n-alkanes in the $C_{10}$-$C_{28}$ range", Fluid Phase Equilibria, 97, 211-242.

Murdock, James W. (1993), Fundamental fluid mechanics for the practicing engineer, CRC Press, 25–27, ISBN 0824788087

Nagahama, K.,(1996),"VLE measurements at elevated pressure for process development", Fluid Phase Equilibria, 116 361-372.

Nagata, I, Gotoh, K, Miyamoto, K, (1995),"Application of the UNIQUAC associated-solution model acid + alkanol and alkanol + hydrocarbon mixtures", Thermochimica Acta ,249 ,89-1 11 .

Nannoolal, Y., J. Rarey and D. Ramjugernath, (2007),"Estimation of Pure Component Properties Part 2: Estimation of Critical Property Data by Group Contribution", Fluid Phase Equilibria, 252(1-2), 1-27.

Nath A.; Bender E., (1981), "On the thermodynamics of associated solutions. I. An analytical method for determining the enthalpy and entropy of association and equilibrium constant for pure liquid substances", Fluid Phase Equilibria, 7, 275.

Ndlovu, M, (2005), "Development of a Dynamic Still for Measuring Low Pressure Vapour-Liquid-Liquid Equilibria (Systems of Partial Liquid Miscibility)", Master of Science in Engineering (Chemical Engineering) Thesis, University of KwaZulu-Natal, South Africa.

Nothnagel, K-H, Abrams, D S and Prausnitz, J M, (1973), "Generalized Correlation for Fugacity Coefficients in Mixtures at Moderate Pressures", Industrial and Engineering Chemistry, Process Design and Development, 12, 25-35.

O'Connell, J P and Prausnitz, J M, (1967), "Empirical Correlation of Second Virial Coefficients for Vapour-Liquid Equilibrium Calculations", Industrial and Engineering Chemistry, Process Design and Development, 6, 245-250.

Oh, B. C., Y. Kim, H. Y. Shin, and H. Kim,(2004), "Vapor–Liquid Equilibria for the system 1-propanol+n-hexane near the Critical Region," Fluid Phase Equilibria, 220, 41-46.

Orbey, H and Sandler, S I, (1996), "A Comparison of Various Cubic Equation of State Mixing Rules for the Simultaneous Description of Excess Enthalpies and Vapour-Liquid Equilibria", Fluid Phase Equilibria, 121, 67-83.

Panayiotou, C and Sanchez, I C, (1991), "Hydrogen Bonding in Fluids: Equation of State Approach", Journal of Physical Chemistry, 95, 10090-10097

Pedersen, K. S.; Michelsen, M. L.; Fredheim, A. O., (1996), "Phase equilibrium calculations for unprocessed well streams containing hydrate inhibitors", Fluid Phase Equilibria, 126, 13.

Peng, D and Robinson, D B, (1976), "A New Two constant Equation of State" Industrial and Engineering Chemistry Fundamentals, 15, 59 -64.

Perrot, Pierre (1998), "A to Z of Thermodynamics", Oxford University Press, ISBN 0-19-856552-6.

Pitzer, K S, Lippmann, D Z, Curl, R F, Huggins, C M and Petersen, D E, (1955), "The Volumetric and Thermodynamic Properties of Fluids. II. Compressibility Factor, Vapour Pressure and Entropy of Vapourization", Journal of the American Chemical Society, 77, 3433.

Pitzer, K S, and Curl, R F, (1957), "Empirical Equation for the Second Virial Coefficients", Journal of the American Chemical Society, 79, 2369 – 2370.

Prausnitz, J M, (1969), "Molecular Thermodynamics of Fluid Phase Equilibria", Prentice Hall Inc. Canada.

Prausnitz, J M, Anderson, T F, Grens, E A, Eckert, CA, O'Connell, J P (1980) "Computer Calculations for Multicomponent Vapour Liquid Equilibria" Prentice- Hall, Englewood Cliffs, NJ.

Prausnitz, J M, Lichtenthaler, R N and De Azevedo, E G, (1986), "Molecular Thermodynamics of Fluid Phase Equilibria", 2nd Edition, Prentice Hall, Englewood Cliffs, New Jersey.

Prausnitz, J M, Lichtenthaler, R N and de Azevedo, E G, (1999), "Molecular Thermodynamics of Fluid-Phase Equilibria", 3rd edition, Prentice-Hall, Upper Saddle River, New Jersey.

Prikhodko, I. V., Letcher, T. M., and de Loos, T. W.,( 1997) "Liquid-Liquid Equilibrium Modeling of Ternary Hydrocarbon +Water + Alkanol Systems", Ind. Eng. Chem. Res., 36, 4391-4396 .

Raal, J.D. and C.J. Brouckaert,(1992), "Vapour-liquid and liquid-liquid equilibria in the system methyl butenol-water", Fluid Phase Equilibria, 74 , 253-270.

Raal, J.D. and A.L. Mühlbauer, (1998), "Phase Equilibria: Measurement and Computation", Taylor and Francis, Bristol.

Rackett, H G, (1970), "Equation of state for saturated Liquids", Journal of Chemical and Engineering Data, 15, 514-517.

Rarey, J., R., Gmehling, J., (1993), "Computer-operated static apparatus for the measurement of vapor-liquid equilibrium data", Fluid Phase Equilibria, 83, 279-287.

Reddy, P, (2006) "Development of a Novel Apparatus for the Measurement of Vapour-Liquid Equilibria at Elevated Temperatures and Moderate Pressures", PhD Thesis, University of KwaZulu-Natal, Durban, South Africa.

Redlich, O and Kister, A T, (1948), "Algebraic Representation of Thermodynamic Properties and the Classification of Solutions", Industrial and Engineering Chemistry, 40, 345- 348

Redlich, O and Kwong, J N S, (1949), "On Thermodynamics of SolutionsV: An Equation of State. Fugacities of Gaseous Solutions", Chemical Reviews ,44, 233 – 244.

Reichl, A., Daiminger, U., Schmidt, A., Davies, M., Hoffmann, U., Brinkmeier, C, Rederc, C., Marquardt, W., (1998), "A non-recycle flow still for the experimental determination of vapor–liquid equilibria in reactive systems", Fluid Phase Equilibria, 153 113-134.

Reid, C R, Prausnitz, J M, and Polling, B E, (1988), "The Properties of Gases and Liquids", 4th Edition, McGraw Hill Book Company, Singapore.

Renon, H and Prausnitz, J M (1968), “Local Compositions in Thermodynamic Excess Functions for Liquid Mixtures”, American Institute of Chemical Engineers Journal, 14, 135-144.

Rogalski, M., and Malanowski, S.,(1980), "Ebuliometers Modified for the Accurate Determination of. Vapor-Liquid Equilibrium", Fluid Phase Equilibria, 5, 97-112.

Scatchard, G. Chem. Rev. 44 (1949) 7 ( as in Apelblat, A, (2007) Erratum to “The concept of associated solutions in historical development: Part 1. The 1884–1984 period” [J. Mol. Liq. 128 (2006) 1–31] Journal of Molecular Liquids 130 (2007) 133–162.)

Salzman , W. R.(2004) Website, “Dynamic Text”,Department of Chemistry, University of Arizona, Tucson, Arizona 85721.

Sandler, S I, Orbey, H, and Lee, B, (1994), “Models for Thermodynamic and Phase Equilibria Calculations. Marcel Dekker, New York.

Sandler, S I, Wolbach, J.P, and Caster,M., Escoledo-Alvarado. G, (1997), “Modeling of thermodynamically difficult systems”, Fluid Phase Equilibria, 136, 15-29.

Sayegh, S G, and Vera, J H, (1980), “Model Free Methods for Vapour Liquid Equilibria Calculations. Binary Systems”, Chemical Engineering Science, 35 , 2247 -2256.

Schad R. C.,(1998), “Make the most of Process Simulation”, Chem. Eng. Progress. 94, no. 1, 21-27.

Sewnarain, R, Raal, J D and Ramjugernath, D, (2002), “Isobaric Vapour-Liquid Equilibria for the Systems Propionic Acid + Butyric Acid, Isobutyric Acid + Butyric Acid, Butyric Acid + Isovaleric Acid, and Butyric Acid + Hexanoic Acid at 14 kPa”, Journal of Chemical Engineering Data, 47, 603-607.

Sivaraman, A. and R. Kobayashi, (1982),“Investigation of Vapor Pressures and Heats of Vaporization of Condensed Aromatic Compounds at Elevated Temperatures”, Journal of Chemical Engineering Data. 27(3) 264-269.

Skjold-Jøgensen, S., (1984), Fluid Phase Equilibria, 16, 317-351. (as in Skjold-Jøgensen, S.,1988).
Skjold-Jøgensen, S.,(1988), “Group Contribution Equation of State (GC-EOS): A Predictive Method for Phase Equilibrium Computations over Wide Ranges of Temperature and Pressures up to 30 MPa”, Ind. Eng. Chem. Res.,27,110-118.

Smith J M, Van Ness, H C,(1996),"Introduction to Chemical Engineering Thermodynamics" 5th Edition, Mc Graw-Hill, Singapore.

Smyth, C P (1955), "Dipole Moment and Molecular Structure", CCP5 Quarterly, 4, 13 -25.

Soave, G, (1972), "Equilibrium Constants from a modified Redlich-Kwong Equation of State", Chemical Engineering Science, 27, 1197 – 1203.

Soo, C-B ; El Ahmar,E.; Coquelet, C. ; Ramjugernath, D. ;Richon, D, (2009), "Vapor–liquid equilibrium measurements and modeling of the n-butane + ethanol system from 323 to 423K" ,Fluid Phase Equilibria,286, 69–77.

Stryjek, R and Vera, J H, (1986), "PRSV: An Improved Peng and Robinson Equation of State for Pure Compounds and Mixtures", The Canadian Journal of Chemical Engineering, 64 ,323-333.

Taha, A.A and Christian, S.D, J. Phys. Chem. 73 (1969) 3430 (as in Apelblat, A, (2007) Erratum to "The concept of associated solutions in historical development: Part 1. The 1884–1984 period" [J. Mol. Liq. 128 (2006) 1–31] Journal of Molecular Liquids 130 (2007) 133–162).

Tamir, A and Wisniak, J, (1975), "Vapour-Liquid Equilibria in Associating Solutions", Chemical Engineering Science, 30, 335-342.

Tsonopoulos, C and Prausnitz, J.M , Chem. Eng. J. 1 (1970) 243 (as in Apelblat, A, (2007) Erratum to "The concept of associated solutions in historical development: Part 1. The 1884–1984 period" [J. Mol. Liq. 128 (2006) 1–31] Journal of Molecular Liquids 130 (2007) 133–162).

Tsonopoulos, C (1974), "An Empirical Correlation of the Second Virial Coefficients", American Institute of Chemical Engineers Journal, 20, 263 – 272.

Tsuboka, T and Katayama, T, (1975), "Modified Wilson Equation for Vapour-Liquid and Liquid-Liquid Equilibria", Journal of Chemical Engineering of Japan, 8 No. 5, 181 -187.

Turton, R., Bailie, R. C., Whiting, W. B., Schaewitz, J. A.,(1998), "Analysis, Synthesis, and Design of Chemical Processes", Prentice Hall.

Twu, C H, Coon, J E and Cunningham, J R, (1993), "An Equation of State for Carboxylic Acids", Fluid Phase Equilibria, 82, 379-388.

Twu, C H and Coon, J E, (1996), "CEOS/$A^E$ Mixing Rules Constrained by vdW Mixing Rule and Second Virial Coefficient", American Institute of Chemical Engineers Journal, 42, 3212-3222.

Uusi-Kyyny, P., Pokki, J-P., Laakkonen, M., Aittamaa, J. and Liukkonen, S., (2002) , "Vapour liquid equilibrium for the binary systems 2-methylpentane + 2-butanol at 329.2 K and n-hexane + 2-butanol at 329.2 and 393.2 K with a static apparatus", Fluid Phase Equilibria, 201, 343-358.

Van der Waals, J. D,(1873), "On the Continuity of the Gaseous and Liquid States"(doctoral dissertation). Universiteit Leiden.

Van Laar, J J, (1910), "The Vapour Pressure of binary mixtures", Zeitschrift feur Physik Chemie, 72, 723 -751. (As given in Walas, 1985).

Van Ness, H.C.; Byer, S.M.; Gibbs, R.E. (1973) "Vapor-liquid equilibrium: Part I. An appraisal of data reduction methods", American Institute of Chemical Engineers Journal, 19, 238-244.

Van Ness, H C and Abbott, M M, (1975), "Vapour Liquid Equilibrium: Part III- Data Reduction with Precise Expressions for $G^E$", American Institute of Chemical Engineers Journal, 21, 1 , 62 – 71.

Van Ness, H C, Pedersen, F and Ramussen, P, (1978), "Part V. Data Reduction by Maximum Likelihood", American Institute of Chemical Engineers Journal, 24, 1055-1063.

Van Ness, H C, and Abbott, M M, (1982), "Classical Thermodynamics of Non-Electrolyte Solutions: With Applications to Phase Equilibria", McGraw Hill, New York.

Van Ness, H C, (1995), "Thermodynamics in the Treatment of Vapour-Liquid Equilibrium Data" Journal of Pure and Applied Chemistry, 67, 6, 859 – 872.

Vawdrey, A.C; Oscarson, J.L; Rowley, R.L; Wilding, W.V, (2004), "Vapor-phase association of *n*-aliphatic carboxylic acids", Fluid Phase Equilibria, 222–223, 239–245.

Walas, S M (1985), "Phase Equilibrium in Chemical Engineering" Butterworth, Boston.

Weast, R C (Editor) (1983 -1984), "Handbook of Chemistry and Physics", 64th Edition, CRC Press, London.

Wertheim, M. S., (1984a), "Fluids with highly directional attractive forces: I. Statistical thermodynamics", Journal of Statistical Physics, 35, 19.

Wertheim, M. S., (1984b), “Fluids with highly directional attractive forces: II. Thermodynamic perturbation theory and integral equations”, Journal of Statistical Physics, 35, 35.

Wertheim, M. S., (1986a), “Fluids with highly directional attractive forces: III. Multiple attraction sites”, Journal of Statistical Physics, 42, 459.

Wertheim, M.S.,(1986b), “Fluids with highly directional attractive forces: IV. Equilibrium polymerization”, Journal of Statistical Physics, 42,477.

Wilson, G M, (1964), “Vapour-Liquid Equilibrium, A New Expression for the Excess Free Energy of Mixing”, Journal of American Chemical Society, Vol. 86, pp 127 – 130.

Wisniewska-Goclowska B., Malanowski S.K., "A new modification of the UNIQUAC equation including temperature dependent parameters", Fluid Phase Equilib., 180, 103-113, 2001.

Wisniak, J and Tamir, A, (1978), “Mixing and Excess Thermodynamic Properties”, Elsevier Scientific Publishing Company, Netherlands.

Wong, D. S. H. and Sandler, S. I. (1992), “A Theoretically Correct Mixing Rule for Cubic Equation of State”, American Institute of Chemical Engineers Journal, 38, 671-680.

http://www.chemguide.co.uk/organicprops/alcohols/background.html accessed on 23 October 2009

http://www.petr0.com/Carboxylic_acid:Physical_properties/encyclopedia.htm

Yerazunis, S, Plowright, J D and Smola, F M, (1964), “Vapour-Liquid Equilibrium Determination by a New Apparatus”, American Institute of Chemical Engineers Journal, Vol.10, pp. 660-665.

Zhao, J., Bao, J. and Hu, Y., (1989), “Excess molar enthalpies of (an alkanol+ a carboxylic acid) at 298.15 K measured with a Picker Calorimeter”, Journal of Chemical Thermodynamics, 21, 811-818.

**APPENDIX**
**A**

# PURE COMPONENT PROPERTIES

The pure component properties used in this project are included in this appendix. The critical pressure, temperature, volume and compressibility were easily obtained from the Dortmund Data Bank (DDB, 2009) and Prausnitz et al.(1980). The acentric factors as well as the dipole moments were equally obtained from Dortmund Data Bank (DDB, 2009). The solvation and association parameters were acquired from Prausnitz (1980). The mean radius of gyration was determined using the group contribution method proposed by Reid et al. (1977). The second virial coefficients were calculated using the correlations discussed in Section 3.4.2 and the liquid molar volumes were evaluated via the Rackett (1970) equation (presented in Tables A-2 and A-3).

The kappa parameter for the Stryjek-Vera (1986) alpha correlation was obtained by regressing the vapour pressure parameter and was presented in Table 7-3.

The pure component properties are presented for the new systems measured on this system as applied to the VLE data procedure. The pure component properties for the test system (comprised of cyclohexane and ethanol) are also included in Table A-1. The data for the test system was obtained from the DDB (2009) and Smith et al. (1996).

| Pure Component Property | 2-Propanol | 2-Butanol | 2-Methyl-1-Propanol | Butyric Acid | Cyclohexane | Ethanol |
|---|---|---|---|---|---|---|
| $T_c$ /K | 508.3 | 536.0 | 547.7 | 624.0 | 553.8 | 516.2 |
| $P_c$ / kPa | 4762.28 | 4194.86 | 4296.18 | 3951.68 | 4080.36 | 6383.48 |
| $V_c$ /$cm^3mol^{-1}$ | 220.0 | 268.0 | 273.0 | 292.0 | 308.0 | 167.0 |
| $Z_c$ | 0.2479 | 0.2523 | 0.2576 | 0.2224 | 0.2729 | 0.2484 |
| DipoleMoment /debye | 1.66 | 1.7 | 1.64 | 1.5 | 0.3 | 1.69 |
| Solvation&Association | 4.5 | 4.5 | 4.5 | 4.5 | 0 | 1.4 |
| Radius of Gyration /Å | 2.726 | 3.182 | 3.14 | 3.61 | 3.261 | 2.25 |
| Acentric Factor (ω) | 0.665 | 0.5760 | 0.5880 | 0.5913 | 0.213 | 0.6300 |
| A | 16.4129 | 15.2925 | 17.6380 | 15.8069 | 13.7612 | 16.8757 |
| B | 3466.589 | 3040.634 | 4492.207 | 4063.33 | 2778 | 3782.90 |
| C | 211.6 | 185.559 | 237.147 | 199.892 | 223.136 | 230.3 |

**Table A-1: Pure component properties used in this project.**

| Temperature | $B_{12}^F$ $cm^3$/mol | $B_{12}^D$ $cm^3$/mol | $B_{12}$ $cm^3$/mol | $V_1^L$ $cm^3$/mol | $V_2^L$ $cm^3$/mol |
|---|---|---|---|---|---|
| 333.15 K | -28.0240 | -2.60E+06 | -2.595E+06 | 78.646 | 87.189 |
| 353.15 K | -11.5262 | -8.24E+05 | -8.241E+05 | 81.449 | 89.339 |
| 373.15 K | 3.4590 | -2.96E+05 | -2.961E+05 | 84.639 | 91.662 |

**Table A-2: Liquid molar volumes and second virial coefficients for the 2-propanol (1) + butyric acid (2) system.**

| Temperature | $B_{12}^F$ $cm^3$/mol | $B_{12}^D$ $cm^3$/mol | $B_{12}$ $cm^3$/mol | $V_1^L$ $cm^3$/mol | $V_2^L$ $cm^3$/mol |
|---|---|---|---|---|---|
| 333.15 K | -52.3371 | -2.72E+06 | -2.715E+06 | 94.405 | 87.189 |
| 353.15 K | -35.7885 | -8.62E+05 | -8.623E+05 | 97.327 | 89.339 |
| 373.15 K | -19.9299 | -3.10E+05 | -3.099E+05 | 100.59 | 91.662 |

**Table A-3: Liquid molar volumes and second virial coefficients for the 2-butanol (1) + butyric acid (2) system.**

| Temperature | $B_{12}^F$ $cm^3$/mol | $B_{12}^D$ $cm^3$/mol | $B_{12}$ $cm^3$/mol | $V_1^L$ $cm^3$/mol | $V_2^L$ $cm^3$/mol |
|---|---|---|---|---|---|
| 333.15 K | -53.410 | -2.72E+06 | -2.717E+06 | 96.699 | 87.189 |
| 353.15 K | -37.5767 | -8.63E+05 | -8.629E+05 | 99.506 | 89.339 |
| 373.15 K | -22.1842 | -3.10E+05 | -3.100E+05 | 102.62 | 91.662 |

**Table A-4: Liquid molar volumes and second virial coefficients for the 2-methyl-1-propanol (1) + butyric acid (2) system.**

| Temperature | $K_1$ /kPa$^{-1}$ | $K_2$ /kPa$^{-1}$ | $K_{12}$ | $Є'_{12}$ /ergs/mol. | $σ'_{12}$ /Å |
|---|---|---|---|---|---|
| 333.15 K | 83.912 | 103.487 | 187.396 | 320.54 | 5.318 |
| 353.15 K | 25.134 | 31.007 | 56.136 | 320.54 | 5.318 |
| 373.15 K | 8.544 | 10.547 | 19.086 | 320.54 | 5.318 |

**Table A-5: Equilibrium constants and cross coeffiecients for the 2-propanol (1) + butyric acid (2) system from chemical theory.**

| Temperature | $K_1$ /kPa$^{-1}$ | $K_2$ /kPa$^{-1}$ | $K_{12}$ | $Є'_{12}$ /ergs/mol. | $σ'_{12}$ /Å |
|---|---|---|---|---|---|
| 333.15 K | 92.514 | 103.487 | 196.067 | 363.50 | 5.428 |
| 353.15 K | 27.713 | 31.007 | 58.738 | 363.50 | 5.428 |
| 373.15 K | 9.422 | 10.547 | 19.974 | 363.50 | 5.428 |

**Table A-6: Equilibrium constants and cross coefficients for the 2-butanol (1) + butyric acid (2) system from chemical theory.**

| Temperature | $K_1$ /kPa$^{-1}$ | $K_2$ /kPa$^{-1}$ | $K_{12}$ | $Є'_{12}$ /ergs/mol. | $σ'_{12}$ /Å |
|---|---|---|---|---|---|
| 333.15 K | 92.655 | 103.487 | 196.187 | 366.02 | 5.431 |
| 353.15 K | 27.755 | 31.007 | 58.774 | 366.02 | 5.431 |
| 373.15 K | 9.437 | 10.547 | 19.986 | 366.02 | 5.431 |

**Table A-7: Equilibrium constants and cross coefficients for the 2-methyl-1-propanol (1) + butyric acid (2) system from chemical theory.**

**APPENDIX**
**B**

## B.1 SOAVE MODIFICATION OF REDLICH-KWONG EQUATION OF STATE

The Soave-Redlich-Kwong (1972) equation of state has gained acceptance over the years amongst many other equation of state. The Van der Waals (1893) which was a modification of the ideal gas law is established as the first success in the development of a cubic equation of state. The landmark of this EOS is the introduction of two constant a (termed the attraction parameter) and b (termed the repulsion parameter) that depend on the specific material. In 1949, Redlich and Kwong modified the Van der Waals EOS, to give an equation that is generally more accurate than both Van der Waals and the ideal gas equation. This was called the Redlich-Kwong (1949) equation of state. However, this equation is disadvantageous in its poor representation of the liquid phase behaviour. Hence, it cannot be used in accurately calculating VLE except in conjunction with some of the liquid phase correlation models. Soave in 1972 then replaced the $a/\sqrt{(T)}$ term of the Redlich-Kwong equation with a function $\alpha(T_r,\omega)$ involving the temperature and the acentric factor. The α function was devised to fit the vapour pressure data of hydrocarbons and the equation does fairly well for these components. This replacement changes the definition of *a* slightly, as the $T_c$ is now to the second power. The modified form of the equation is:

$$P = \frac{RT}{V_m - b} - \frac{a(T)}{(V_m + \varepsilon b)(V_m + \sigma b)} \tag{B.1}$$

where P is the gas pressure, R is the universal gas constant, T the absolute temperature ,$V_{m,}$ is the molar volume , *a* is a constant that corrects for attractive potential of molecules, and *b* is a constant that corrects for volume while for the Soave-Redlich-Kwong EOS (1972): ε = 0 and σ = 1

$$a(T) = a(T_c)\alpha(T_r, \omega) \tag{B.2}$$

$$b(T) = b(T_c) \tag{B.3}$$

where

$$a(T_c) = 0.42747 \frac{R^2 T_c^2}{P_c} \tag{B.4}$$

$$b(T_c) = 0.08664\frac{RT_c}{P_c} \tag{B.5}$$

$$\alpha(T_r, \omega) = \left[1 + \kappa(1 - T_r^{1/2})\right]^2 \tag{B.6}$$

where

$$\kappa = 0.480 + 1.574\omega - 0.176\omega^2 \tag{B.7}$$

and

$$T_r = \frac{T}{T_c} \tag{B.8}$$

where $T_r$ is the reduced temperature, $T_c$ and $P_c$ are the critical temperature and pressure respectively and ω is the acentric factor for the species.

The fugacity coefficient can be calculated from the expression:

$$\ln \hat{\phi}_i = (Z - 1) - \ln\frac{(V_m - b)}{V_m} - \frac{a(T)}{\sigma bRT}\ln\left(\frac{V_m + \sigma b}{V_m}\right) \tag{B.9}$$

## B.2 PENG-ROBINSON EQUATION OF STATE

The Peng-Robinson equation developed by Peng and Robinson (1976) is presented in the standard form.(Smith,2005)

$$P = \frac{RT}{V_m - b} - \frac{a(T)}{(V_m + \varepsilon b)(V_m + \sigma b)} \tag{B.10}$$

$$a(T_c) = 0.45724\frac{R^2 T_c^2}{P_c} \tag{B.11}$$

$$b(T_c) = 0.07780\frac{RT_c}{P_c} \tag{B.12}$$

The constant *a* (related to the intermolecular attraction force) is dependent on temperature while *b* (related to molecular size) is considered to be temperature independent. $\varepsilon = 1 - \sqrt{2}$, $\sigma = 1 + \sqrt{2}$ as applied in the Peng-Robinson equation.

$$a(T) = a(T_c)\alpha(T_r, \omega) \tag{B.13}$$

where

$$\alpha(T_r, \omega) = \left[1 + \kappa(1 - T_r^{1/2})\right]^2 \tag{B.14}$$

and $$\kappa = 0.37464 + 1.54226\omega - 0.26992\omega^2 \tag{B.15}$$

$$T_r = \frac{T}{T_c} \tag{B.8}$$

In a polynomial form:

$$A = \frac{aP}{R^2T^2} \tag{B.16}$$

$$B = \frac{bP}{RT} \tag{B.17}$$

$$Z^3 - (1-B)Z^2 + (A - 3B^2 - 2B)Z - (AB - B^2 - B^3) = 0 \tag{B.18}$$

To calculate the fugacity coefficient of species *i*, the following equation is employed:

$$\ln \hat{\phi}_i = \frac{\bar{b}_i}{b}(Z-1) - \ln\frac{(V_m - b)Z}{V_m} + \frac{a/bRT}{\varepsilon - \sigma}\left(1 + \frac{\bar{a}_i}{a} - \frac{\bar{b}_i}{b}\right)\ln\frac{V_m + \sigma b}{V_m + \varepsilon b} \tag{B.19}$$

where $\bar{a}_i$ and $\bar{b}_i$ are partial properties of the parameters *a* and *b* respectively.

The mixture parameters are obtained from the following mixing rules:

$$a = \sum_i \sum_j x_i x_j a_{ij} \tag{B.20}$$

$$b = \sum_i x_i b_i \tag{B.21}$$

$$a_{ij} = (1 - \delta_{ij})(a_i a_j)^{0.5} \tag{B.22}$$

$\delta_{ij}$ is the empirically determined binary interaction parameter. The Peng- Robinson EOS has the advantage over the Soave EOS in that it gives more accurate vapour pressures and equilibrium ratios (Peng and Robinson, 1976).

On this project, the Stryjek-Vera modified form of Peng-Robinson EOS was used. Stryjek and Vera (1986) modified the dependence of the attractive term of the Peng-Robinson EOS on temperature and on the acentric factor. This was done with a view of coming up with an EOS applicable to a wide variety of substances (non-polar, polar associating and non-associating alike), they retained Equations (3.54) to (3.57) for the Peng-Robinson EOS but proposed a new equation for $\kappa$. the new expression is:

$$\kappa = \kappa_o + \kappa_1\left(1+T_r^{0.5}\right)\left(0.7-T_r\right) \qquad \text{(B.23)}$$

with

$$\kappa o = 0.378893 + 1.4897153\omega - 0.17131848\omega^2 + 0.0196554\omega^3 \qquad \text{(B.24)}$$

Based on the above expression, $\kappa_1$ is an adjustable parameter characteristic of each pure component and is found from regressing vapour pressure data. Stryjek and Vera (1986) tabulated values of this parameter for a number of components, which were obtained through correlation of vapour pressure data at reduced temperatures. The same mixing rules and expressions for the fugacities are used as in the Peng-Robinson EOS.

## B.3 THE WONG AND SANDLER MIXING RULE

The cubic equations of state (Soave 1972, Peng and Robinson, 1976 and Stryjek and Vera modified Peng and Robinson, 1986) use similar mixing rules when applied to mixtures. These mixing rules are known as the *Van der Waal one fluid theory classical mixing rules* and the mixture *a* and *b* parameters are respectively given by equation 3.70 and 3.71.

In the original Soave (1972) EOS the cross parameter $a_{ij}$ is given by:

$$a_{ij} = \left(1-k_{ij}\right)\left(a_i a_j\right) \qquad \text{(B.25)}$$

and for the Stryjek Vera form of Peng-Robinson EOS :

$$a_{ij} = \left(1-\delta_{ij}\right)\left(a_i a_j\right)^{0.5} \qquad \text{(B.22)}$$

The foregoing classical mixing rules, although having been used successfully for some highly non-ideal and complex systems, are not generally applicable and are limited in that they do not have predictive capabilities. Due to the limitations of the classical mixing rules, Wong and Sandler (1992) developed a mixing rule which when used in conjunction with any cubic equation of state (CEOS) can be used to predict high-pressure vapour-liquid equilibrium from VLE data measured at low pressures. Their mixing rule when applied to a CEOS gives second virial coefficients that have quadratic composition dependence and thus is consistent with statistical mechanics (Wong and Sandler 1992). The correct use of the excess Helmholtz energy at infinite pressure in the mixing rule produces the correct low and high densities without being density dependent. The density-independent Wong and Sandler mixing rule is one of the five novel classes of mixing rules as described by Raal and Mühlbauer (1998). These include:

- The density-dependent mixing rules (DDMR),
- Classical mixing rules (CMR),
- Composition-dependent mixing rules (CDMR),
- Density-independent mixing rules (DIMR) and
- Local composition mixing rules (LCMR).

The reader is referred to the above-mentioned text for a greater and more detailed discussion of these mixing rules.

The Wong and Sandler (1992) mixing rule was chosen for this project due its applicability in simple mixtures containing hydrocarbons and inorganic gases and mixtures containing polar, aromatic and associating species over a wide range of pressures.

It gives the mixture parameters $a_m$ and $b_m$ as:

$$\frac{a_m}{RT} = \frac{QD^o}{(1-D^o)} \tag{B.26}$$

and

$$b_m = \frac{Q}{(1-D^o)} \tag{B.27}$$

where Q and $D^o$ are given by the equations:

$$Q = \sum_i \sum_j x_i x_j \left( b - \frac{a}{RT} \right)_{ij} \tag{B.28}$$

$$D^o = \sum_i x_i \frac{a_i}{b_i RT} + \frac{A_\infty^E}{cRT} \tag{B.29}$$

The fugacity coefficient can then be computed from any CEOS by substituting it in the equation:

$$\ln \phi_i = \int_V^{\infty} \frac{1}{RT}\left(\left(\left[\frac{\partial P}{\partial n_i}\right]\right)_{T,V,n_i} - \frac{1}{V}\right)dV - \ln\left(\frac{PV}{RT}\right) \tag{B.30}$$

When evaluating fugacities using the above equation, the partial derivatives of the mixture $a_m$ and $b_m$ parameters are needed. These are given by the equations:

$$\frac{\partial n b_m}{\partial n_i} = \frac{1}{(1-D^o)}\left(\frac{1}{n}\frac{\partial n^2 Q}{\partial n_i}\right) - \frac{Q}{(1-D^o)^2}\left(1 - \frac{\partial n D^o}{\partial n_i}\right) \tag{B.31}$$

$$\frac{1}{RT}\left(\frac{1}{n}\frac{\partial n^2 a_m}{\partial n_i}\right) = D^o \frac{\partial n b_m}{\partial n_i} + b_m \frac{\partial n D^o}{\partial n_i} \tag{B.32}$$

The corresponding partial derivatives of Q and $D^o$ are given respectively by:

$$\left(\frac{1}{n}\frac{\partial n^2 Q}{\partial n_i}\right) = 2\sum_j x_j \left(b - \frac{a}{RT}\right)_{ij} \tag{B.33}$$

and

$$\frac{\partial n D^{\circ}}{\partial n_i} = \frac{a_i}{b_i RT} + \frac{\ln \gamma_i^{\infty}}{c} \tag{B.34}$$

with c being a constant and:

$$\ln \gamma_i^{\infty} = \frac{1}{RT}\frac{\partial n A_{\infty}^E}{\partial n_i} \tag{B.35}$$

For the Stryjek-Vera form of Peng-Robinson EOS,

$$c = \frac{1}{\sqrt{2}}\ln(\sqrt{2}-1) \tag{B.36}$$

While for the Soave-Redlich-Kwong EOS,

$$c = -\ln(\frac{1}{2}) \tag{B.37}$$

Wong and Sandler (1992) showed that $A^E$ is much less pressure dependent than $G^E$ (an advantage which allows for the prediction of high pressure VLE from low-pressure VLE), thus:

$$\overline{G}^{E} = \overline{A}^{E}(T, x, P = low) = \overline{A}^{E}(T, x, P = \infty) \tag{B.38}$$

From this relation, any expression of $G^E$ at low pressure can be substituted for $A^E$. Using the NRTL equation for this purpose we have:

$$\frac{A_{\infty}^{E}}{RT} = \sum_{i} x_i \left( \frac{\sum_{j} x_j \tau_{ji} g_{ji}}{\sum_{k} x_k g_{ki}} \right) \tag{B.39}$$

and

$$\ln \gamma_i^{\infty} = \frac{\sum_{j} x_j \tau_{ji} g_{ji}}{\sum_{k} x_k g_{ki}} + \sum_{j} \frac{x_j g_{ij}}{\sum_{k} x_k g_{kj}} \left( \tau_{ij} - \frac{\sum_{l} x_l \tau_{lj} g_{lj}}{\sum_{k} x_k g_{kj}} \right) \tag{B.40}$$

The following equation is used for the evaluation of the cross parameters:

$$\left( b - \frac{a}{RT} \right)_{ij} = \frac{\left( b_i - \frac{a_i}{RT} \right) + \left( b_j - \frac{a_j}{RT} \right)}{2} (1 - k_{ij}) \tag{B.41}$$

In the above equation the parameter $k_{ij}$ is obtained by regression of data for binary mixtures following the procedure detailed in Section 3.7.2. In addition to this parameter, the coefficients in the expression chosen for the Helmholtz free energy are needed since the NRTL model was used. Thus, a total of four parameters were used in the regression.

# APPENDIX C

## C-1: Overall Deviation of the models for all the systems measured at three different isotherm.

| SRK ΔP | SRK Δy | VEOS ΔP | VEOS Δy | PRSV ΔP | PRSV Δy | HOC-CT ΔP | HOC-CT Δy |
|---|---|---|---|---|---|---|---|
| 0.0702 | 0.0110 | 0.0924 | 0.0102 | 0.1003 | 0.0115 | 0.0549 | 0.0169 |
| 0.0368 | 0.0076 | 0.0624 | 0.0098 | 0.0598 | 0.0098 | 0.0458 | 0.0086 |
| 0.0247 | 0.0085 | 0.0364 | 0.0103 | 0.0370 | 0.0103 | 0.0449 | 0.0114 |
| 0.0914 | 0.0065 | 0.1102 | 0.0087 | 0.1235 | 0.0082 | 0.0668 | 0.0137 |
| 0.1324 | 0.0164 | 0.1536 | 0.0186 | 0.1677 | 0.0174 | 0.0667 | 0.0158 |
| 0.0247 | 0.0244 | 0.0367 | 0.0288 | 0.0326 | 0.0259 | 0.0714 | 0.0060 |
| 0.0744 | 0.0019 | 0.0994 | 0.0027 | 0.1193 | 0.0033 | 0.0660 | 0.0049 |
| 0.0637 | 0.0046 | 0.1000 | 0.0082 | 0.1040 | 0.0084 | 0.0634 | 0.0044 |
| 0.0298 | 0.0137 | 0.0425 | 0.0178 | 0.0565 | 0.0153 | 0.0499 | 0.0042 |
| **0.0609** | **0.0105** | **0.0815** | **0.0128** | **0.0890** | **0.0122** | **0.0589** | **0.0095** |

**Table C-1: Average deviations of the models on all the systems measured on this project**

## C-2: The Effect of Dimerization on the fugacity and fugacity coefficient of Carboxylic Acid-Alcohol binary mixture

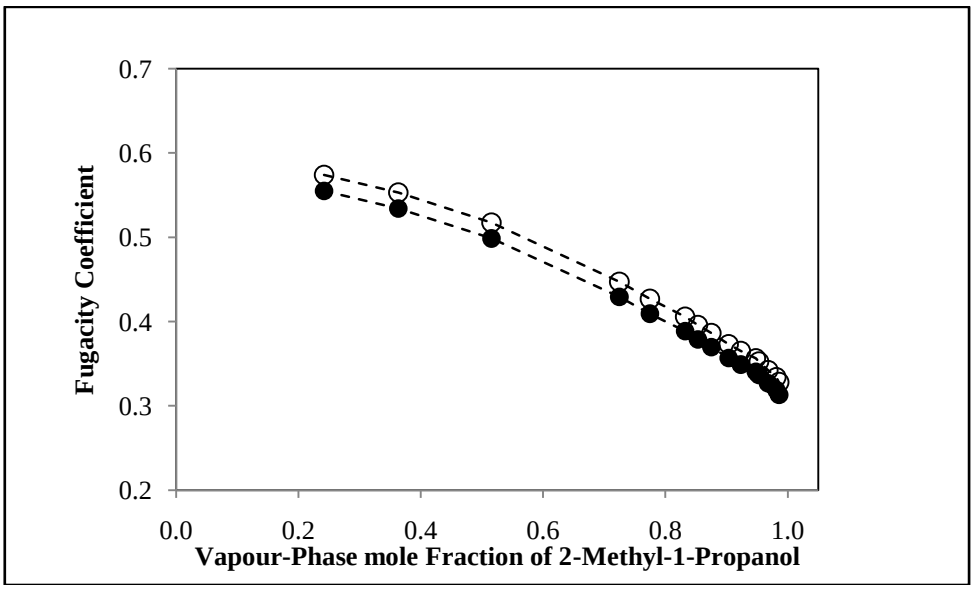


**Figure C-1: Fugacity coefficients for saturated mixtures of 2-methyl-1-propanol (1) and butyric acid (2) at 373.15K. Calculations based on chemical theory shows large deviations from ideal behaviour.**

The plot above is based on the chemical theory of vapour-phase imperfection and on experimental vapour-liquid equilibrium data for the binary systems. In the system 2-methyl-1-propanol (1) + butyric acid (2), the fugacity coefficient for $y_1$ =1 is slightly higher than fugacity coeffficent for $y_2$ =1 because pure butyric acid has a stronger tendency to dimerize with itself than does 2-methyl-1-propanol at 373.15 K. However, since strong dimerization occurs between all three possible pairs (i.e the monomer of 2-methyl-1-propanol, monomer of butyric acid and the dimer complex), the fugacity coefficients for the two components are not severely different from each other and as shown, give nearly parrallel curves when plotted against composition. This plot also shows that as $y_1$ is near zero, there is little dimerization, hence, the fugacity coefficients for the two components are close to unity.

## C-3: Temperature dependence of dimerization contribution to the second virial coefficients

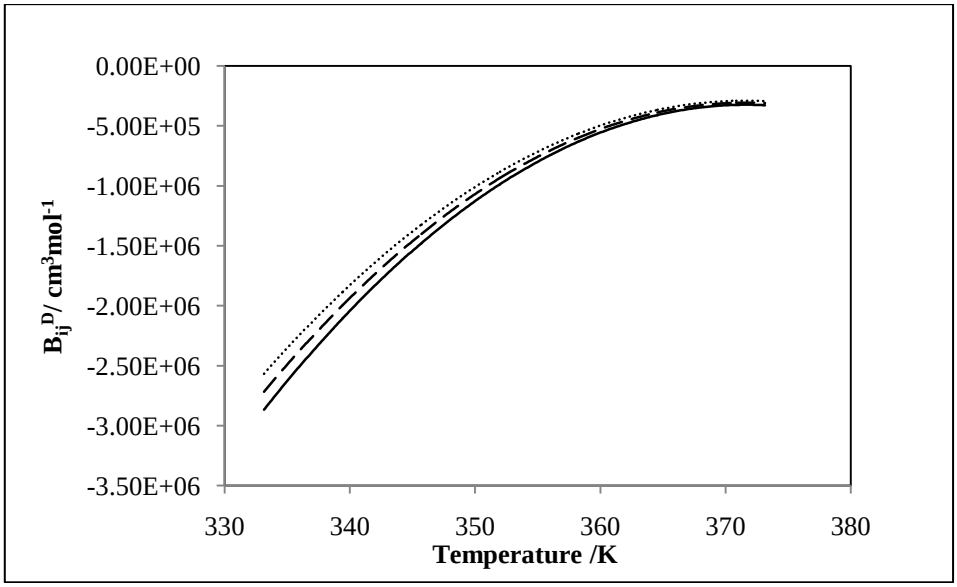


**Figure C-2: Dimerization contribution to Second virial coefficients for 2-methyl-1-propanol (1) + butyric acid binary system (**----), $B_{11}$; (−), $B_{22}$ ; (- - -) , $B_{12}$

The plot shows the temperature dependence of the second virial coefficients for dimerization ($B_{ij}^{D}$) $B_{11}$, $B_{12}$ and $B_{22}$ for 2-methyl-1-propanol+Butyric acid binary system at 333.15, 353 and 373.15K. The plot shows that the intermolecular forces between like molecules are similar just as the diploe-dipole moments to those between unlike molecules and therefore the curve $B_{12}$ lies between the curves for $B_{11}$ and $B_{22}$.

**APPENDIX**
**D**

# THERMODYNAMIC CONSISTENCY

This appendix contains the graphs utilized in the determination of the thermodynamic consistency of the measured VLE data. Two consistency tests were conducted for each set of experimental data, namely the point test and the direct test. The deviation of the model pressures and vapour compositions from the experimental data are presented for the point test while the direct test applying the chemical theory has been presented in the discussion section.

## D.1 2-Propanol (1) + Butyric Acid (2) System

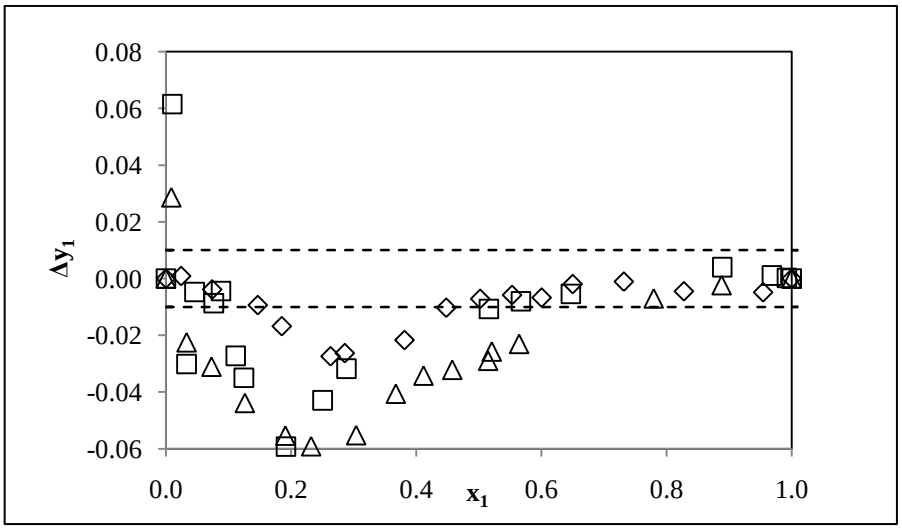


**Figure D-1: Graph of the deviation of the VEOS (Tsonopoulos)-NRTL model vapour compositions from the experimental values for the 2-Propanol (1) + Butyric acid (2) system. (**◊),T = 333.15K, ; (□) ,T = 353.15K, ; (Δ) ,T = 373.15K; ----- 0.01 line

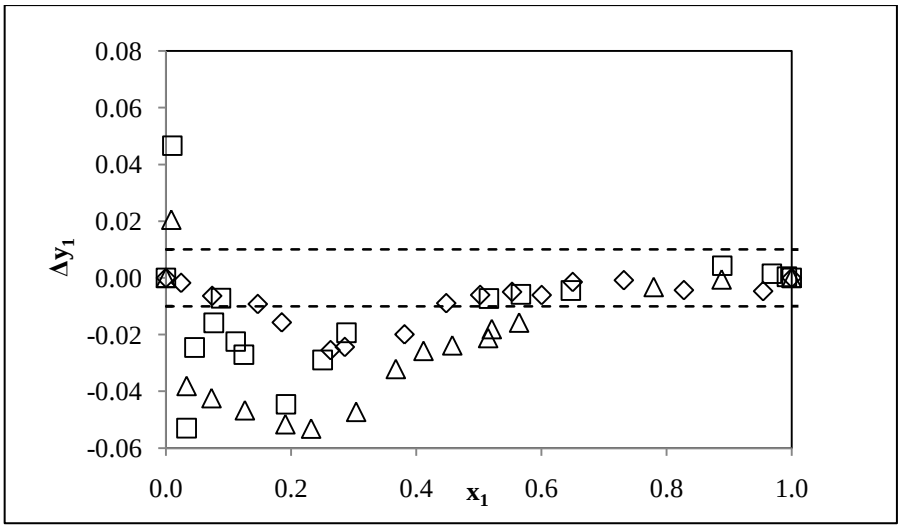


**Figure D-2: Graph of the deviation of the PRSV-WS-NRTL model vapour compositions from the experimental values for the 2-Propanol (1) + Butyric acid (2) system. (**◊),T = 333.15 K, ; (□) ,T = 353.15 K, ; (Δ) ,T = 373.15 K; ----- 0.01 line

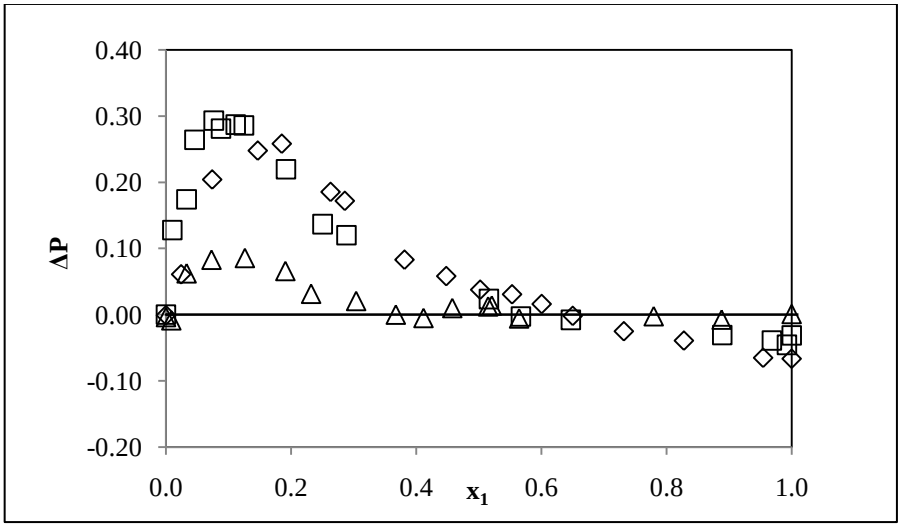


**Figure D-3: Graph of the deviation of the SRK-WS-NRTL model pressure calculated from the experimental pressure values for the 2-Propanol (1) + Butyric acid (2) system. (**◊),T = 333.15 K, ; (□) ,T = 353.15 K, ; (Δ) ,T = 373.15 K; − Zero line

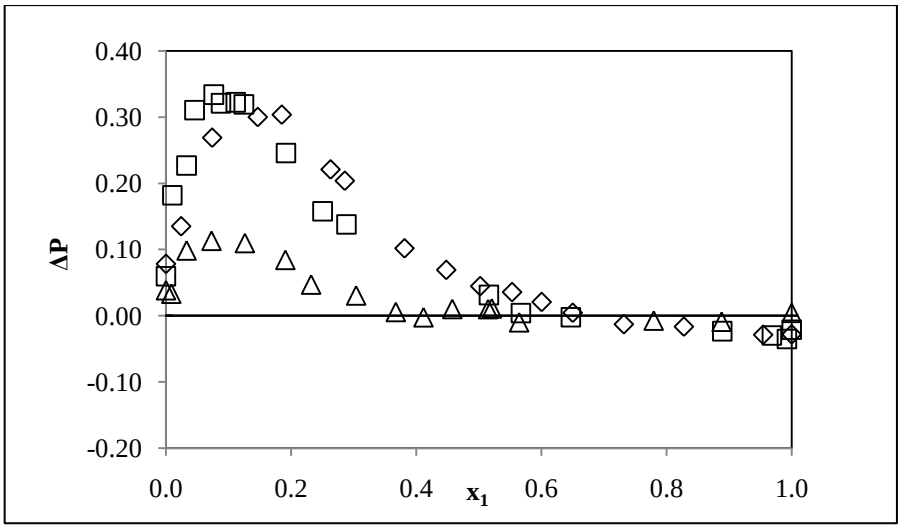


**Figure D-4: Graph of the deviation of the VEOS (Tsonopoulos)-NRTL model pressure calculated from the experimental pressure values for the 2-Propanol (1) + Butyric acid (2) system. (**◊),T = 333.15 K, ; (□) ,T = 353.15 K, ; (Δ) ,T = 373.15 K; − Zero line

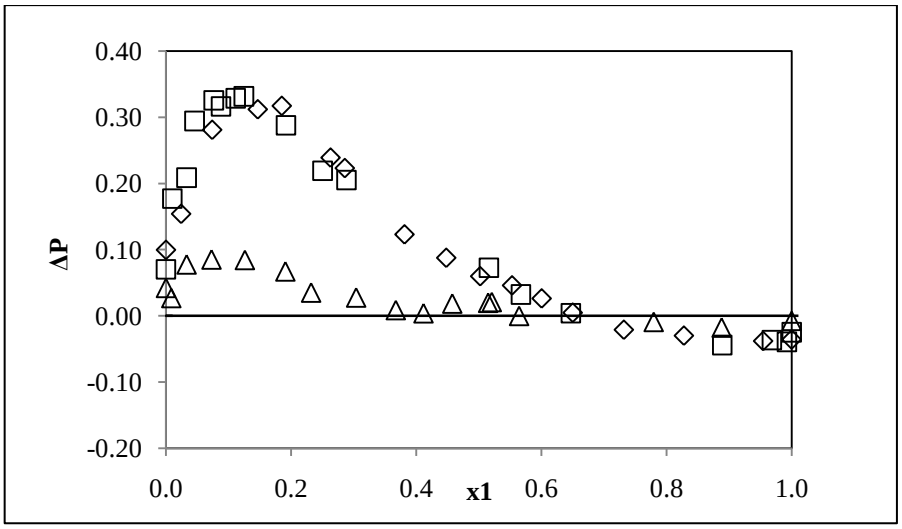


**Figure D-5: Graph of the deviation of the PRSV-WS-NRTL model pressure calculated from the experimental pressure values for the 2-Propanol (1) + Butyric acid (2) system.** (◊),T = 333.15 K, ; (□) ,T = 353.15 K, ; (Δ) ,T = 373.15 K; − Zero line

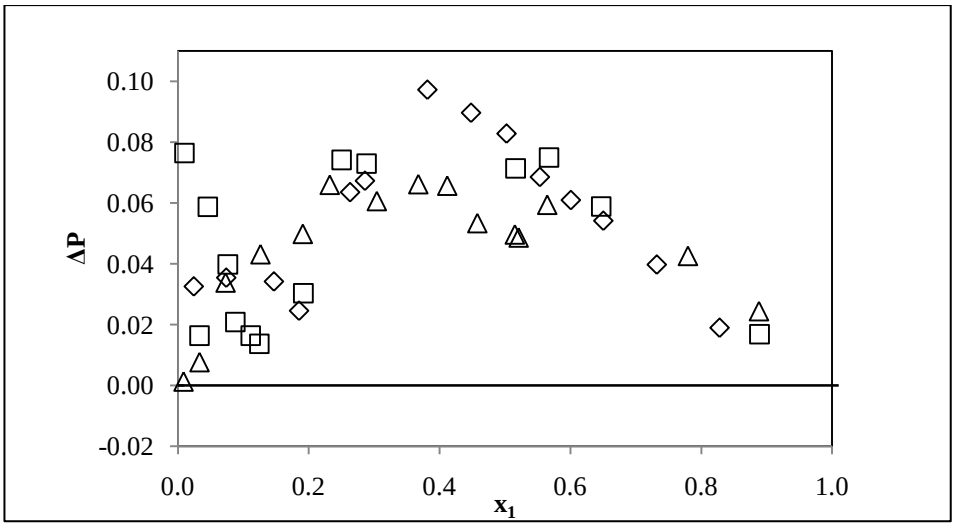


**Figure D-6: Graph of the deviation of the NRTL model (with Chemical Theory) pressure calculated from the experimental pressure values for the 2-Propanol (1) + Butyric acid (2) system. (**◊),T = 333.15 K, ; (□) ,T = 353.15 K, ; (Δ) ,T = 373.15 K; − Zero line

## D.2 2-Butanol (1) + Butyric Acid (2) System

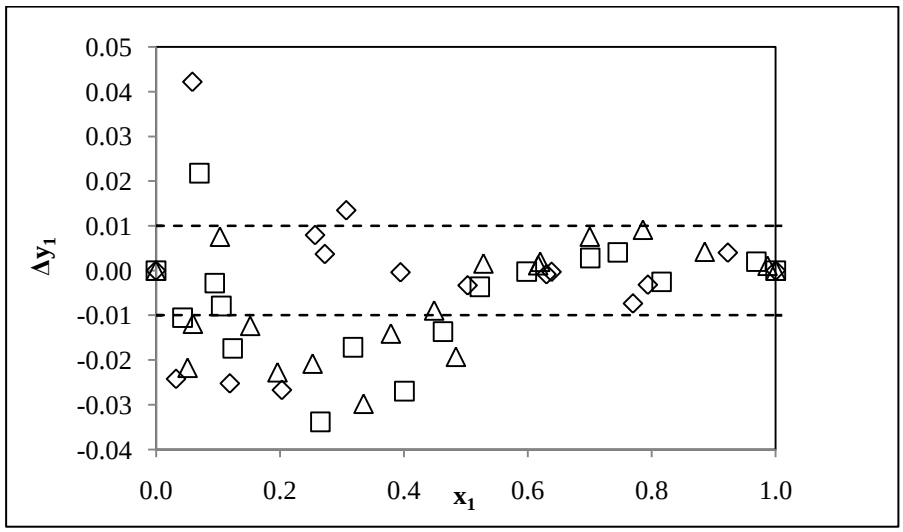


**Figure D-7: Graph of the deviation of the VEOS (Tsonopoulos)-NRTL model vapour compositions from the experimental values for the 2-Butanol (1) + Butyric acid (2) system. (**◊),T = 333.15 K, ; (□) ,T = 353.15 K, ; (Δ) ,T = 373.15 K; ----- 0.01 line

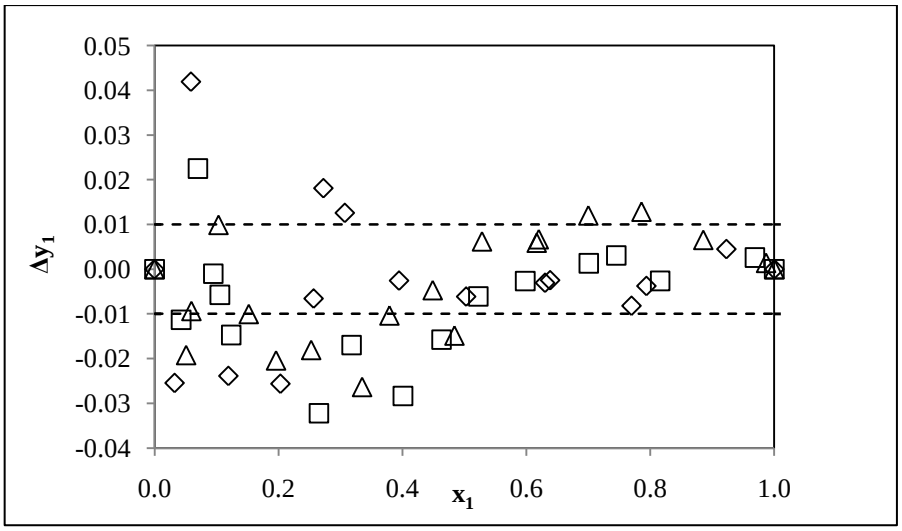


**Figure D-8: Graph of the deviation of the PRSV-WS-NRTL model vapour compositions from the experimental values for the 2-Butanol (1) + Butyric acid (2) system. (**◊),T = 333.15 K, ; (□) ,T = 353.15 K, ; (Δ) ,T = 373.15 K ; ----- 0.01 line

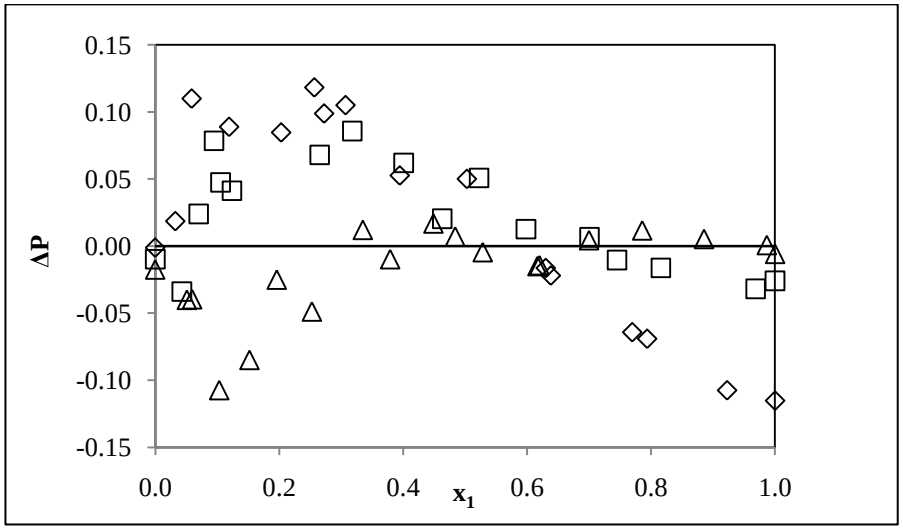


**Figure D-9: Graph of the deviation of the SRK-WS-NRTL model pressure calculated from the experimental pressure values for the 2-Butanol (1) + Butyric acid (2) system. (**◊),T = 333.15 K, ; (□) ,T = 353.15 K, ; (Δ) ,T = 373.15 K ; − Zero line

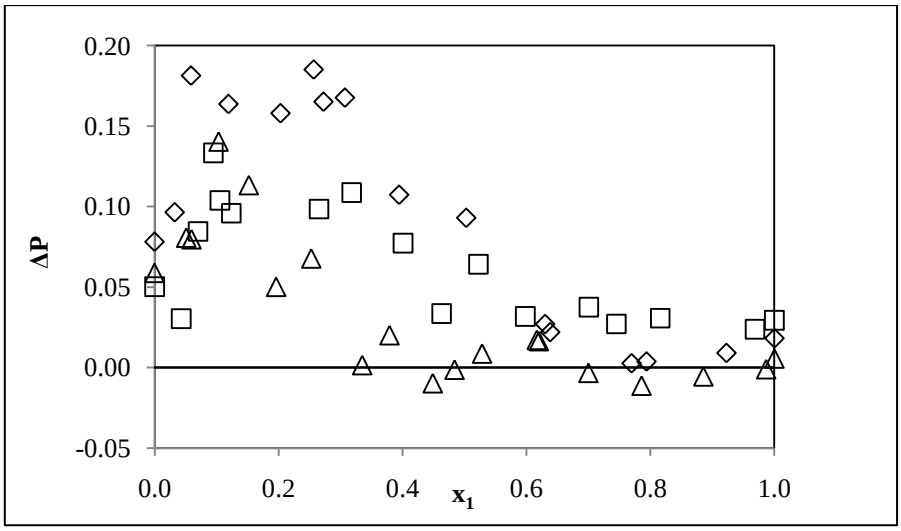


**Figure D-10: Graph of the deviation of the VEOS (Tsonopoulos)-NRTL model pressure calculated from the experimental pressure values for the 2-Butanol (1) + Butyric acid (2) system. (**◊),T = 333.15 K, ; (□) ,T = 353.15 K, ; (Δ) ,T = 373.15 K; − Zero line

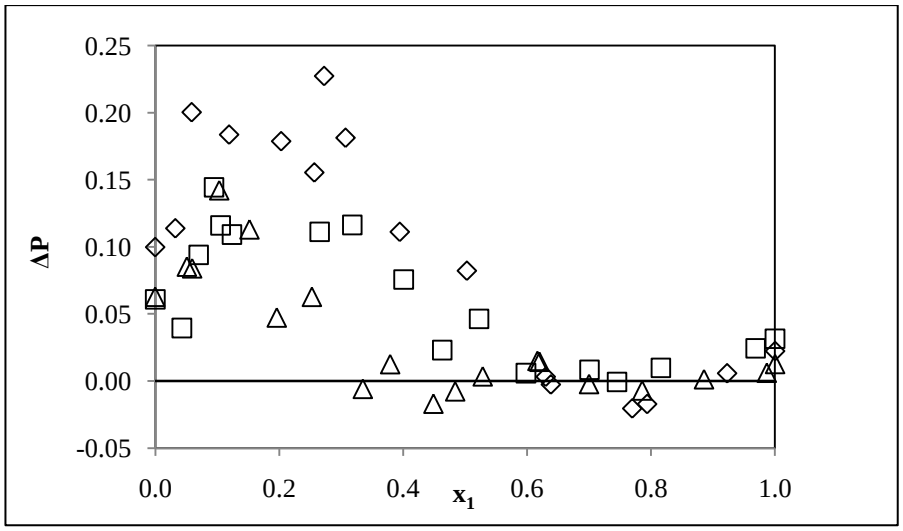


**Figure D-11: Graph of the deviation of the PRSV-WS-NRTL model pressure calculated from the experimental pressure values for the 2-Butanol (1) + Butyric acid (2) system. (**◊),T = 333.15 K, ; (□ ) ,T = 353.15 K, ; (Δ) ,T = 373.15 K ; − Zero line

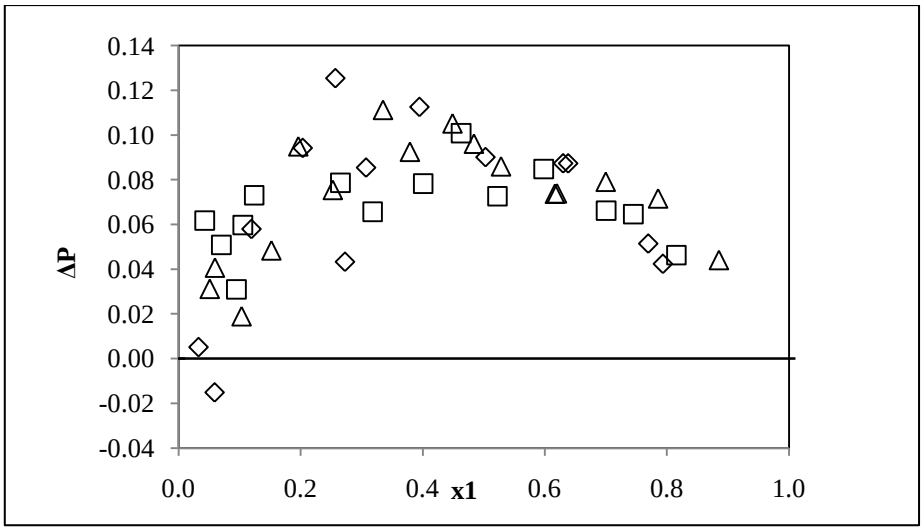


**Figure D-12: Graph of the deviation of the NRTL model (with Chemical Theory) pressure calculated from the experimental pressure values for the 2-Butanol (1) + Butyric acid (2) system. (**◊),T = 333.15 K, ; (□) ,T = 353.15 K, ; (Δ) ,T = 373.15 K; − Zero line

## D.3 2-Methyl-1-Propanol (1) + Butyric Acid (2) System

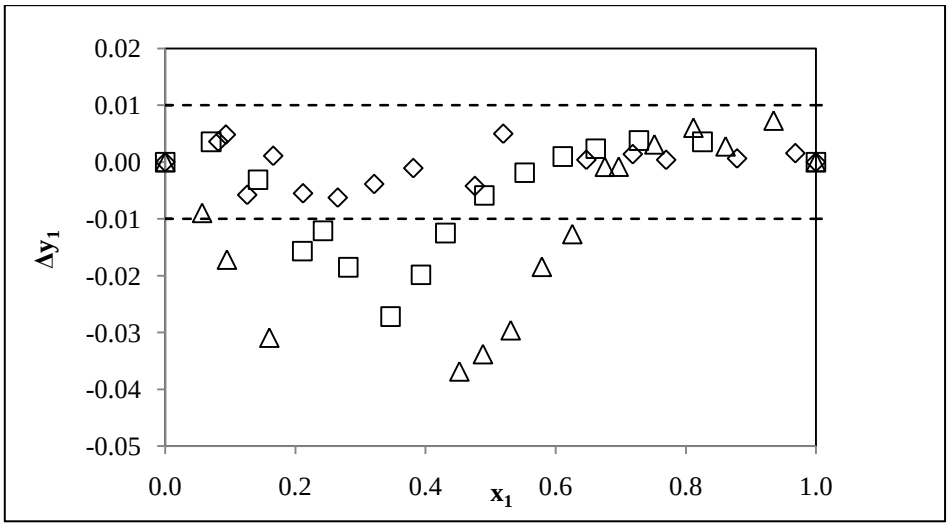


**Figure D-13: Graph of the deviation of the VEOS (Tsonopoulos)-NRTL model vapour compositions from the experimental values for the 2-Butanol (1) + Butyric acid (2) system. (**◊),T = 333.15 K, ; (□) ,T = 353.15 K, ; Δ ,T = 373.15 K; ----- 0.01 line

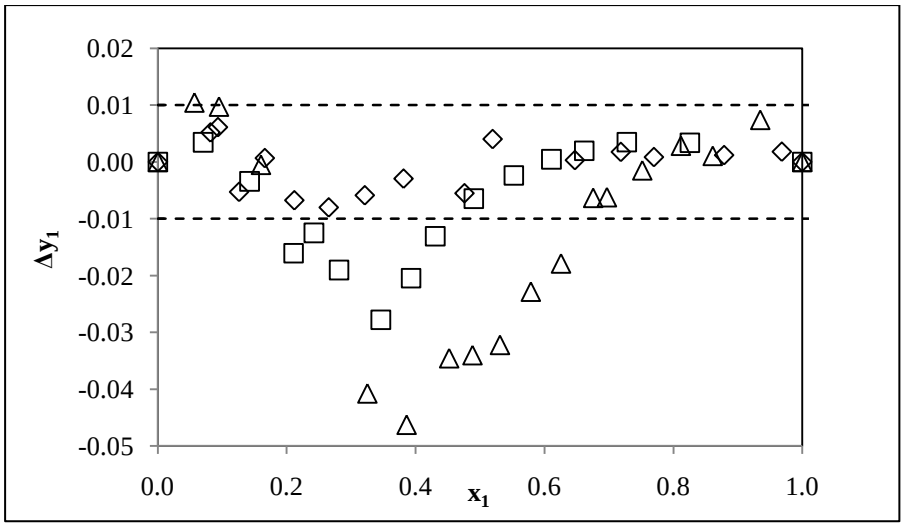


**Figure D-14: Graph of the deviation of the PRSV-WS-NRTL model vapour compositions from the experimental values for the 2-Butanol (1) + Butyric acid (2) system. (**◊),T = 333.15 K, ; (□) ,T = 353.15 K, ; (Δ) ,T = 373.15 K; ----- 0.01 line

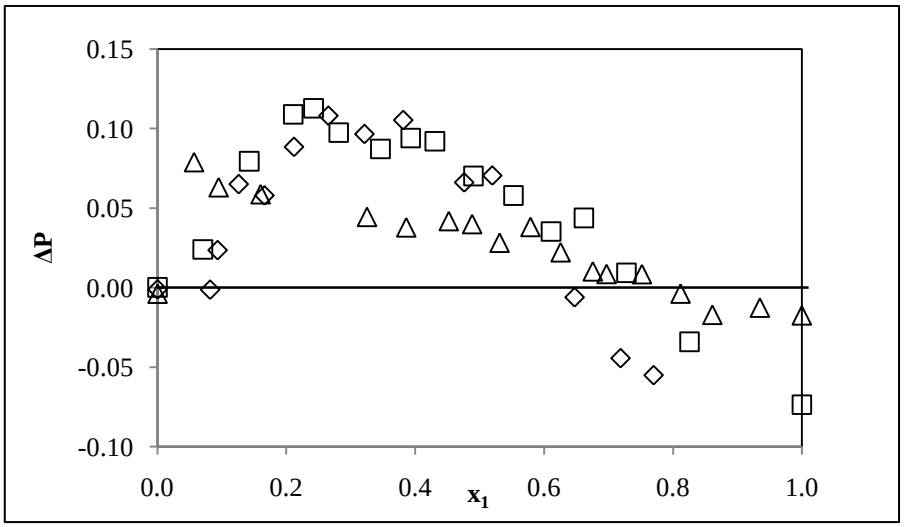


**Figure D-15: Graph of the deviation of the SRK-WS-NRTL model pressure calculated from the experimental pressure values for the 2-Butanol (1) + Butyric acid (2) system. (**◊),T = 333.15 K, ; (□) ,T = 353.15 K, ; (Δ) ,T = 373.15 K; − Zero line

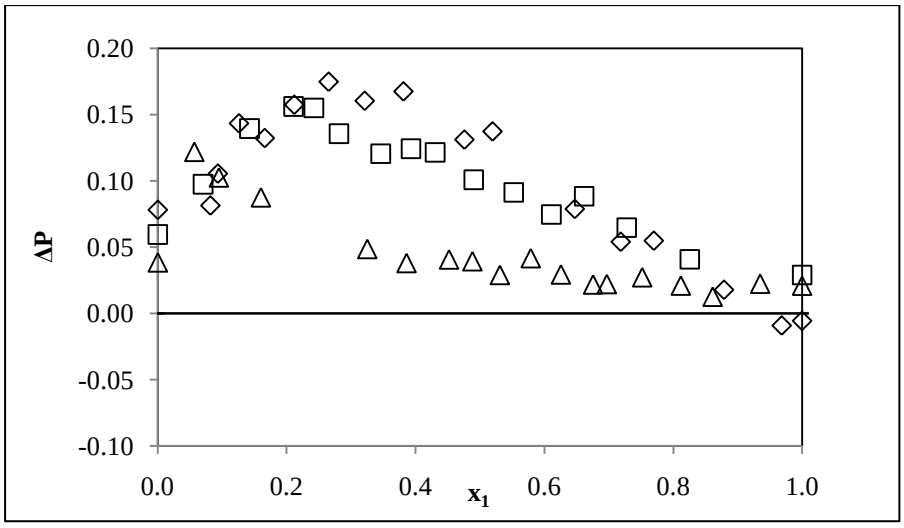


**Figure D-16: Graph of the deviation of the VEOS (Tsonopoulos)-NRTL model pressure calculated from the experimental pressure values for the 2-Butanol (1) + Butyric acid (2) system. (**◊),T = 333.15 K, ; (□) ,T = 353.15 K, ; (Δ) ,T = 373.15 K; − Zero line

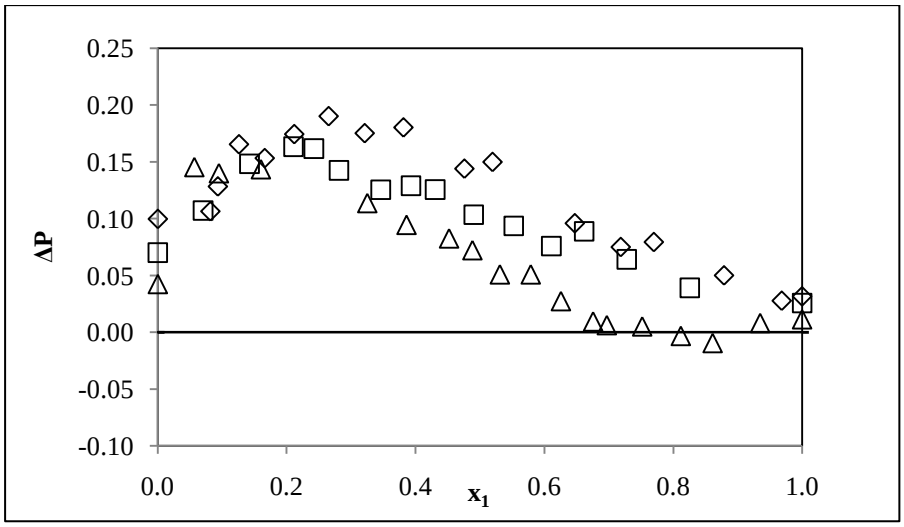


**Figure D-17: Graph of the deviation of the PRSV-WS-NRTL model pressure calculated from the experimental pressure values for the 2-Butanol (1) + Butyric acid (2) system. (**◊),T = 333.15 K, ; (□) ,T = 353.15 K, ; (Δ) ,T = 373.15 K; − Zero line

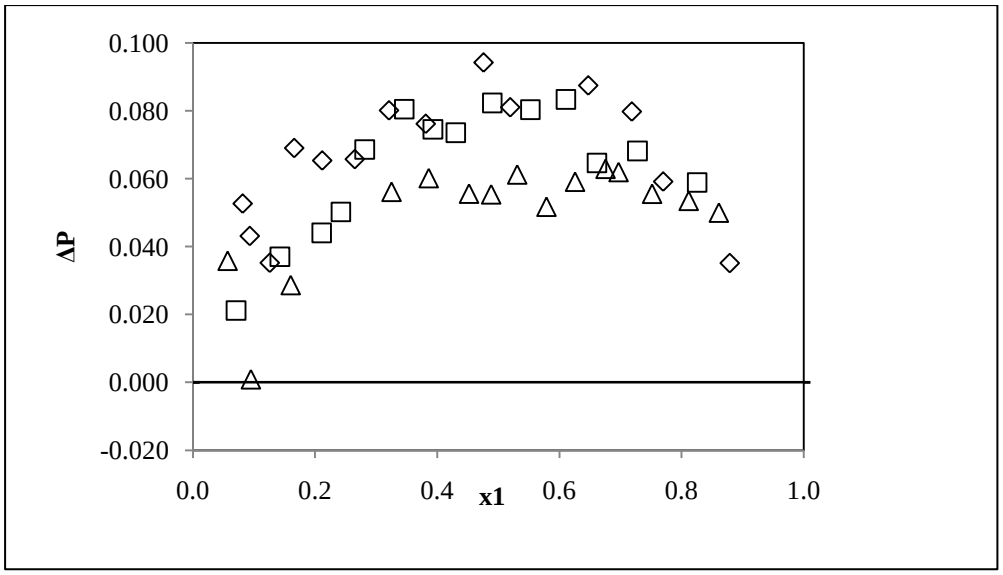


**Figure D-18: Graph of the deviation of the NRTL model (with Chemical Theory) pressure calculated from the experimental pressure values for the 2-Butanol (1) + Butyric acid (2) system. (**◊),T = 333.15 K, ; (□) ,T = 353.15 K, ; (Δ) ,T = 373.15 K ; − Zero line

# APPENDIX
# E

## E-1: Guide for Estimating Unknown Parameter for the Chemical Theory

Estimation of parameters used in the chemical theory could be challenging; especially when it involves $C_4$ acids and above since the $C_1$-$C_3$ are commonly found in literature.

The second virial coefficients are the most sensitive to the values of the critical temperature. Hence, using the correct critical properties is important. As mentioned in Appendix A, the critical properties were obtained from DDB, 2009. The values of the radius of gyration ($R_D$) were obtained from Prausnitz et al.(1980) as well as values of dipole moment from McClellan (1974) as cited by Prausnitz et al.(1980). However, the solvation of the systems measured was neglected based on the theoretical ground that in "pure" solvation, neither species associates (Prausnitz et al., 1980). Hence, only the association parameters were used. The association parameters could not be found in any of the literature. However, Prausnitz et al. (1980) advise that where the parameter of the components is not available, the association parameter for a chemically similar system can be use (i.e. acetic and propionic acid which could be found in Prausnitz el al., 1980). In addition, it has been reported that association parameters must be obtained when specific ("chemical") interactions can occur. Since these are difficult to estimate à priori, it was advised that reasonable approximations be made by choosing a value for a chemically similar system. Thus, 4.5 were chosen for the alcohols studied on this project.

It should be mentioned that in the course of this project, when the value of 5.0 or 5.5 were used for the association parameters for the alcohols, the vapour-phase nonidealities was more accounted for. However, the activity coefficient was not well correlated with the model as in the case when 4.5was employed as the association parameter. Hence, a conclusion was reached to use 4.5 for the acids as well as the alcohols.

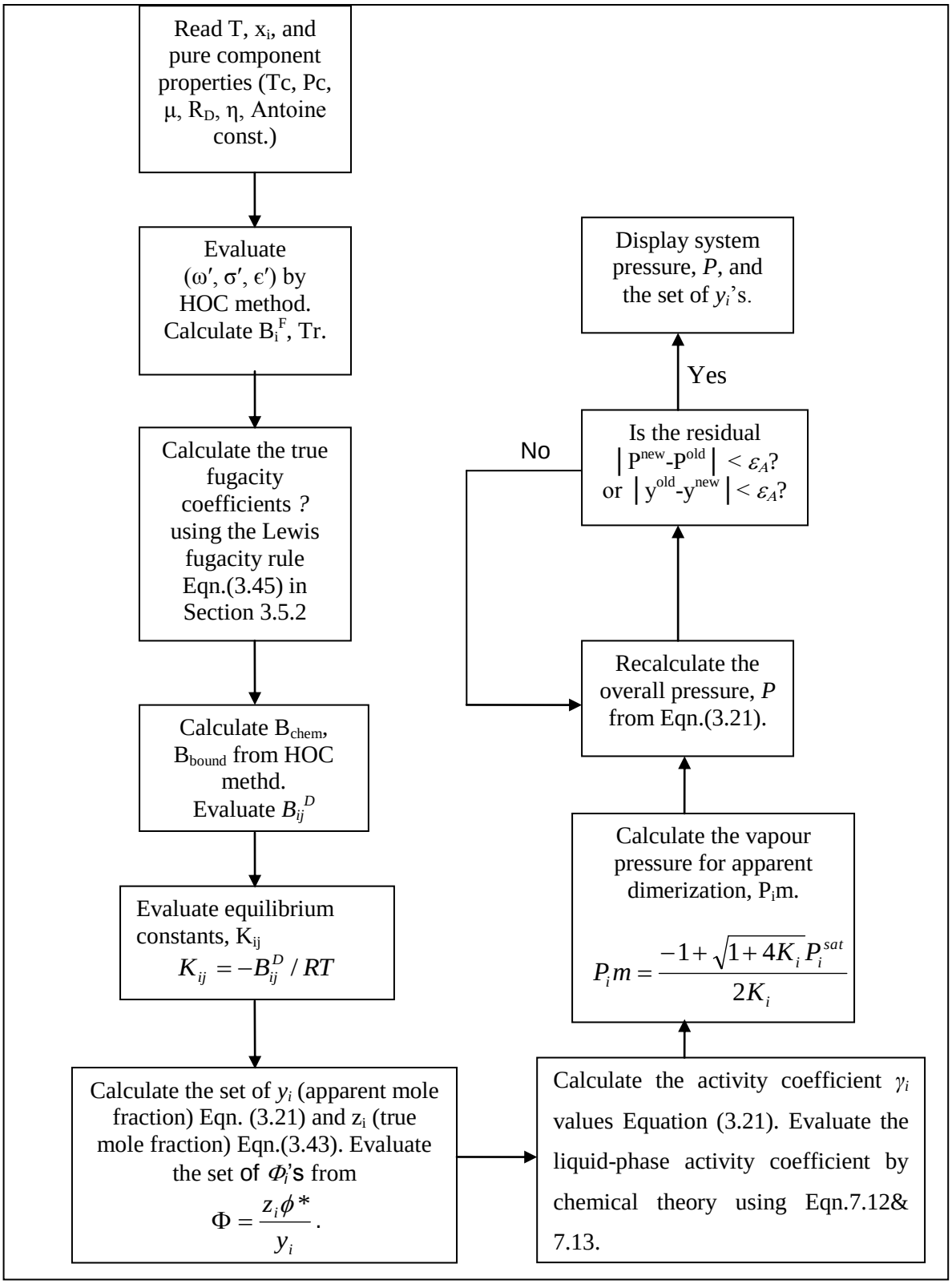


**E-2: Flow diagram showing the routine procedure for the chemical theory.**